UNIVERSITY OF SOUTHAMPTON

FACULTY OF NATURAL AND ENVIRONMENTAL SCIENCES

School of Ocean & Earth Science

Evolution and mineralization of volcanic arc sequences: Tyrone Igneous Complex, Northern Ireland

by

Steven P. Hollis

A thesis submitted for the degree of
Doctor of Philosophy

Submitted August 2012
Corrected version January 2013

Declaration of authorship

I, Steven Philip Hollis declare that the thesis entitled

Evolution and mineralization of volcanic arc sequences: Tyrone Igneous Complex, Northern Ireland

and the work presented in the thesis are both my own, and have been generated by me as the result of my own original research. I confirm that:

- this work was done wholly or mainly while in candidature for a research degree at this University;
- where any part of this thesis has previously been submitted for a degree or any other qualification at this University or any other institution, this has been clearly stated;
- where I have consulted the published work of others, this is always clearly attributed;
- where I have quoted from the work of others, the source is always given. With the exception of such quotations, this thesis is entirely my own work;
- I have acknowledged all main sources of help;
- where the thesis is based on work done by myself jointly with others, I have made clear exactly what was done by others and what I have contributed myself;
- parts of this work have been published as:

Cooper, M.R., Q.G., Crowley, **Hollis, S.P.**, Noble, S.R., Roberts, S., Chew, D., Earls, G, Herrington, R., & Merriman, R.J. (2011). *Age constraints and geochemistry of the Ordovician Tyrone Igneous Complex, Northern Ireland: Implications for the Grampian orogeny.* Journal of the Geological Society, London, v. 168, p. 837-850

Hollis, S.P., Roberts, S., Cooper, M.R., Earls, G., Herrington, R., Condon, D.J., Cooper, M.J., Archibald, S.M., & Piercey, S.J. (2012). *Episodic arc-ophiolite emplacement and the growth of continental margins: Late accretion in the Northern Irish sector of the Grampian-Taconic orogeny.* GSA Bulletin, v. 124. p. 1702-1723.

Signed: 

Date: 18/01/2013

Abstract

The Tyrone Igneous Complex of Northern Ireland forms an integral part of the Grampian-Taconic orogen, linking the well documented sectors of Scotland, western Ireland and Newfoundland. The orogen records the accretion of a series of peri-Laurentian affinity arcs, ophiolites and microcontinental blocks to the Laurentian margin between the Late Cambrian and Middle Ordovician. The Tyrone Igneous Complex is broadly divisible into two distinct units: the c. 484-480 Ma ophiolitic Tyrone Plutonic Group and the structurally overlying c. 475-469 Ma arc-related Tyrone Volcanic Group. Both were intruded by a synvolcanogenic and syncollisional, to post-collisional high-level ensialic intrusive suite between c. 470 and 464 Ma associated with their coeval obduction to an outboard peri-Laurentian microcontinental block, the Tyrone Central Inlier, at c. 470 Ma. The Tyrone Plutonic Group is principally composed of amphibolite-facies layered and isotropic gabbros, sheeted dolerite dykes and rare pillow lavas. Tholeiitic suprasubduction affinity geochemical characteristics, Nd-isotope constraints, zircon inheritance, and the presence of late Fe-Ti enriched post-obduction dykes suggest the Tyrone Plutonic Group formed above a N-dipping subduction zone by the propagation of a spreading centre into a microcontinental block.

The Tyrone Volcanic Group is characterized by mafic to intermediate lavas, tuffs, rhyolite, banded chert, ironstone and argillaceous sedimentary rocks cut by numerous high-level synvolcanogenic intrusive rocks. Geochemical signatures are consistent with formation in an evolving peri-Laurentian island-arc which underwent several episodes of rifting. High LILE and LREE enrichment, calc-alkaline geochemical signatures and strongly negative εNd_t values suggest the Tyrone arc was at least partially founded on a fragment of microcontinental crust, which may have rifted off the Tyrone Central Inlier during the formation of the Tyrone Plutonic Group. Stong temporal, stratigraphic, and geochemical correlations with elements within the Annieopsquotch Accretionary Tract of Newfoundland suggest the Tyrone Igneous Complex represents a third phase of arc-ophiolite obuction in the Irish Caledonides during the Grampian-Taconic orogeny and may potentially host significant VMS mineralization.

Through a combination of field mapping and petrochemistry several stratigraphic horizons have been identified in the Tyrone Igneous Complex, favourable for the formation and preservation of VMS deposits. Each is closely associated with hydrothermal alteration, synvolcanogenic faults and high-level synvolcanogenic intrusions of dolerite, gabbro, diorite and tonalite. Episodic rifting is recorded by the eruption of: abundant non-arc type Fe-Ti enriched eMORB ('icelandite'), island-arc tholeiite, OIB-like alkali basalt, high-temperature tholeiitic rhyolites with flat to U-shaped REE profiles, and high-Zr rhyolites, within the calc-alkaline dominated sequence. Rift related mafic lavas occur in the hangingwall to VMS-style mineralization and are closely associated with ironstones (often Au-bearing) and/or argillaceous sedimentary rocks representing volcanic quiescence. Extensive hydrothermal alteration, characterized by Na-depletion, high Ba/Sr, Bi, Sb, Ni, CCPI, AI and variable MgO and CaO, allows specific target areas to be identified. In the lower bimodal-mafic Tyrone arc and backarc, hydrothermal alteration is associated with Zn-Cu mineralized float. Pb-Zn-Cu-Au mineralization occurs in silicified auriferous rhyolite domes/flows and/or volcaniclastic rocks of the syncollisional bimodal-felsic upper Tyrone arc. Ophiolite hosted Cu mineralization is characterized by chalcopyrite stringers hosted in sheeted dyke sequences.

"In the outside world, I am a simple geologist... but in here, I am Valkorn, Defender of the Alliance"

- Randy Marsh

Contents

List of figures

List of tables

Acknowledgements

I would first and foremost like to thank my supervisors Stephen Roberts, Mark Cooper, Garth Earls, Richard Herrington and Stephen Piercey for their support, guidence and friendship over the past few years.

My parents Robert and Coral are thanked for their enduring belief and encouragement. This thesis would not have been possible without them.

Catriona, James, Alex, Sarah and Chris – thanks for a great four years.

Aurum Exploration Services and Dalradian Gold personnel are thanked for their hospitality and assistance during fieldwork, particularly Gavin Berkenheger, Raymond Keenan, Hilary Clarke, Sandy Archibald and Vaughan Williams. I would also like to thank the Dalradian Gold, Major and SLR teams for a great year, especially Marty, the geos (Susan, Nikki, Ana and Orla), Damien, Andy, Keith, Shane, Steve, Jake, Lee, Angela, Tomac, and Charlie. Alan – I will miss our chats and all the questions.

I am indebted to many individuals for invaluable field discussions, including: David Chew, John Dewey, Paul Ryan, Jack Casey, Stephen Daly, Robin Taggart, Rob Chapman, Ian Mitchell, Simon Bottrell and many others. Dan Condon, Quentin Crowley and Stephen Noble are also thanked for U-Pb zircon geochronology.

This project was supported through the generosity of the BGS University Funding Initiative, Dalradian Resources, the Geological Survey of Northern Ireland, University of Southampton, Metallum Resources and the Natural History Museum, London. Funding for U-Pb zircon dating was made possible through a combination of Northern Ireland Department of Enterprise Trade and Investment and Northern Ireland Environment Agency funding.

Matthew Cooper, Ian Croudace, John Spratt and Andy Milton are thanked for help with labwork. Bob and John – sorry about the state of the rock saw and for all those thin sections.

B. Bingen, K. Goodenough, M. Young, D. Schofield, Cees van Staal and anonoymous revewiers are thanked for reviewing the manuscripts in this thesis.

Stephen Daly and Rex Taylor are thanked for many constructive comments on this thesis.

Definitions and abbreviations

Alk	- alkali basalt
BGS	- British Geological Survey
BON	- boninite
CA	- calc-alkalic
CAI	- calc-alkaline subgroup 1 (see Chapter 4)
CAII	- calc-alkaline subgroup 2 (see Chapter 4)
CAB	- calc-alkaline basalt
CHUR	- chondritic uniform reservior
DDH	- diamond drillhole
EM	- electromagnetics
eMORB	- enriched mid ocean ridge basalt
EMPA	- electron microprobe analysis
Fe-Ti	- Fe-Ti enriched
GSI	- Geological Survey of Ireland
GSNI	- Geological Survey of Northern Ireland
HFSE	- high field strength elements
HREE	- heavy rare earth elements
IAT	- island arc tholeiite
ICP-MS	- inductively coupled plasma mass spectrometry
ID-TIMS	- isotope dilution thermal ionization mass spectrometry
OIB	- ocean island basalt
LILE	- large ion lithophile elements
LOI	- loss on ignition
LOTI	- low-Ti tholeiite
LREE	- light rare earth elements
NERC	- Natural Environment Research Council
NIGL	- NERC Isotope Geosciences Laboratory
nMORB	- normal mid ocean ridge basalt
NOCS	- National Oceanography Centre, Southampton
REE	- rare earth elements
RTP	- reduced to pole
SEM	- scanning electron microscope
sd	- standard deviation
SSZ	- suprasubduction zone
TCI	- Tyrone Central Inlier
TMI	- total magnetic intensity
TPG	- Tyrone Plutonic Group

TVG - Tyrone Volcanic Group

VMS - volcanogenic massive sulphide

XRF - x-ray fluorescence

εNd_t - epsilon Nd value at age t

τ_{DM} - depleted mantle model age at age t

$^{87}Sr/^{86}Sr_i$ - initial $^{87}Sr/^{86}Sr$ ratio

Chapter 1: Introduction - Accretionary orogens and implications for mineralization

1.1 Natural complexity in accretionary orogens

Accretionary orogens form at sites where oceanic lithosphere is subducted at continental margin and in intraoceanic settings due to the progressive closure of ocean basins. The orogen results in the growth of continental crust through the accretion of: blocks of allochthonous crust (e.g Waldron & van Staal 2001), fragments of oceanic plateaus and seamounts (e.g. Ryan & Dewey 2004), and/or dismembered or relatively complete arc and ophiolite sequences (e.g. Dewey & Shackleton 1984; Dewey 2005; Zagorevski et al. 2009a). Long lived collisional orogens, may produce multiple sutures along terrane boundaries which play a crucial role in determining the metallogenic signatures of accretionary orogens (see Bierlein et al. 2009). Understanding lithospheric processes involved in these orogens is crucial for reconstructing the growth of continental crust (e.g. Draut et al. 2004, 2009) and ultimately understanding the metallogeny of accreted terranes for mineral exploration (van Staal 2007). Accretionary processes have been recongized to span from the Archaean (e.g. Superior Province, Yilgarn Craton: Sengör & Natal'in 2004) to the present day (e.g. Taiwan; reviewed in Byrne et al. 2011), with arc-continent collision zones producing a significant amount of the world's mineral wealth from porphyry Cu-Mo-Au, epithermal Au-Ag, volcanogenic massive sulphide (VMS), and orogenic Au deposits (Brown et al. 2011a).

Through the study of fossil and modern orogens, and the use of geodynamic models (e.g. Afonso & Zlotnik 2011; Boutelier & Chemenda 2011; also see Gerya 2011), it is evident that there is not a paradigm that uniquely defines arc-continent collision (reviewed in Brown et al. 2011a). Natural complexities in key first order parameters such as the nature of the margin (e.g. shape, thickness, presence of reentrants, hydration, composition) and arc-trench complex (e.g. shape of trench, arc thickness, nature of the arc basement, hydration, composition), results in considerable variation between orogens (references in Brown et al. 2011a; see Fig. 1.1). Furthermore, a range of vectors and convergence rates are possible (e.g. 2cm/yr in Lesser Antilles arc to 24cm/yr in N Tonga arc). Arc and ophiolite complexes may be obducted (e.g. Lushs Bight, Bay of Islands: van Staal et al. 2007) or underplated to continental margins (e.g. Annieopsquotch Accretionary Tract: Zagorevski et al. 2009a) depending on their relative age at the time of accretion and tectonic position (e.g. Stern 2004). Forearcs

may be preserved or completely lost due to the location of failures in the overriding plate, which are determined by sites of lithospheric weakness (Boutelier & Chemenda 2011). Suprasubduction zone ophiolites (Pearce et al. 1984b) can form in a wide variety of tectonic environments and be preserved by various mechanisms (e.g. Stern 2004; Dewey & Casey 2011; Gerya 2011; discussed below). Modern subduction systems and therefore accretionary orogens can be further complicated by the presence of transform faults, oceanic plateaus, outriding microcontinental blocks and triple junctions, which bring about significant along-strike variations (van Staal et al. 1998). These along-orogen variations may result in: diachronous collision, oubduction significantly outboard of the continental margin onto microcontinental blocks (van Staal et al. 2007), arc-arc collisions (Huon-Finisterre in Solomon Sea, Halmahera-Sangihe in Molucca Sea: references in Zagorevski et al. 2008) or arc-plateau collisions (e.g. Solomon arc – Ontong Java Plateau, see Calvert 2011).

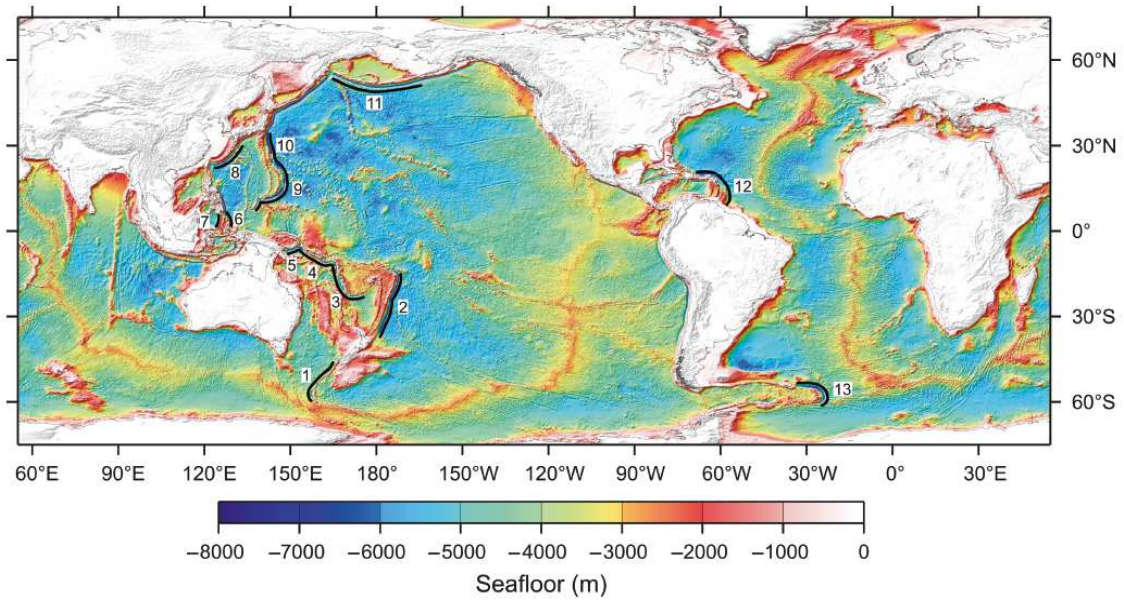

Figure 1.1. Location of modern intraoceanic subduction zones. Trenches are indicated by heavy black lines. 1, MacQuarie; 2, Tonga-Kermadec; 3, Vanuatu (New Hebrides); 4, Solomon; 5, New Britain; 6, Halmahara; 7, Sangihe; 8, Ryuku; 9 – Mariana; 10, Izu-Bonin (Ogasawara); 11, Aleutian; 12, Lesser Antilles; 13, South Sandwich. From Gerya (2011).

1.1.1 Nature of the continental margin

Some of the largest variations across and within individual orogens are due to the natural complexity of rifted margins and intraoceanic arcs. Rifted margins develop during continental breakup due to lithospheric extension, thinning and the eventual rupture of continental crust (reviewed in Reston & Manatschal 2011). Consequently, these margins become the eventual sites of continent-continent and/or arc-continent collisions, due to the closure of the ocean basins they surround. Rifted continental

margins can be broadly divided into magma-poor (i.e. 'non-volcanic') and magma-rich (i.e. 'volcanic') types, complicated by the presence of hybrid margins with characteristics of both (reviewed in Reston & Manatschal 2011). Magma-poor margins are typically c. 150-400 km wide, overlain by several km-thick sedimentary cover sequences, and often underplated by serpentinized mantle (references in Brown et al. 2011a; Reston & Manatschal 2011; Fig. 1.2). Extreme crustal thinning can occur from c. 30-35km to a few km over 100-200km, resulting in large amounts of accommodation space for sedimentary sequences to accumulate; these can in turn form the thick deforming pile of some orogens (Reston & Manatschal 2011). For example, the Dalradian Supergroup of Scotland and NW Ireland can reach a thickness of up to c. 10km at any one locality (reviewed in Daly 2009). A total cumulative thickness of c. 25km records the migration of the depocentre with time (see Anderton 1982; Daly 2009), with a depositional duration of approximately 370 Myr (c. 920-550 Ma: Daly 2009, also see Tanner & Sutherland 2007).

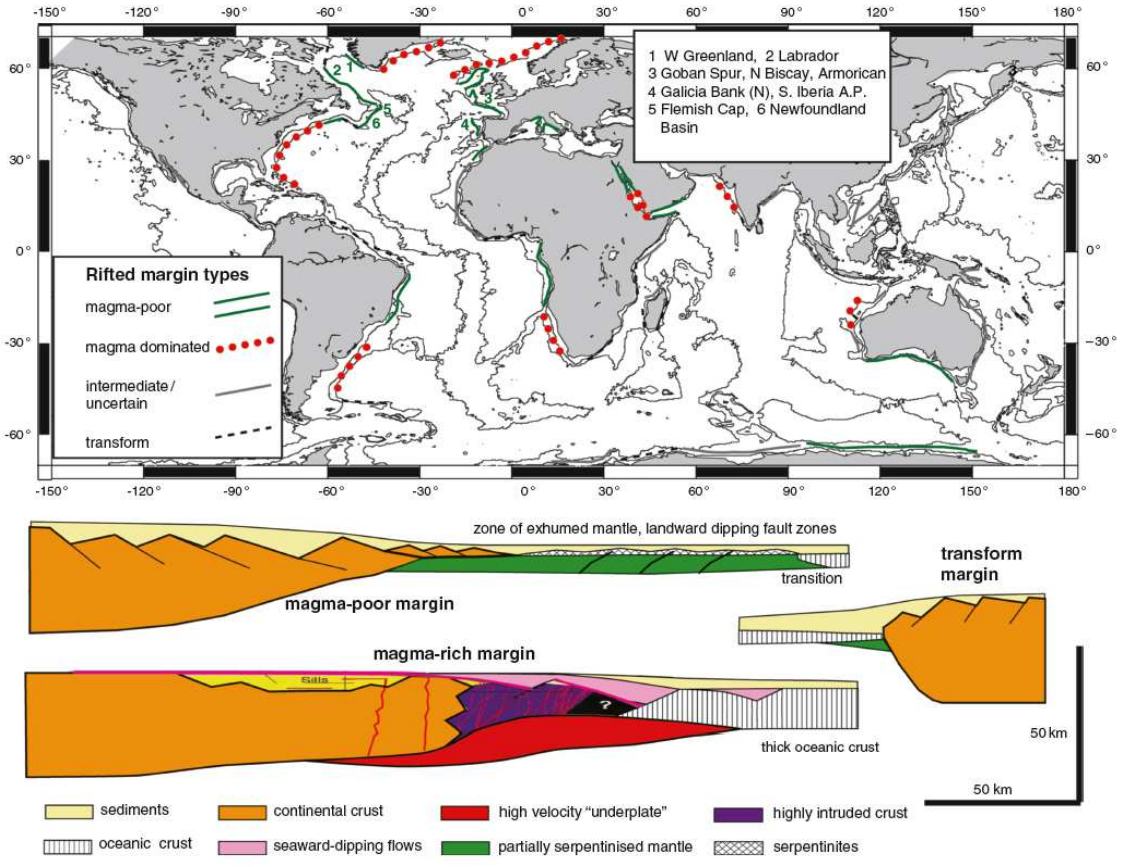

Figure 1.2. Worldwide distribution of different margin types and cartoon sections summarising the architecture of a magma-poor, magma-rich and transform margin types (from Reston & Manatschal 2011).

Magma-rich margins by contrast are much narrower, thicker, and contain substantial accumulations of subaerial basalts and intrusive sequences at or near the base of the crust (Reston & Manatschal 2011; Fig. 1.2). Total thicknesses of igneous rocks emplaced during rifting and breakup often greatly exceeds 10km (Reston & Manatschal 2011). Thick underplates commonly occur as the crust thins substantially from >>20km to <10km across distances of up to c. 50km (Reston & Manatschal 2011). Transform margins (Fig. 1.2) form a separate class of rifted margins. They exhibit little magmatism, are marked by abrupt changes in crustal thickness, and are characterized extreme strain localization (Reston & Manatschal 2011). Localized mantle serpentinization can occur due to the presence of deeply penetrating facture zones.

These differences between transform, magma-poor and magma-rich margins will directly affect their crustal composition and physical properties (e.g. geometry, rheology, density), which are intimately linked to their subductability (Afonso & Zlotnik 2011) and behaviour during orogenesis (Brown et al. 2011a). It is perhaps no surprise that magma-poor margins are more commonly preserved in fossil orogens, whereas magma-rich margins are rarely recognised. Extensional detachments that allow broad zones of mantle to be unroofed at continent-ocean transitions in magma-poor margins may act as zones where subduction initiates, and/or may be reactivated during collision (see Reston & Manatschal 2011). Transforms have also suggested as sites for the initiation of subduction, where they juxtapose oceanic plates of contrasting age and density (see Stern 2004; Gerya 2011). By contrast, large underplates and extrusions of mafic lava will increase the strength and density of magma-rich margins. Subduction is unlikely to initiate along these margins, which are more likely to form the downgoing slabs during eventual convergence (Reston & Manatschal 2011). Furthermore, thick underplates on magma-rich margins may be transformed to eclogite if the margin is partially subducted. The presence of significant quantities of eclogite would favour further subduction and the destruction of these magma-rich margins. These margins are also characterized by faster convergence velocities once they begin to subduct (see numerical models in Afonso & Zlotnik 2011). The age of the subducting slab can also vary significantly, with subduction favouring the loss of older, cold and dense oceanic crust. Although along-strike variations in the age of subducting slabs are not typically large within individual orogens (±10 Myr), through between orogens these ages can be significant (e.g. c.150 Ma Pacific Plate subducting under Mariana arc to c. 0 Ma along parts of the Solomon arc: Gerya 2011). Subducting oceanic crust attached to continental margins can also display large variations in topography (e.g. ridges, seamounts) which will also affect subduction and may

influence the chemisty of the overlying arc. Remnant slices may be preserved as ophiolites.

The presence of thick rift-related sedimentary basins (e.g. Rockall Trough, NW Irish margin) will also dictate how the arc-system reacts with the continental margin during arc-continent collision (Brown et al. 2011a). Any rift basins formed before final breakup occurred may be preserved, as the crust will be significantly weaker and a focus for deformation (see Reston & Manatschal 2011). Additional complications during orogenesis are manifested from compositional and rheological variations in continental crust along strike or with depth, and its original degree of hydration.

The rheology of continental lithosphere will directly affect its subductability and the duration of its subduction (see Afonso & Zlotnik 2011). Until a depth of c. 250-300km subducted continental crust will remain buoyant with respect to the surrounding mantle; past this point ('of no return') it becomes significantly denser, inhibiting its return to the surface (see Afonso & Zlotnik 2011). In the Banda arc system continued subduction of the passive continental margin has occurred to depths of at least 400km with no slab break-off, as viewed by tomography (references in Harris 2011). The exhumation of high- and ultra-high pressure rocks is strongly controlled by serpentinized subduction channels which form from the hydration of the overriding plate and incorporation of subducted upper oceanic crust (Gerya 2011). An array of clockwise and counter clockwise P-T paths can be produced, which may be preserved within a single mélange (see Gerya 2011).

1.1.2 Nature of the arc

Intraoceanic arcs also display significant across- and along-strike structural and compositional variation. Although some arc systems show fairly uniform compositions of upper, middle and lower crust, as derived from the inversion of seismic velocity data (see Calvert 2011; DeBari & Greene 2011), others vary considerably (see references in Gerya 2011). Arcs vary in thickness from c. 10km (e.g. parts of Izu-Bonin arc) to c. 35km (e.g. Aleutian arc) over a strike length of c. 300km (Calvert 2011), with thickness variations up to c. 25km within individual arc systems (e.g Izu-Bonin-Mariana; references in Brown et al. 2011a). Generally, thin crust is obducted or underplated depending on its composition (i.e. buoyancy relative to the passive continental margin), whereas thick arc crust may be accreted to the edge of the margin (Calvert 2011). The crustal thickness of an arc is directly related to the amount of extension it has undergone, and the addition of laterally and temporally variable magmatic additions (references in Gerya 2011). For example, the Bonin arc has been subjected to at least three episodes of extension, resulting in a 400km wide arc and forearc with

crustal thickness ranging between c. 10 and 22km (Calvert 2011). These thickness variations will dictate how the arc behaves during subsequent collision and the character of preserved crust (Calvert 2011).

Arcs subjected to little extension are likely to be characterized by relatively thick mafic middle and lower crustal sequences, which may be less susceptible to obduction (Calvert 2011). If there has been substantial intra-arc rifting and basin development (e.g. Annieopsquotch Accretionary Tract: Zagorevski et al. 2009a), arc-splitting may occur, resulting in the formation of new oceanic crust at a spreading centre (e.g. Mariana arc: references in Brown et al. 2011a). Subsequent collision with a continental margin may give the impression that two distinct arcs have collided with an associated ophiolite.

These variations associated with the nature of the arc also have important implications for which parts of the overriding plate are preserved during orogenesis, as the arc area and backarc spreading centre are the weakest parts of the overriding plate subjected to compression (Boutelier & Chemenda 2011). Areas where the crust is significantly thin will be the focus for failure in the overriding plate. Results of physical modelling have demonstated that: (i) failure in the overriding plate in the arc area, along a fault zone dipping in the same direction as subduction, leads to subduction of the forearc block (e.g. Taiwan); (ii) failure in the arc or backarc spreading centre, along a continent-dipping fault zone, can lead to subduction reversal (e.g. Grampian orogeny); and (iii) failure in the backarc towards the ocean will lead to the loss of the entire arc plate (models described in Boutelier & Chemenda 2011). This last scenario was suggested to explain the emplacement of the young Oman ophiolite onto the Arabian continental lithosphere associated with the loss of an immature volcanic arc (see Boutelier & Chemenda 2011).

Variations in arc rifting occur due to plate tectonic configurations (e.g. presence of propagating rifts, triple junctions etc.) and the density of the downgoing slab (e.g. slab rollback). Most modern oceanic subduction systems are characrterised by backarc rifts (with the notable exceptions of the Aleutian and Solomon arcs; Gerya 2011). Well-organized seafloor spreading occurs normally at least over part of the length of the backarc, due to the action of slab-pull (Gerya 2011). Backarc rifting typically preceeds slab break-off, which occurs after the length of subducted slab reaches a critical value (Boutelier & Chemenda 2011). Plate configurations may also influence whether the arc system is dominated by slab rollback or 'forward subduction'. Numerical modelling has demonstrated that "when both the arc and continental plate are free to move (e.g. bounded by mid-ocean ridges), the system evolves as 'forward subduction', rather than

by slab rollback" (i.e. it is free to 'slide'; see Afonso & Zlotnik 2011). This system favour a circulation pattern typical of corner flow in the mantle wedge and the continuous replenishment of fertile hot mantle, favouring larger degrees of melting (Afonso & Zlotnik 2011). The composition of the basement on which the arc is built (e.g. oceanic crust or a fragment of continental crust) will also directly influence how the arc behaves prior to and during arc-continent collision (e.g. its buoyancy; Brown et al. 2011a). The prearc basement of modern intraoceanic arcs are extremely variable and include those built on oceanic crust formed at backarc spreading centres, earlier intraoceanic arcs, accretionary complexes and oceanic plateaus; only the Aleutian arc is built on 'normal ocean crust' (Gerya 2011). Other arc systems may be partially founded on fragments of microcontinental crust (e.g. Ordovician Buchans-Robert's Arm arc: Zagorevski et al. 2009a).

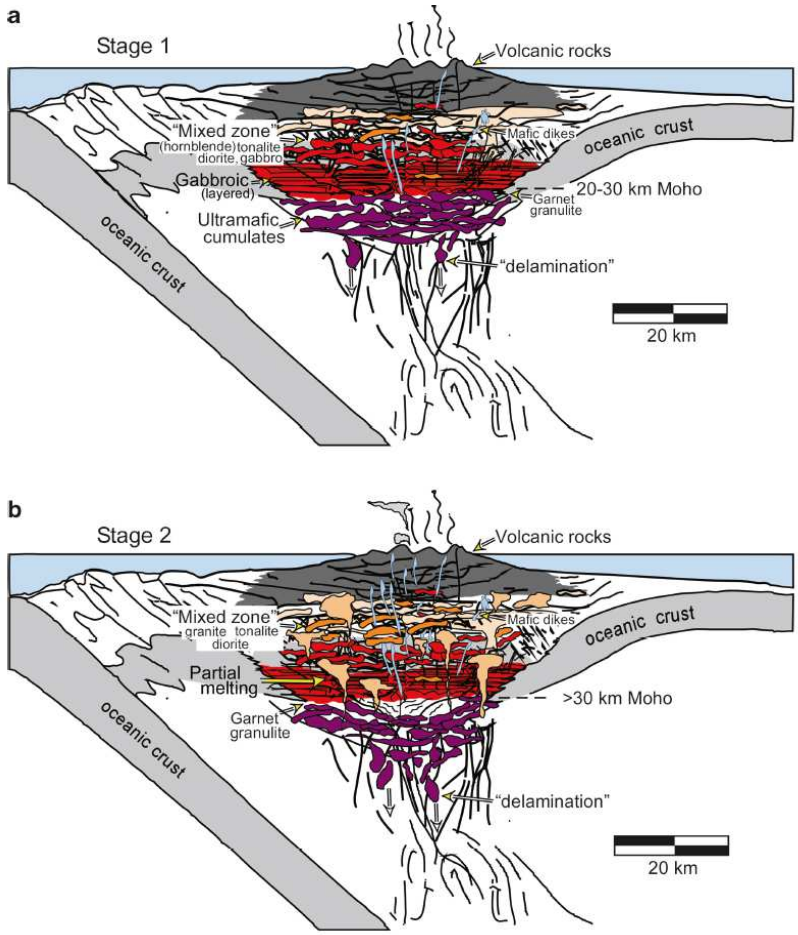

Figure 1.3. Evolution of an arc associated with arc-continent collision. (a) During stage 1 the arc is dominated by crystal fractionation and mingling/mixing processes with arc crust generally <30km thick during early arc development. (b) During stage two the arc has thickened by contraction possibly during collision with another terrane. Crustal melting can be extensive.

Note the presence of abundant partial melting and the emplacement of large bodies of granite, tonalite and diorite during contraction. From DeBari & Greene (2011).

Arcs may also vary from extensional (e.g. Tonga) with associated spreading, to neutral or mildly compressional (e.g. Aleutian arc), to strongly compressional in the case of the Solomon arc (which is in collision with the Ontong Java Plateau; Calvert 2011). These variations may occur with time and/or along strike. The geochemical character of the arc will change as it approaches the continental margin (e.g. due to sediment input: Draut et al. 2004), and undergoes compression (see Fig 1.3). Significant along strike compositional and thickness variations can result if the arc varies in age (i.e degree of evolution) before collision. Forearcs may also vary in width, thickness (9-16km over 50km), composition, structure and rheology depending on whether they are accretionary in nature or are undergoing tectonic erosion (Brown et al. 2011a). Most modern arcs are currently not accreting sediments, with the notable exceptions of the Lesser Antilles and Aleutian arcs (Gerya 2011).

1.2 From subduction initiation to final accretion

It appears that no single paradigm explains the variety of arc-continent collision, with an astonishing amount of variation in these natural systems, which will affect the way the orogen develops. The next section describes the variety of ophiolites preserved in the rock record, the tectonic scenarios which lead to the inception of subduction, and ophiolite formation/preservation, and briefly, the duration of orogenesis.

1.2.1 The inception of subduction and ophiolite formation

Ophiolites represent fragments of upper mantle and oceanic crust accreted to continental margins during continent-continent and arc-continent collisions, ridge-trench interactions and/or subduction-accretion events (references in Dilek & Furnes 2011). Although widespread in orogens, ophiolites are often intermittent both across- and along-strike, and along rifted continental margins (Dewey & Casey 2011). The following nine suites were termed ophiolites by Dewey (2003), with the tectonic setting in which they form directly controlling their characteristics and ultimately their states of preservation (simplified from Dewey & Casey 2011, references therein):

(i) Oceanic crust and mantle of intra-arc/backarcs (e.g. Leka ophiolite, Norweigan Caledonides). Backarc ophiolites are typically difficult to obduct and are frequently dismembered (e.g. Stern 2004).

(ii) Narrow Red Sea type oceans.

(iii) Narrow pull-apart oceans, in transtensional segments of major strike-slip faults (e.g. Cayman Trough, Gulf of California).

(iv) Alpine-type; subcontinental mantle pulled up beneath continental extensional detachments at rifted margins (e.g. Galician margin). These ophiolites will lack a sheeted dyke complex, and have an association of lherzolite intruded by gabbro and dolerite with pillow basalt.

(v) Oceanic crust and mantle clipped as thin sheets from ocean ridge crests where they enter subduction zones at RTT (ridge-trench-trench) triple junctions (e.g. Nicoya Complex, S Costa Rica).

(vi) Transforms exactly at continental margins that uplift MORB thin crust (e.g. E Oman).

(vii) Steady-state diachonous conversion from ridge to trench or tranpressive transform (e.g. Macquarie Ridge, Macquarie Island between New Zealand and Antarctica).

(viii) Mafic and ultramafic rock suites scraped and clipped off subducting plates from seamounts, oceanic plateaus and fracture zones (e.g. South Connemara Group, w. Ireland).

(ix) Large flat obducted slabs with the full 'Penrose sequence', up to 12km thick (e.g. Bay of Islands, Semail). These rocks are characterized by the following association from base to top: harzburgite, dunite, layered gabbro, isotropic or weakly layered gabbro with trondhjemites at the top, mafic sheeted dyke complex, pillow basalt and sediment. Possible models for the origin of these 'Penrose' ophiolites are discussed in Dewey & Casey (2011). They concluded that they are generated in the forearcs of oceanic island arcs, "where an arc-normal and arc-cutting spreading ridge joined a trench at an RTT (ridge-trench-trench) triple junction". The RTT triple junction results from the conversion of a ridge/transform/ridge system into a subduction zone, which providing the polarity is constant will lead to two RTT triple junctions forming. Ophiolite formation will occur at the ridge site on the upperplate, whereas the ridge on the lower plate is progressively subducted (see Dewey & Casey 2011).

It is clear from the above summary that ophiolites can form in a variety of tectonic settings, with classic 'Penrose-type' large ophiolite slabs (e.g. Shetland ophiolite, Bay of Islands ophiolite) prosposed to form in forearc settings. The well preserved nature of these ophiolites is directly attributable to their formation in forearc settings as they will be easily obducted during arc-continent collision (see Stern 2004). Other types of ophiolite which form in different tectonic settings are more dismembered and/or fragmental, and may be scraped or clipped off ridges, seamounts and plateaus of downgoing slabs, or form in backarc basins (which are more difficult to obduct; Stern 2004).

Although it is clear how most types of ophiolite form/are preserved, there is still debate about how subduction zones are initiated. One method proposed by Dewey & Casey (2011) has already been discussed (=change of a transform/fracture zone into a trench). Countless other mechanisms have been proposed over the last four decades. These include, but are not limited to (from review of Gerya 2011, references therein):

(i) Plate rupture within an oceanic plate or at a passive margin
(ii) Reversal of the polarity of an existing subduction zone
(iii) Sediment or other topographic loading at continental/arc margins
(iv) Forced convergence at oceanic fracture zones
(v) Spontaneous initiation of retreating subduction at oceanic fracture zones/transforms separating plates of contrasting age;
(vi) Tensile decoupling of the continental and oceanic lithosphere due to rifting
(vii) Rayleigh-Taylor instability due to a lateral compositional buoyancy contrast within the lithosphere
(viii) Addition of water into the lithosphere
(ix) Spontaneous thrusting of the buoyant continental/arc crust over the oceanic plate
(x) Small-scale convection in the sub-lithospheric mantle
(xi) Interaction of thermal-chemical plumes with the lithosphere

Recently, Stern (2004) has suggested there are two main types of subduction initiation: induced and spontaneous. Induced subduction can occur following the jamming of a previously active subduction zone by buoyant crust (e.g. arc, microcontinental block, oceanic plateau). This may lead to either transference (e.g. Indo-Asian collision, references in Stern 2004) or subduction reversal (e.g. Grampian orogeny: Dewey 2005). Transference results in the new subduction zone forming outboard of the previous one. Polarity reversal leads to the new subduction zone forming behind the magmatic arc (Fig. 1.4). Both of these processes are characterized by strong compression and uplift. The exact locations of the new trench will depend heavily on preexisting lithospheric weaknesses and fracture zone orientations.

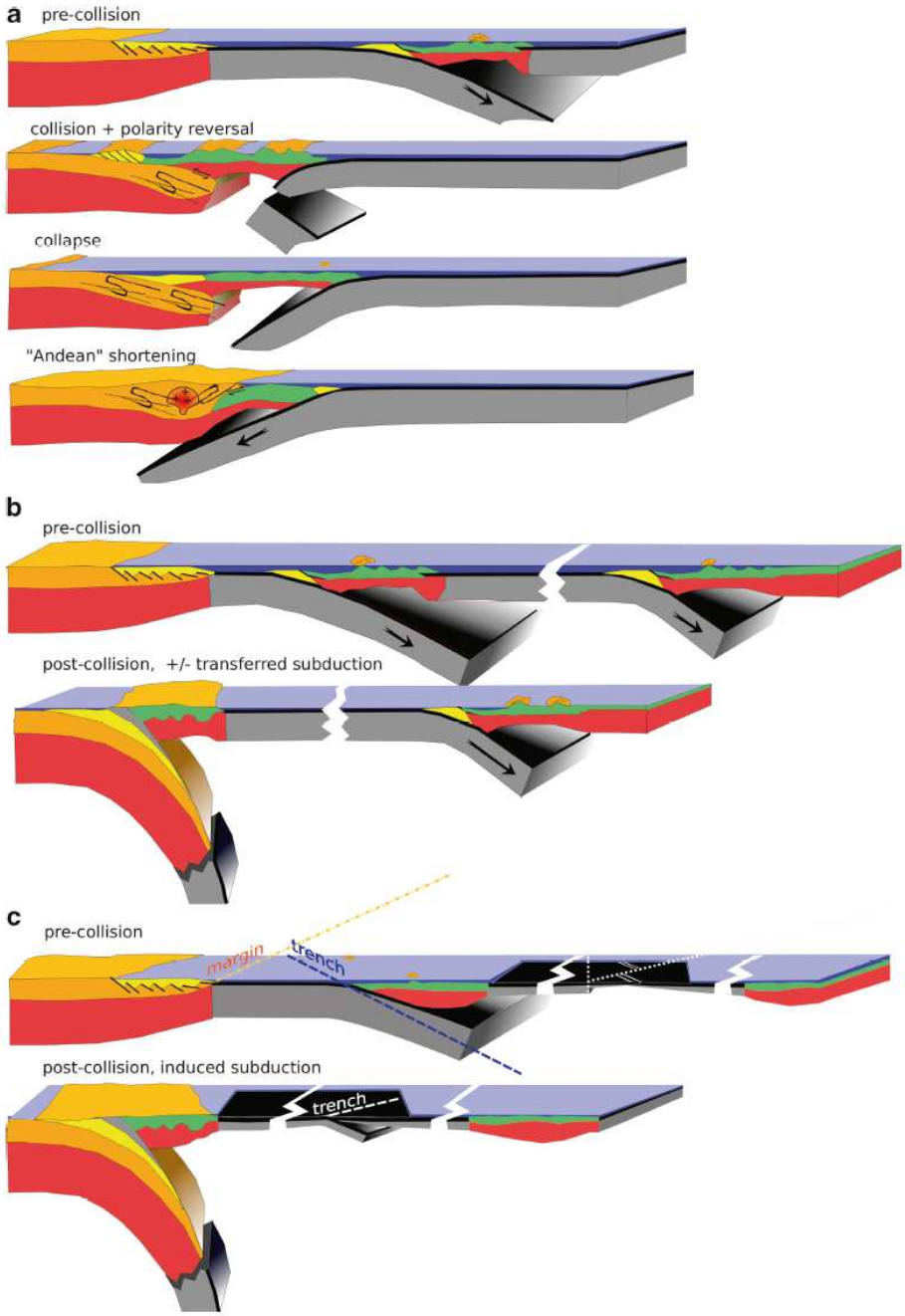

Figure 1.4. Tectonic models for arc-continent collision and subsequent processes (from Brown et al. 2011a). (a) Collision is followed by a subduction reversal (induced reversal of Stern 2004), which is followed by collapse and an Andean shortening phase (e.g. western Ireland: Grampian orogeny; Dewey 2005; Ryan & Dewey 2011). (b) Collision is followed by continued subduction outboard of the continental margin. This may occur by transference or by a preexisting subduction zone (e.g. Urals; Brown et al. 2011b). (c) Collision is followed by induced subduction if the collision is oblique. Transforms within the backarc will be subparallel to the convergence zone resulting in induced subduction. The sense of subduction will depend on the relative offset of the transform.

Spontaneous subduction results from the instability of old lithosphere compared to its underlying mantle (Stern 2004; Gerya 2011; Fig. 1.4). This may occur at transform/fracture zones (e.g. Dewey & Casey 2011), or a passive continental/arc margin. Unlike induced subduction initiation, this process begins with rifting and seafloor spreading (Stern 2004). The rock record should therefore allow discrimination between spontaneous and induced processes in fossil orogens. Key differences between magma-rich and magma-poor margins may explain reasons why some old continental passive margins have not formed subduction zones (e.g. magma-rich margins off eastern N America; Fig 1.2).

1.2.2 Duration of arc-continent collision:

In Brown et al.'s (2011a) summary of arc-continent collision (Fig 1.5), it is clear that despite the complexities outlined, many orogens such as the Wopmay, Taconic, Grampian and Kamchatka, are similar in terms of their duration. The first sign of arc-continent collision in these fossil orogens is the arrival of sediment into the subduction zone. This has been shown to systematically affect the chemistry of the overlying arc (e.g. Draut et al. 2004). Oceanic subduction is typically short lived for approximately 12 to 20 Myr before arc-continent collision. In these orogens subduction reversal occurs c. 5 and 10 Myr after arc-continent collision begins. Subcontinental subduction then proceeds until further (unrelated) orogenesis (Fig. 1.5). Reasons for why these processes occur have already been discussed (e.g. failures in the overriding plate in the correct orientation can lead to subduction reversal; see Boutelier & Chemenda 2011). However, in other orogens, such as the South Urals (reviewed in Brown et al. 2011b), there is a prolongued period of arc-continent collision (c. 20-30 Myr), followed by subsidence and no reversal. In this instance, "...the upper plate on which the arc is built is rheologically strong and there is less work required to deform the continental margin that to induce subduction in the backarc region" (Brown et al. 2011a p. 486). A strong backarc is characteristic of one which has not undergone significant extension. Despite these differences, it is clear from Figure 1.5 that arc-continent collision appears to last between 20 to >50 My (Brown et al. 2011a), confirming the earlier hypothesis of Dewey (2005) that orogeny can be brief.

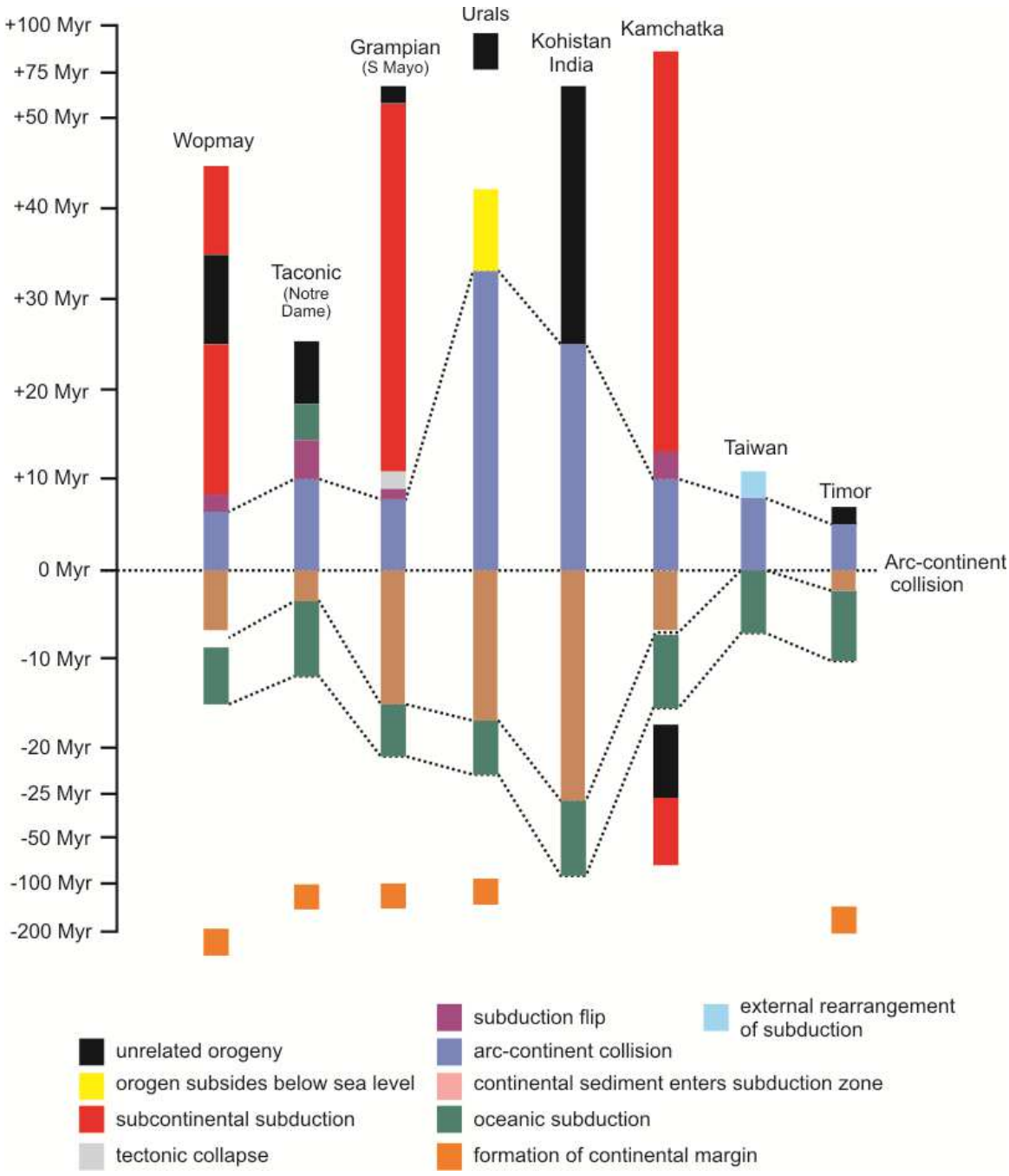

Figure 1.5. Duration of several arc-continent orogens (adapted after Brown et al. 2011a). Zero on the relative timescale represents the time of the arrival of the continental margin at the subduction zone (from Brown et al. 2011a).

1.3 Implications for mineralization

The geochemical characteristics of source magmas are an important constraint on the metal budget of different deposit types. For example, VMS deposits associated with primitive tholeiitic oceanic arcs are typically Cu, Cu-Zn or Zn-Cu rich whereas those associated with evolved calc-alkaline magmas are polymetallic (e.g. Herrington et al. 2005; Piercey 2007; see section 1.4 for detailed discussion). This is primarily due to the composition of the underlying footwall rocks from where metals are leached (e.g. Piercey 2007). Deposits which may be preserved during arc-continent collision include: (i) orthomagmatic podiform Cr deposits and extension-related Cu-rich VMS deposits in suprasubduction zone ophiolites and primitive oceanic crust; (ii) Zn-Cu rich VMS deposits in nascent or immature oceanic arcs; and (iii) porphyry Cu-Mo-Au deposits and epithermal Au-Ag deposits, and/or polymetallic VMS deposits in more evolved arcs (Herrington & Brown 2011).

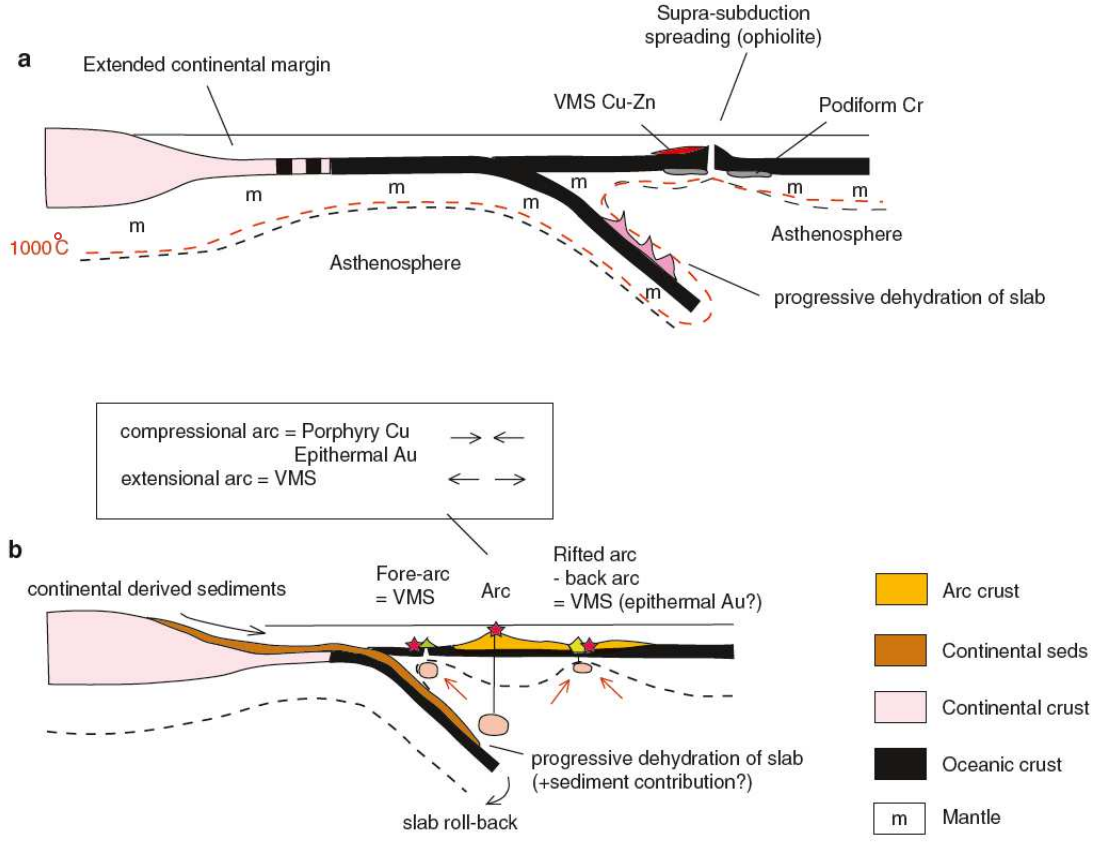

Figure 1.6. Simplified sections showing: (a) an early suprasubduction (infant arc) setting, with ophiolite formation and key related mineral deposits; (b) a maturing arc setting with fore-arc and backarc rifting and possible magma source regions. Subduction of continentally derived sediment enters the subduction channel and yields components to metasomatise the sub-arc mantle wedge. From Herrington & Brown (2011).

Dewatering of the slab and an addition of subducted sediment profoundly affects the geochemistry of associated magmas, changing their isotopic and geochemical ratios (e.g. Draut et al. 2004). This contamination from subducted sediments may be observed c. 2-5 Myr after their first subduction, although it is virtually impossible to differentiate these contaminated magmas, from those associated with mature arcs, or arcs founded on continental crust (references in Herrington & Brown 2011). Systematic changes as the arc approaches the margin (e.g. more negative εNd, more radiogenic Sr) suggests subducted sediment was directly involved (e.g. Draut et al. 2004). Au-rich VMS mineralization on Wetar, Indonesia (e.g. Scotney et al. 2005) coincides with the formation of contaminated magmas during the collisional stage, suggesting fluids released may be implicated in the formation of these mineral deposits (Herrington et al. 2011; see Chapter 7 for further discussion; Fig. 1.7c). Slowing of the subducting slab might also provide an effective way for transporting components from subducted sediment to the overlying mantle, as this would allow higher temperatures to build in the downgoing slab (Herrington & Brown 2011).

It has been recognised in many VMS camps worldwide that rift-related alkalic lavas occur in the hangingwall sequences of VMS deposits in ensialic/evolved arcs (e.g. Bathurst Mining Camp, Urals; see section 1.4; Piercey 2007). In the Urals, alkaline to shonshonitic magmas represent the culmination of volcanism in the Magnitogorsk arc, and are interbedded with sediments across the arc and onto the continental margin (i.e. they are significantly post-collisional). Their association with late Cu-Au porphyry mineralization is consistent with an increased contribution of subducted slab into the source region (references in Herrington & Brown 2011). This again highlights the importance of the source region, particularly for forming Au-rich deposits.

If subduction reversal occurs, this will result in the formation of Andean-type margins, where ensialic arc systems can contain significant Cu-Mo-Au and/or epithermal Au-Ag mineralization (Fig. 1.7c), or even VMS mineralization if the arc is extensional (Fig. 1.7d; Allen et al. 2002). Mineralization may also be preserved in the passive margin which formed prior to collision (e.g. during the original stage of continental breakup). For example, if the margin underwent significant extension (prior to arc-continent collision), SEDEX or even VMS mineralization may occur (e.g. Dalradian Supergroup – see Chapter 7; see Colman & Cooper 2000). Orogenic Au deposits form late in the evolution of arc-continent collision events (Fig. 1.7b), representing orogen-wide fluxes of thermal energy and deeply-sourced auriferous fluids in response to the thermal relaxation of geotherms (Bierlein et al. 2009).

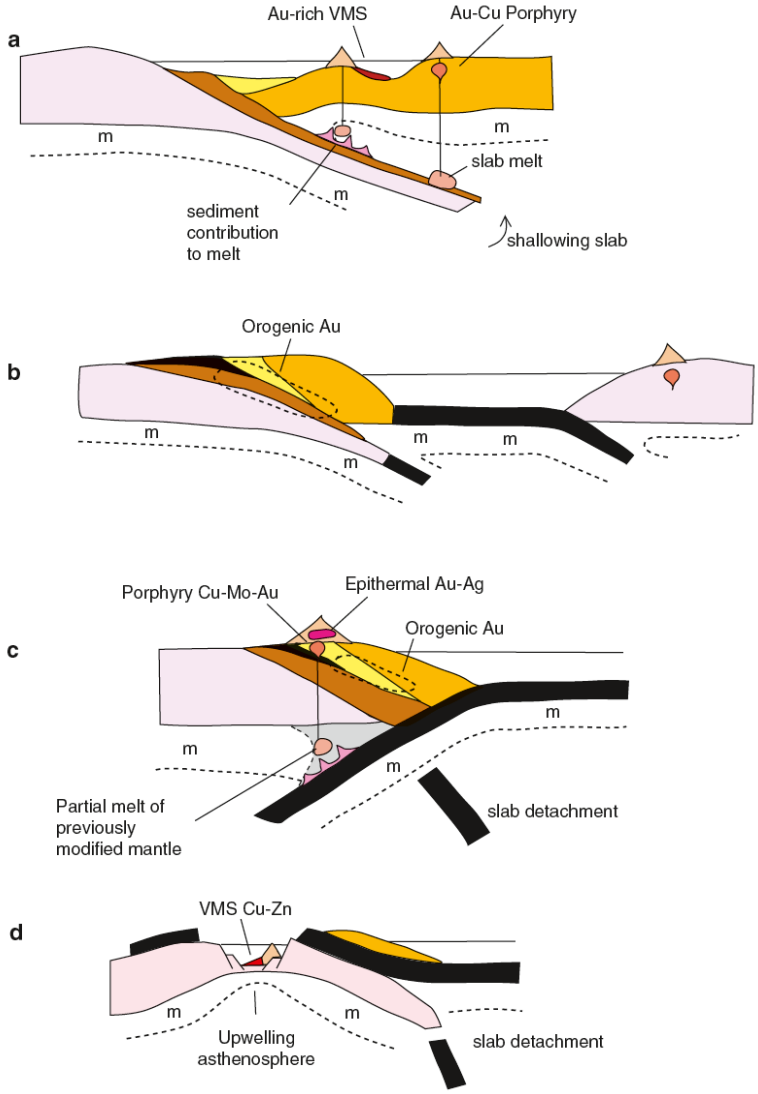

Figure 1.7. Possible scenarios which may occur during/after the arc-continent collision process with effects on mineral deposit systems. (a) Contamination of generated melts by subducted sediment may lead to Au-rich VMS. Melting of the downgoing slab may lead to Au-Cu porphyry mineralization. (b) Accretion and obduction may lead to orogenic Au mineralization. Subduction initiation outboard of the collision zone by induced transference may lead to new mineralization in a separate arc system, which may then be accreted. (c) Subduction polarity reversal may result in the metasomatism of previously modified or new subcontinental mantle leading to porphyry Cu-Au and/or epithermal Au-Ag mineralization. (d) Post-collisional extension may result in VMS mineralization.

1.4 Tectonic control on VMS mineralization

It has already been demonstrated that the natural complexity of subduction systems and continental margins can lead to large variations in orogens. Furthermore, this variation has important implications for the formation and preservation of mineral deposits. Tectonic setting directly determines the metal budgets of VMS deposits (and to some degree whether they are replacive or effusive), through host rock composition and lithofacies associations (see following).

1.4.1 VMS classification: a function of tectonic setting

Volcanogenic massive sulfide (VMS) deposits represent a major source of Zn, Cu, Pb, Ag, and Au within the Earth's crust, with some individual deposits containing significant amounts of Co, Sn, Se, Mn, Cd, In, Bi, Te, Ga, Ge, As, Sb and Hg (Galley et al. 2007a). Following the characterization of modern massive sulphide mineralization at hydrothermal vent sites (see Hannington et al. 2005), VMS deposits have been classically viewed as mound-shaped to tabular, stratiform accumulations of sulphide minerals (i.e. concordant massive lenses), underlain by discordant to semi-concordant stockworks of veins and disseminated sulphides enveloped by distinctive alteration halos (e.g. Hannington et al. 1998; Galley et al. 2007; Fig. 1.8). Deposits form through the precipitation of sulphides from metal-enriched fluids either at or near the seafloor from hydrothermal convection and mixing with ambient seawater. Heat is ultimately derived from contemporaneous volcanism (i.e. high-level subvolcanic intrusions) with fluids focused from high temperature reaction zones through synvolcanogenic faults or fissures towards the seafloor (e.g. Franklin et al. 2005; Fig. 1.9).

Over the last 30 years a number of different classification schemes have been used to characterize and explain the natural variation in VMS deposits (e.g. tonnage, grade, mineralogy, nature of alteration, effusive or replacive mineralization). These include base-metal content (e.g. Franklin et al. 1981; Large 1992; Franklin et al. 2005; Fig. 1.10), gold content (Hannington et al. 1999; Poulsen & Hannington 1995; Sillitoe et al. 1996; Mercier-Langevin et al. 2011; Fig. 1.11), geologic setting (i.e. teconic regime: Sawkins 1976) and host rock composition (Divi et al. 1979; Morton & Franklin 1987; Barrie & Hannington 1999; Herrington et al. 2005; Galley et al. 2007a; see below). As metals are ultimately leached from host rocks during hydrothermal circulation (although there may be a minor magmatic input: see de Ronde 1995; Hannington et al. 2005) the chemical composition of the host succession directly determines the metal content of the VMS deposit which forms (see discussion of Franklin et al. 2005). Irrespective of which classification scheme is used, both the metal content and host

rocks of VMS deposits are directly controlled by tectonic setting (Piercey 2007; Rogers et al. 2007).

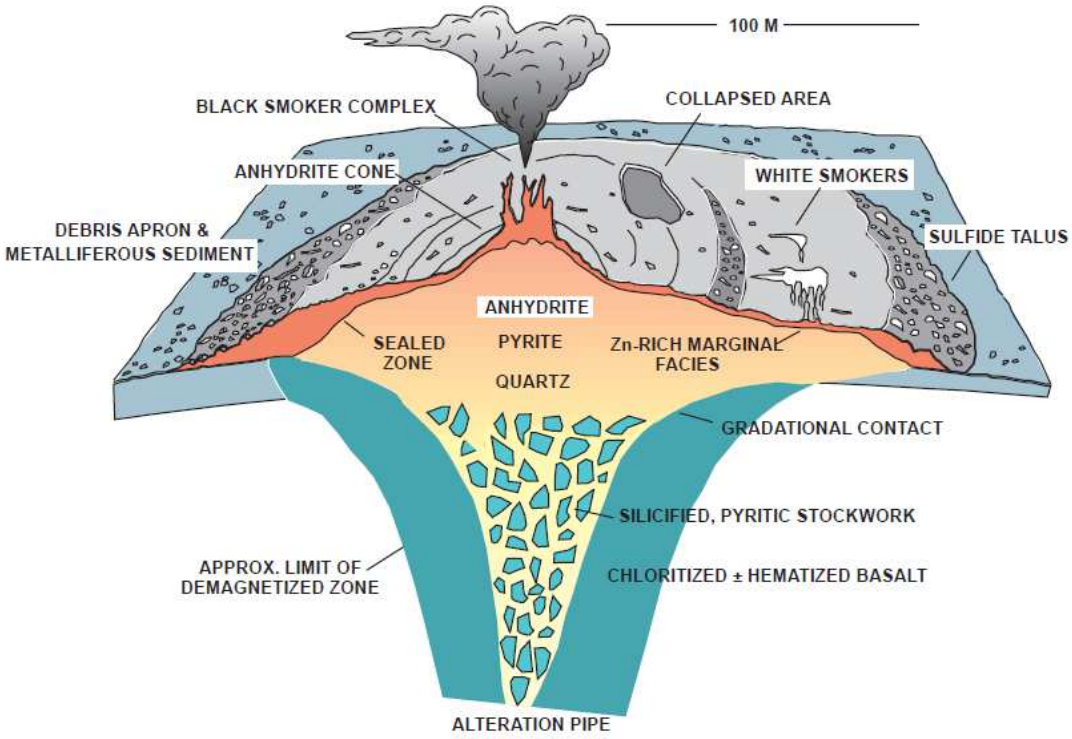

Figure 1.8. Schematic diagram of the modern TAG sulphide deposit on the Mid-Atlantic Ridge, which represents a classic cross-section of a VMS deposit (from Galley et al. 2007).

A classic example is the Urals, where the progressive evolution of the Magnitogorsk arc system, and its host stratigraphy, is reflected by an associated change in the metal ratios of preserved VMS deposits (Fig. 1.12 to 1.13). Boninitic rocks of the forearc to the Magnitogorsk arc host Cu-(Zn) and Cu-Co deposits, with the latter restricted to fragments within the main arc-continent collision suture (Herrington et al. 2005). This Cu-Co rich mineralogy is believed to reflect the ultramafic footwall source rocks (Herrington et al. 2005). Primitive arc-tholeiites host Cu or Cu-Zn deposits (e.g. Buribai deposit), which as the arc matured gave way to polymetallic Zn-Pb-Cu deposits (often Au rich) associated with calc-alkaline felsic volcanics (e.g. East Podolsk, Balta Tau) (Herrington et al. 2005). Large rifts associated with thick bimodal tholeiite sequences higher in the stratigraphy host the giant Cu-Zn deposits of Sibay, Uzelga and Uchaly, and are associated with a change of the arc-system at this time into more calc-alkalic compositions. These rocks in turn host VMS deposits such as Alexandrinka (10Mt at 5.5% Zn, 4.4% Cu, 2.2 g/t Au). In summary, an increase of felsic material (rhyolite-dacite) is associated with the replacement of Cu dominated deposits by Cu-Zn or Zn-Cu, with a switch to calc-alkaline magmatism accompanied by increasing Pb, Zn, Ba, Au and Ag.

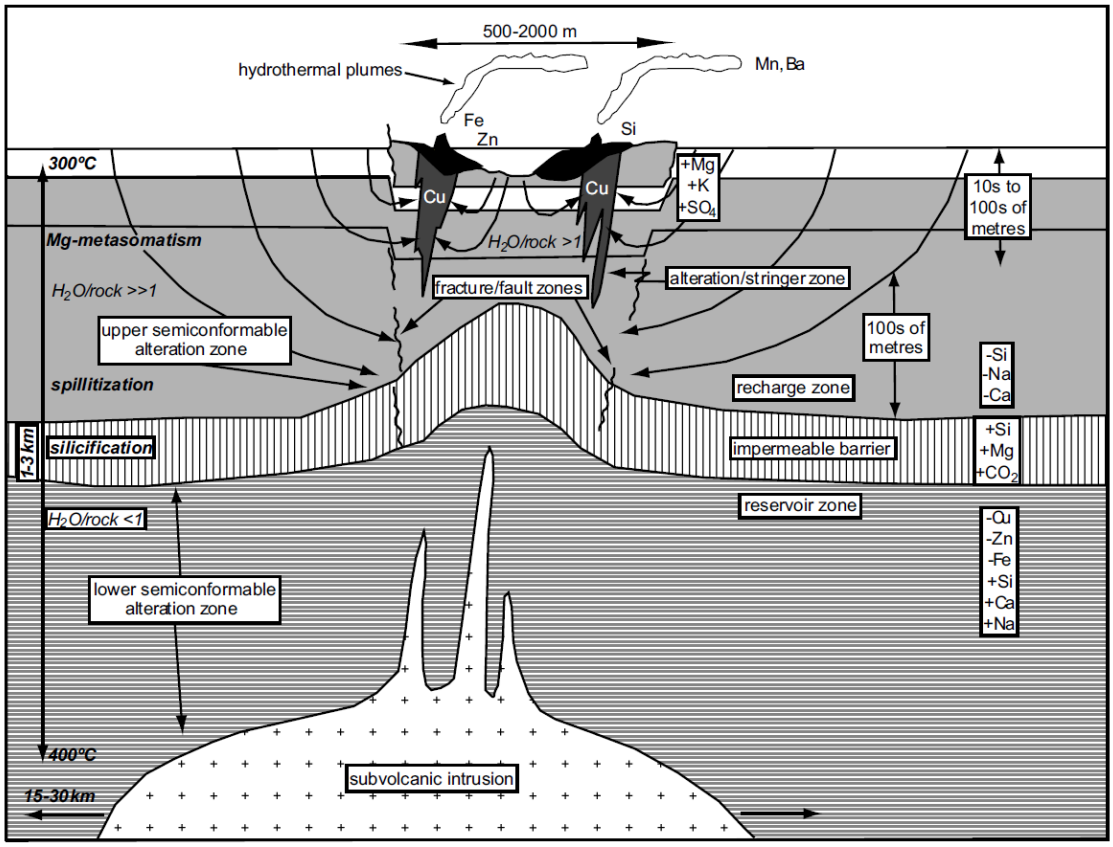

Figure 1.9. Model for the setting and genesis of VMS deposits (from Piercey 2010, after Franklin et al. 2005; Galley et al. 2007a).

1.4.2 Host-rock classification scheme: implications for metal budget

There is now general acceptance and widespread use of the host-rock classification scheme, which places VMS deposits into the following six groupings (after Barrie & Hannington 1999; Herrington et al. 2005; Franklin et al. 2005; Galley et al. 2007a; Piercey, 2010; Piercey & Hinchey 2012; see Fig. 1.14). Sequence boundaries for the following six VMS classes are defined by major-time stratigraphic breaks, faults, or major subvolcanic intrusions in their footwall sequences (see Franklin et al. 2005). Hangingwall rocks of the same time-stratigraphic sequence are also included.

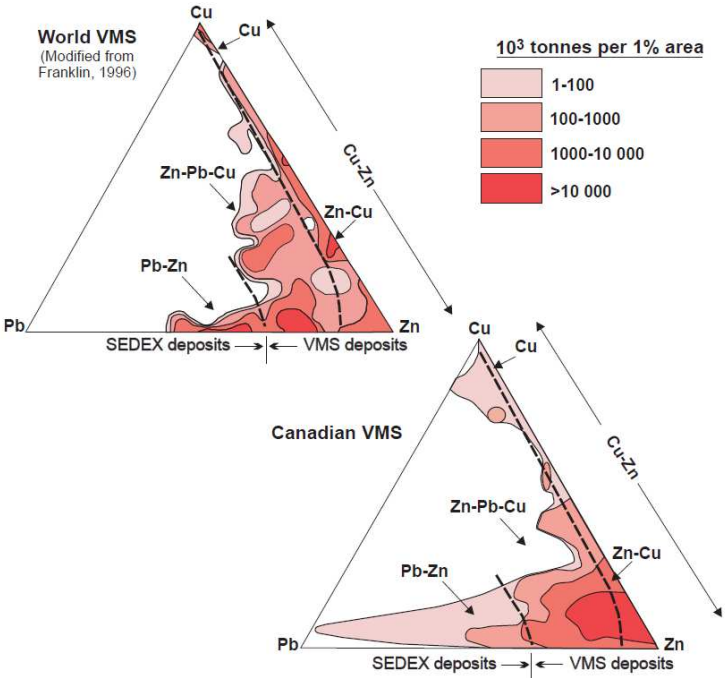

Figure 1.10. Base metal classification scheme worldwide and in Canadian VMS deposits as defined by Franklin et al. (1981) and modified by Large (1992). From Galley et al. (2007a). Canada has a larger proportion of Zn-Cu deposits due to the abundance of Precambrian primitive oceanic arcs settings. SEDEX, sedimentary exhalative mineralization.

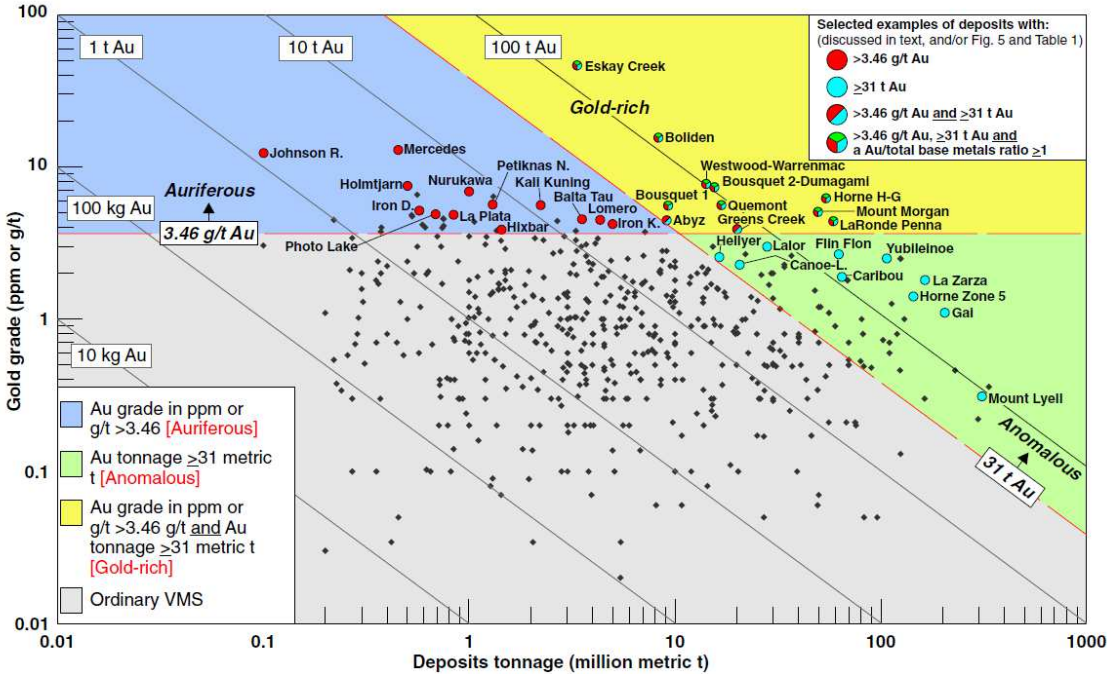

Figure 1.11. Plot of Au grade against tonnage for world VMS deposits showing boundaries for ordinary, Au-rich, anomalous and auriferous VMS deposits (from Mercier-Langevin et al. 2011).

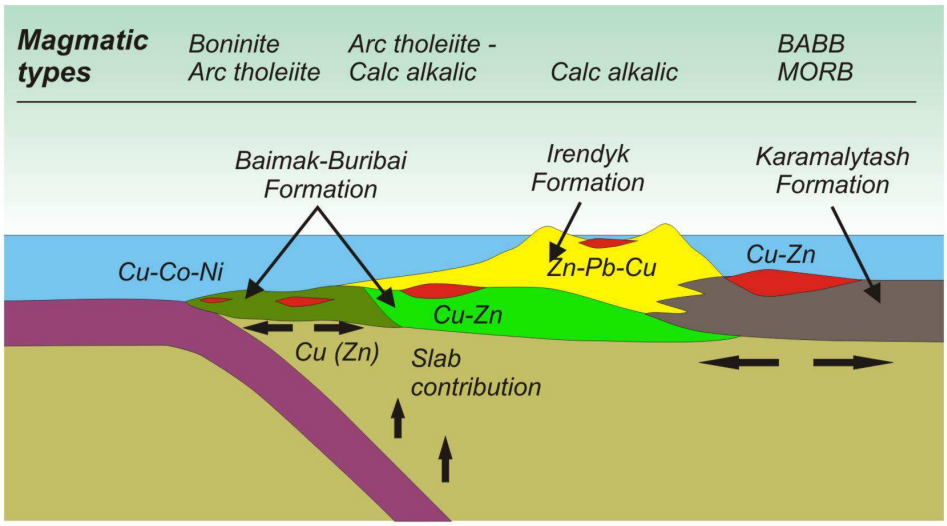

Figure 1.12. VMS deposit type in different tectonic regimes of the Magnitogorsk arc system (from Herrington et al. unpublished). Horizontal arrows indicate rifting and the upwelling of asthenosphere.

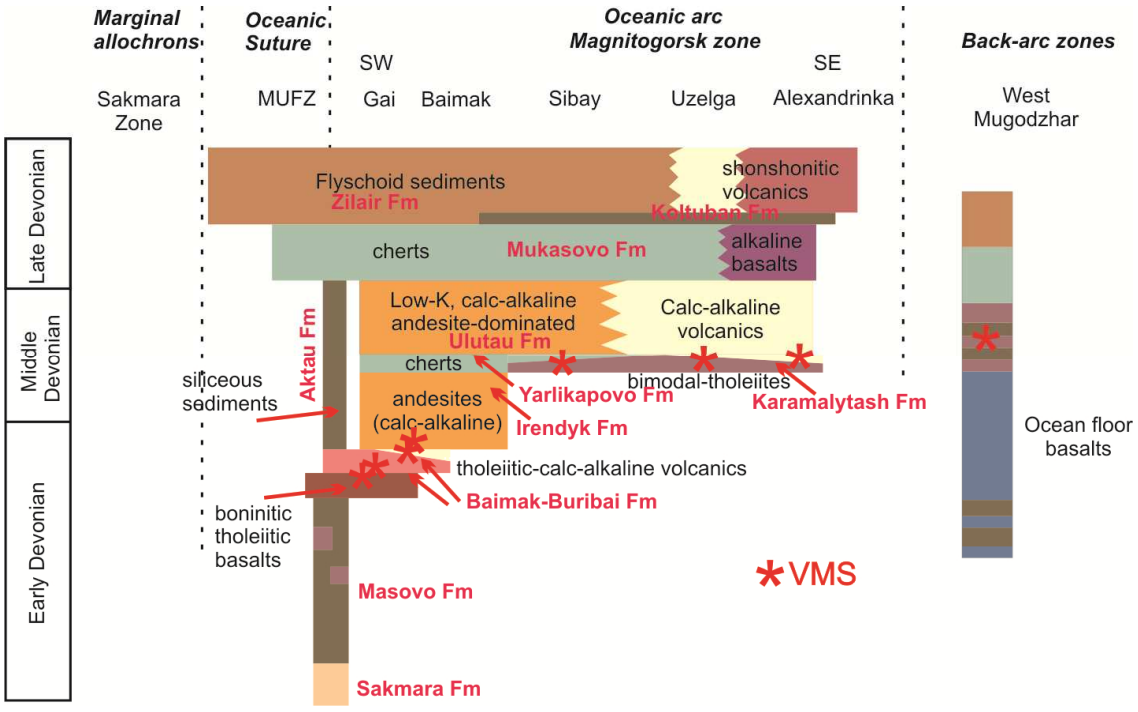

Figure 1.3 Stratigraphic correlations across the volcanic arc sequences of the Magnitogorsk and contiguous zones (after Herrington et al. 2005).

1. Mafic (=Cyprus-type) deposits occur in mafic-dominated host-rock assemblages with <10% sediment, typical of primitive oceanic backarcs and ophiolites. These VMS deposits are Cu-(Zn) rich and are typically hosted within basaltic flows or sheeted dykes. Classic examples include VMS deposits of the Cyprus and Oman ophiolites.

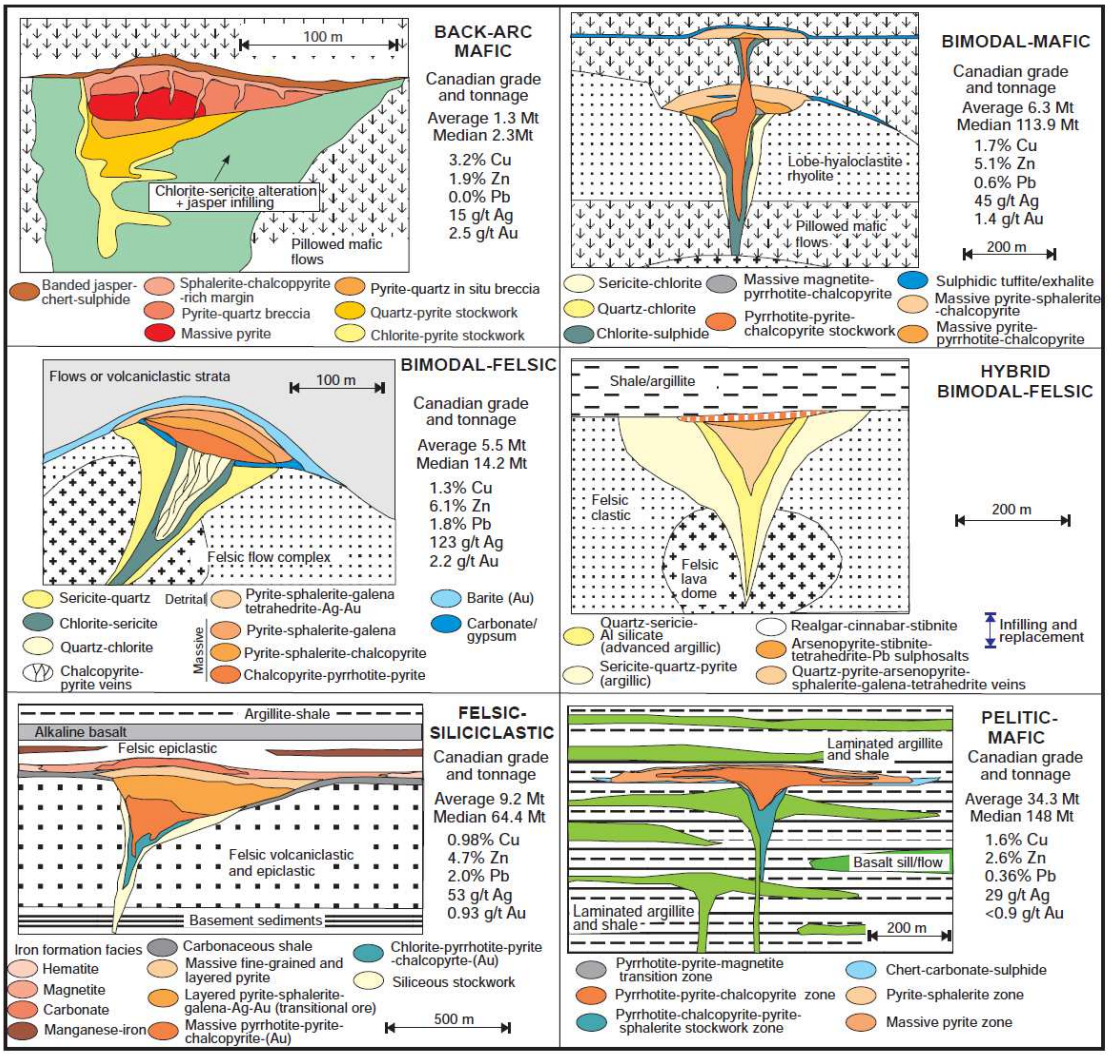

Figure 1.14. Representation of the lithological classifications modified from Barrie and Hannington (1999) by Franklin et al. (2005), with the addition of the hybrid bimodal-felsic classification. Average and median sizes are representative for Canadian deposits (from Galley et al. 2007a).

2. Mafic-siliciclastic (or mafic pelitic, =Besshi-type) deposits occur in sequences rich in sedimentary rocks interlayered with abundant basaltic intrusive and extrusive rocks typical of mature oceanic backarcs. Sedimentary rocks are often carbonaceous or turbiditic. Minor felsic rocks can occur and ultramafic rocks may be present. These VMS deposits are typically Cu-Co-Au enriched. The Besshi deposits of

Japan, Outokumpu deposits of Sweden, and Windy Craggy deposit in Canada represent classic examples. The 297 Mt Windy Craggy deposit represents a supergiant deposit (i.e. >150 Mt, Franklin et al. 2005) due to its immense tonnage.

3. Bimodal-mafic (=Noranda-type) deposits occur in mafic-dominated settings with up to 25% felsic rocks, typical of incipient-rifted suprasubduction zone oceanic arc terranes. VMS deposits are typically felsic hosted, Zn-Cu rich and often polymetallic. Classic examples include the deposits of the Noranda, Flin Flon, Snow Lake and Kidd Creek camps of Canada.

4. Bimodal-felsic (=Kuroko-type) deposits occur in felsic-dominated settings where felsic rocks occur in greater abundance than mafic rocks and only minor sedimentary rocks are present. These settings are typical of incipient-rifted suprasubduction epicontinental or evolved arcs. These VMS deposits are polymetallic (Zn-Pb-Cu-Au-Ag-Ba) and often high grade. Classic examples include the Kuroko deposits of Japan, the Skelleftea camp of Sweden, and the 'classic Buchans' deposits of the Buchans-Robert's Arm Belt Newfoundland (e.g. Lucky Strike, Oriental).

5. Felsic-siliciclastic (or bimodal siliciclastic, =Iberian Pyrite Belt-type or Bathurst-type) deposits occur in siliciclastic dominated environments with abundant felsic rocks and <10% mafic rocks, typical of mature epicontinental or evolved backarcs. These settings are often shale rich, graphitic and associated with iron formations. Volcanic rocks are typically volcaniclastic and consequently VMS deposits typically occur as replacive rather than effusive orebodies. These VMS deposits are often high tonnage and polymetallic. Classic examples include the Bathurst camp of New Brunswick (e.g. van Staal et al. 2003), Iberian Pyrite Belt (Carvalho et al. 1999) and Finlayson Lake (e.g. Piercey et al. 2001).

6. Hybrid bimodal-felsic (=Eskay Creek-type) deposits are similar to bimodal-felsic deposits but contain additional features associated with shallower water and a more hybrid nature between epithermal and VMS deposits. Deposits may include aluminous alteration, precious metal enrichments, and enrichments in the epithermal suite elements (e.g. Bi-Te-Hg-Sb-As). Classic examples include Eskay Creek and those of the Bousquet-LaRonde camp. The presence of an epithermal suite of elements may suggest a direct magmatic input (see below).

For subvolcanic intrusions to provide a direct (i.e. magmatic) source of metal to the deposit they must be emplaced at a relatively shallow levels in the crust (2 to 5km depth) (see de Ronde 1995; Hannington et al. 2005). Metals may be introduced

directly to the seafloor, mix with fluids generated during convection, or be introduced later as a superimposed component (Franklin et al. 2005). Deep penetrating faults are required if magmatic fluids and metals are to reach the seafloor intact. Evidence for a magmatic source in VMS deposits includes (references in Franklin et al. 2005):

(i) fluid inclusions with salinities greater than seawater, which may indicate the presence of magmatic fluids associated with supercritical phase separation;

(ii) differences in the composition of sea-floor vent gases (e.g. N_2, Ar, He and CO_2) reflecting their association with different magma types and associated tectonic settings;

(iii) isotope studies of O, H, S and Pb which indicate a magmatic input into the hydrothermal fluid;

(iv) anomalous trace element compositions in some VMS ores (e.g. Bi, Se, Co, high Se/S: Kidd Creek bornite zone);

(v) melt inclusions in footwall rocks which contain significant amounts of base metals (e.g. Bathurst and PACMANUS); and

(vi) Au-rich VMS deposits are characterized by enrichments in Cu, Co, Bi, Te, In and Sn and/or the presence of argillic alteration, which are comparable to high sulphidation Cu-Au deposits where metals are magmatic in origin.

1.4.3 Lithofacies association: effusive and replacive deposits

Each of these main VMS classes outlined above, based on the host rock classification scheme of Barrie & Hannington (1999) and subsequent workers, may be further subdivided into flow-, volcaniclastic- or sediment-dominated settings on the basis of the predominant VMS-hosting lithofacies (reviewed in Franklin et al. 2005). The lithofacies which host specific VMS deposits has been known to vary in many camps worldwide even when the deposits are hosted by the same petrogenetic sequence (e.g. bimodal-felsic, mafic-dominated). The following account is after Franklin et al. (2005) who provided an extensive review of the following lithofacies associations.

Flow-dominated lithofacies typically include coherent ultramafic, mafic and/or felsic lava flows and domes and their associated autoclastic deposits (autobreccia, hyaloclastite and their redeposited equivalents). Synvolcanogenic intrusives occur as dykes, sills and less often as cryptodomes (with associated peperite). Volcaniclastic and sedimentary rocks form a minor component, with the latter including carbonaceous argillite and immature wacke, minor carbonate and/or chemical sediments (e.g. exhalite: Noranda district; tuffite: Matagami district). VMS deposits associated with flow-dominated lithofacies are typically effusive rather than replacive, with many interpreted to occur within synvolcanogenic subsidence structures (e.g.

grabens and calderas: Noranda and Flin Flon districts, Canada; Sibay, Gai and Uchaly deposits, Urals).

Volcaniclastic-dominated lithofacies are characterized by a wide variety of volcaniclastic rocks with subordinate flows and domes (± autobreccia, hyaloclastite, and their redeposited equivalents), cryptodomes (associated peperite and/or fluidal breccia) and lesser synvolcanogenic dykes, and clastic sedimentary rocks (typically in the hangingwall of VMS deposits). VMS deposits within volcaniclastic-dominated lithofacies are typically replacive, due to the higher porosity of volcaniclastic sediments and possible cap rocks inhibiting hydrothermal fluids from reaching the seafloor. Most VMS deposits which formed below the seafloor occur within lithofacies dominated by volcaniclastic (either pumice- or glass-rich) and/or terrigneous clastic sedimentary rocks (wacke, sandstone, and lesser mudstone). These deposits are often sheet-like with broad diffusive alteration zones due to channelized flow along specific stratigraphic units. Carbonate units deposited at the seafloor may inhibit the upward flow of hydrothermal fluids, acting as 'chemical traps', thereby concentrating metals through the open-space filling, and dissolution and/or replacement of host-rocks.

Sedimentary-dominated lithofacies are dominated by terrigneous clastic sedimentary rocks and are composed primarily of wacke, sandstone, siltstone, mudstone and carbonaceous mudstone. Lesser amounts of chert, carbonate, marl, and iron formation can also occur. VMS deposits are spatially associated with subordinate mafic or felsic, flow or volcaniclastic horizons in these sequences. The sedimentary-dominated lithofacies can be further subdivided into a siliciclastic association (wacke, sandstone, argillite, siltstone and iron formation: e.g. Bathurst district and Iberian Pyrite Belt) and a pelitic association (argillite, carbonaceous argillite, siltstone, marl and carbonate: e.g. Windy Craggy deposit of British Columbia). VMS deposits associated with sedimentary-dominated lithofacies (i.e. mafic-siliciclastic and felsic-siliciclastic types) are typically higher tonnage than those associated with flow- or volcaniclastic-dominated lithofacies (e.g. Bathurst No. 12, Windy Craggy, Rio Tinto).

1.5 Project Rationale and subsequent chapters

The Tyrone Igneous Complex of the Midland Valley Terrane, Northern Ireland, has been a target for base metal exploration since the early 1970s. Although previous work by Riofinex and Ennex International highlighted a number of Au and Cu targets, no occurrences of any size were delineated (e.g. Leyshon & Cazalet 1978; Clifford et al. 1992; Gunn et al. 2008, unpublished Ennex International reports). The recent completion of a high-resolution airborne geophysical survey (part of the Tellus Project: Geological Survey of Northern Ireland [GSNI] 2007), new geochemical analyses and U-

Pb geochronology (carried out by the Geological Survey of Northern Ireland) has significantly improved our understanding of the geological evolution of the complex and its potential to host significant VMS mineralization.

This PhD project was set up to:

(i) investigate the evolution of Tyrone Igneous Complex and its role within the Grampian – Taconic orogeny;

(ii) assess and utilize the recent Tellus geophysical survey of Northern Ireland (Tellus Project) to better understand the regional geology of the area; and

(iii) identify specific stratigraphic horizons and target areas for further exploration through a combination of field geology, petrography, alteration-lithogeochemistry, soil geochemistry and geophysics.

The following is an outline of the subsequent chapters to this thesis:

Chapter 2: Methods

This chapter outlines all of the methods for subsequent chapters.

Chapter 3: Age and geochemistry of the Tyrone Igneous Complex

This chapter forms the basis of a published paper: Cooper, M.R., Q.G., Crowley, Hollis, S.P., Noble, S.R., Roberts, S., Chew, D., Earls, G, Herrington, R., & Merriman, R.J. (2011). *Age constraints and geochemistry of the Ordovician Tyrone Igneous Complex, Northern Ireland: Implications for the Grampian orogeny.* Journal of the Geological Society, London, v. 168, p. 837-850. This paper provides a temporal and geochemical framework for the evolution of the Tyrone Igneous Complex in the Grampian orogeny, and includes nine new high-resolution U-Pb zircon ages and a new geochemical dataset.

Chapter 4: Episodic arc-ophiolite accretion in the Grampian-Taconic orogeny

This chapter forms the basis of a published paper: Hollis, S.P., Roberts, S., Cooper, M.R., Earls, G., Herrington, R., Condon, D.J., Cooper, M.J., Archibald, S.M., & Piercey, S.J. (2012). *Episodic arc-ophiolite emplacement and the growth of continental margins: Late accretion in the Northern Irish sector of the Grampian-Taconic orogeny.* GSA Bulletin, v. 124, p. 1702-1723. This paper provides the first detailed stratigraphic and petrochemical account of the Tyrone Volcanic Group and three new U-Pb zircon ages.

Chapter 5: Evolution and emplacement of the Tyrone ophiolite

This chapter forms the basis of a submitted manuscript: Hollis, S.P., Cooper, M.R., Roberts, S., Herrington, R., Earls, G., & Condon, D.J. (Submitted). *Late obduction of the Northern Irish, Tyrone ophiolite during the Grampian-Taconic orogeny: Links to central Newfoundland?* Journal of the Geological Society, London. This manuscript provides a detailed model for the evolution of the Tyrone Plutonic Group based on a new U-Pb zircon age, field relationships, geochemistry and mineral chemical data.

Chapter 6: Timing arc evolution in the Irish Caledonides

This chapter forms the basis of a submitted manuscript: Hollis, S.P., Cooper, M.R., Roberts, S., Earls, Herrington, R., G., & Condon, D.J. (Submitted). *New stratigraphic, geochemical and U-Pb zircon constraints from Slieve Gallion, Northern Ireland: a correlation of the Irish Caledonide arcs.* Journal of the Geological Society, London. This manuscript provides a detailed stratigraphic and petrochemical study of the Slieve Gallion Inlier (part of the Tyrone Volcanic Group) and two new U-Pb zircon ages.

Chapter 7: Implications for VMS mineralization in Co. Tyrone

This chapter forms the basis of a manuscript to be submitted to Mineralium Deposita: Hollis, S.P., Roberts, Earls, G., Herrington, R., S., Cooper, M.R. & Piercey, S.J. *Petrochemistry and hydrothermal alteration within the Tyrone Arc: Targeting VMS mineralization in Northern Ireland.* This manuscript demonstrates how detailed field mapping combined with extensive petrochemistry and alteration lithogeochemistry has identified 'fairways' for VMS mineralization in Northern Ireland. Areas of interest are highlighted and suggestions are made for forthcoming exploration. This chapter presents new mineral chemical and whole rock geochemical data (ironstones and drillcore) from the Tyrone Volcanic Group.

Chapter 8: Conclusions and future work

This chapter concludes the main results of the thesis and presents a number of suggestions for further work in the Tyrone Igneous Complex and surrounding terranes.

Additional published work completed during the couse of this PhD (in collaboration with authors listed) is detailed below:

- Cooper, M.R., Crowley, Q.G., **Hollis, S.P.**, Noble, S.R. & Henney, P.J. (Submitted). A new U-Pb age constraint for a Late Caledonian intrusion suite in the north of

Ireland: Constraining the timing of slab break-off in the Grampian terrane. *Journal of the Geological Society, London.*

- Takai, K., Mottl, M.J., Nielsen, S.H.H. & **the IODP Expedition 331 Scientists.** 2012. IODP Expedition 331: Strong and Expansive Subseafloor Hydrothermal Activities in the Okinawa Trough. *Scientific Drilling*, **13**, 19-27.
- **Expedition 331 Scientists.** Integrated Ocean Drilling Program Expedition 331. Preliminary report. 1st September – 3rd October, 2010.

Chapter 2: Methods

2.1 Geological mapping and sampling

Approximately six months of fieldwork was undertaken over the Tyrone Igneous Complex during two main field seasons in spring-summer 2009 and 2010. Due to poor exposure across much of the area (<2%), geological mapping at 1:10,000 scale (on Ordnance Survey of Northern Ireland [OSNI] basemaps) was restricted to areas with significant exposure (e.g. Slieve Gallion Inlier, Tanderagee-Granagh, Crosh, Beaghbeg). Within the Tyrone Volcanic Group exposure is primarily restricted to stream sections, drainage ditches, sand and gravel pits, and quarry floors; abundant peat and thick glaciofluvial deposits obscure bedrock over much of the complex. Exceptions include areas where resistive lithologies create local topographic highs (e.g. tonalite intrusive rocks and basaltic horizons). Geo-referenced Geological Survey of Northern Ireland (GSNI) fieldsheets covering the Tyrone Igneous Complex were available prior to fieldwork. All outcrops recorded on GSNI fieldsheets in the Tyrone Volcanic Group were examined. Key exposures within the Tyrone Plutonic Group and Tyrone Central Inlier were also visited during 2010.

During 2011, doctoral studies were suspended for industry placement with Dalradian Resources Ltd. Throughout the employment period a considerable amount of time was spent prospecting in the Tyrone Volcanic Group, logging new drillcore at Cashel Rock, Tullybrick and Broughderg, and mapping areas of the volcanic succession (e.g. Formil). All the historic Ennex International drillcore available was examined, approximately 2 km in total. Half-core samples were also collected from rock types of interest to characterize the observed hydrothermal alteration.

Over 450 rock samples were collected from the Tyrone Igneous Complex, of which over 95% were from the Tyrone Volcanic Group. Samples collected were >2 kg in weight so all signs of weathering, alteration and veining could be removed and a fresh core of rock obtained. Every effort was made to collect the least altered and most representative samples from outcrop. Cut and cleaned samples were crushed for whole rock geochemical analysis using a flypress. Sheets of paper and clean plastic bags were used to minimize contact between the flypress and the sample. Samples collected during 2009 (SPH01-SPH207) were powdered using an agate ball and mill system to avoid W, Co and Ta contamination from tungsten carbide. Later samples collected during 2010 (SPH208-onwards) were powdered using a Cr-steel TEMA.

2.2 BGS whole rock geochemistry

Prior to the commencement of this PhD a numer of samples were collected from the Tyrone Igneous Complex for whole rock geochemistry. These samples were analysed at the British Geological Survey, Keyworth. Results were provided by M.R. Cooper and are presented in Chapter 3. They are distinguished from subsequent samples collected during the course of this PhD by their JTP and MRC prefixes. Major elements were determined for twenty-eight powdered whole-rock samples on fused glass beads by X-ray Fluorescence Spectrometry (XRF). Samples were dried at 105 °C before loss on ignition (LOI) and fusion. LOI was determined after 1 hour at 1050 °C. Fe_2O_3t represents total iron expressed as Fe_2O_3. SO_3 represents sulphur retained in the fused bead after fusion at 1200 °C. Trace elements were analysed on pressed powder-pellets by XRF. Rare earth elements were determined by inductively coupled plasma mass spectrometry (ICP-MS). Samples were subjected to an $HF/HClO_4/HNO_3$ attack with residues fused with NaOH before solutions were combined.

2.3 X-ray fluorescence spectrometry and LOI

Samples collected during the course of this PhD are presented in Chapters 4 to 7. Major-elements were determined for powdered whole-rock samples on fused glass beads by XRF at the University of Southampton. Trace-elements were analysed on powder-pellets by XRF. All analyses were undertaken using a Philips® MagiX-Pro 4kW Rh X-ray tube. Geochemical Reference Materials were used to construct calibrations for individual elements. Interferences created from element overlaps are accounted for by the Philips Magix-PRO software.

Before preparation of powder pellets and fusion beads, LOI was determined for three reasons: (i) heating Pt-Au crucibles in the presence of sulphides may cause damage to the metal structure of the crucible; (ii) major element totals, following the analysis of the bead, should sum to 100% providing a check on the quality of the analysis; and (iii) LOI is a useful alteration index when applied to hydrothermally altered rocks. To determine LOI, approximately 10-15g of sample powder was dried at 110°C for ~6 hours to remove any atmospheric water absorbed. Following cooling in a dessicator, LOI was determined using fused ceramic crucibles:

$$LOI = 100 \times (Y - Z) / (Y - X)$$

where: X = crucible weight; Y = weight of crucible plus sample prior to ignition; Z = weight of crucible plus sample after ignition at 950°C for ~6 hours.

Fusion beads were created using a mixture of 0.5g di-lithium tetraborate flux and 5g of homogenized rock powder. The mixture was heated on a gas burner until a homogonous melt was produced, which was then cooled on a Pt-Au dish. Pressed power pellets were made by mixing ~10g of powder with 8-12 drops of polyvinyl acetate (PVA) glue. The exact amount required was dependent on rock type and the abundance of clay minerals.

2.3.1 Data quality, precision & accuracy

As previously stated, major element totals following LOI should sum to 100% since the sample:flux ratio will not change when calcined material is used. Of 100 samples analysed from the Tyrone Volcanic Group (Chapter 4), major element sums ranged between 97.45 and 102.92 wt.%, with 69% between 98 and 101 wt.%. An average of 100.13 wt.% was produced for the dataset with a standard deviation of 1.37.

To further determine the quality of the data obtained, precision and accuracy of the dataset was determined for each element. Precision was determined by duplicate analysis of three SPH-prefixed samples (SPH13 rhyolite, SPH29 basalt, SPH47 granodiorite) and a range of international reference materials. Precision is presented as %RSD (percent relative standard deviation) in Table 2.1, using:

$$\% \text{ RSD} = 100\% \times S_i / \mu_i$$

where: μ_i = mean value of element i over a series of analytical runs; S_i = standard deviation of the mean from the series of analytical runs for element i

As a general rule (Jenner 1996):

% RSD 0-3% = excellent precision; 3-7% = very good precision; 7-10% good precision, >10% poor precision.

Accuracy was determined using a range of international reference materials and is presented as %RD (percent relative difference) in Table 2.2, using:

$$\% \text{ RD} = 100\% \times (\mu_i - \text{STD}_i) / \text{STD}_i$$

where: μ_i = mean value of element i over a series of analytical runs; STD_i = known or certified value of element I in the standard or reference material.

As a general rule (Jenner 1996):

% RD = ± 0-3% = excellent accuracy; ±3-7% = very good accuracy; ±7-10% = good accuracy, ±>10% = poor accuracy.

Detection limits for major elements were 0.05 wt%. Detection limits for trace elements were: 10ppm = Ba & Ce; 5ppm = V, Co & Sc; 4ppm = La; 3ppm = Pb; 2ppm = Cr, Ni, Cu,

Zn, Ga, Zr, Y & Nb; 1ppm = Rb & Sr. Results below detection were assigned values of 0.5x their detection limit. The limit of determination is the concentration that has a quantifiable error associated with it and is set at 3 times the detection limit. Data below determination limits are associated with large errors.

Element	JB1A Basalt M=2 T=6	BEN Basalt M=2 T=7	SPH29 Basalt M=5 T=10 Sc=4	JA1 Andesite M=1 T=6	JG3 Granodiorite M=2 T=5	SPH47 Granodiorite M=6 T=11 Sc=4	JR1 Rhyolite M=2 T=0	JR2 Rhyolite M=0 T=5	SPH13 Rhyolite M=7 T=11 Sc=4	JG1A Granite M=5 T=5
SiO_2	0.13	1.74	1.07	No Rep.	0.32	0.56	0.09	Not An.	0.36	0.21
TiO_2	2.19	6.29	2.01	No Rep.	0.04	3.45	5.38	Not An.	3.84	2.69
Al_2O_3	0.16	4.61	1.60	No Rep.	0.99	4.31	0.76	Not An.	3.53	0.67
Fe_2O_{3T}	0.66	7.83	0.81	No Rep.	0.15	0.67	2.1	Not An.	2.74	1.79
Mn_3O_4	2.59	**11.05**	1.62	No Rep.	1.40	4.64	1.11	Not An.	1.62	1.75
MgO	1.18	**17.11**	1.09	No Rep.	0.87	1.48	**10.73**	Not An.	1.90	2.71
CaO	0.36	**10.22**	4.32	No Rep.	0.25	2.82	0.81	Not An.	2.60	0.65
Na_2O	5.07	6.22	7.03	No Rep.	0.67	2.34	0.89	Not An.	2.24	3.76
K_2O	3.79	1.48	1.33	No Rep.	0.00	2.48	0.77	Not An.	3.49	1.52
P_2O_5	4.70	6.29	3.46	No Rep.	3.03	5.04	4.68	Not An.	8.05	4.48
Sc	Not An.	Not An.	3.35	Not An.	Not An.	**13.13**	Not An.	Not An.	7.27	Not An.
V	1.05	1.77	3.54	0.19	1.68	1.74	Not An.	B. Det	1.06	2.17
Cr	0.30	1.30	3.88	7.60	2.08	**18.89**	Not An.	**11.16**	**19.62**	1.71
Co	**29.36**	**45.10**	**37.95**	**39.23**	2.22	**45.36**	Not An.	B. Det	**49.56**	3.54
Ni	0.92	0.57	9.01	B. Det	3.02	**53.58**	Not An.	**11.42**	**47.15**	6.70
Cu	1.71	1.68	3.84	2.30	6.20	**14.58**	Not An.	B. Det	3.60	5.90
Zn	0.58	0.58	0.88	0.53	0.31	3.62	Not An.	1.26	1.88	0.82
Ga	4.16	2.62	2.28	2.34	0.56	1.94	Not An.	2.62	2.91	0.84
Rb	3.79	2.35	**22.43**	**10.02**	2.37	1.65	Not An.	1.85	3.44	0.37
Sr	1.03	0.59	1.51	0.25	1.36	0.87	Not An.	2.60	1.98	0.25
Zr	0.64	2.52	1.13	1.37	0.86	0.75	Not An.	0.51	2.18	0.88
Ba	1.62	2.48	7.75	2.95	3.36	2.33	Not An.	B. Det	2.66	2.08
Pb	B. Det	B. Det	B. Det	B. Det	5.96	**21.66**	Not An.	3.05	**10.62**	1.68
Y	4.32	4.42	3.92	4.02	7.12	6.59	Not An.	0.92	6.69	3.89
Nb	0.38	0.45	2.79	B. Det	1.50	3.07	Not An.	1.12	4.69	1.61
La	9.00	6.21	B. Det	B. Det	**25.98**	**11.03**	Not An.	**22.56**	**18.51**	**19.54**
Ce	**11.15**	6.74	9.07	B. Det	B. Det	**12.58**	Not An.	**10.93**	**21.74**	**18.71**
Th	5.03	4.49	B. Det	B. Det	5.81	4.38	Not An.	3.79	9.38	6.31

Table 2.1. Precision for XRF data (%RSD). B. Det, below determination limit; Not An, not analysed; No Rep, no repeats. M and T refer to number of repeats for major and trace elements respectively. Bold values reflect poor precision after Jenner (1996).

Element	JB1A Basalt M=2 T=6	BEN Basalt M=2 T=7	JA1 Andesite M=1 T=6	JG3 Granodiorite M=2 T=5	JR1 Rhyolite M=3 T=1	JR2 Rhyolite M=0 T=5	JG1A Granite M=5 T=5
SiO_2	0.73	0.01	0.79	-0.08	0.11	Not An.	0.40
TiO_2	-1.39	-4.72	-4.27	-3.04	-8.72	Not An.	-5.43
Al_2O_3	0.12	1.40	-1.56	0.36	-0.24	Not An.	-1.39
Fe_2O_{3T}	-2.06	-5.48	-2.17	0.21	-4.82	Not An.	-2.92
Mn_3O_4	-0.38	-7.61	0.75	1.58	-0.15	Not An.	6.04
MgO	-1.83	**12.27**	-1.66	-0.44	**38.16**	Not An.	1.66
CaO	-0.32	-6.21	-0.07	1.86	2.14	Not An.	-0.88
Na_2O	-1.18	3.91	-0.98	-1.16	-0.83	Not An.	-1.23
K_2O	1.08	-7.73	0.30	-0.65	-0.62	Not An.	0.56
P_2O_5	-1.65	-6.62	-6.19	8.60	-8.97	Not An.	3.83
Sc	Not An.	Not An.	Not An.	Not An.	Not An.	Not An.	Not An.
V	-2.92	**13.08**	4.94	7.65	Not An.	B. Det	**36.65**
Cr	-1.12	9.52	**146.35**	**218.13**	Not An.	**343.1**	**304.09**
Co	**163.82**	**107.19**	**445.00**	**251.11**	Not An.	B. Det	**315.59**
Ni	-6.89	3.41	B. Det	**24.2**	Not An.	**692.9**	**54.56**
Cu	-2.41	9.37	-0.73	**75.92**	Not An.	B. Det	**308.38**
Zn	-5.75	3.14	-3.63	-7.40	Not An.	-8.60	-9.92
Ga	1.39	3.78	-1.05	-6.20	Not An.	-8.13	-3.39
Rb	**-21.8**	2.13	0.31	-5.05	Not An.	-0.88	-5.43
Sr	1.11	0.68	-1.79	-3.41	Not An.	**121.00**	-1.78
Zr	-0.29	3.55	6.55	-0.69	Not An.	4.49	-1.83
Ba	0.37	0.34	-2.92	-3.44	Not An.	B. Det	-5.95
Pb	B Det	B Det	B. Det	2.22	Not An.	-4.29	-2.42
Y	5.42	5.67	9.43	9.48	Not An.	**10.37**	**11.09**
Nb	-7.08	0.46	B. Det	1.36	Not An.	**24.38**	**21.93**
La	-3.2	-3.59	B. Det	**-16.02**	Not An.	-3.67	**-22.25**
Ce	-1.54	-7.19	B. Det	B. Det	Not An.	-7.53	**-30.36**
Th	2.17	0.82	B. Det	-7.00	Not An.	**-26.71**	**-34.22**

Table 2.2. Accuracy for XRF data (%RD). B. Det, below determination limit; Not An, not analysed. M and T refer to number of repeats for major and trace elements respectively. Bold values reflect poor accuracy after Jenner (1996).

The precision and accuracy of the data is excellent to very good for the vast majority of elements (after Jenner 1996). However, a number of the period 4 transition metals show poor accuracy and precision across the vast majority of the international standards and repeats used (Co, Cr, Ni & Cu, possibly Sc, Pb & Zn). Comparison of different analytical 'runs' suggests the machine was poorly calibrated for some of these elements during runs 4 (SPH>207) and 5 (drillcore). For example on runs 1 and 3 international standard BEN (basalt) produced Co concentrations of 62.0 (R1), 64.9 (R3) and 66.3 (R3) ppm, compared to a known value of 60 ppm. By contrast run 4 produced concentrations between 168.0 and 171.0 ppm. Considerably higher Co concentrations for JA1 (also JB1a) were also measured during runs 4 and 5 compared to their known values for these standards (111.0 to 113.8 ppm measured, compared to actual value of 38.1 ppm). Ni and Cu values also were considerably elevated for the more felsic standards as they approached the determination limit for these elements. Only Co data from runs 1 to 3

are used. Co data was not used from runs 4 or run 5 (drillcore). Accuracy and precision was generally good to poor (i.e < 10%) for Y, La, Ce, Th and Nb. However, these elements were also analysed by inductively coupled mass spectrometry which gives better accuracy and precision.

Element	JB1A Basalt	BEN Basalt	JA1 Andesite
Cr actual	392.0	360.0	6.4
Cr Run 1	-	385.0	-
Cr Run 3	385.6	**391.1 to 193.6**	**15.7**
Cr Run 4	387.0 to 389.0	**395.0 to 401.0**	**15.0 to 17.0**
Cr Run 5	388	-	**13.9**
Co actual	38.1	60.0	11.0
Co Run 3	40.3	64.9 to 66.3	12.0
Co Run 4	**111.0 to 113.0**	**168.0 to 171.0**	**68.0 to 71.0**
Co Run 5	**113.8**	-	**70.7**
Ni actual	140.0	267.0	1.7
Ni Run 3	129.2	273.5 to 275.3	**8.0**
Ni Run 4	130.0 to 132.0	276.0 to 278.0	**9.0**
Ni Run 5	128.9	-	**8.2**

Table 2.3. Measured and actual concentrations for various standards (ppm) demonstrating poorer calibration for Co, Cr and Ni during later runs (values in bold).

2.4 Inductively coupled plasma mass spectrometry

Rare earth-elements (plus Rb, Ba, Sr, Zr, Nb, Y, Hf, Ta, Th, U) were determined by inductively coupled plasma mass spectrometry (ICP-MS) at the University of Southampton using HF/HNO_3 digestion. Samples were measured on a Thermo Scientific Xseries 2. To ensure complete digestion of zircons and other resistant minerals, repeated digests were made until no residue was visible. The procedure is outlined in the Appendix.

Accuracy (%RD) and Precision (%RSD) was checked against a range of international standards (Table 2.4). Precision is excellent to very good for the majority of elements (after Jenner, 1996). Only Ta and Th showed poor precision (%RSD >10). Accuracy (%RD) was excellent to good for the majority of elements over a range of international standards (Table 2.4). Exceptions include: basaltic rocks generally showed poor accuracy for Ta, Ba, Sc and Nb; and rhyolitic rocks showed poor accuracy for Sc and the MREE. Poor accuracy for Zr, Hf and the HREE for JGB-1 gabbro may suggest incomplete digestion of zircons in coarse grained igneous rocks. Elements duplicated by both

XRF and ICP-MS analysis include: Ba, Rb, Sr, Th, Zr, La, Ce, Y and Nb. Plotting these data against each other produces a strong correlation for all elements except Zr (again indicative of incomplete zircon digestion) (also see Fig. 2.2):

$Ba_{ICP\text{-}MS} = 1.0439 * Ba_{XRF}$ $R^2=0.9293$
$Sr_{ICP\text{-}MS} = 1.0295 * Sr_{XRF}$ $R^2=0.9111$
$Rb_{ICP\text{-}MS} = 1.0592 * Rb_{XRF}$ $R^2=0.8302$
$Th_{ICP\text{-}MS} = 0.9566* Th_{XRF}$ $R^2=0.8557$
$Nb_{ICP\text{-}MS} = 0.9964 * Nb_{XRF}$ $R^2=0.9073$
$Y_{ICP\text{-}MS} = 0.9018 * Y_{XRF}$ $R^2=0.8038$
$La_{ICP\text{-}MS} = 1.1808 * La_{XRF}$ $R^2=0.8759$

The Zr dataset can be split into three groupings, showing the effectiveness of the HF technique on zircon digestion (Fig. 2.2). 'Good' digestion (ICP-MS data ± 25% of XRF data) was restricted to basalts, basaltic andesites, feldspar-porphyritic andesites, gabbros, mafic tuffs and cherts. 'Moderate' digestion (ICP-MS data -25 to -65% of XRF data) was common for andesitic to rhyolitic tuffs, rhyolites, quartz diorite, some cherts and pillow lavas, and various lithologies from the Tyrone Plutonic Group (plagiogranite, aplite). Poor dissolution (ICP-MS data less than -65% of XRF data) was a common feature of all ironstones and the vast majority of coarse grained intermediate to felsic intrusive rocks (tonalite, quartz porphyry, granodiorite, granite).

'Good' (complete?) digestion: $Zr_{ICP\text{-}MS} = 0.9462 * Zr_{XRF}$ $R^2=0.7618$
'Moderate' digestion: $Zr_{ICP\text{-}MS} = 0.5294* Zr_{XRF}$ $R^2=0.8866$
Poor digestion: $Zr_{ICP\text{-}MS} = 0.1268 * Zr_{XRF}$ $R^2=0.3013$

Zr concentrations from XRF data was used for subsequent chapters as this has shown to be both precise and accurate for a suite of international standards and various rock types. Good correlation between XRF and ICP-MS data for the LREEs, Nb and Y suggests these elements were largely unaffected by incomplete zircon dissolution (Fig. 2.1). Comparsion between results obtained from the BGS (Section 2.2) and repeat analysis on the same rocks made at NOCS confirms this, with a good correlation for the majority of elements, plus La/Sm, La/Yb and Dy/Yb (Fig 2.2). A slight artificial steepening of some REE profiles (to ~1.25x of La/Yb) occurs due to Incomplete zircon digestion (see Fig. 2.2). Poor correlation between BGS and NOCS data for Hf suggests this element was not liberated by the HF technique at NOCS. The BGS technique uses $HF/HClO_4/HNO_3$ attack and fusion with NaOH and is considered effective for zircon dissolution. Hf (and Ta) data obtained from digestions made at NOCS was not used for subsequent chapters.

Element	BHVO-2 Basalt N=6		BIR-1 Basalt N=6		JB-1A Basalt N=6		JB-3 Basalt N=6		JGB-1 Gabbro N=2		JR1 Rhyolite N=2	
	%RSD	%RD	%RSD	%RD	%RSD	%RD	%RSD	%RD	%RSD	%RD	%RSD	%RD
Sc	2.07	-0.13	1.69	1.86	1.85	-4.81	1.97	2.63	0.91	-2.60	4.63	**11.93**
Rb	1.27	5.36	3.14	4.33	1.49	4.06	0.87	1.36	0.88	**-11.32**	8.00	2.22
U	1.61	0.5	5.75	**10.00**	1.53	-0.64	0.94	-3.30	1.57	**-22.95**	1.69	-4.81
Sr	1.13	-3.14	1.35	-2.49	1.64	-1.39	0.64	0.82	0.92	-1.55	1.93	-4.40
Y	1.25	3.06	1.20	2.43	1.50	-3.26	0.85	0.37	0.63	-5.25	0.83	1.15
Zr	0.96	3.45	1.50	7.24	1.54	0.28	1.01	0.25	0.98	**-13.60**	0.96	-.1.96
Nb	4.49	-4.14	3.26	-1.18	1.19	-2.78	1.81	**-18.03**	1.21	**-32.49**	1.57	-0.39
Cs	1.17	0.17	7.90	**-26.19**	1.58	7.96	0.60	1.26	1.00	**-17.31**	0.57	1.78
Ba	1.22	-1.74	0.65	**-10.75**	1.66	3.15	0.78	-2.10	0.87	-4.76	6.91	2.39
La	1.30	-0.80	1.55	-3.28	1.47	-1.23	1.20	-4.33	0.70	-4.50	0.07	-1.17
Ce	1.12	-0.88	1.74	-2.70	1.49	0.88	1.07	-0.55	1.04	0.48	0.79	-0.40
Pr	1.25	-0.35	1.24	0.59	1.61	-1.12	0.58	5.35	0.95	0.91	0.75	7.08
Nd	1.23	-1.04	1.19	-1.42	1.54	-1.34	0.76	0.68	1.19	-4.41	0.69	0.21
Sm	1.46	-0.29	1.95	-2.99	1.52	-1.56	0.88	-1.02	0.94	-5.04	0.99	-4.26
Eu	1.44	-1.22	1.75	-2.67	1.33	-0.13	0.68	-0.54	1.08	-2.20	1.56	**-10.33**
Gd	1.24	-1.12	1.31	-2.75	2.07	-1.51	1.09	-0.85	1.71	2.01	2.72	10.45
Tb	1.46	0.78	1.65	-0.69	1.80	-3.03	0.73	0.94	1.06	-6.38	1.63	-2.28
Dy	1.43	-2.15	1.09	-0.88	1.54	-1.45	0.60	-0.52	1.00	8.59	1.35	**10.28**
Er	1.26	-3.06	1.16	-1.05	1.60	-.088	0.74	5.31	0.95	-5.11	1.73	**12.96**
Yb	1.3	0.09	1.36	-0.11	1.57	-458	0.86	-0.61	0.79	**-11.26**	2.24	3.82
Lu	1.75	2.07	0.97	-0.20	1.49	-.097	0.75	-2.14	0.79	-6.89	1.2	2.54
Hf	1.53	-0.65	1.82	-1.98	1.63	-2.36	0.68	-0.6	0.97	**-10.09**	2.18	2.86
Ta	**18.01**	2.81	**118.33**	**316.43**	1.86	6.81	2.76	11.00	**29.70**	7.87	**58.73**	-5.27
Th	1.35	-4.75	**15.69**	0.00	1.57	-4.89	1.21	-1.59	1.81	**-14.03**	0.86	-2.28

Table 2.4. Accuracy (%RD) and precision (%RSD) for ICP-MS data. N refers to number of repeats. Bold values reflect poor accuracy after Jenner (1996).

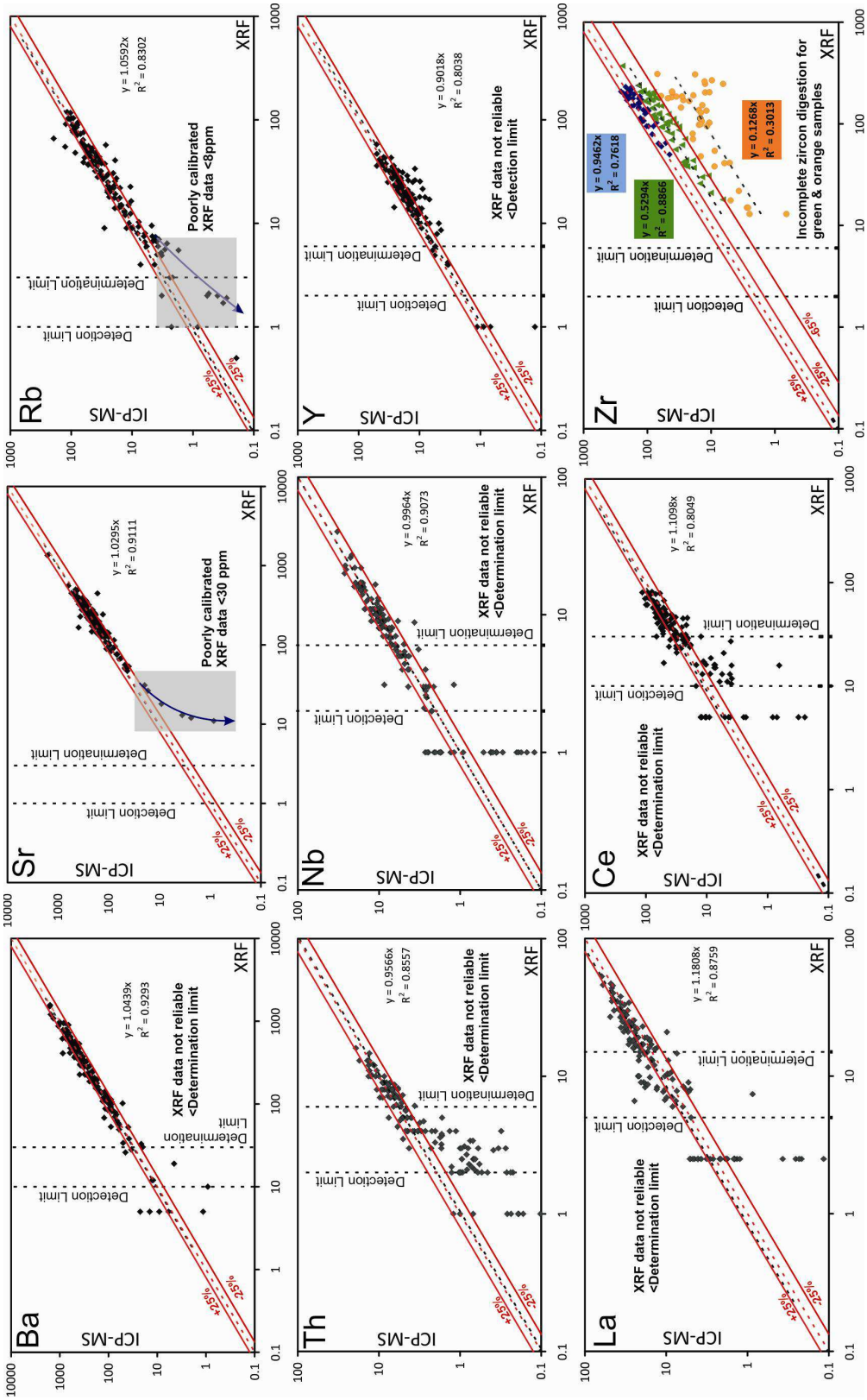

Figure 2.1. Correlations between XRF and ICP-MS data for Ba, Sr, Rb, Th, Nb, Y, La, Ce and Zr. Dotted red line shows perfect 1:1 correlation. XRF data shows a good correlation with ICP-MS data for the majority of elements above their determination limits (set at 3x detection limits).

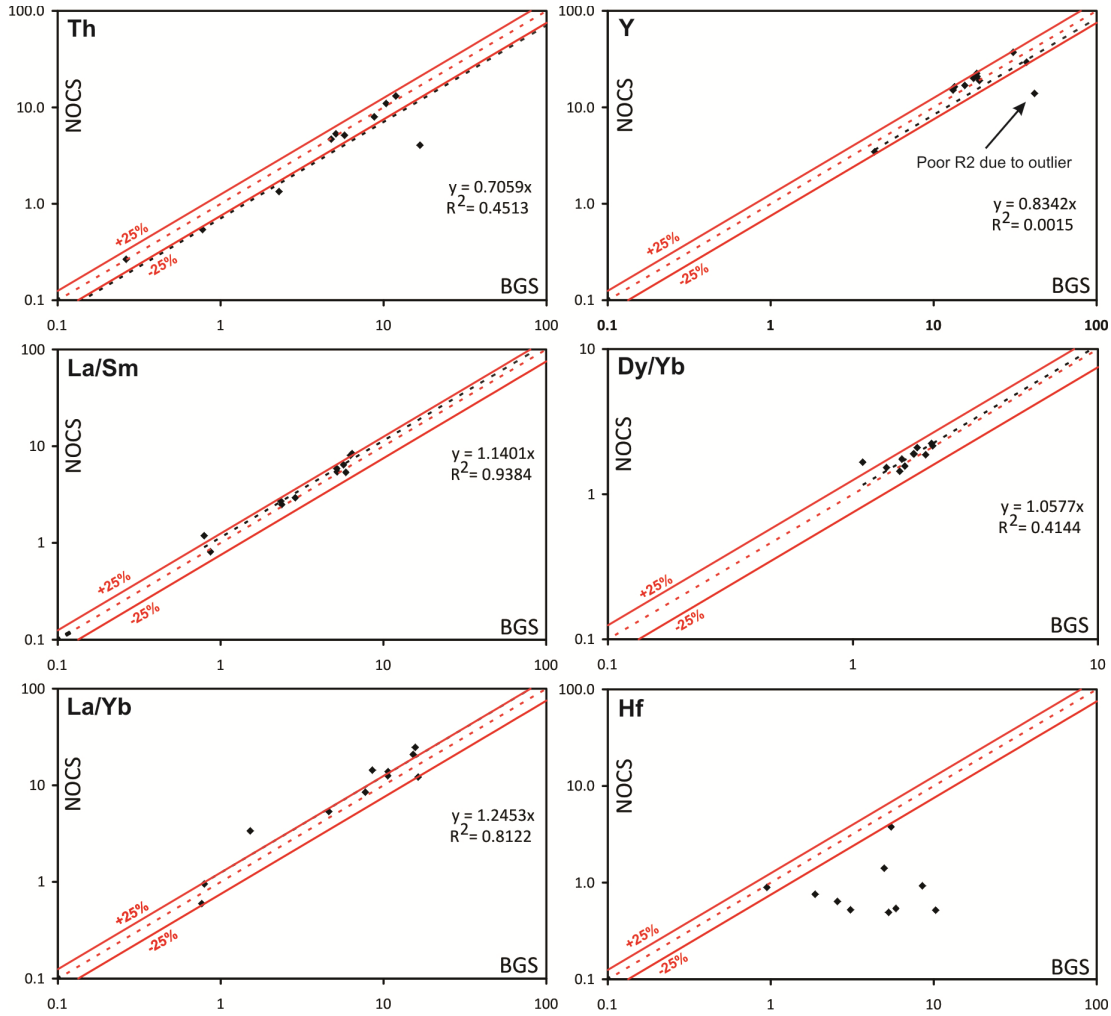

Figure 2.2. Correlations between ICP-MS data carried out at the NOCS and at the BGS for Th, Y, La/Sm, Dy/Yb, La/Yb and Hf. All elements and ratios show good correlations except for Hf. Slightly steeper REE profiles (to 1.25x) from NOCS analyses suggest some HREE were retained in undigested phases. Poor correlation for Hf suggests this element (along with Ta) was retained in undigested phases.

2.5 Thermal ionization mass spectrometry

Strontium was isolated for Sr isotope analysis using approximately 80µl columns containing Sr-Spec resin and elution with 3M HNO_3 to remove interfering elements (see Appendix). The purified Sr samples were collected with water and loaded onto a single outgassed Ta filament using a Ta activator solution. Samples were run using a multi dynamic peak jumping routine on a VG Micromass Sector 54 thermal ionization mass spectrometer (TIMS) at the University of Southampton. The ratios were corrected using an exponential fractionation correction relative to $^{86}Sr/^{88}Sr$ of 0.1194. NIST-987 was run as a standard in each run and the long term average for $^{87}Sr/^{86}Sr$ is 0.710243 ± 18 (2sd n=93). An age correction was performed to account for radioactive decay and ingrowth of ^{87}Sr; values for that time (=age of the sample) are reported as $^{87}Sr/^{86}Sr_i$. Modern CHUR was taken to be 0.7045 and 0.0827 for $^{87}Sr/^{86}Sr$ and $^{87}Rb/^{86}Sr$ respectively. The decay constant of ^{87}Sr is 1.42×10^{-11} yr^{-1}.

Neodymium was isolated for Nd isotope analysis using 6.5ml Dowex AG50W-X8 (200-400 mesh) cation columns and Ln-spec reverse phase columns (see Appendix). Neodymium isotope ratios were measured using a VGMicromass Sector 54 thermal ionization mass spectrometer (TIMS) at the University of Southampton. $^{143}Nd/^{144}Nd$ was measured in multidynamic mode, exponentially corrected for instrumental fractionation relative to $^{146}Nd/^{144}Nd = 0.7219$. The JNdi standard gave a value of 0.512091 ± 14 (2sd, n=20), with data corrected to 0.512115 (Tanaka et al. 2000). An age correction was performed (DePaolo & Wasserburg 1976) to account for radioactive decay and ingrowth of ^{143}Nd; values for that time are reported as εNd_t. Modern CHUR was taken to be 0.512638 and 0.1967 for $^{143}Nd/^{144}Nd$ and $^{147}Sm/^{144}Nd$ respectively (Hamilton et al. 1983). The decay constant of ^{147}Sm is 6.54×10^{-12} yr^{-1}. Depleted mantle model ages (τ_{DM}) were calculated after DePaolo (1981) assuming present day $^{143}Nd/^{144}Nd$ and $^{147}Sm/^{144}Nd$ values of 0.51315 and 0.2137.

2.6 Electron microprobe analysis

Electron microprobe analyses (EPMA) were completed at the Natural History Museum, London on a Cameca SX-50 electron microprobe equipped with a wavelength dispersive system. Analyses were conducted at 20 keV and 20 nA and counting times ranged from 10 to 50s for spot analysis. The detection limits for elements measured are given in Table 3.5. Analyses we performed on polished thin sections.

Element	Minimum (ppm)	Maximum (ppm)	Mean (ppm) N=280	Standard Deviation N=280
Na	211	604	270.65	49.37
Mg	131	341	176.03	26.45
Al	161	331	213.10	18.83
Si	172	322	233.91	19.39
P	97	575	161.19	47.70
K	225	460	342.26	40.38
Ca	191	372	270.46	37.15
Ti	127	282	142.84	20.98
Cr	140	213	154.11	9.03
Mn	244	368	311.12	613.31
Fe	234	389	171.18	20.56
Co	0	5318	263.66	464.94
Ni	258	412	285.48	28.87
F	0	38853	860.18	2543.83
Ce	470	688	516.32	31.02
Ba	453	686	506.68	40.06
V	72	292	136.25	20.79

Table 2.5. Detection limit ranges for elements determined by microprobe analysis (in ppm). Ranges vary due to the composition of the mineral being analysed.

2.7 U-Pb zircon geochronology

Prior to the commencement of this PhD study several samples were selected for U-Pb zircon geochronology at the NERC Isotope Geosciences Laboratory (NIGL) by Mark Cooper. All sample preparation, analysis and age dating was completed by NIGL staff. Quentin Crowley and Stephen Noble carried out all U-Pb geochronology in Chapter 3. Dan Condon carried out all U-Pb geochronology in Chapters 4-6. Recalculated U-Pb zircon ages of the Draut et al. (2009) dataset (Chapter 3) were carried out by Quentin Crowley.

2.7.1 Age dating for Chapter 3

Heavy mineral concentrates were obtained at the NERC Isotope Geosciences Laboratory using standard crushing techniques, a Gemini™ table, modified superpanner, a Frantz LB1 magnetic separator and heavy liquids. Minerals were selected for analysis by hand picking in alcohol under a binocular microscope and either air-abraded or chemically abraded to improve concordance following Krogh (1982) and Mattinson (2005). Chemically abraded zircons were first annealed at 850 °C for 48 hours prior to partial dissolution in 29N HF at 180 °C for 12 hrs (McConnell et al. 2009). Dissolutions, spiking and chemical separations follow Krogh (1973) with modifications after Corfu & Noble (1992). Procedural blanks of MRC prefixed samples ranged from c. 20 pg to ≤10 pg Pb and <0.5 pg U, whereas sample JTP prefixed samples had procedural blanks of 2 pg Pb and 0.1pg U.

Correction for common Pb, in excess of the laboratory blank, was made using a Stacey and Kramers (1975) model Pb composition calculated for the $^{207}Pb/^{206}Pb$ age of the analyses, with a 2 % error on the compositions propagated through data reduction calculations. Data were either obtained on a VG354 or Thermo Electron Triton using either a Daly detector or SEM respectively. U-Pb Concordia and upper and lower intercept age calculations followed Ludwig (1998, 2003) using the decay constants and measurement uncertainties of Jaffey et al. (1971). Uncertainties quoted for isotope ratios and ages are at the 2σ level, and all data are plotted with 2σ error ellipses.

2.7.2 Age dating for Chapters 4 to 6

Zircons were isolated using conventional mineral separation techniques. Prior to isotope dilution thermal ionization mass spectrometry (ID-TIMS) analyses zircons were subject to a modified version of the chemical abrasion technique (Mattinson 2005). U-Pb ID-TIMS analyses utilized the EARTHTIME ^{205}Pb-^{233}U-^{235}U (ET535) tracer solution. Measurements at the NERC Isotope Geosciences Laboratory were performed on a Thermo Triton TIMS. Pb analyses were measured in dynamic mode on a MassCom SEM detector and corrected for 0.14 ± 0.04%/u. mass fractionation. Linearity and dead-time corrections on the SEM were monitored using repeated analyses of NBS 981 and U500. Uranium was measured in static Faraday mode on 10^{11} ohm resistors or for signal intensities < 15 mV, in dynamic mode on the SEM detector. Uranium was run as the oxide and corrected for isobaric interferences with an $^{18}O/^{16}O$ composition of 0.00205 (IUPAC value and determined through direct measurement at NIGL). Single analysis U-Pb dates and uncertainties were calculated using the algorithms of Schmitz and Schoene (2007) and a $^{235}U/^{205}Pb$ ratio for ET535 of 100.18 ± 0.1%. All common Pb in the analyses was attributed to the blank and subtracted based on the isotopic composition and associated uncertainties analysed over time. The $^{206}Pb/^{238}U$ ratios and dates were

corrected for initial ^{230}Th disequilibrium using an assumed Th/U[magma] of 3 ±1 applying the algorithms of Schärer (1984) resulting in an increase in the $^{206}Pb/^{238}U$ dates of ~100 kyr. Weighted mean $^{206}Pb/^{238}U$ dates and associated uncertainties were calculated using Isoplot (Ludwig 1991).

Errors for U-Pb dates are reported in the following format: ±X(Y)[Z], where X is the internal or analytical uncertainty in the absence of systematic errors (tracer calibration and decay constants), Y includes the quadratic addition of tracer calibration error (using a conservative estimate of the standard deviation of 0.1% for the Pb/U ratio in the tracer), and Z includes the quadratic addition of both the tracer calibration error and additional ^{238}U decay constant errors of Jaffey et al. (1971). All analytical uncertainties are calculated at the 95% confidence interval. These $^{238}U/^{206}Pb$ dates are traceable back to SI units via the gravimetric calibration of the EARTHTIME U-Pb tracer and the determination of the ^{238}U decay constant (Condon et al. 2007; Jaffey et al. 1971). The mean square weighted deviation (MSWD) has been calculated for each population used for weighted mean calculations all fall within the range expected for a single population of a given sample size (Wendt & Carl 1991).

2.8 Tellus Project

An airborne geophysical survey covering the whole of Northern Ireland was flown in 2005 and 2006 as part of the Tellus project (see GSNI 2007). This project was funded by the Northern Ireland Department of Enterprise Trade and Investment and by the Rural Development Programme through the Northern Ireland Programme for Building Sustainable Prosperity (Chacksfield 2010). The aircraft used was a De Havilland Twin Otter which carried magnetic, electromagnetic and radiometric sensors, and was operated as a joint venture between the British Geological Survey (BGS) and the Geological Survey of Finland (GSNI 2007). Two frequency EM datasets (3 and 14 kHz) were acquired over the Tyrone Igneous Complex and the western half of Northern Ireland in 2005 and four-frequency datasets (0.9, 3, 12 and 25 kHz) across the eastern half in 2006. Survey lines were orientated at 165° or 345°, 200 m apart, at a flight height of >56 m in rural areas, rising to >244 m over urban areas. Typical survey speed was 70 m/s, with tie lines bearing 075. Two Scintrex Caesium Vapour Model CS2 magnetometers were employed to derive magnetic intensity. Sensitivity was 0.001 nT with a sample interval of 0.1 seconds (~7 m). Electromagnetic data was acquired through a vertical-coplanar transmitter/receiver configuration. A Tx-Rx coil separation of 21.36 m was used with a sample interval of 0.25 seconds (~17.5 m). The radiometric data were acquired using self-calibrating Exploranium GR-820/3 gamma-ray spectrometers with a sample interval of 1.0 sec (~70 metres). Energy

'windows' for Thorium, Uranium, Potassium and Total Count were sampled (Beamish et al. 2007). Further detail on survey specification and geophysical data processing are presented within Beamish et al. (2007, and references therein). The BGS regional gravity data is herein grouped together with the Tellus dataset. Land data coverage for Northern Ireland is approximately 1 station per 1.25km^2. Regional gravity surveys were carried out between 1959 and 1960 (Beamish et al. 2007). This dataset was processed by Martin Moloney (Dalradian Gold Ltd.).

Maps and raw data from the Tellus geophysical survey were provided by the Geological Survey of Northern Ireland. All maps are shaded from the NNW, and include:

- Apparent Conductivity. Low frequency (3005 Hz or 3125 Hz)
- Apparent Depth. Low frequency (3005 Hz or 3125 Hz)
- Digital Elevation Model (precision ~10m).
- Radioactivity Dose Rate.
- Ternary Image. RGB = K-Th-U
- Radioactivity. Potassium.
- Radioactivity. Potassium over Thorium Rate.
- Radioactivity. Equivalent Thorium.
- Radioactivity. Equivalent Uranium.
- Total Magnetic Intensity, reduced to pole.
- First Vertical Derivative of the Pole-reduced Total Magnetic Intensity.
- Second Vertical Derivative of the Pole-reduced Total Magnetic Intensity.
- Tilt Derivative of the Pole-reduced Total Magnetic Intensity.
- Analytic Signal Amplitude of the Total Magnetic Intensity.

In addition, georeferenced rasters of GSNI fieldsheets were provided, along with 1:10,000 scale topographic maps, orthophotographs, and the complete Tellus geochemical dataset over Northern Ireland.

2.9 Historic mineral exploration datasets

A wide range of historic mineral exploration datasets and reports were provided by the GSNI, Metallum Resources, Dalradian Resources and Aurum Exploration Services personnel for licences covering the Tyrone Igneous Complex. Most of these datasets were digitally captured by Aurum Exploration Services personnel from original A0 map sheets over the past several years. Datasets which were provided included (but were not limited to):

- Historic prospecting and float database

- Historic pan concentrates database
- Soil sampling database
- Pionjar base of till geochemical database
- Ground magnetic survey database
- Ground VTEM survey database
- Ground IP survey database
- Drilling and trenching database
- Historic assays from diamond drilling
- Historic drillhole logs
- Licence renewal and interim reports to the GSNI
- Internal company reports and consultant reports

Chapter 3: Age and geochemistry of the Tyrone Igneous Complex

This chapter forms the basis of a published paper: Cooper, M.R., Crowley, Q.G., Hollis, S.P., Noble, S.R., Roberts, S., Chew, D., Earls, G, Herrington, R., & Merriman, R.J. (2011). *Age constraints and geochemistry of the Ordovician Tyrone Igneous Complex, Northern Ireland: Implications for the Grampian orogeny.* Journal of the Geological Society, London, v. 168, p. 837-850. U-Pb geochronology was carried out by Q. Crowley and S.P Noble. Samples were collected by M.R. Cooper and other GSNI staff. Geochemical data was provided by M.R. Cooper, analysed at the BGS and interpreted by S. Hollis.

Abstract

The Tyrone Igneous Complex is one of the largest areas of ophiolitic and arc-related rocks exposed along the northern margin of Iapetus within the British and Irish Caledonides. New U-Pb zircon data and regional geochemistry, suggest the Tyrone Plutonic Group represents the uppermost portions of a c. 480 Ma suprasubduction zone ophiolite accreted onto an outboard segment of Laurentia prior to 470.3 ± 1.9 Ma. The overlying Tyrone Volcanic Group formed as an island arc which collided with the Laurentian Margin during the Grampian phase of the Caledonian orogeny. Early magmatism is characterized by transitional to calc-alkaline, light rare earth element-enriched island-arc signatures, with an increasing component of continentally-derived material up sequence. Tholeiitic rhyolites with flat to U-shaped rare earth element profiles and light rare earth element-depleted basalts, located stratigraphically above a c. 473 Ma rhyolite of the upper Tyrone Volcanic Group, suggest initiation of intra-arc rifting at c. 475 Ma. Metamorphic cooling ages from the Tyrone Central Inlier imply arc-continent collision occurred before 468 ± 1.4 Ma, with the emplacement of the Tyrone Volcanic Group onto the Tyrone Central Inlier (Chew et al. 2008). A suite of 470.3 ± 1.9 Ma to 464.3 ± 1.5 Ma calc-alkaline intrusions are associated with the continued closure of Iapetus.

3.1 Introduction

The Grampian phase of the Caledonian orogeny records collision between the passive continental margin of Laurentia and a Lower Paleozoic oceanic arc(s) during the Early to Middle Ordovician (Dewey & Shackleton 1984). Predating final closure of the Iapetus Ocean, this was the first orogenic event to affect the southeast margin of Laurentia, broadly equivalent to the Taconic event of the Appalachians (van Staal et al. 1998). Widespread c. 490-480 Ma ophiolite obduction (Chew et al. 2010) was followed by polyphase deformation and metamorphism of thick post-Grenville, Neoproterozoic cover sequences along the Laurentian margin, such as the Dalradian Supergroup (c. 475 to 465 Ma; reviewed in Chew 2009). Orogeny was remarkably short-lived due to an associated subduction polarity reversal (Friedrich et al. 1999; Dewey 2005).

In Scotland, the colliding volcanic arc (Midland Valley terrane) is separated from the Laurentian margin by the Highland Boundary Fault (Fig. 3.1a), a continuation of the Baie Verte - Brompton Line of Newfoundland and the Fair Head - Clew Bay Line of Ireland (Fig. 3.1b). Ophiolitic rocks are preserved within this fault zone as the Highland Border ophiolite of Scotland, part of the Highland Border Complex, (Tanner 2007) and the dismembered Deer Park ophiolitic mélange of western Ireland, part of the accretionary Clew Bay Complex (Ryan et al. 1983). Remnants of the colliding arc(s) are represented within the Irish Caledonides as the Lough Nafooey, Tourmakeady and Charlestown groups of western Ireland (e.g. Ryan et al. 1980; Clift & Ryan 1994; Draut et al. 2004), and Tyrone Volcanic Group of Northern Ireland (Cooper et al. 2008; Draut et al. 2009). The South Mayo Trough represents the fore-arc to post-collisional foreland basin of the colliding Lough Nafooey arc (Dewey & Ryan 1990).

The Dunnage Zone of central Newfoundland and Maritime Canada includes a complex association of Cambro-Ordovician arc and backarc complexes of both intra-oceanic and continental affinity which were accreted to the Laurentian margin during the Taconic event (van Staal et al. 2007) (Fig. 3.1b). Peri-Laurentian tracts of the Notre Dame and Dashwoods Subzones are separated from those of peri-Gondwanan affinity within the Exploits Subzone by the Red Indian Line (Williams et al. 1988). Within the Notre Dame Subzone, three distinct phases of the Taconic event are recognized (van Staal et al. 2007). Broad correlations have been made between the Caledonides and Newfoundland Appalachians (e.g. van Staal et al. 1998), although exact correlations between terranes often remain contentious.

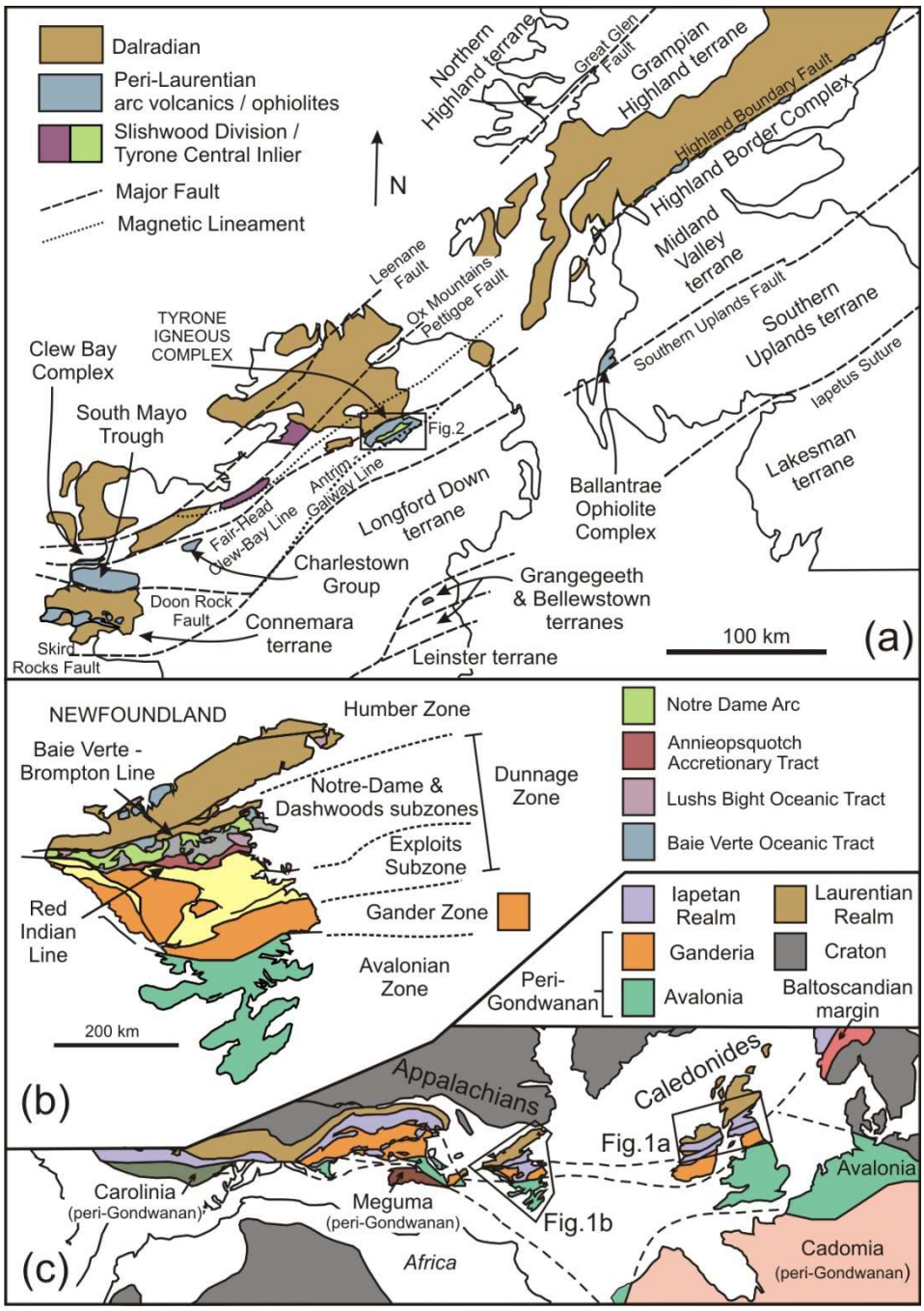

Figure 3.1. (a) Setting of the Tyrone Igneous Complex and other comparable ophiolite and volcanic arc associations in Britain and Ireland (after Hutton et al. 1985; Parnell et al. 2000: Chew et al. 2008). (b) Simplified regional geology of Newfoundland (after van Staal et al. 2007). (c) Early Mesozoic restoration of North Atlantic region and Appalachian-Caledonian orogen (after Pollock et al. 2009).

The Tyrone Igneous Complex of Northern Ireland provides one of the most complete sections through an accreted arc within the Grampian belt of the Caledonides. Whole rock geochemical data published by Angus (1977) and Draut et al. (2009) detail the evolution of the complex, constrained by four U-Pb zircon dates (Hutton et al. 1985; Cooper et al. 2008; Draut et al. 2009). These data nevertheless only partially characterize the geochronology and geochemistry of the entire complex. This paper (Cooper et al. 2011) presents a total of nine new U-Pb zircon ages, which are combined with existing U-Pb and biostratigraphical age constraints, field relations and new regional geochemistry to shed further light on the Grampian orogenic evolution of the Caledonide – Appalachian orogen (Fig. 3.1c).

3.2 Tyrone Igneous Complex

The Ordovician Tyrone Igneous Complex extends over an area of about 350km^2 in the counties of Tyrone and Londonderry, Northern Ireland, and is one of the most extensive areas of ophiolitic and arc-related rocks exposed along the northern margin of Iapetus within the British and Irish Caledonides. Building on the comprehensive survey of Hartley (1933), the Tyrone Igneous Complex was divided into two distinct units: the Tyrone Plutonic Group and the Tyrone Volcanic Group (Cobbing et al. 1965; Geological Survey of Northern Ireland 1979, 1983, 1995). The complex overlies sillimanite-grade paragneisses of the Tyrone Central Inlier, which based on detrital zircon age profiling, appears to be of upper Dalradian, Laurentian affinity (Chew et al. 2008). Both the Tyrone Igneous Complex and Tyrone Central Inlier are intruded by a suite of arc-related tonalitic to granitic intrusions (Cooper & Mitchell 2004; Fig. 3.2).

3.2.1 Tyrone Central Inlier

The Tyrone Central Inlier is composed of a thick sequence of psammitic and semipelitic paragneisses (Hartley 1933) termed the Corvanaghan Formation (GSNI 1995). Metamorphism is characterized by a prograde assemblage of biotite + plagioclase + sillimanite + quartz ± muscovite ± garnet in pelitic lithologies (c. 670 ± 113 °C, 6.8 ± 1.7 kbar; Chew et al. 2008), with corderite locally observed (Hartley 1933). Recent detrital zircon age profiling suggests an upper Dalradian, Laurentian affinity for these metasedimentary rocks, with Paleoproterozoic Nd model ages overlapping with those from both the Argyll and Southern Highland groups (Chew et al. 2008), while in situ Hf isotope analysis of zircon rims from c. 470Ma granitoid rocks that cut the Tyrone Central Inlier paragneisses yield negative ε_{Hf}470 values of approximately −39. This isotopic signature requires an Archaean source, suggesting rocks similar to the Lewisian Complex of Scotland occur at depth beneath the Tyrone Central Inlier (Flowerdew et al. 2009). The Tyrone Central Inlier is believed to

represent part of an outboard segment of Laurentia, most likely detached as a microcontinent prior to arc-continent collision and reattached during the Grampian event (Chew et al. 2010).

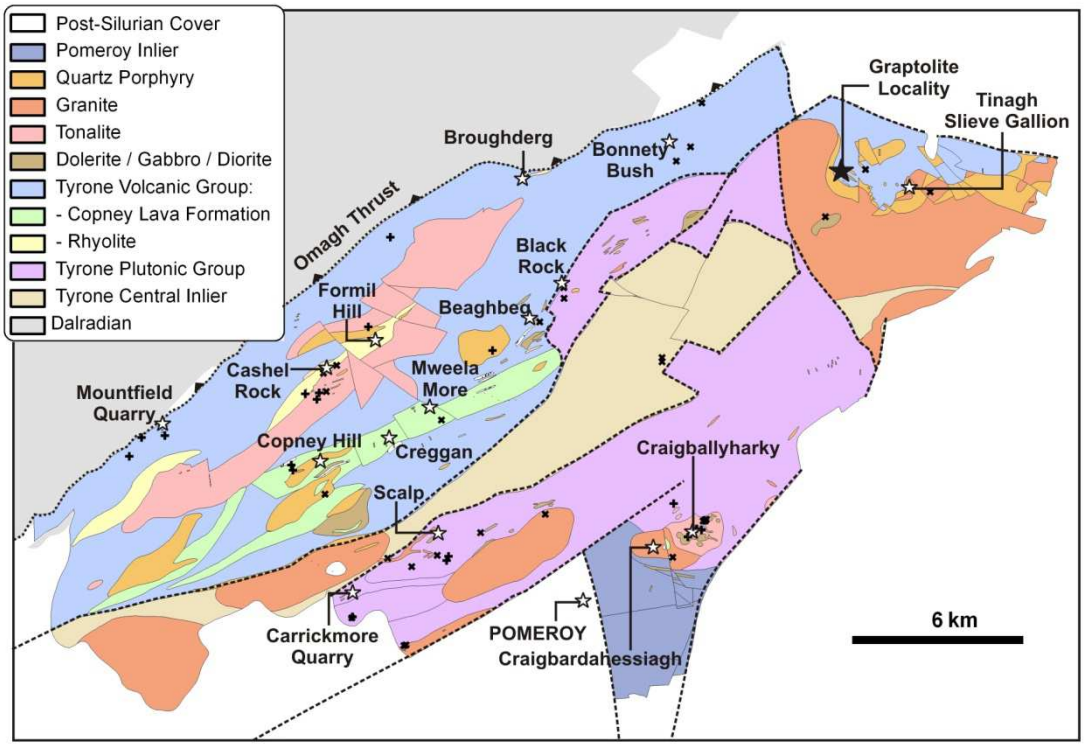

Figure 3.2. Simplified geological map of the Tyrone Igneous Complex showing locations sampled or discussed in this study (after GSNI, 1979, 1983, 1995). Crosses and plus symbols mark sample locations of Draut et al. (2009) and the new analyses presented here. Copney Pillow Lava Formation and Rhyolite are divisions within the Tyrone Volcanic Group.

3.2.2 Tyrone Plutonic Group

The Tyrone Plutonic Group forms the southern, structurally lower portion of the Tyrone Igneous Complex and consists mainly of variably tectonised and metamorphosed, layered, isotropic and pegmatitic gabbros (Cobbing et al. 1965; Cooper & Mitchell 2004). Olivine gabbro at Scalp (Fig. 3.2) displays cumulate layering, reflecting textural and compositional variations (see Cooper & Mitchell 2004), with gabbro locally altered to hornblende schist (Cobbing et al. 1965). At Black Rock (Fig. 3.2), coarse-grained hornblende gabbro is in contact with, and contains xenoliths of, an early-formed suite of dolerite, itself intruded by younger 1-2 m wide, basalt and dolerite dykes (Cooper & Mitchell 2004). Irregular veins of pegmatitic gabbro are closely associated. In Carrickmore Quarry, parallel NE-SW trending dolerite dykes display two-sided, and more commonly one-sided, chilled margins characteristic of a sheeted dyke complex

(Hutton et al. 1985). Pillow lavas are scarce within the group, and are present as a roof-pendant within the Craigballyharky intrusion (e.g. Angus 1977; Fig. 3.2).

Although exposure is poor, this association of rock types and their field relations strongly supports the view of Hutton et al. (1985) that the Tyrone Plutonic Group represents the upper parts of a dismembered ophiolite sequence. Previous geochemistry has shown the sequence to be of suprasubduction affinity (Draut et al. 2009). Based on a magma-mixing relationship between gabbro and tonalite at Craigballyharky, Hutton et al. (1985) considered the Tyrone Plutonic Group to be contemporaneous with the Tyrone Volcanic Group. A U-Pb zircon 472 $^{+2}/_{-4}$ Ma age determination of a tonalite from Craigballyharky along with magma relationships was taken as evidence for the age of the ophiolite and for the timing of obduction (Hutton et al. 1985). However, recent U-Pb zircon dating of gabbro from Craigballyharky yielded a significantly older age of 493 ± 2 Ma for the Tyrone Plutonic Group (Draut et al. 2009) which is discussed later.

3.2.3 Tyrone Volcanic Group

The Tyrone Volcanic Group forms the upper part of the Tyrone Igneous Complex and is comprised of basic to intermediate pillow lavas, tuffs, rhyolites, banded chert, ferruginious jasperoid (ironstone) and argillaceous sedimentary rocks. The predominant "background" lithology in the Tyrone Volcanic Group is a pale-greenish grey, schistose, chlorite-epidote-sericite tuff, which varies from fine-grained ash to coarse-grained lapilli tuff (Cooper & Mitchell 2004). Previous research suggests that there is evidence for at least three volcanic cycles within the Tyrone Volcanic Group; each commencing with basaltic lavas, with cycle tops characterized by the presence of laminated chert and/or mudstone at Tanderagee, Bonnety Bush and Broughderg respectively (Hutton et al. 1985; Cooper & Mitchell 2004). The base of the lowest cycle is represented by the Copney Pillow Lava Formation, with rhyolite at Formil Hill (Fig. 3.2) taken as the top of cycle two (Cooper & Mitchell 2004). Biostratigraphical correlation and a robust U-Pb zircon age constraint of 473 ± 0.8 Ma from the Formil Hill rhyolite, suggest an age for the upper Tyrone Volcanic Group within the Australasian Castlemainian (Ca1) Stage of the Arenig (Cooper et al. 2008; Fig. 3.3).

Draut et al. (2009) provided the first geochemical study of the Tyrone Volcanic Group. They suggested it formed within an oceanic arc which assimilated considerable detritus from the Laurentian margin and made a correlation with the Lough Nafooey arc of western Ireland. Although Cobbing et al. (1965) considered the Tyrone Volcanic Group to unconformably overlie the Tyrone Central Inlier, both Harley (1933) and more recent work (Cooper & Mitchell 2004; Draut et al. 2009) favoured a tectonic contact

between the units. Nowhere are contacts exposed with either the Tyrone Plutonic Group or the Tyrone Central Inlier.

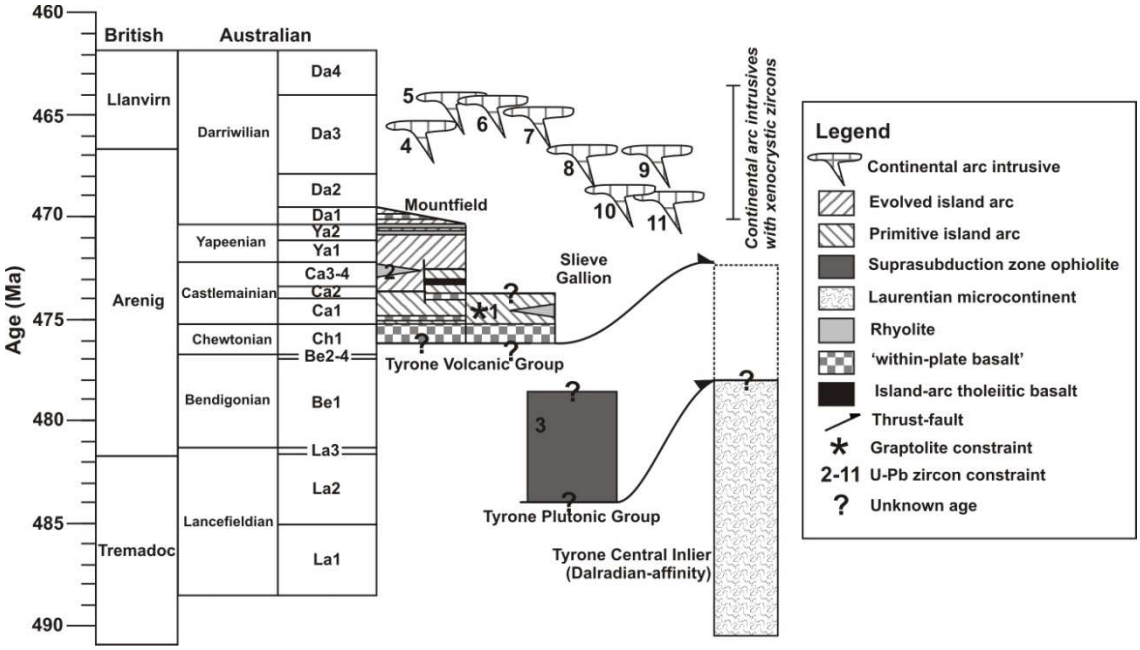

Figure 3.3. Tectonostratigraphic evolution of the Tyrone Igneous Complex during the Ordovician. Stratigraphy after Cooper and Mitchell (2004), Cooper et al. (2008); Draut et al. (2009), Hollis et al. (unpublished). The standard British Ordovician stages and the Australian graptolite zones are after Sadler et al. (2009). Biostratigraphic and U-Pb zircon ages: 1. Ca1 graptolite age of Cooper et al. (2008); 2. Formil Rhyolite of Cooper et al. (2008); 3. Scalp layered gabbro; 4. Laght Hill tonalite; 5. Pomeroy granite; 6. Copney quartz porphyry; 7. Craigbardahessiagh granodiorite; 8. Slieve Gallion granite; 9. Golan Burn tonalite; 10. Cregganconroe quartz-monzodiorite; 11. Craigballyharky tonalite (3-11 ages herein). Note: U-Pb age of Draut et al. (2009) for the Craigballyharky gabbro is not shown (see following).

3.2.4 Late Intrusive Rocks

Several large granitic to tonalitic intrusions cut the Tyrone Igneous Complex and Tyrone Central Inlier (Fig. 3.2). All show an I-type affinity except an intrusion of muscovite granite at Tremoge Glen (Fig. 3.2). A series of high-level sills and dykes of porphyryitic dacite cut all levels of the complex. Strong large ion lithophile element (LILE) and light rare earth element (LREE) enrichment, coupled with zircon inheritance and strongly negative εNd_t values, suggest that assimilation of Dalradian-affinity metasedimentary material was an integral part of their petrogenesis (Draut et al. 2009).

Field relations at Craigballyharky show roof pendants of Ordovician pillow basalt and sheeted dolerite enclosed within tonalite, demonstrating the Tyrone Plutonic Group

was in its present structural position prior to intrusion (Cobbing et al. 1965; Angus 1977; GSNI 1979). Granodiorite at Craigbardahessiagh contains pendants of Ordovician volcanic rocks and ironstone, and tonalite from Craigballyharky (Cobbing et al. 1965; Angus 1977; GSNI 1979). Tonalite from Craigballyharky and Leaghan (i.e. Cashel Rock; Fig. 2) has yielded U-Pb zircon ages of 472 $^{+2}/_{-4}$ Ma (Hutton et al. 1985) and 475 ± 10 Ma (Draut et al. 2009) respectively.

3.3 Sampling and analytical methods

A range of stratigraphic levels in the Tyrone Volcanic Group were sampled for geochemical analysis, as were key localities from the Tyrone Plutonic Group and several large tonalitic to granitic intrusions. A total of four Tyrone Plutonic Group, nine Tyrone Volcanic Group, and fifteen arc-related intrusive suite samples were analysed for major, trace and rare-earth elements at the British Geological Survey (BGS) in Nottingham. Results are presented in the Appendix (3.2). Nine samples were dated by U-Pb TIMS geochronology at the NERC Isotope Geoscience Laboratory. Three samples were collected from the Tyrone Plutonic Group – the layered gabbro at Scalp, pegmatitic gabbro at Black Rock and sheeted dykes from Carrickmore Quarry (Fig. 3.2), however only the layered gabbro (JTP207) produced sufficient zircon for successful age dating. Eight samples from the arc-related intrusive suite, including tonalite, granodiorite, granite, porphyritic dacite and quartz-monzodiorite yielded abundant zircon suitable for U-Pb TIMS geochronology. See Chapter 2 for further detail concerning methods.

3.4 Results

All samples examined from the Tyrone Igneous Complex have been subjected to low-grade metamorphism (sub-greenschist to epidote-amphibolite facies) and hydrothermal alteration, which has determined the approaches used in the interpretation of the geochemistry. Within the upper Tyrone Volcanic Group, volcanogenic base and precious metal mineralization has led to a variety of alteration types (see Chapter 7). Primary minerals are rarely well preserved except in late granitic to tonalitic intrusive rocks.

4.4.1 Geochemistry

The hydrothermal alteration and low-temperature metamorphism prevalent across the Tyrone Igneous Complex suggests that the use of mobile elements for whole rock classification and deducing magma affinity will be compromised. In particular,

elements such as SiO_2, Na_2O, K_2O, CaO, MgO and FeO, and the low-field strength elements (LFSE: Cs, Rb, Ba, Sr), are considered mobile under these conditions (MacLean 1990). By contrast, Al_2O_3, TiO_2, Th, V, Ni, Cr, Co, the high field strength elements (HFSE: Nb, Hf, Ta, Zr, Y, Sc, Ga) and rare earth elements (REE: minus Eu ± Ce) typically remain immobile (e.g. Pearce & Cann 1973; Wood 1980; MacLean 1990; Rollinson 1993; Barrett & MacLean 1999). In light of these results, particular attention is given to the immobile-element geochemistry of the Tyrone Igneous Complex. Although mass change associated with hydrothermal alteration may alter the absolute concentrations of immobile elements, inter-element ratios will remain constant (MacLean 1990).

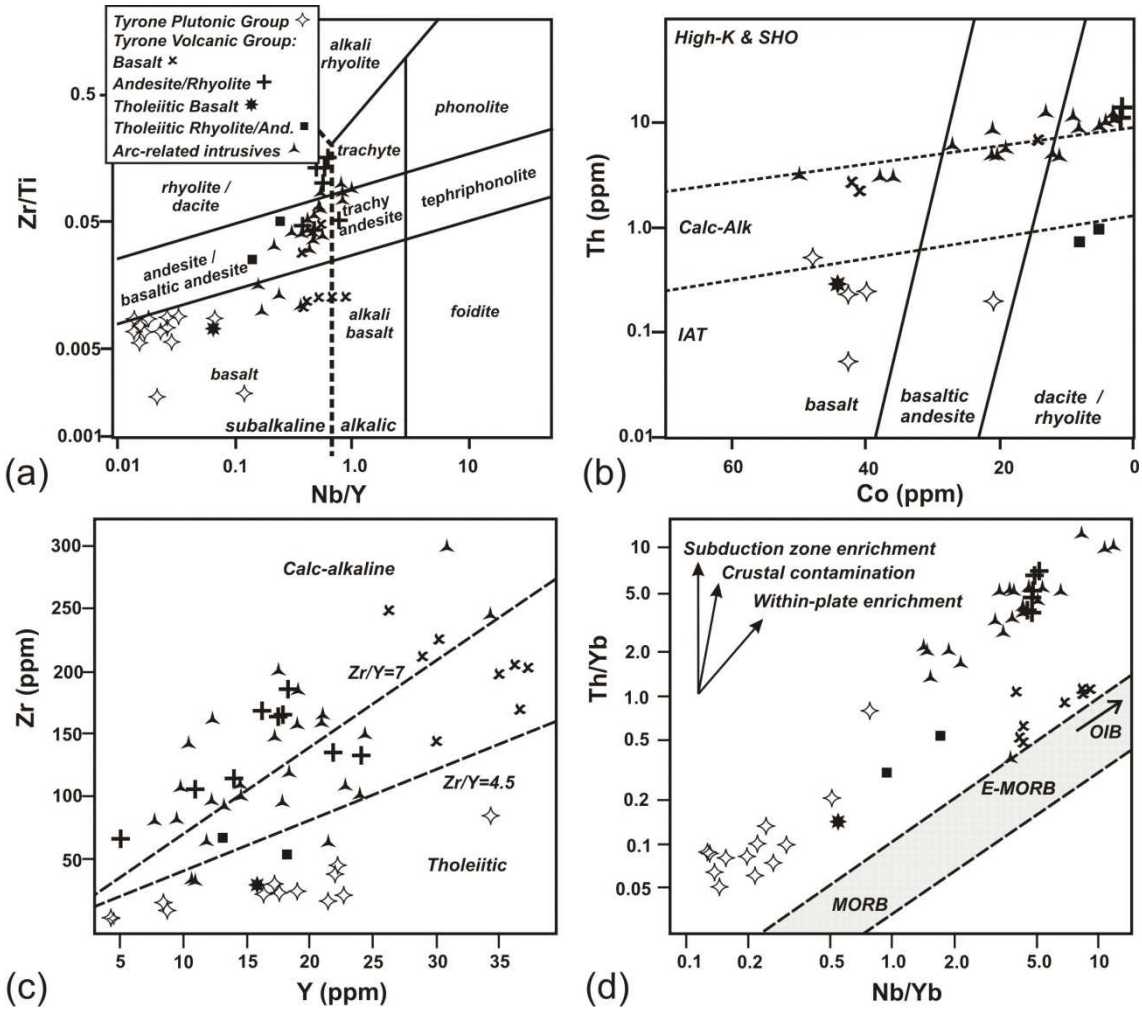

Figure 3.4. Geochemical analyses from the Tyrone Igneous Complex; data of Draut et al. (2009) also included. (a) Nb/Y against Zr/Ti after Winchester & Floyd (1977) modified by Pearce (1996). (b) Th-Co plot after Hastie et al. (2007). (c) Zr against Y after Barrett and MacLean (1999). (d) Th/Yb against Nb/Yb after Pearce (1983). Calc-alk, calc-alkaline; e-MORB, enriched mid-ocean ridge basalt; MORB, mid-ocean ridge basalt; OIB, ocean-island basalt, IAT, island arc tholeiite; SHO, shonshonite. Note Co data used are from BGS dataset and considered reliable.

Tyrone Plutonic Group

Rocks from the Tyrone Plutonic Group are tholeiitic and basaltic in composition (Fig. 3.4a-c), with positive Pb, negative Nb and modest Ti anomalies (Fig. 3.5a). Geochemical signatures are similar to those previously reported by Draut et al. (2009) (Fig.3.4 and 3.5a) and are typical of basalts generated in a suprasubduction environment (Pearce et al. 1984b; Fig. 3.4d). Th concentrations are variable (~1 to 100x primitive mantle), all samples show weak LREE depletion relative to heavy rare earth elements (HREE) (Fig. 3.5a), and HFSE concentrations are generally less than those of normal mid ocean ridge basalt. Aphanitic basaltic rocks (e.g. MRC343 and MRC340) classify as island-arc tholeiitic basalts according to Meschede (1986), Wood (1980), Pearce and Norry (1979) and Pearce and Cann (1973).

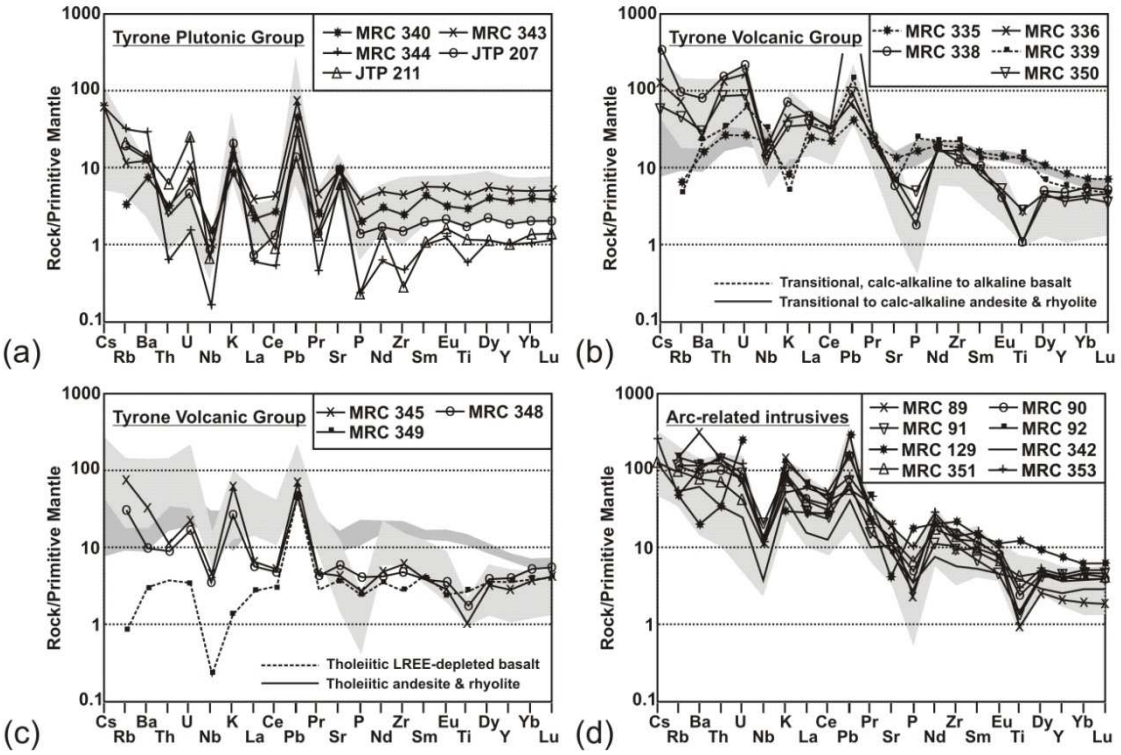

Figure 3.5. Multi-element variation diagrams for samples from the Tyrone Plutonic Group (a), Tyrone Volcanic Group (b,c) and arc-related intrusives (d). Shading reflects Draut et al. (2009) data for each respective group. Primitive mantle normalization values after Sun and McDonough (1989). Variable Rb and Sr reflects hydrothermal alteration.

Tyrone Volcanic Group

All basalts analysed from the Tyrone Volcanic Group, except those from Bonnety Bush (MRC349), are LILE- and LREE-enriched. Most display pronounced negative Nb anomalies (Fig. 3.5b), range from subalkaline (transitional to calc-alkaline) to

borderline alkalic in composition (Fig.3.4a,c), and plot within the enriched-mid ocean ridge basalt (e-MORB) fields of Wood (1980) and the within-plate/volcanic-arc fields of Meschede (1986) and Pearce and Norry (1979). Samples from around Mountfield are alkalic, of within-plate affinity, and do not display the classic HFSE depletion of suprasubduction zone magmatism (Draut et al. 2009). Tholeiitic basalt (e.g. low Zr/Y) from Bonnety Bush (MRC349) has Pb and Nb anomalies typical for arc-related volcanism, yet has low LILE concentrations, limited Ti anomalies and is LREE depleted relative to HREE (Fig. 3.5c). Immobile element ratios from this locality (e.g. Sc/Y, Ti/Sc, Ti/V, Sm/Yb, Th/Nb and Zr/Nb) are similar to those from the Tyrone Plutonic Group.

All rocks of andesitic to rhyolitic composition (Fig. 3.4a and 3.4b), except those from Beaghbeg and Bonnety Bush (MRC345 & MRC348), are subalkaline and transitional to calc-alkaline in nature (Fig. 3.4c). They are LILE- and LREE-enriched, and have lower HREE concentrations than associated basalts. Consideration of the data within multi-element variation diagrams (Fig. 3.5c) suggests they are typical of arc-related volcanism (e.g. negative Nb anomalies and HFSE depletion). Tholeiitic rhyolitic tuff from Beaghbeg (MRC345) and strongly altered andesitic tuff from Bonnety Bush (MRC348) are unusual within the Tyrone Volcanic Group, in that they display modest LILE enrichment (>10x primitive mantle), and LREE and HREE concentrations around 10x chondrite. Primitive-mantle normalized multi-element variation diagrams show flat to 'U' shaped REE profiles (Fig. 3.5c).

Late arc-related Intrusive Rocks

Calc-alkaline, arc-related intrusive rocks cut both the Tyrone Igneous Complex and the Tyrone Central Inlier (Fig. 3.2). These rocks display geochemical affinities similar to the LILE- and LREE-enriched rhyolites and andesites of the Tyrone Volcanic Group (Fig. 3.4 and 3.5b,d), with granitic rocks classified as volcanic-arc granites according to their Ta-Yb systematics (Pearce et al. 1984a).

3.4.2 U-Pb Geochronology

Calculated U-Pb ages for samples analysed herein are presented in the Appendix (3.1), along with additional information. The U-Pb ages (Fig. 3.6), range in age from 479.6 ± 1.1 Ma to 464.3 ± 1.5 Ma. All samples display evidence of zircon inheritance. Gabbro from the Tyrone Plutonic Group (JTP207) was dated at 479.6 ± 1.1 Ma, with inherited ages of c. 1015 Ma and c. 2100 Ma. All samples investigated from the arc-related intrusive suite range in age between c. 470 Ma and 464 Ma (Fig. 3.6). Granite from Slieve Gallion (MRC92, 466.5 ± 3.3 Ma) and granodiorite from Craigbardahessiagh (MRC91, 464.9 ± 1.5 Ma) both contain Mesoproterozoic inherited zircons. Zircons analysed from quartz porphyry (dacite) from Copney (MRC90, 465 ± 1.7 Ma) and

tonalite from Craigballyharky (MRC128, 470.3 ± 1.9 Ma) both contain inherited components dated at c. 2100 Ma. Our U-Pb zircon age of the tonalite from Craigballyharky is within error of that proposed by Hutton et al. (1985).

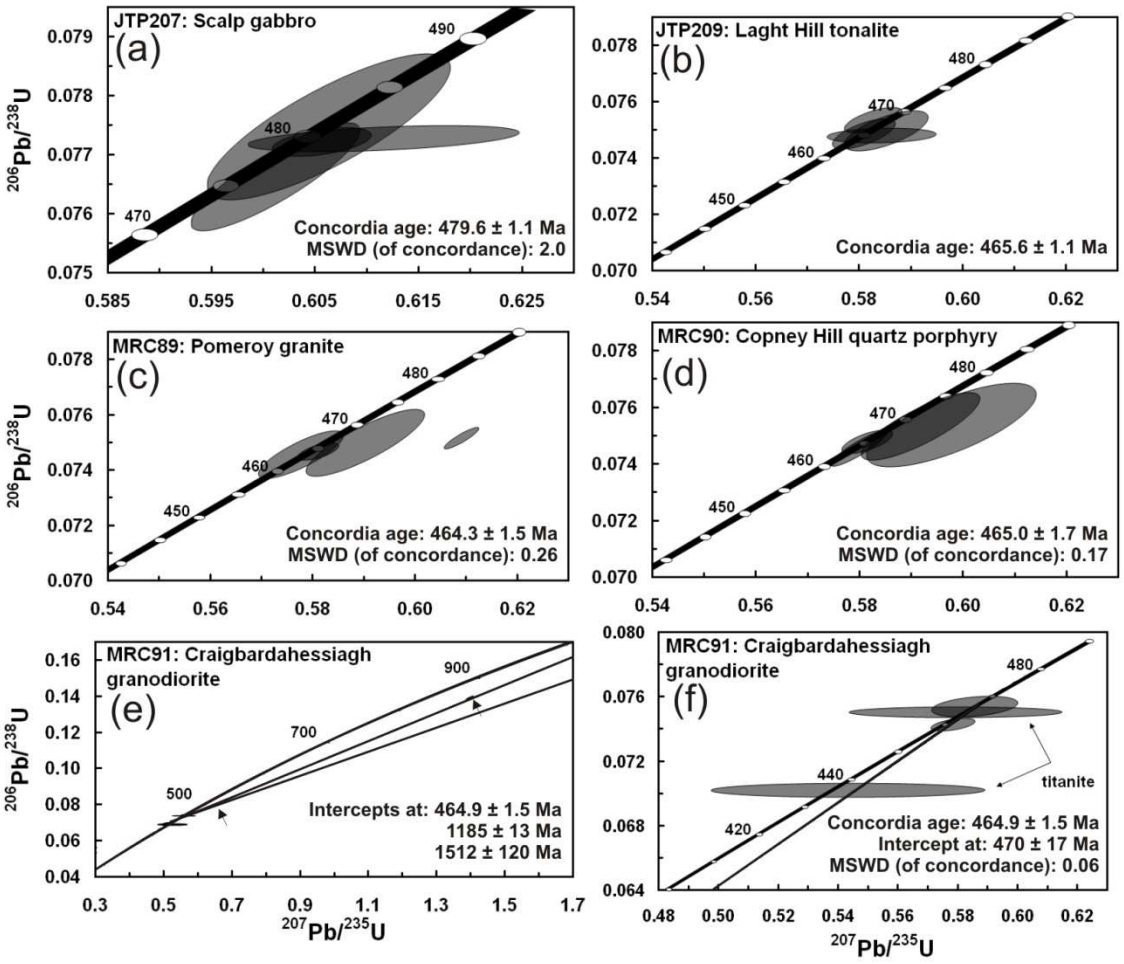

Figure 3.6. $^{206}Pb/^{238}U$-$^{207}Pb/^{235}U$ concordia diagrams. (a) JTP207 Scalp layered gabbro. (b) JTP209 Laght Hill tonalite. (c) MRC89 Pomeroy granite. (d) MRC90 Copney quartz porphyry. (e and f) All data-point error ellipses are 2 σ.

3.5. Discussion

Using the new U-Pb geochronology and geochemical data presented herein we can refine current models for the evolution of the Tyrone Igneous Complex and timing of the Grampian orogeny within Ireland.

3.5.1 Development of the Tyrone Plutonic Group

Field relationships and geochemical evidence including negative Nb anomalies and HFSE depletion suggests the Tyrone Plutonic Group represents the uppermost portions

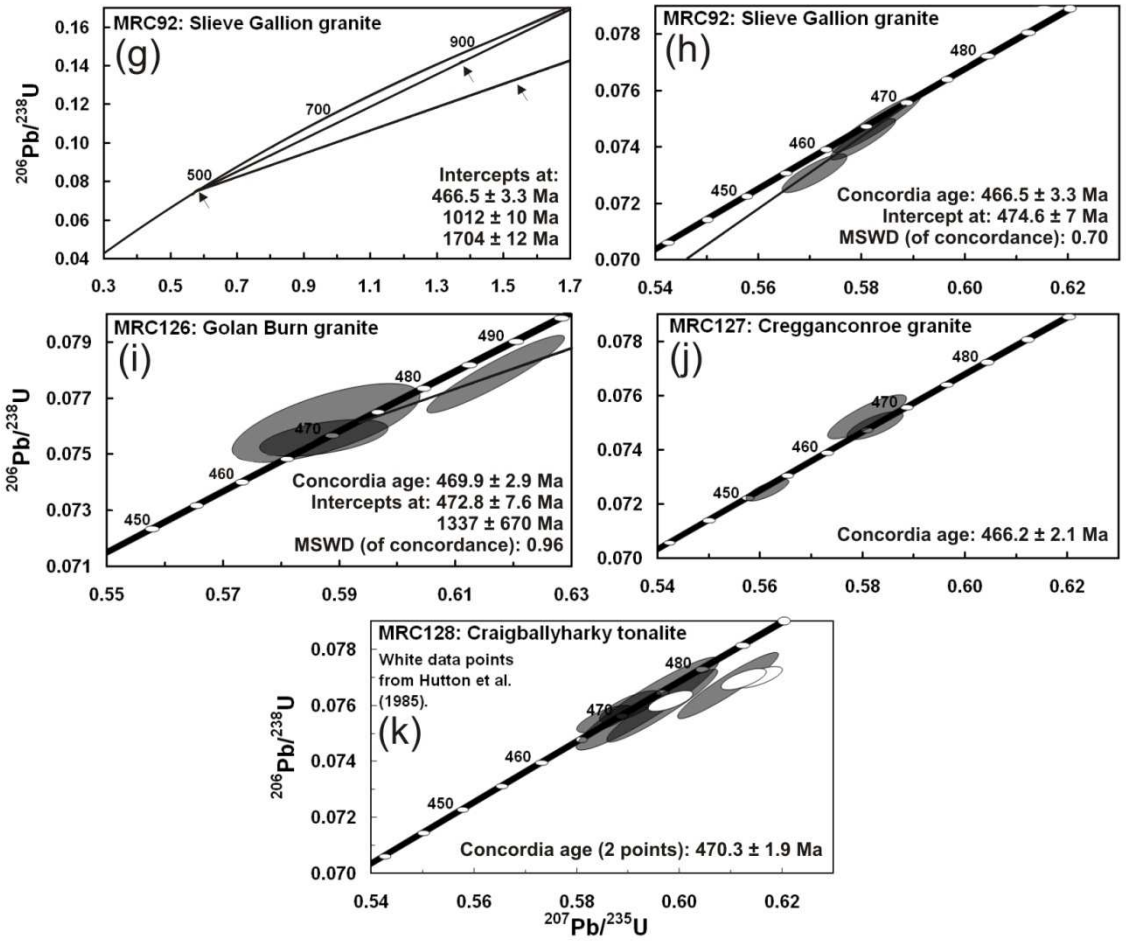

Figure 3.6. (continued) MRC91 Craigbardahessiagh granodiorite. (g and h) Slieve Gallion granite. (i) MRC126 Golan Burn tonalite. (j) MRC127 Cregganconroe quartz-monzodiorite. (k) Craigballyharky tonalite, with data of Hutton et al. (1985) also shown. All data-point error ellipses are 2σ.

of a suprasubduction zone ophiolite which was emplaced onto an outboard segment of Laurentia, the Tyrone Central Inlier, during the Grampian event. Though fault bounded, the Tyrone Plutonic Group and Tyrone Volcanic Group were previously considered contemporaneous based on a magma-mixing relationship between gabbro and 472 $^{+2}/_{-4}$ Ma tonalite at Craigballyharky (Hutton et al. 1985). However, recent work by Draut et al. (2009) reported an age of 493 ± 2 Ma for the Craigballyharky gabbro which is too old considering the magma-mixing relationship observed with c. 470 Ma tonalite (MRC128 at 470.3 ±1.9 Ma; also 472 $^{+2}/_{-4}$ Ma of Hutton et al. 1985). The zircon age of 493 Ma derived by Draut et al. is a $^{206}Pb/^{238}U$ age of three reversely discordant analyses. The reverse discordance is a probable analytical artifact of the SIMS data, possibly attributed to high uranium content of the zircons. Draut et al. (2009) also presented zircon ages from the Craigballyharky gabbro of approximately 470 Ma, but disregarded them as sample contamination. These three apparently younger zircons give a mean $^{206}Pb/^{238}U$ age of 473.2 ± 1.6 Ma (2σ). We therefore propose that the

Craigballyharky gabbro, which is LREE-enriched, is considerably younger than that proposed by Draut et al. (2009) and belongs to the arc-related intrusive (c. 470-464 Ma) suite. This scenario also agrees with the magma-mixing relationship observed and a $\varepsilon Nd_{t=470\ Ma}$ value of -5.89 (Draut et al. 2009).

Our new U-Pb zircon age determination from the layered gabbro at Scalp (JTP207, 479.6 ± 1.1 Ma), suggests that formation of the Tyrone Plutonic Group initiated at c. 480 Ma (Fig. 3.7a). Two inherited grains at c. 1015 and c. 2100 from the Scalp layered gabbro signify that material of this age was present at depth by c. 480 Ma. Their occurrence in the ophiolitic Tyrone Plutonic Group may reflect subduction of peri-Laurentian metasediments under the Tyrone ophiolite during formation or formation at a spreading centre adjacent to continental crust (see Chapter 5). Primitive geochemical characteristics presented herein (JTP207) are inconsistent with alternate explanations, which would require intrusion of the Scalp gabbro after ophiolite emplacement with xenocrystic zircons derived during emplacement through the Tyrone Central Inlier. As zircons of c. 2100 Ma are not present in abundance in peri-Laurentian sources (Cawood et al. 2007), including the Tyrone Central Inlier (Chew et al. 2008), their occurrence as xenocrysts may signify a difference in age signature of the basement underlying the region at this time.

3.5.2 Emplacement of the Tyrone Plutonic Group

Obduction of the Tyrone Plutonic Group onto the Tyrone Central Inlier must have occurred prior to c. 470 Ma (Fig. 3.7b-c). Two intrusions dated here at c. 470 Ma (MRC128, 470.3 ± 1.9 Ma; MRC126, 469.9 ± 2.9 Ma) cut the Tyrone Plutonic Group in its present structural position upon the Tyrone Central Inlier. At Craigballyharky, tonalite (MRC128) contains roof-pendants of LREE-depleted basalt derived from the Tyrone Plutonic Group. Whole rock and isotope geochemistry (see Draut et al. 2009) and zircon inheritance from these granitic to tonalitic stitching intrusions suggests they ascended through continental crust. Zircon inheritance (MRC128, MRC126) is compatible with derivation from the underlying Tyrone Central Inlier (Chew et al. 2008), although the source of the c. 2100 Ma signature remains elusive and may be due to discordance.

Lithological Unit	Age (Ma)	Calculated On	Additional Information
Scalp Layered Gabbro (JTP207)	479.6 ± 1.1	Three concordant zircon analyses	Two zircon fractions gave inherited ages of *c.* 1015 Ma (concordant) and 2100 Ma (upper intercept anchored at 479.6 Ma).
Laght Hill Tonalite (JTP209)	465.6 ± 1.1	Four concordant analyses	This tonalite provided a low yield of inheritance free zircon.
Golan Burn Tonalite (MRC126)	469.9 ± 2.9	Two concordant zircon analyses	Zircons separated from this sample were generally free from inheritance, but contained melt and mineral inclusions. Three zircon analyses yielded concordant to near-concordant analyses. Third analysis shows a small degree of inheritance.
Cregganconroe Quartz-monzodiorite (MRC127)	466.2 ± 2.1	Two concordant zircon analyses	A small proportion of zircons from this sample displayed visible inherited components and these were avoided. A third point was discordant along a shallow Pb-loss trajectory.
Craigballyharky Tonalite (MRC128)	470.3 ± 1.9	Two concordant zircon analyses	These new data are consistent with that of Hutton *et al.* (1985) for the same sample site. Plotting these new U-Pb data with those of Hutton *et al.* gives a lower intercept age of 471.2 $^{+2.0}/_{-2.3}$ Ma and an upper intercept of 2101 $^{+400}/_{-350}$ Ma indicating an inherited component at *c.* 2100 Ma.
Pomeroy Granite (MRC89)	464.3 ± 1.5	Two concordant zircon analyses.	The zircons analysed are predominantly acicular neocrystalline with rare visible inherited cores.
Copney Quartz Porphyry (MRC90)	465.0 ± 1.7	Two concordant zircon analyses.	Zircons recovered are very similar to those described for the Pomeroy granite. A discordia yields a lower intercept age of 464.6 ± 2.3 Ma and an upper intercept of *c.* 2150 Ma.
Craigbardahessiagh Granodiorite (MRC91)	464.9 ± 1.5	One analysis each of titanite and zircon are concordant	Zircons show both inheritance and Pb-loss, while some titanites analysed exhibit Pb loss. Most data plot near 465 Ma on the concordia diagram, but two zircon analyses show a significant Mesoproterozoic (*c.* 1185 - 1512 Ma) inherited component.
Slieve Gallion Granite (MRC92)	466.5 ± 3.3	One concordant analysis	This granite contains both core-free zircons and those with clearly visible cores. Two analyses of inherited zircons have Mesoproterozoic ages from *c.* 1000 Ma to 1700 Ma. Three analyses of core-free grains are concordant to slightly discordant, and yield an upper intercept age of 474.6 $^{+7.1}/_{-6.9}$ Ma. The most concordant analysis has an age of 466.5 ± 3.3 Ma and this is considered to be the best estimate of the intrusion age.
Previous Geochronology:			
Leaghan tonalite of Draut et al. (2009)	475 ± 10	Ten zircon analyses	U-Pb zircon SHRIMP. Archaean cores identified in three zircon grains using SHRIMP and LA-MC-ICP-MS.
Craigballyharky Gabbro of Draut et al. (2009)	493 ± 2	Three concordant zircon analyses	U-Pb zircon SHRIMP. The weighted mean $^{238}U/^{206}Pb$ age of the oldest three concordant ages from the gabbro was 493 ± 2 Ma. Three younger zircons with ages around *c.* 470 Ma were attributed to contamination.
Formil Rhyolite of Cooper et al. (2008)	473.0 ± 0.8	Three concordant zircon analyses.	U-Pb zircon TIMS. No inheritance noted by authors.
Craigballyharky Tonalite of Hutton et al. (1985)	471+2-4 Ma	Three zircon size fractions.	U-Pb zircon TIMS. Analyses are moderately discordant and define a discordia line with an upper intercept of 2030 $^{+630}/_{-500}$ Ma and lower intercept of 471 $^{+2}/_{-4}$ Ma.

Table 3.1. Calculated U-Pb zircon ages and additional information for analysed samples. Previously published U-Pb geochronology for Tyrone Igneous Complex also included.

Sillimanite-bearing metamorphic assemblages and leucosomes in paragneisses within the Tyrone Central Inlier are cut by granite pegmatites (Chew et al. 2008). The main fabric of the leucosomes yielded a ^{40}Ar–^{39}Ar biotite cooling age of 468 ± 1.4 Ma (Chew et al. 2008), which implies the Tyrone Central Inlier was metamorphosed and deformed under a thick, high-temperature succession prior to 468 ± 1.4 Ma (c. 670 ˚C, 6.8 kbar of Chew et al. 2008), consistent with ophiolite emplacement prior to c. 470 Ma (Fig. 3.7c). The lack of an ultramafic succession within the Tyrone Plutonic Group may be explained by post-obduction excision. In western Ireland, late extensional detachments associated with the Deep Park ophiolitic mélange juxtapose high-pressure, low-temperature blueschist facies rocks alongside lower-pressure Barrovian metasedimentary rocks (e.g. Chew et al. 2010).

Rocks of the South Mayo Trough, western Ireland, the fore-arc to the Lough Nafooey arc, record significant quantities of ophiolite-derived sediment entering the basin from c. 478 Ma (Chew 2009); systematic changes in Mg, Cr, Ni (Wrafter & Graham 1989) and detrital chrome spinel (Dewey & Mange, 1999) suggest the progressive unroofing on a ophiolite prior to the exhumation of the Grampian metamorphic belt (Fig. 3.7a). It is possible that obduction of the Tyrone Plutonic Group was also initiated at or shortly after c. 480 Ma. Evidence from certain ophiolites suggests that the timing of magmatism and obduction may be very closely spaced. For instance, age constraints from the Oman-UAE ophiolite indicate that the latest, seafloor, rift-related magmatism occurred less than 1 m.y. prior to obduction (Styles et al. 2006; Goodenough et al. 2010).

3.5.3 Development of the Tyrone Volcanic Group

Geochemical variation within the Tyrone Volcanic Group is predominantly characterized by transitional to calc-alkaline island-arc signatures, with strong enrichment in the LILE and LREE, high La/Sm and an increasing component of continentally derived material up sequence (see Draut et al. 2009). Th/Yb-Nb/Yb systematics imply the magmas were similar to eMORB in composition, but enriched in subduction zone components (e.g. Th, Cs, Rb, Ba, Pb). Draut et al. (2009) proposed the observed increase in La/Sm, LILE- and LREE-enrichment, and lowering of εNd_t values reflects the approach of the arc to the continental margin, subduction of continental detritus and magmatism during arc-continent collision. Although the strongly negative εNd_t values and LILE- and LREE-enrichment within the Tyrone Volcanic Group are also consistent with formation within an ensialic arc, the occurrence of primitive basalt at several stratigraphic horizons and the absence of zircon inheritance within the c. 473 Formil rhyolite (the only dated sample which *sensu stricto* belongs to the Tyrone

Volcanic Group, Cooper et al. 2008), suggest an oceanic-affinity for the early Tyrone arc or this area was founded upon thinned crust associated with rifting.

Tholeiitic rhyolite and silicified andesite from Beaghbeg and Bonnety Bush are unusual within the Tyrone Volcanic Group in that they display flat to 'U-shaped' chondrite-normalized REE profiles. According to Piercey (2007) tholeiitic rhyolites with U-shaped REE profiles typically form from the melting of mafic (to andesitic) substrates, and are often associated with forearc rifting, intra-arc rifting or rifting during the initiation of backarc basin activity. These lavas stratigraphically underly the 473 ± 0.8 Ma rhyolite of Cooper et al. (2008) and are closely associated with primitive tholeiitic and LREE-depleted island-arc basalt from Bonnety Bush. If the tholeiitic rhyolites of Beaghbeg mark the initiation of intra-arc rifting, then the LREE-depleted basalts of Bonnety Bush are a likely consequence of the same process, representing eruption onto the floor of the newly formed basin.

Basalt at Mountfield, towards the top of the sequence (Cooper et al. 2008), is borderline alkalic, of within-plate affinity, lacks the prominent HFSE depletion of subduction-related magmatism, and displays weakly positive εNd_t values. Draut et al. (2009) suggested this basalt formed at a late stage in the orogen when no strong underthrusting occurred, and is perhaps associated with a reversal in subduction polarity and/or gravitationally induced loss of the lower crust. Although the Mountfield basalts are geochemically consistent with formation in a seamount, their close association with strongly LILE- and LREE enriched rhyolite, argillaceous sedimentary rocks, abundant tuff and chert makes this unlikely.

3.5.4 Correlatives across the Grampian – Taconic orogen

In the British and Irish Caledonides, recent work on the Highland Border Ophiolite has demonstrated that generation of oceanic crust in Scotland was underway by 499 ± 8 Ma, with high-grade obduction-related metamorphism constrained to c. 490 ± 4 Ma (Chew et al. 2010). Similarly, in western Ireland high-grade metamorphism within the Deer Park Complex, part of the Clew Bay Complex (Fig. 3.1), was underway by 514 ± 3 Ma, prior to exhumation at 482 ± 1 Ma (Chew et al. 2010). Together these dates suggest a correlation between these ophiolites and the c. 510-501 Ma Lushs Bight Oceanic Tract of Newfoundland. As the Highland Border and Deerpark Complex ophiolites experienced metamorphism and deformation at least 15 m.y. before the Grampian event (c. 475-465 Ma), Chew et al. (2010) suggested early obduction may have occurred substantially outboard of the Laurentian margin onto peri-Laurentian microcontinental blocks.

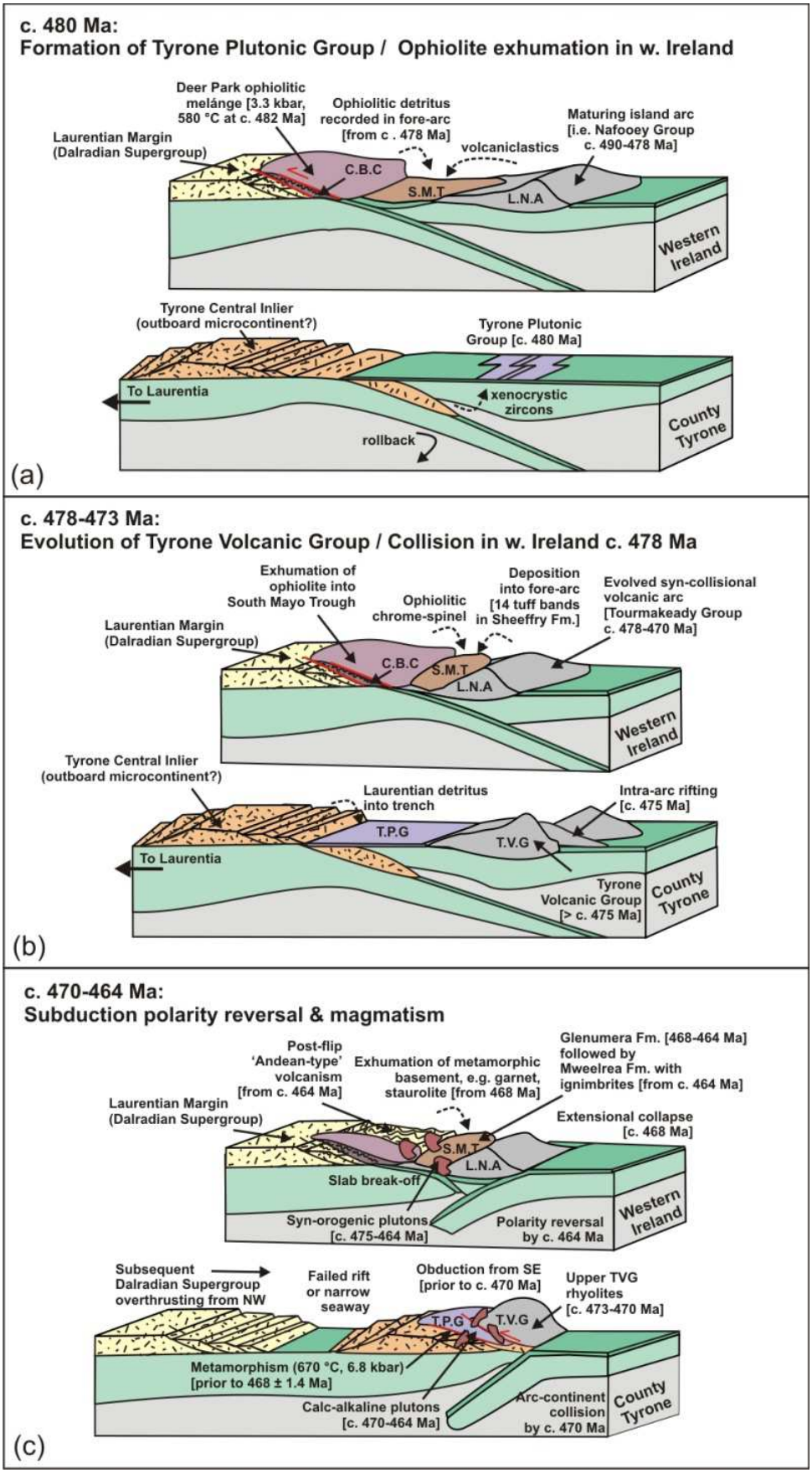
c. 480 Ma:
Formation of Tyrone Plutonic Group / Ophiolite exhumation in w. Ireland
Deer Park ophiolitic melánge [3.3 kbar, 580 °C at c. 482 Ma]
Ophiolitic detritus recorded in fore-arc [from c . 478 Ma]
Maturing island arc [i.e. Nafooey Group c. 490-478 Ma]
Laurentian Margin (Dalradian Supergroup)
volcaniclastics
C.B.C
S.M.T
L.N.A
Western Ireland
Tyrone Central Inlier (outboard microcontinent?)
Tyrone Plutonic Group [c. 480 Ma]
To Laurentia
xenocrystic zircons
rollback
County Tyrone
(a)
c. 478-473 Ma:
Evolution of Tyrone Volcanic Group / Collision in w. Ireland c. 478 Ma
Exhumation of ophiolite into South Mayo Trough
Ophiolitic chrome-spinel
Deposition into fore-arc [14 tuff bands in Sheeffry Fm.]
Evolved syn-collisional volcanic arc [Tourmakeady Group c. 478-470 Ma]
Laurentian Margin (Dalradian Supergroup)
C.B.C
S.M.T
L.N.A
Western Ireland
Tyrone Central Inlier (outboard microcontinent?)
Laurentian detritus into trench
Intra-arc rifting [c. 475 Ma]
T.P.G
T.V.G
To Laurentia
Tyrone Volcanic Group [> c. 475 Ma]
County Tyrone
(b)
c. 470-464 Ma:
Subduction polarity reversal & magmatism
Post-flip 'Andean-type' volcanism [from c. 464 Ma]
Exhumation of metamorphic basement, e.g. garnet, staurolite [from 468 Ma]
Glenumera Fm. [468-464 Ma] followed by Mweelrea Fm. with ignimbrites [from c. 464 Ma]
Laurentian Margin (Dalradian Supergroup)
Extensional collapse [c. 468 Ma]
S.M.T
L.N.A
Slab break-off
Syn-orogenic plutons [c. 475-464 Ma]
Polarity reversal by c. 464 Ma
Western Ireland
Subsequent Dalradian Supergroup overthrusting from NW
Failed rift or narrow seaway
Obduction from SE [prior to c. 470 Ma]
Upper TVG rhyolites [c. 473-470 Ma]
T.P.G
T.V.G
Metamorphism (670 °C, 6.8 kbar) [prior to 468 ± 1.4 Ma]
Calc-alkaline plutons [c. 470-464 Ma]
Arc-continent collision by c. 470 Ma
County Tyrone
(c)

Fig. 3.7 (previous page). Tectonic model for the formation of the Tyrone Igneous Complex during the Early to Middle Ordovician, illustrating contrasts with the Nafooey-Tourmakedy arc system of western Ireland. (a) Ophiolite exhumation in western Ireland occurs at c. 480 Ma, around the same time as maturation of the Lough Nafooey arc and formation of the Tyrone Plutonic Group. (b) Formation of the Tyrone Volcanic Group occurs between >c. 475 Ma and 470 Ma, synchronous with arc-continent collision in western Ireland and development of the Tourmakeady Group. (c) Subduction polarity reversal in western Ireland occurs prior to c. 464 Ma. In Northern Ireland, arc-continent collision occurs prior to the intrusion of a suite of c. 470-464 Ma continental intrusives. Ages after Draut et al. (2004). Dewey (2005), Cooper et al. (2008), Chew et al. (2008, 2010). C.B.C, Clew Bay Complex; L.N.A, Lough Nafooey arc; S.M.T, South Mayo Trough; T.P.G, Tyrone Plutonic Group; T.V.G, Tyrone Volcanic Group. Note: timescales of Ryan & Dewey (2011) were not available at time of publishing.

Following obduction, a primitive oceanic-arc, represented locally by the Lough Nafooey Group of western Ireland (Lough Nafooey arc), was active by c. 490 Ma (Chew et al. 2010; Fig. 3.7a). Granitoid boulders of this age indicate the assimilation of crustal material (εNd_t ~0, Chew et al. 2007). This ophiolite – oceanic arc complex is preserved within Newfoundland as the c. 490 Ma Baie Verte Oceanic Tract and the overlying c. 487-476 Ma oceanic Snooks Arm arc/backarc (see van Staal et al. 2007). Collision between the Lough Nafooey arc and the Laurentian margin occurred at c. 478 Ma (Fig. 3.7b). The Tourmakeady Group (c. 478-470) records volcanism during peak deformation and regional metamorphism within the Dalradian Supergroup (Draut et al. 2004).

Ages similar to the one of the Tyrone Plutonic Group (479.6 ± 1.1 Ma) have been reported from the Ballantrae Complex of Scotland (e.g. 483 ± 4 Ma, Bluck et al. 1980) and the Annieopsquotch ophiolite belt of Newfoundland (481 to 478 Ma, Dunning & Krogh 1985). Development of the Tyrone Plutonic Group at c. 480 Ma outboard of the Tyrone Central Inlier suggest a temporal correlation to the Annieopsquotch ophiolite belt, although all components of the Annieospquotch Accretionary Tract were progressively underplated to the Dashwoods microcontinent above a west-dipping subduction zone (Zagorevski et al. 2009a). As contacts between the Tyrone Plutonic Group, Tyrone Volcanic Group, and Tyrone Central Inlier are unexposed it remains unclear exactly how the Tyrone Igneous Complex was obducted.

Similarly, it is at present unclear whether the Tyrone Volcanic Group (and Tyrone Plutonic Group) developed above a north- or south-dipping subduction zone; both are plausible. In the former case, correlation to the Lough Nafooey arc of western Ireland would be permitted, as suggested by Draut et al. (2009) and shown in Figure 3.7. Current geochronology from the Tyrone Volcanic Group, although limited, is consistent

with correlation either to the Tourmakeady Group of western Ireland (the syn-collisional stage of the Nafooey arc, also see Draut et al. 2009), or the Buchans Group and correlative Roberts Arm Group of the Anniopsquotch Accretionary Tract (see Zagorevski et al. 2009a). Both the Buchans arc and its continental basement were accreted to the Dashwoods microcontinent prior to c. 468 Ma accompanied by the intrusion of dominantly arc-like continental plutons within the Annieopsquotch Accretionary Tract and adjacent Notre Dame Arc (Lissenberg et al. 2005). This intrusive suite is comparable in age to those seen in Tyrone (c. 470-464 Ma; Fig. 3.2), Connemara (Cliff et al. 1996; Friedrich et al. 1999; McConnell et al. 2009) and also those intruding the NE Ox Mountains Slishwood Division (Flowerdew et al. 2005). Future lithogeochemistry and U-Pb geochronology may shed further light on the development of this enigmatic arc system.

3.6 Conclusions

The U-Pb geochronology and geochemistry presented herein refine current models of formation for the Tyrone Igneous Complex and the Grampian orogenic system within the British and Irish Caledonides. Geochemical variation within the Tyrone Plutonic Group is typical for a suprasubduction zone ophiolite and our new U-Pb zircon age of 479.6 ± 1.1 Ma constrains the timing of development of the Tyrone Plutonic Group. Obduction onto the Tyrone Central Inlier must have occurred prior to 470.3 ± 1.9 Ma, although this may have been initiated as early as c. 480-478 Ma.

Geochemical analyses of the Tyrone Volcanic Group indicates that it formed within an oceanic volcanic arc receiving an increasing component of continentally derived material from the Laurentian margin. Magmatism associated with the maturing arc is strongly LILE- and LREE-enriched and calc-alkaline in nature. Tholeiitic rhyolites with U-shaped REE profiles and LREE-depleted basalts mark the initiation and formation of an intra-arc basin at c. 475 Ma. Arc-obduction can be constrained to c. 470 Ma in Northern Ireland. Eight new U-Pb ages from the arc-related intrusive suite range from 470.3 ± 1.9 to 464.9 ± 1.5 Ma and are associated with continued closure of the Iapetus Ocean.

Chapter 4: Episodic arc-ophiolite accretion in the Grampian orogeny

This chapter forms the basis of a paper currently in press: Hollis, S.P., Roberts, S., Cooper, M.R., Earls, G., Herrington, R., Condon, D.J., Cooper, M.J., Archibald, S.M., & Piercey, S.J. (2012). *Episodic arc-ophiolite emplacement and the growth of continental margins: Late accretion in the Northern Irish sector of the Grampian-Taconic orogeny.* GSA Bulletin, v. 124, p. 1702-1723. Some sections have been considerably expanded (e.g. stratigraphy, geochemistry). Note: references to Cooper et al. (2011) refer to chapter 3.

Abstract

In order to understand the progressive growth of continental margins and the evolution of continental crust we must first understand the formation of allochthonous ophiolitic and island-arc terranes within ancient orogens and the nature of their accretion. During the early Paleozoic closure of the Iapetus Ocean a diverse set of arc terranes, oceanic tracts and ribbon-shaped microcontinental blocks were accreted to the passive continental margin of Laurentia during the Grampian-Taconic orogeny. In the northern Appalachians in central Newfoundland, Canada, three distinct phases of arc-ophiolite accretion have been recognized. New field mapping, high-resolution airborne geophysics, whole-rock and Nd-isotope geochemistry, and U-Pb zircon geochronology within the Tyrone Volcanic Group of Northern Ireland has allowed all three episodes to be correlated into the British and Irish Caledondies. The Tyrone Volcanic Group (c. 475-469 Ma) is characterized by mafic to intermediate lavas, tuffs, rhyolite, banded chert, ferruginous jasperoid and argillaceous sedimentary rocks cut by numerous high-level intrusive rocks. Geochemical signatures are consistent with formation within an evolving peri-Laurentian island-arc/backarc which underwent several episodes of intra-arc rifting prior to its accretion at c. 470 Ma to an outboard peri-Laurentian microcontinental block. Outriding microcontinetal blocks play a fundamental role within the orogen, explaining the range of ages for Iapetan ophiolites and the timing of their accretion, as well as discrepancies between the timing of ophiolite emplacement and the termination of the Laurentian Cambrian-Ordovician shelf sequences. Accretion of the Tyrone arc and its associated suprasubduction zone ophiolite represents the third stage of arc-ophiolite emplacement to the Laurentian margin during the Grampian-Taconic orogeny in the British and Irish Caledonides.

4.1 Introduction

Understanding the temporal development of allochthonous ophiolitic and island-arc terranes within ancient orogens is an integral part of reconstructing the growth of continental margins (Zagorevski et al. 2009a) and the evolution of continental crust (Draut et al. 2004, 2009). The Caledonian–Appalachian orogen (Fig. 4.1) is one of the best preserved and most intensely studied examples of a long-lived collision zone within the geologic record (c. 510-400 Ma). Early Paleozoic closure of the Iapetus Ocean resulted in the accretion of a diverse set of arc terranes, ribbon-shaped microcontinents and oceanic tracts to the Laurentian margin during Grampian–Taconic orogenesis (e.g., van Staal et al. 1998; Dewey 2005; van Staal et al. 2007). Subsequent collisions with Baltica and Avalonia resulted in the assembly of Euramerica, prior to the construction of Pangaea during the Variscan–Alleghanian–Ouachita orogeny (Nance et al. 2010).

The Canadian Appalachians provide a clear template for the interpretation of analogous segments of the Laurentian margin. Within the analogous British and Irish Caledonides extensive post-Ordovician cover sequences obscure crucial relationships, and terrane excision and repetition are common. Despite recognized similarities across the orogen (Colman-Sadd et al. 1992; Winchester & van Staal 1995; van Staal et al. 1998), a number of specific terrane correlations remain contentious when extended into the British and Irish Caledonides. In contrast with the Grampian orogeny, three main phases of arc-ophiolite accretion have been recognized during the Taconic orogeny (van Staal et al. 2007).

Peri-Laurentian ophiolitic remnants of Iapetus are well documented within the Caledonides; and include the Ballantrae Ophiolite Complex (Oliver et al. 2002), Highland Border Ophiolite (Tanner & Sutherland 2007), Shetland Ophiolite (Flinn & Oglethorpe 2005), Deer Park Complex (Ryan et al. 1983), and Tyrone Plutonic Group (Hutton et al. 1985; Cooper et al. 2011) (Fig. 4.1, Fig. 4.2a). Collision between the passive continental margin of Laurentia and the Lough Nafooey arc of western Ireland (and any buried along strike equivalent in the Midland Valley terrane of Scotland) during the Grampian orogeny, was associated with the polyphase deformation and metamorphism of thick Laurentian sequences, such as the Neoproterozoic Dalradian Supergroup, and the emplacement of suprasubduction zone ophiolites (Dewey & Shackleton 1984). Examination of the Lough Nafooey arc and its associated forearc-successor basin, the South Mayo Trough, allows a detailed reconstruction for arc-continent collision in western Ireland (Clift & Ryan 1994; Dewey & Mange 1999; Mange et al. 2003; Draut et al. 2004; Mange et al. 2010). Timing of peak metamorphism and

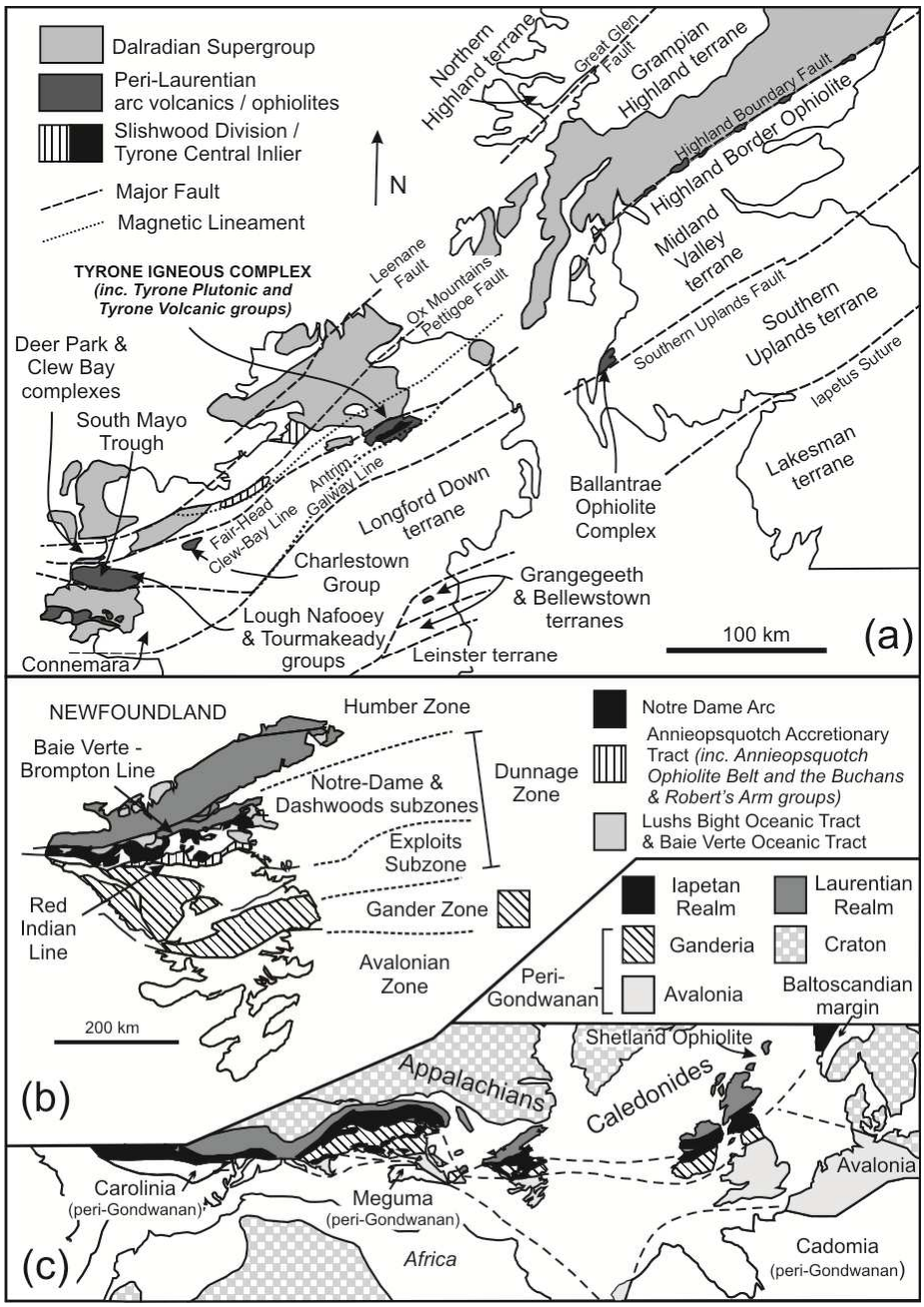

Figure 4.1 (a) Setting of the Tyrone Igneous Complex and other comparable ophiolite and volcanic arc associations in Britain and Ireland (after Cooper et al. 2011). (b) Simplified regional geology of Newfoundland (after van Staal et al. 2007). (c) Early Mesozoic restoration of North Atlantic region and Appalachian-Caledonian orogen (after Pollock et al. 2009).

regional deformation is constrained by Sm-Nd garnet ages of c. 473-465 Ma for Barrovian metamorphism in the Scottish Highlands (Baxter et al. 2002) and c. 475-468 Ma U-Pb zircon ages from synorogenic intrusive rocks in western Ireland (Friedrich et al. 1999a,b). Recent U-Pb zircon geochronology from the Irish Caledonides (e.g. Flowerdew et al. 2005; Chew et al. 2008) is consistent with the above interpretations.

The Tyrone Igneous Complex of Northern Ireland comprises a tectonically dissected ophiolite and a relatively complete island-arc sequence, accreted to an outboard segment of Laurentia during the Grampian orogeny. Despite its potential importance, research has been hampered by poor exposure and has therefore focused primarily on graptolite biostratigraphy and U-Pb zircon geochronology (e.g. Hartley 1936; Hutton & Holland 1992; Cooper et al. 2008, 2011). Recent work characterized the geochemical affinity of the Tyrone arc (=Tyrone Volcanic Group), its associated suprasubduction ophiolite (=Tyrone Plutonic Group) and a late suite of continental calc-alkaline intrusive rocks (Draut et al. 2009; Cooper et al. 2011; Fig. 4.2a).

New field mapping and high-resolution airborne geophysics, have enabled the volcanic succession to be placed in a detailed structural and stratigraphic context for the first time. This is complemented by an extensive new whole-rock and Nd-isotopic geochemical dataset, which combined with new and previous U-Pb zircon geochronology, details the evolution of the Tyrone arc during the Grampian phase of the Caledonian orogeny.

4.2 Regional geology

Rocks of Grampian age are exposed in the British and Irish Caledonides as inliers that represent geologically distinct terranes (Fig. 4.1a). The NE-SW trending Fair Head – Clew Bay Line of Ireland is generally accepted as the correlative to the Highland Boundary Fault of Scotland (Fig. 4.1a) and the Baie Verte – Brompton Line of the Newfoundland Appalachians (Max & Riddihough 1975; Max et al. 1983; Fig. 4.1b). This major tectonic structure separates metamorphosed, Laurentian rift and passive-margin sequences of the Hebridean, Northern Highland and Southern Highland terranes, from lower-grade remnants of the Iapetus Ocean to the south (Park et al. 2002; Strachan et al. 2002). The Midland Valley Terrane is bounded by the Highland Boundary Fault to the north and the Southern Uplands Fault to the south, and includes a series of allochthonous ophiolitic and island-arc components buried by extensive Upper Paleozoic cover rocks (Oliver et al. 2002). The Southern Uplands and Longford – Down terranes of Scotland and Ireland are widely considered to represent accretionary complexes associated with north-directed subduction and the post-Grampian closure of the Iapetus Ocean (Graham 2009).

The Tyrone Igneous Complex underlies c. 350km^2 within the Midland Valley Terrane and is one of the largest areas of ophiolitic and arc-related rocks exposed along the Laurentian margin of Iapetus within the British and Irish Caledonides (Fig. 4.1a). It is

broadly divisible into the ophiolitic Tyrone Plutonic Group (c. 480 Ma) and the younger arc-related Tyrone Volcanic Group (c. >475-469 Ma) (Cooper et al. 2008; Cooper et al. 2011; Fig. 2a). The northwestern edge of the Tyrone Igneous Complex is bounded by the Omagh Thrust, which has emplaced Neoproterozoic metasedimentary rocks of the Dalradian Supergroup above the Tyrone Volcanic Group (Alsop & Hutton 1993). Within the central regions of the complex, the structurally underlying metamorphic basement is exposed, termed the Tyrone Central Inlier (Geological Survey of Northern Ireland: GSNI 1979). A suite of granitic to tonalitic plutons (c. 470-464 Ma) intrude both the Tyrone Igneous Complex and Tyrone Central Inlier (Cooper et al. 2011).

The Tyrone Central Inlier (Fig. 2) is a thick monotonous sequence of psammitic and semi-pelitic paragneisses (Hartley 1933) termed the Corvanaghan Formation (GSNI 1995). A prograde metamorphic assemblage is characterized by biotite + plagioclase + sillimanite + quartz ± muscovite ± garnet in pelitic lithologies (Chew et al. 2008), with cordierite locally observed (Hartley 1933). A published ^{207}Pb-^{206}Pb zircon age of 467 ± 12 Ma from syn-tectonic leucosomes (Chew et al. 2008) suggest a Grampian age for the metamorphism and deformation of the Tyrone Central Inlier. Metamorphic cooling ages from post-tectonic muscovite-bearing pegmatites, quartz–K-feldspar porphyritic dykes and coarse grained quartzo-feldspathic sheets imply the Tyrone Central Inlier was metamorphosed and deformed under a thick, hot sequence (c. 670 ± 113 °C, 6.8 ± 1.7 kbar) prior to 468 ± 1.4 Ma (Chew et al. 2008).

Recent detrital zircon age profiling on a sample of psammitic gneiss identified prominent U-Pb age peaks at c. 1050 Ma, 1200 Ma and 1500 Ma, with more restricted peaks at c. 1800 Ma, 2500-2700 Ma and 3100 Ma (Chew et al. 2008). Deposition must have occurred after 999 ± 23 Ma, the age of the youngest dated zircon (Chew et al. 2008). These ages are consistent with a Laurentian-affinity for these Late Neoproterozoic metasedimentary rocks. Paleoproterozoic Nd model ages and a significant c. 2.5-2.7 Ga U-Pb zircon population may suggest an upper Dalradian Supergroup affinity for the Tyrone Central Inlier (Chew et al. 2008). The Tyrone Central Inlier is interpreted to represent part of an outboard segment of Laurentia, possibly detached as a microcontinent prior to arc-continent collision during the initial stages of the opening of Iapetus (Chew et al. 2008). Extremely negative εHf_{470Ma} values within zircon overgrowths imply hidden Archean crust may lie at depth under NW Ireland (Flowerdew et al. 2009).

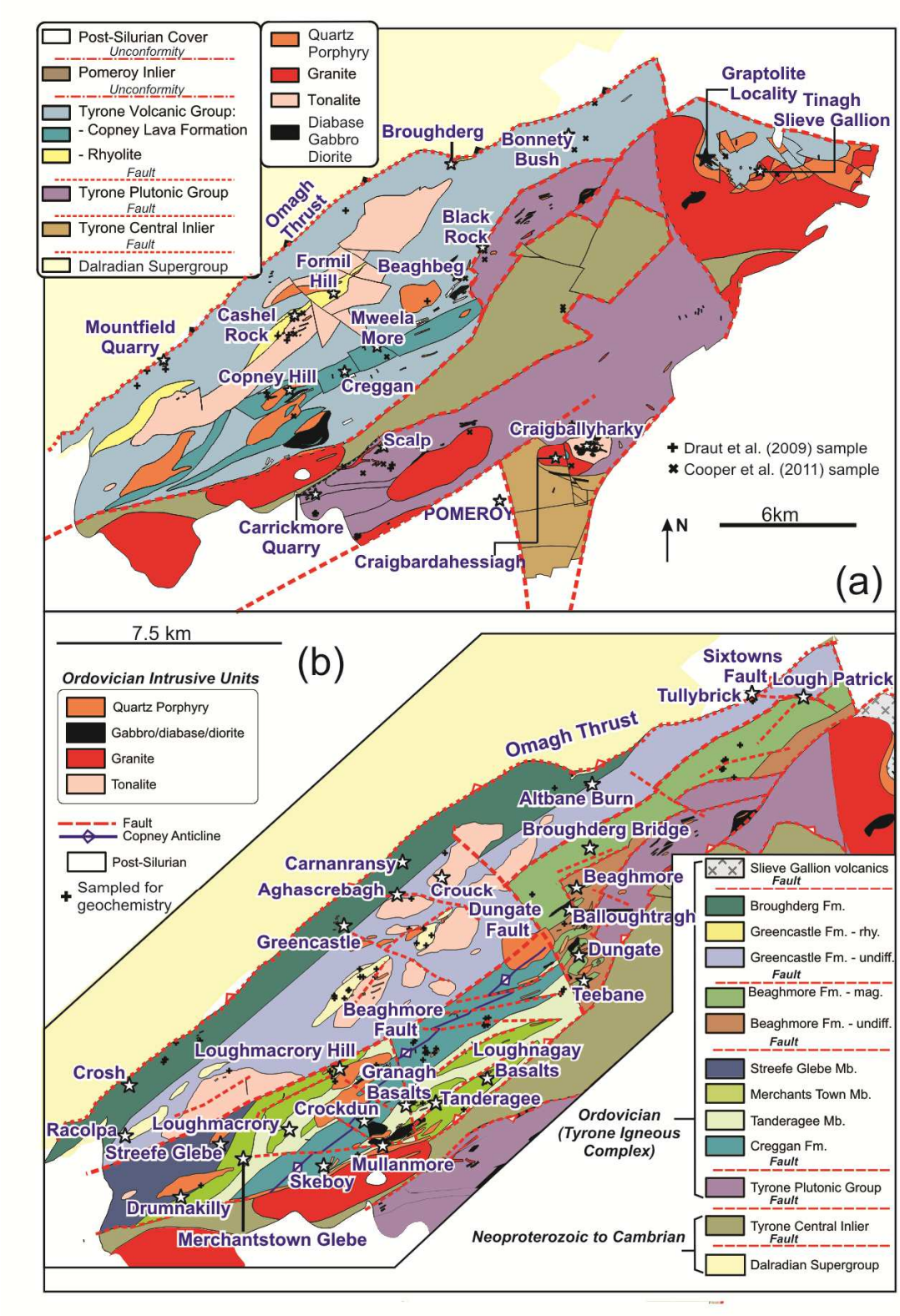

Figure 4.2 (a) Previous geological map of the Tyrone Igneous Complex (after GSNI 1979, 1983, 1995; Cooper et al. 2011). Crosses and plus symbols mark sample locations of Draut et al. (2009) and Cooper et al. (2011). Copney Pillow Lava Formation and Rhyolite are divisions within the Tyrone Volcanic Group. (b) New geological map of the Tyrone Volcanic Group.

Since the ophiolitic nature of the Tyrone Plutonic Group (Fig. 4.2a) was initially recognized by Hutton et al. (1985), a consensus has emerged that the group represents the uppermost portion of a dismembered suprasubduction zone ophiolite (Chew et al. 2008; Draut et al. 2009; Cooper et al. 2011). The Tyrone Plutonic Group is characterized by layered, isotropic and pegmatitic gabbros, sheeted dolerite dykes and the occurrence of rare pillow lavas (Angus 1970; Hutton et al. 1985; Cooper & Mitchell 2004). Layered gabbro has provided a U-Pb zircon age of 479.6 ± 1.1 Ma (Cooper et al. 2011). Accretion to the Tyrone Central Inlier must have occurred prior to the intrusion of a 470.3 ± 1.9 Ma tonalite which contains inherited Proterozoic zircons and roof pendants of ophiolitic material (Hutton et al. 1985; Cooper et al. 2011).

The Tyrone Volcanic Group forms the upper part of the Tyrone Igneous Complex and comprises mafic to intermediate pillowed and sheeted lavas, tuffs, rhyolite, banded chert, ferruginous jasperoid (ironstone) and argillaceous sedimentary rocks (Cooper & Mitchell 2004; Fig. 4.2a). The Tyrone Volcanic Group is interpreted to have formed within a peri-Laurentian island arc/backarc, which was accreted to the Tyrone Central Inlier following emplacement of the Tyrone Plutonic Group (Draut et al. 2009; Cooper et al. 2011). A high-precision U-Pb zircon age of 473 ± 0.8 Ma for rhyolite is in close agreement with biostratigraphic age constraints from the Slieve Gallion volcanic succession, which place the upper Tyrone Volcanic Group within the Australasian Castlemainian (Ca1) Stage of the uppermost Floian of the Lower Ordovician (c. 474-475 Ma: Cooper et al. 2008; Sadler et al. 2009). Large ion lithophile element (LILE) and light rare earth element (LREE) enrichment and strongly negative εNd_t values indicate the arc was formed close to or upon the Laurentian margin (either autochthonous margin or microcontinental block) and was contaminated by continental material (Draut et al. 2009; Cooper et al. 2011).

A late suite of I-type, calc-alkalic, tonalitic to granitic plutons intrude the Tyrone Igneous Complex and Tyrone Central Inlier associated with a syn- to post-collisional continental arc (Draut et al. 2009). Recent U-Pb zircon geochronology indicates these were intruded between c. 470 and 464 Ma (Cooper et al. 2011). Strong LILE- and LREE-enrichment, coupled with zircon inheritance and strongly negative εNd_t values, suggest that assimilation of Dalradian affinity metasedimentary rocks was an integral part of their petrogenesis (Draut et al. 2009; Cooper et al. 2011). Similar plutons intrude Connemara (Cliff et al. 1996; Friedrich et al. 1999a,b; McConnell et al. 2009) and the NE Ox Mountains Slishwood Division (Flowerdew et al. 2005) (Fig. 4.1a).

The Late Ordovician to Early Silurian Pomeroy Inlier unconformably overlies both the Craigbardahessiagh granodiorite (464.9 ± 1.5 Ma, Cooper et al. 2011) and Tyrone Plutonic Group. Uplift and erosion of the Tyrone Central Inlier and Tyrone Igneous Complex occurred by Middle Caradoc times (Cooper & Mitchell 2004). The Lisbellaw Inlier exposed some 50 km to the SW, comprises a 300m thick succession of fossiliferous mudstone and silty mudstone (with some greywacke beds). A 40 m thick clast-supported conglomerate near the middle of the succession is dominated by purplish and greenish-grey quartzite, with minor vein quartz, jasper and granite. Palaeocurrent data imply sediments were derived from the N and NE (Cooper & Mitchell 2004).

4.3 Tellus geophysics

Understanding the structural and stratigraphic relationships between and within the Tyrone Igneous Complex and Tyrone Central Inlier has previously been hampered by poor exposure. However, a recently completed regional airborne geophysical survey over Northern Ireland has helped in resolving the crustal structure of the region. Magnetic, radiometric and electromagnetic (EM) data were acquired over the entirety of Northern Ireland during 2005-2006 as part of the Tellus Project (see GSNI 2007). Total magnetic intensity (reduced to pole), first vertical derivative and analytic signal maps over the Tyrone Igneous Complex are shown in Figure 4.3a-c. Two frequency EM datasets (3 and 14 kHz) were acquired over the Tyrone Igneous Complex and the western half of Northern Ireland in 2005 (Fig. 4.3d) and four-frequency datasets (0.9, 3, 12 and 25 kHz) across the eastern half in 2006. Further detail on survey specification and geophysical data processing are summarised within Beamish et al. (2007) and Chapter 2.

The lower Tyrone Volcanic Group, Tyrone Plutonic Group and Tyrone Central Inlier are all characterized by short-wavelength magnetic anomalies (Gunn et al. 2008). Within the lower Tyrone Volcanic Group, laterally extensive magnetic highs correspond to units of pillowed, massive and sheet-flow basalt (e.g. Copney Pillow Lava Formation; GSNI 1979, 1995), magnetite-rich jaspers and local bodies of magnetite-bearing gabbro (e.g. at Beaghmore) and dolerite (e.g. at Tanderagee) (Figs. 4.2 and 4.4). By contrast, the upper Tyrone Volcanic Group is predominantly non-magnetic, except within the vicinity of Cashel-Formil and Broughderg where gold and base-metal mineralization is prevalent (Leyshon and Cazalet 1978; Clifford et al. 1992; Gunn et al. 2008). Geophysical characteristics of the Tyrone Plutonic Group and Tyrone Central Inlier will be discussed in subsequent chapters. Faulted contacts between the Tyrone Plutonic Group, Tyrone Volcanic Group and Tyrone Central Inlier are best discriminated

with the EM imagery, with boundaries corresponding well to previous mapping (GSNI 1979, 1995). New subdivisions within the Tyrone Volcanic Group recognized through Tellus geophysics and fieldwork are outlined below. Major ENE-trending reactivated Caledonian and Carboniferous faults (e.g. Omagh Thrust, Tempo-Sixmilecross Fault) are apparent from sharp magnetic features which offset Palaeogene dykes (Cooper et al. 2012), as are previously unrecognized faults such as the herein named Beaghmore, Dungate and Sixtowns faults which truncate basaltic subdivisions of the Tyrone Volcanic Group.

4.4 Stratigraphy

Combined with recent geological survey, the Tellus Geophysical Survey of Northern Ireland has allowed the Tyrone Volcanic Group to be placed in a detailed structural and stratigraphic framework for the first time. New formations have become apparent and the Tyrone Volcanic Group has been further subdivided (Fig. 4.2b). As previously only one formal stratigraphic unit, the Copney Pillow Lava Formation, was recognized (GSNI 1995), we herein introduce several new formations. Stratigraphic terminology is according to the International Stratigraphic Guide and the North American Stratigraphic Code. South of the Beaghmore Fault, three formations have been recognized within the lower Tyrone Volcanic Group: the Creggan, Loughmacrory and Beaghmore formations (Fig. 4.2b). The Dungate Fault separates the Creggan and Loughmacrory formations to the west from the Beaghmore Formation to the east of this structure (Fig. 4.2b). This study has redefined the boundaries of the Copney Pillow Lava Formation (GSNI 1979, 1995) and renamed this unit based on its type locality to the Creggan Formation. Consequently, the former name is redundant. North of the Beaghmore Fault, the upper Tyrone Volcanic Group is divided into the Greencastle and Broughderg formations (Fig. 4.2b). Formations do not correlate across the major faults and consequently three distinct structural blocks have been identified: Southwestern – Creggan and Loughmacrory formations; Eastern – Beaghmore Formation; Northwestern – Greencastle and Broughderg formations (Fig. 2b). Each formation is summarized in Figure 4.4 along with the geochemical affinity of the mafic and felsic units present (discussed below). A variety of intrusive units cut the Tyrone Volcanic Group (Figs. 4.2b and 4.4). All units in the lower Tyrone Volcanic Group have been subjected to varying degrees of hydrothermal alteration and are characterized by regional sub- to greenschist-facies metamorphic assemblages (see Chapter 7).

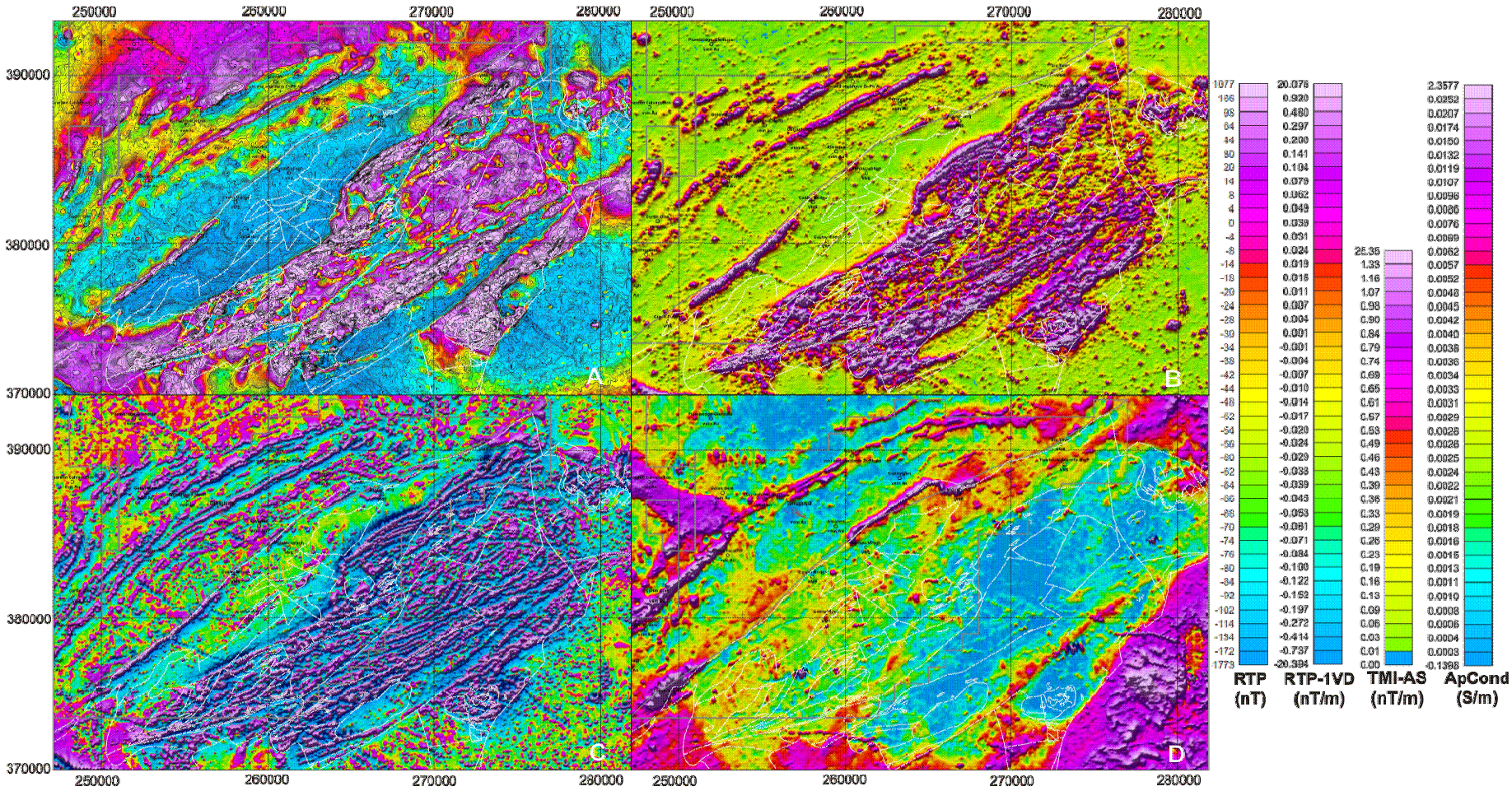

Figure 4.3. Results of the Tellus airbourne geophysical survey of Northern Ireland. (a) Total magnetic intensity map, reduced to pole (RTP), (b) Total magnetic intensity, analytic signal (TMI-AS), (c) Total magnetic intensity map, first vertical derivative (RTP-1VD), (d) EM low frequency (ApCond). All maps show original GSNI linework (GSNI 1979, 1983, 1995) as in Figure 4.2a. Grid references are according to Irish Grid. See Chapter 7 maps for interpreted linework.

4.4.1 Lower Tyrone Volcanic Group

The lower part of the Tyrone Volcanic Group is restricted to south of the Beaghmore Fault (southwestern and eastern blocks) and is dominated by basaltic to andesitic lavas and volcaniclastic rocks, with subsidiary agglomerate, layered chert, ferruginous jasperoid (ironstone), finely-laminated argillaceous sedimentary rocks and rare rhyolite breccia, deformed into the SW-NE trending upright Copney Anticline (Fig. 4.2).

Creggan Formation

The Creggan Formation, exposed along the length of the Copney Anticline, is characterized by pillowed, massive and sheet-flow basalt/basaltic andesite, with lesser layered chert, basaltic agglomerate and rare mafic volcaniclastic crystal tuff, associated with dykes of dolerite and diorite (Fig. 4.4). The current extent of the Creggan Formation is similar to an unnamed unit mapped by Hartley (1933). It is at least 1.3 km thick with its lower portions unexposed, and extends along strike for approximately 12 km.

Pillow lavas of fine- (locally plagioclase-phyric) to medium-grained ophitic basalt, with well-exposed triple junctions, characterize the lower part of the formation (Fig. 4.5a). Pale pink to red chert and fine-grained hyaloclasite breccias crop out between pillow structures (Cooper & Mitchell 2004). Pillows are typically <40 cm in width (though may be as large as 1.5m), variably epidotised, vesicular and may show radial cooling fractures. Type localities for the formation are well exposed at Creggan, Mweela More and Copney. Rare occurrences of thin, chloritised and feldspathic crystal tuff beds and white/cream or grey-and-green-banded chert are exposed at Mweela More (Fig. 4.5c).

Within the upper part of the formation vesicular massive and sheet-flow basalt dominates, locally associated with volcanic agglomerate and subordinate weakly-foliated chloritised crystal tuff. Volcanic agglomerate (Fig. 4.5b) contains fine-grained chloritised basalt and rare jasper. Units vary between clast and matrix supported varieties with subrounded to angular fragments (typically <20 cm in length) within a coarse grained chloritic matrix of basaltic tuff (Cooper & Mitchell 2004). Thin (<10 m) dykes of diorite and dolerite cut the formation.

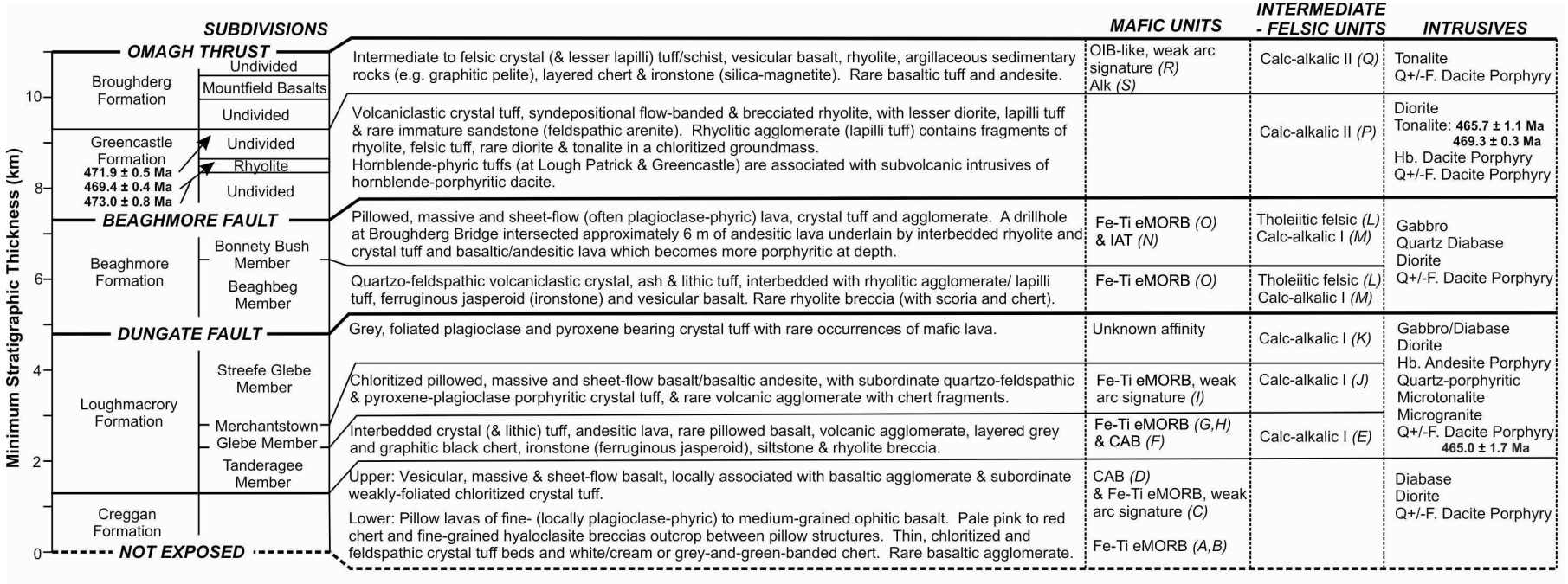

Figure 4.4. Stratigraphy of the Tyrone Volcanic Group. All unit thicknesses are minimum values. This study has redefined the boundaries of the Copney Pillow Lava Formation (GSNI 1979, 1995) and renamed this unit to the Creggan Formation. The base of the overlying Loughmacrory Formation is marked by the first occurrence of hornblende-porphyritic andesite, ironstone, argillaceous sedimentary rocks, rhyolite breccia or quartzo-feldspathic volcaniclastic tuff. The 'Granagh Basalts' have been placed within the Tanderagee Member of the Loughmacrory Formation and are believed to be broadly equivalent to similar rocks exposed on Copney Hill ('Copney Basalts'). The 'Loughnagay Basalts' are believed to be broadly equivalent to the Merchantstown Glebe Member. The base of the Broughderg Formation is placed at the first occurrence of chert, argillaceous sedimentary rocks or basalt north of the Beaghmore Fault. Mafic and intermediate to felsic petrochemical suites refer to those discussed in geochemistry section. Letters in parantheses refer to geochemical plots of figure 4.7.

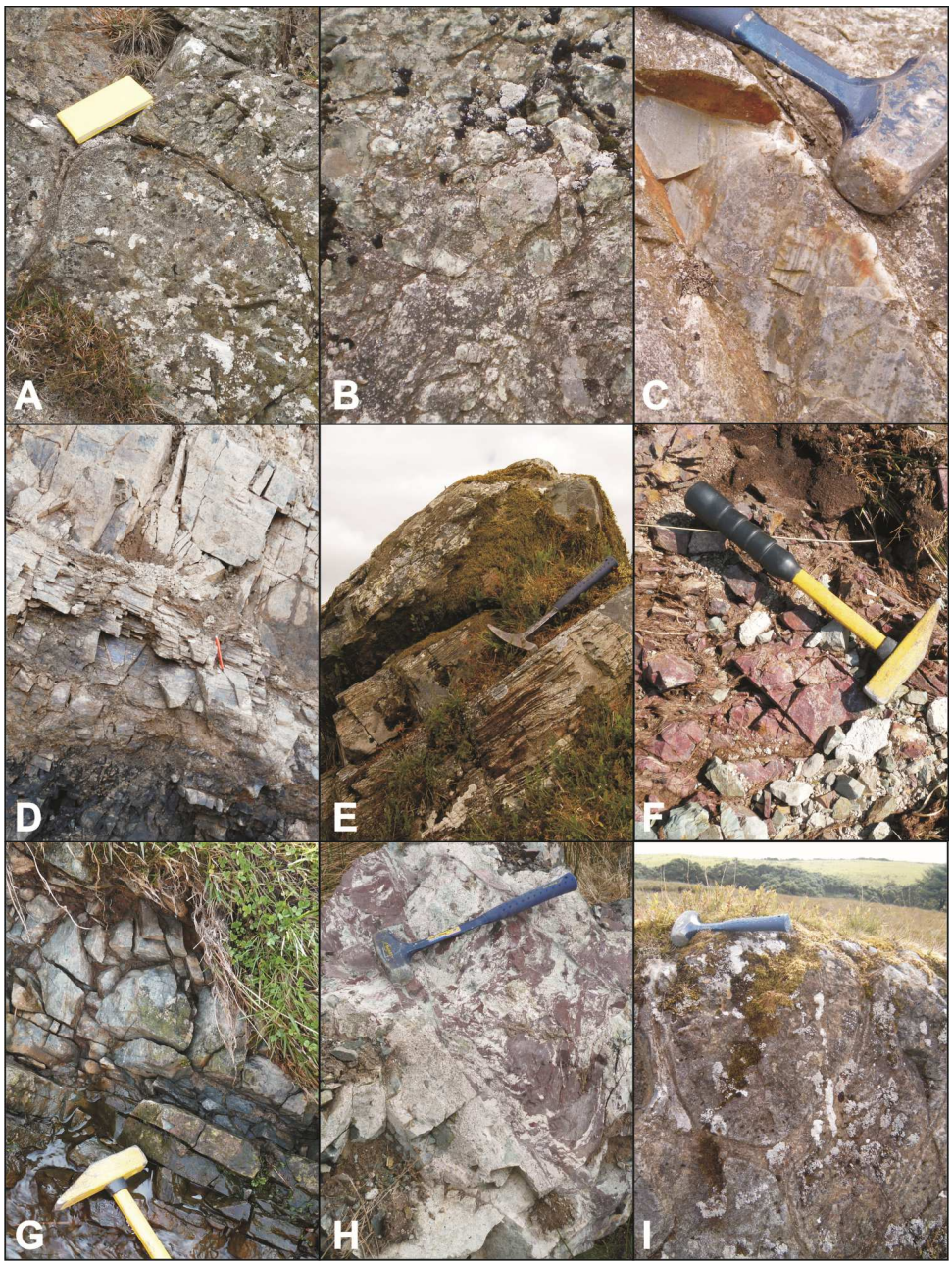

Figure 4.5. Field photographs from the Tyrone Volcanic Group. (a) Pillow lavas typical of those exposed at Mweela More and Creggan (Creggan Formation). (b) Basaltic agglomerate exposed at Creggan (Creggan Formation). (c) Layered chert associated with thin horizons of crystal and lithic tuff at Mweela More (Creggan Formation). (d) Interbedded tuff, siltstone and chert at Tanderagee (Tanderagee Member – Loughmacrory Formation). (e) Andesite and layered chert at Tanderagee (Tanderagee Member - Loughmacrory Formation). (f) Ironstone and layered grey chert at Tanderagee (Tanderagee Member – Loughmacrory Formation). (g) Bedded tuffs at Tanderagee (Tanderagee Member – Loughmacrory Formation). (h) Angular clasts of laminated red siltstone within green-foliated andesite, west of Loughnagay (Tanderagee Member - Loughmacrory Formation). (i) Pillowed lava at Loughmacrory Hill (Merchantstown Glebe Member - Loughmacrory Formation).

Figure 4.5. (continued) (j) Vesicular sheeted basalt at Teebane (Beaghbeg Member – Beaghmore Formation). (k) Rhyolite breccia at Teebane with chert and scoria fragments (Beaghbeg Member – Beaghmore Formation). (l-m) Ironstone at Beaghbeg (Beaghbeg Member – Beaghmore Formation). (n-o) Sheared agglomerate at Beaghbeg with rhyolitic clasts (Beaghbeg Member – Beaghmore Formation). (p) Tuff with quartz pebbles (Beaghbeg Member – Beaghmore Formation). (q-r) Ironstone at Bonnety Bush (Bonnety Bush Member – Beaghmore Formation).

Figure 4.5. (continued) (s-t) Flow banded and sheared rhyolite at Cashel Rock with xenoliths of diorite and rhyolite (Greencastle Formation). (u) Tonalite xenolith in flow-banded and sheared rhyolite at Cashel Rock (Greencastle Formation). (v) Sheared felsic tuff near Racolpa (Greencastle Formation). (w) Scrappy outcrop of chloritic tuff (typical of upper Greencastle Formation). (x) Sheared silicified and sericitic tuff in Carnaranransy Burn (lowermost Broughderg Formation). (y) Boulder of reduced ironstone with bedded pyrite from Broughderg (Broughderg Formation). (z-a*) Thrusting and graphitic pelite at McNally's Bridge near the Omagh Thrust (upper Broughderg Formation).

Loughmacrory Formation

Obscured by drift across much of its length, the overlying Loughmacrory Formation is exposed as a >3.5 km thick sequence dominated by interbedded andesitic lava and tuff which extends for across a maximum strike length of 13 km (Figs. 4.2b, 4.4). Its base is marked by the first occurrence of hornblende-phyric andesite, ferruginous jasperoid (ironstone), argillaceous sedimentary rocks or thick tuff. The top of the formation is absent north of the Creggan Formation, cut by the Beagmore Fault. Three broad divisions are recognized: the Tanderagee, Merchantstown Glebe, and Streefe Glebe members; named after their type localities. Intrusions of hornblende-andesite porphyry, quartz-porphyritic microtonalite, diorite, ophitic dolerite/gabbro and microgranite cut the formation, some of which are synvolcanogenic (see Chapter 7).

The Tanderagee Member directly overlies the Creggan Formation and comprises a 1 km thick sequence of interbedded crystal (and lithic) tuff (Fig. 4.5g), andesitic lava, rare pillow basalt, volcanic agglomerate, layered grey and graphitic black chert, ferrugineous jaspeoid (Fig. 4.5f), argillaceous sedimentary rocks (Fig. 4.5d-e, h) and rhyolite breccia (Fig. 4.4). Exposure is primarily confined to a series of gravel pits and stream sections between Tanderagee and Mullamore, and isolated outcrops around the townland of Loughmacrory. Tuff varies between well-sorted, coarse and finely-bedded to fine and foliated. Crystal tuffs include hornblende-, pyroxene-plagioclase, and quartzo-feldspathic bearing types. Original sedimentary structures are rare, although fine laminae, cross-laminae and grading in fine chloritic tuff can be observed. Imbricated sub-rounded pebbles of grey-chert and angular to sub-rounded ironstone also occur in coarse tuff. Lavas are typically plagioclase or hornblende-phyric, vesicular and sheeted. Pillow structures are rare but present on the W side of Copney Hill and N of Loughmacrory. Volcanic agglomerate is similar to that within the Creggan Formation, although clasts of chert, jasper and rhyolite can be locally dominant.

Originally mapped as part of the Copney Pillow Lava Formation (GSNI 1979, 1995), the Merchantstown Glebe Member is a 500 m thick sequence of chloritized pillowed (Fig. 4.5i), massive and sheet-flow basalt/basaltic andesite, with subordinate quartzo-feldspathic and pyroxene-plagioclase porphyritic crystal tuff and rare volcanic agglomerate with chert fragments (Fig. 4.4). Exposure is of poor quality and infrequent, confined predominantly to farmland, although its mapped extent corresponds well with a strong magnetic high revealed through Tellus geophysics (Fig. 4.3). The overlying Streefe Gleebe Member is a 2 km thick succession of grey, foliated plagioclase and pyroxene bearing crystal tuff intruded by a large body of quartz-porphyry (Figs. 4.2b, 4.4). Rare occurrences of mafic lava may be more extensive than

current exposure suggests as the majority of the succession is highly magnetic (Fig. 4.3).

Beaghmore Formation

The Beaghmore Formation is approximately 2.5 km thick and broadly divisible into the Beaghbeg Member and stratigraphically younger Bonnety Bush Member. The formation is characterized by crystal, aphyric and lapilli tuff, agglomerate, basalt and ferruginous jasperoid (ironstone; Fig. 4.5l); and is intruded by bodies of quartz dolerite, diorite and gabbro (Fig. 4.4).

The stratigraphically older Beaghbeg Member is composed predominantly of crystal and lithic tuff, interbedded with rhyolitic agglomerate (Fig. 8d), ironstone (Fig. 4.5l-m) and vesicular basalt (4.5j), exposed immediately east of the Dungate Fault with a strike length of less than 3.5 km (Figs. 4.2b, 4.4). Agglomerate contains angular isolated clasts up to 70 cm of pale pink to grey felsite (Fig. 4.5n-o) and rare banded cream chert and ironstone. Tuffs are typically fine-grained, quartzo-feldspathic and extensively sercitised and chloritised. Several units have abundant well-rounded pebbles of quartz up to 3 cm in length (Fig. 4.5p). Other beds contain large angular blocks of basalt and/or fragments of ironstone. Sills of quartz dolerite, diorite and gabbro cut the member.

The overlying Bonnety Bush Member is strongly defined from Tellus magnetics (total magnetic intensity, reduced to pole: 4.2b, 4.3), with a strong magnetic high between Evishessan and Brackagh for approximately 13 km. Exposure is poor and infrequent, with basaltic lava, crystal tuff and agglomerate confined to stream sections and isolated outcrops amongst substantial drift. Pillowed, massive and sheet-flow, vesicular and/or plagioclase-phyric basalt is best exposed around Evishessan Bridge, Keerin Road and between Beaghmore and Crockglass. Ennex drillhole DDH-107-1 at Broughderg Bridge intersected approximately 6 m of andesitic lava underlain by interbedded rhyolite and crystal tuff and basaltic-andesitic lava which becomes more porphyritic at depth. At Bonnety Bush remote outcrops and boulders of foliated basaltic tuff and agglomerate with lesser ironstone form a low rise on a flat glacial outwash plain. Foliated basaltic tuff and sheared agglomerate are replaced by green and purple chlorite with inclusions of epidote set in a matrix of quartz, feldspar and white mica. These are overlain by ironstone (Fig. 4.5q-r) and pale green to grey foliated chloritic tuff. Lapilli of felsic material and lenticular lenses of purple to maroon ironstone are present within the latter. Overlying andesitic tuffs are strongly silicified. Ironstone float occurs for ~12 km along strike from Boley to

Beaghmore/Evishessan Bridge (coincident with ground magnetic anomalies), suggesting these horizons are laterally extensive.

Directly south of Beaghbeg, around Teebane and Dungate, is a well-exposed south-dipping sequence of sheeted chloritised basalt (Fig. 4.5j) interbedded with lesser volcaniclastic tuff, feldspar-phyric andesite, volcanic agglomerate (lapilli tuff) and rare rhyolite breccia. The gradational southerly replacement of volcaniclastic tuff by basalt implies the succession can be ascribed to the upper Beaghbeg Member. Rare rhyolitic breccias at Teebane are matrix supported with small (<7 cm) angular fragments of scoria, chert and felsic volcanics (Fig. 4.5k).

4.4.2 Upper Tyrone Volcanic Group

North of the Beaghmore Fault, the Greencastle and Broughderg formations of the upper Tyrone Volcanic Group are exposed as a conformable sequence dipping between 35 and 60° NW (Fig. 4.2b). Dalradian metasedimentary rocks of the Argyll Group (see McFarlane et al. 2009) overlie the succession along its western edge separated by the low angle Omagh Thrust, which dips around 30° NW (Alsop & Hutton 1993). The cross cutting nature of the Omagh Thrust provides a relatively complete section through the upper part of the Tyrone Volcanic Group, which has been metamorphosed to chlorite-grade greenschist facies. Further south, subgreenschist-facies metamorphic assemblages are preserved around Formil (Fig. 4.2). Hydrothermal alteration and associated Zn-Pb-Cu(Au) mineralization are widespread within the Greencastle and Broughderg formations. Mineralization is characterized by pyrite-sphalerite-galena-chalcopyrite in locally silicified, sericitic and/or chloritic tuff/rhyolite (e.g. Fig.4.5w) (Leyshon & Cazalet, 1978; Clifford et al. 1992; Gunn et al. 2008). Between Racolpa and Broughderg bodies of tonalite and sills of quartz ± feldspar porphyry intrude both formations (Fig. 4.2).

Greencastle Formation

The Greencastle Formation is a relatively thick succession dominated by chloritic, locally sericitized and siliceous quartzo-feldspathic crystal tuff (Fig. 4.5v-w), flow banded and brecciated rhyolite (Fig. 4.5s-u), rhyolitic lapilli tuff, lesser diorite, rare arkosic sandstone and localized occurrences of hornblende-phyric tuff (Fig. 4.4). The formation extends for a strike length of approximately 30 km between Racolpa and Brackagh (Fig. 4.2). The flow-banded rhyolites are strongly deformed and sheared. Intermittent exposures over approximately 15 km between Formil Hill and Racolpa are unlikely to represent a single depositional unit; several intrusions and/or flows are most likely. At depth, rhyolite contains large angular fragments of diorite and is cut by thin sheets of quartz ± feldspar porphyry (e.g. DDH-106-220 and DDH-106-223). Dark

green schistose tuffs can contain feldspar crystals up to 5 mm in length. At Lough Patrick and around Greencastle hornblende-phyric tuffs are present associated with subvolcanic intrusives of hornblende-phyric dacite. Rhyolitic agglomerate near Mulnafye contains fragments of flow-banded rhyolite, felsic tuff and rare xenoliths of diorite and tonalite in a chloritised groundmass.

Between Oxtown and Broughderg laccolithic (?) bodies of tonalite and sills of quartz ± feldspar porphyry intrude the upper Tyrone Volcanic Group. Field-relations and U-Pb zircon geochronology imply several generations of tonalite occur within the succession. At Cashel Rock two generations of tonalite are easily identified; early tonalite is foliated and present as xenoliths within both a younger unfoliated tonalite and syndepositional rhyolite of the Greencastle Formation (Fig. 4.5u). Unfoliated tonalite from Cashel Rock has produced a U-Pb zircon age of 465.6 ± 1.1 Ma (Cooper et al 2011). Abundant sills of quartz ± feldspar porphyry intrude tonalite and both formations of the upper Tyrone Volcanic Group.

Broughderg Formation

The Greencastle Formation is conformably overlain by the Broughderg Formation, the base of which is taken at the first occurrence of chert, argillaceous sedimentary rocks or basalt north of the Beaghmore Fault. The Broughderg Formation is a diverse succession of intermediate to felsic crystal and lesser lapilli tuff/schist (Fig. 4.5x), rhyolite (e.g. around Crosh), vesicular basalt, argillaceous sedimentary rocks (Fig. 4.5z,a*), layered chert and black ironstone (silica-magnetite) with bedded pyrite (Fig. 4.5y). Rare occurrences basaltic tuff and andesite are also associated with the Broughderg Formation. The formation is at least 1.7 km thick and extends for a strike length of approximately 25 km (Fig. 4.2b). Exposure is predominantly restricted to the Quarries of Mountfield, and numerous stream sections between Glencurry Burn and Broughderg.

SW of Mountfield, the formation is best exposed in stream sections draining southern flanks of Ashmeanagh Mountain. Within Glencurry Burn graphitic pelite and banded cherts are exposed. Further NE towards Mountfield, Dalradian metasedimentary rcks of Glenscallop Burn are underlain by graphitic pelite with thin chert and rhyolite bands. This sequence is in turn underlain by andesites, rhyolite and tuffs. Tuffs may be locally banded, and range from dark green to pale grey. Large quartz-feldspar crystals are set in a micaceous matrix. Cherts and tuffs are locally replaced by jasper/ironstone (Hartley, 1933). Within the disused Mountfield Quarries Dalradian metasedimentary rocks of the Argyll Group (McFarlane et al. 2009) can be seen directly overlying tuffs of the Tyrone Volcanic Group. In the working Mountfield Quarry, tuffs

alternate with vesicular basalt and andesite, rhyolite (which can display chilled margins against tuffs) and graphitic pelite with thin chert bands.

Further NE between Cashel Bridge and Carnanransy Burn, fine dark green lava and volcaniclastic crystal tuffs/schists are interbedded with grey phyllite, and thinly bedded chert. At Broughderg two Ennex drillholes (DDH-91-1 and DDH-91-2) intersected dark green pyritiferous tuffs interbedded with fine-grained magnetite-bearing acid intrusives and ironstone (see Chapter 7). Clasts of acid material were observed in crystal tuff at the base of DDH-91-1. These rocks are in turn overlain by a thick succession of chloritic tuff (± magnetite) graphitic pelite and layered grey chert.

SE of Broughderg Forest, a well exposed sequence occurs within a series of streams draining the western flank of Mullaghacoula. Well-bedded, banded, foliated and chloritic tuffs are interbedded with, and eventually succeeded by, schistose tuff, well-cleaved black shale, blue-black finely laminated crystalline chert, and graphitic pelite. Agglomerate, crystal tuff, and rare striped tuff with cherty lamellae occur lower in the section. Further NE in Altbane Burn, thrusting and associated deformation has led to repetition of the uppermost sequence. Thrusting preferentially occurs along thick beds of graphitic pelite, with crenulated chloritic schist associated with sheared metavolcanics (Fig. 4.5z,a*).

A brief deformational history of the Tyrone Volcanic Group is presented in the Appendix, based on the results of the entire thesis.

4.5 Geochemistry

Volcanic rocks from all major stratigraphic horizons within the Tyrone Volcanic Group were sampled for whole-rock geochemical analysis (see Chapter 2). Major elements and trace elements were determined by X-ray fluorescence analysis. Rare earth-elements (REE), plus Nb, Hf, Ta, Th, U, were determined by inductively coupled plasma mass spectrometry (ICP-MS) on the same samples. Neodymium isotope ratios were determined using a VGMicromass Sector 54 thermal ionization mass spectrometer (TIMS). Results are presented in the Appendix (4.x). Geochemical analyses of Draut et al. (2009) and Cooper et al. (2011 – Chapter 3) are also included where appropriate.

Under low-grade metamorphic conditions and during hydrothermal alteration most major elements (e.g. SiO_2, Na_2O, K_2O, CaO) and the low field strength elements (LFSE: Cs, Rb, Ba, Sr, U, except Th) are mobile (MacLean 1990). As the primary mineral assemblages within the Tyrone Volcanic Group have been hydrothermally altered and metamorphosed under sub- to lower-greenschist facies conditions, the following account is based on demonstrably immobile elements. In addition to Al_2O_3, TiO_2, Th, V, Co and Sc, the high-field strength elements (HFSE, e.g. Nb, Hf, Ta, Zr, Y), and REE (minus Eu ± Ce) are herein considered to be immobile during metamorphism and hydrothermal alteration (e.g. Pearce & Cann 1973; MacLean 1990; Jenner 1996). Results for lithostratigraphic units identified within the Tyrone Volcanic Group are presented in Figures 4.6 and 4.7. Multi-element variation diagrams show a distinction between different petrochemical suites of basalt/basaltic andesite (CAB, Fe-Ti eMORB, IAT, OIB-like, Alk) and intermediate to felsic lavas and volcaniclastics (CA-I, TF, CA-II) in each formation (Figs. 4.4, 4.6-4.7). Petrochemical suites identified are detailed below in relation to the newly presented stratigraphy (see Fig. 4.4) and summarised in the Appendix. Several episodes of rifting within the Tyrone Volcanic Group are evident from Figure 4.6 through a return to more primitive geochemical compositions (e.g. lower SiO_2, Zr/TiO_2, Zr/Y and higher Nb/Y) at several stratigraphic levels and the eruption of Fe-Ti enriched eMORB (see below). This most likely reflects rift-related magmatism and the tapping of a different source region, as only Fe-Ti enriched eMORB and alkalic basalts of the Tyrone Volcanic Group are associated with higher Nb/Y values (Fig 4.6a); magmas of arc-affinity have low Nb/Y values.

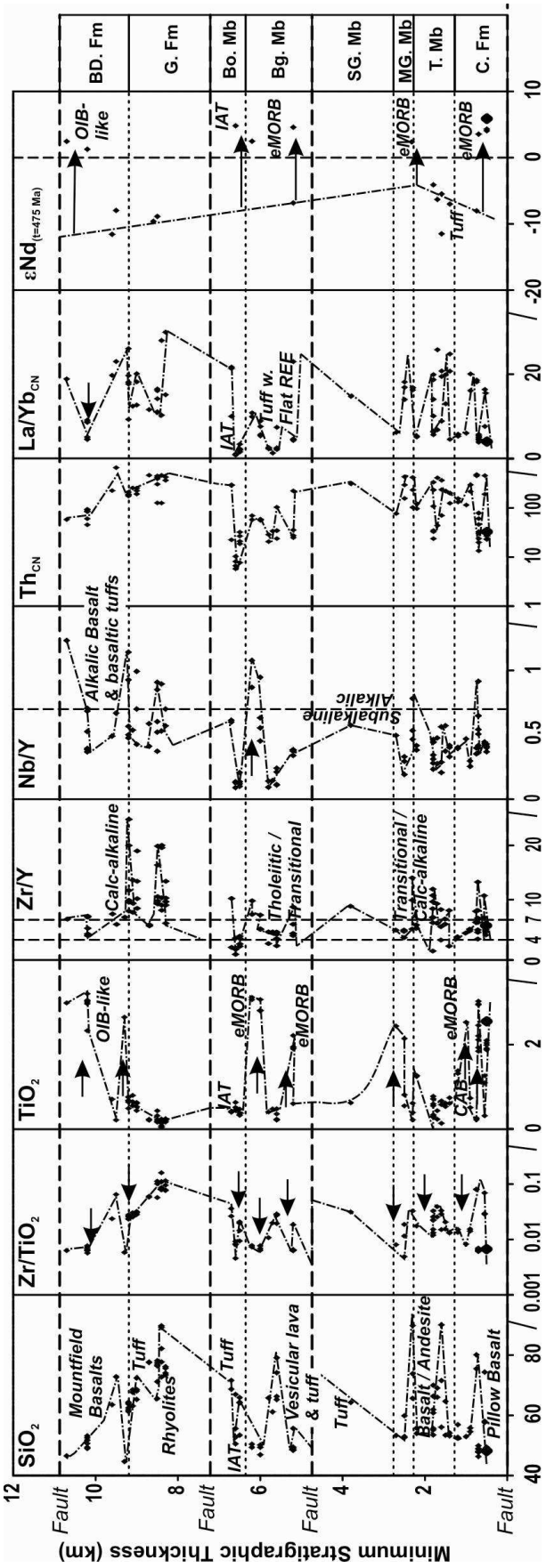

Figure 4.6a. Geochemical analyses from the Tyrone Igneous Complex; data of Draut et al. (2009) and Cooper et al. (2011) also included. Arrows indicate episodes of rifting and a return to more primitive geochemical signatures. BD. Fm, Broughderg Formation; Bg. Mb, Beaghbeg Member; Bo; Mb, Bonnety Bush Member; C. Fm, Creggan Formation; MG. Mb, Merchantstown Glebe Member; SG. Mb, Streefe Glebe Member; T. Mb, Tanderagee Member.

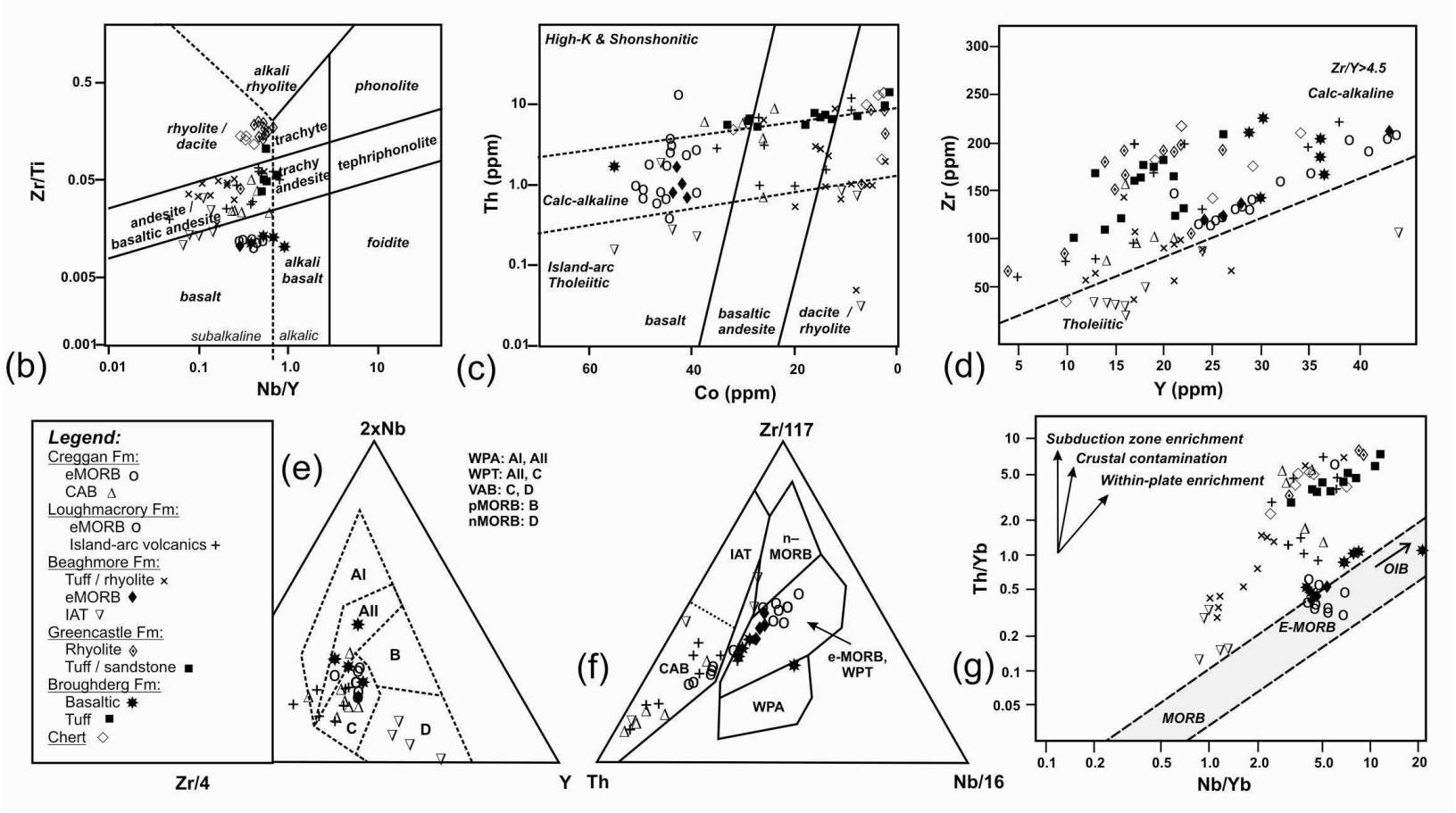

Figure 4.6 (b-g). Geochemistry of the Tyrone Volcanic Group. (b) Zr-Ti against Nb-Y diagram (after Winchester & Floyd 1977; modified after Pearce 1996). (c) Th-Co diagram (after Hastie et al. 2007). (d) Zr-Y diagram (Zr/Y ratio cut off values from Ross & Bédard 2009). (e) Zr-Nb-Y discrimination diagram (after Meschede 1986). (f) Zr-Th-Nb discrimination diagram (after Wood, 1980). (g) Th-Yb against Nb/Yb diagram (after Pearce 1983).

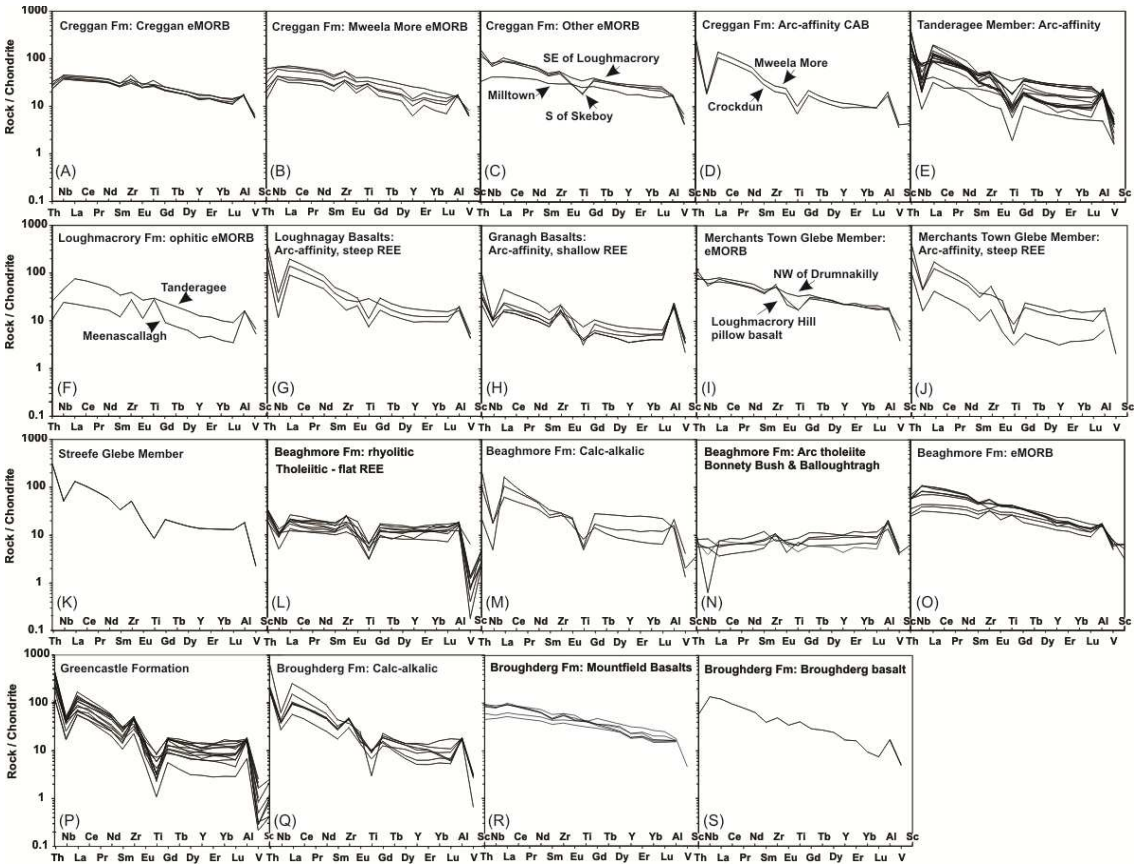

Figure 4.7. Multi-element variation diagrams for samples from the Tyrone Volcanic Group. Chondrite normalization values after McDonough and Sun (1995). Analyses of Draut et al. (2009) and Cooper et al. (2011) also included.

4.5.1 Lower Tyrone Volcanic Group

Three geochemically distinct suites of basalt/basaltic andesite and two geochemically distinct suites of intermediate to felsic lavas and volcaniclastic rocks have been recognized within the lower Tyrone Volcanic Group (southwestern and eastern structural blocks; Fig. 4.2b):

Calc-alkaline basalt (CAB)

Subalkaline (Nb/Y 0.19 to 0.47), borderline to calc-alkaline (Zr/Y 4.3 to 10.6, most >5), LILE- and LREE-enriched (La/Yb_{CN} 4.3-10.6) basalt/basaltic andesite (SiO_2 52.6-61.9 wt.%; Zr/Ti <0.03). These rocks display pronounced negative Nb (Th/Nb_{CN} 1.4-15.0) and HFSE anomalies characteristic of island arc rocks (Pearce & Cann 1973; Pearce & Norry 1979; Wood 1980; Shervais 1982; Meschede 1986; Fig. 4.7d-e, 4.7g-h, 4.7j). Further subdivisions can be made between those which display steep REE profiles (e.g. Loughnagay Basalts; Fig. 4.7g) and those with shallower REE profiles (e.g. Granagh

Basalts; Fig. 4.7h). Fe_2O_{3T} (8.1-14.0%), TiO_2 (0.3-2.5%) and P_2O_5 (0.13-0.32%) enrichment is variable.

Fe-Ti enriched mid-ocean ridge basalt (Fe-Ti eMORB)

Subalkaline to alkalic (Nb/Y, 0.36-1.1, most <0.6), moderately LILE- and LREE-enriched (La/Yb_{CN} 2.6-7.6), and strongly Fe-Ti-P-enriched (8.4-16.6 wt % Fe_2O_{3T}, 1.1-3.1wt.% TiO_2, 0.10-0.44wt % P_2O_3) basalt/basaltic andesite (Zr/Ti <0.02). These rocks are of 'within-plate' and/or eMORB affinity on various discrimination diagrams (e.g. Pearce & Cann 1973; Pearce & Norry 1979; Wood 1980; Shervais 1982; Meschede 1986); and lack a distinctive island-arc signature (Th/Nb_{CN} 0.4-2.2). εNd_t values are moderately primitive (+2.4 to +5.9). Al_2O_3 concentrations (13.2-16.3%, most <14.5%) are generally lower than CAB (13.6-17.3%). Highest Fe and Ti enrichment occurs in basalts with low SiO_2, Al_2O_3 and Cr. Fe-Ti basalts can display either, weakly positive or less often negative Nb, Zr and Ti anomalies on multi-element variation diagrams (e.g. Figs. 4.7a-c, 4.7f, 4.7i). Variable MgO enrichment (4.0-10.9 wt.%) is due to locally developed chloritisation and/or silica-epidote-carbonate alteration. Samples analysed from Mweela More display negative Y anomalies (Fig. 4.7b). Y mobilization may be due to the action of carbonate rich fluids (e.g. Hynes 1980).

Island arc tholeiite (IAT)

Tholeiitic (Nb/Y <0.15; Zr/Y 1.8-4.5), moderately LILE-enriched (Th 5.8-10.3x chondrite) and LREE-depleted (La/Yb_{CN} 0.54-1.43) basalt, with a distinctive island-arc signature (Th/Nb 1.0-16.6). (Fig. 4.7n). Basalt from Bonnety Bush has a primitive εNd_t value of +4.8. SiO_2 (50.5-66.9 wt.%) and MgO (1.1-8.6 wt.%) concentrations are variable due to extensive chlorite and/or silica-epidote alteration.

Calc-alkalic evolved (CA-I)

No intermediate to felsic volcanic rocks have been identified within the Creggan Formation. Intermediate to rhyolitic lavas and tuffaceous rocks present within the Loughmacrory and Beaghmore formations are predominantly transitional to calc-alkaline (Zr/Y 3.1-13.3, most >6), LILE- and LREE-enriched (Th ~20-420 x chondrite) with steep REE profiles ($LaYb_{CN}$ 3.1-16.9), and display island-arc geochemical characteristics such as prominent Nb and HFSE anomalies (Figs. 4.7e, 4.7j-k). Quartz-porphyritic rhyolite from Tanderagee has a εNd_t value of -11.5, whereas volcaniclastic tuffs have produced εNd_t values between -4.1 and -7.0.

Tholeiitic felsic (TF)

Intermediate to rhyolitic tuffaceous rocks present within the Beaghmore Formation at Beaghbeg and Bonnety Bush can be geochemically distinct from those of the

Loughmacrory Formation. These rocks are tholeiitic (Zr/Y 0.8-4.4), variably LILE enriched (Th ~22-300 x chondrite) and with flat to U-shaped REE profiles. All tuffs display strong arc-like geochemical characteristics (Fig. 4.7l-m).

Petrochemical Stratigraphy

The lower part of the Creggan Formation is dominated by pillowed Fe-Ti enriched within-plate basalt/basaltic andesite (Fe-Ti eMORB) associated with rare agglomerate and layered chert. Strongly LILE- and LREE-enriched, island-arc calc-alkaline basalt/basaltic andesite (CAB) occurs only within the upper part of the formation (e.g. Mweela More, Crockdun; Fig. 4.7c-d). Although contacts across the lower Tyrone Volcanic Group are typically poorly exposed, at Mweela More island-arc basalt (CAB) and within-plate basalt (Fe-Ti eMORB) are clearly non-tectonic. Pillowed flows of Fe-Ti eMORB affinity are interlayered with, or intruded by, massive and non-pillowed CAB. Cherts associated with both suites in the Creggan Formation display LREE-enriched arc-like signatures (e.g. Fig. 4.7e). High Al_2O_3, steep REE profiles, and negative Ti and Nb anomalies in these cherts suggest the presence of arc derived components; whereas strongly negative εNd_t values (-8.0 from Mweela More) and Proterozoic τ_{DM} ages (1.7 Ga) imply the presence of continentally-derived components.

In the overlying Loughmacrory Formation, mafic lavas are characterized by both strongly LILE- and LREE-enriched, island-arc calc-alkaline basalt/basaltic andesite (CAB, e.g. Tanderagee, Granagh, Merchantstown Glebe; Fig. 4.7e, 4.7g-h, 4.7j), and Fe-Ti eMORB (e.g. Tanderagee, Mweenascallagh). The latter is present at several stratigraphic horizons within the Tanderagee (Fig. 4.7f) and Merchantstown Glebe members (Fig. 4.7i). Fe-Ti eMORB lavas, LREE-enriched calc-alkaline volcaniclastic tuffs (CA-I) and layered cherts of island-arc affinity are interbedded within the Loughmacrory Formation. At Meenascallagh, ophitic Fe-Ti eMORB intrudes a sequence of calc-alkaline volcanics (CA-I) which characterize the rest of the formation.

The Beaghmore Formation is characterized by abundant Fe-Ti eMORB (e.g. Teebane and north of Beaghbeg), tholeiitic island-arc basalt/basaltic andesite (IAT; Bonnety Bush and Balloughtragh), tholeiitic rhyolite and volcaniclastic rocks with flat to U-shaped REE profiles (TF), and rare LREE-enriched volcaniclastic tuffs (CA-I). Within the Beaghbeg Member calc-alkaline LREE-enriched, island-arc feldspar-phyric andesitic tuff is interbedded with Fe-Ti eMORB, which is in turn overlain by tholeiitic felsic volcaniclastic rocks which display flat to U-shaped REE profiles (TF) and ferruginous jasperoid (ironstone). Strongly LILE- and LREE-enriched volcanic and tuffaceous rocks (CA-I) are restricted to three samples from Teebane (SPH195), Beaghbeg (SPH19) and

Bonnety Bush (SPH184). In the overlying Bonnety Bush Member CA-I affinity tuffs overly tholeititic and LREE-depleted basalts (IAT) and ironstone.

4.5.2 Upper Tyrone Volcanic Group

In the upper Tyrone Volcanic Group, basalt and extensively altered basaltic tuff is restricted to the Broughderg Formation. Two geochemically distinct suites have been recognized (OIB and Alk, summarized below), both of which are interbedded with strongly LILE- and LREE-enriched intermediate to felsic island-arc volcaniclastic rocks (CA-II). Chert from Carnanransy Burn (upper Tyrone Volcanic Group: Broughderg Formation) has high Al_2O_3 (15.24 wt.%) and Fe_2O_{3T} (7.66 wt.%), steep REE profiles (La/Yb_{CN} 12.0) and displays calc-alkaline, arc-like geochemical characteristics.

OIB-like (OIB)

Around Mountfield, basalt (SiO_2 44.7-53.2 wt.%) is subalkaline to borderline alkalic (Nb/Y 0.37-0.70); LILE (Th ~45-100x chondrite), FeO_T (13.4-16.0 wt.%), TiO_2 (2.3-3.2 wt.%) and P_2O_5 (0.2-0.6 wt.%) enriched; and displays weak to absent negative Nb (Th/Nb_{CN} 0.95-1.1) and Ti anomalies on multi-element normalized diagrams (Fig. 4.7r). Chondrite-normalized REE profiles show modest LREE enrichment relative to the HREE (La/Yb_{CN} 3.1-6.2). Immobile-element variation profiles are similar to ocean-island basalts (Fig. 4.7r). Samples classify as within-plate basalt and/or e-MORB (Pearce & Cann 1973; Pearce & Norry 1979; Wood 1980; Shervais 1982; Meschede 1986). εNd_t values are less primitive than mafic rocks of the lower Tyrone Volcanic Group (+1.3, Draut et al. 2009) and τ_{DM} ages are c.1.4 Ga.

Alkalic (Alk)

Basaltic tuff (SPH189, SiO_2 46.5 wt.%) from Broughderg is alkalic (Nb/Y 1.2) and similarly LILE (~60x chondrite), FeO_T (14.3 wt.%), TiO_2 (3.0 wt.%) and P_2O_5 (0.6 wt.%) enriched. However, this sample displays strongly positive Nb (Th/Nb_{CN} 0.4), Zr and Ti anomalies on multi-element variation diagrams (Fig. 4.7s), and has produced a εNd_t value of +2.5 and a τ_{DM} age of c. 2.0 Ga. Chondrite-normalized REE profiles show steeper LREE enrichment relative to the HREE (La/Yb_{CN} 12.8) and are similar to eMORB.

Calc-alkalic (*CA-II*)

All non-basaltic samples analyzed from the Greencastle and Broughderg formations are in many respects geochemically similar (Figs. 4.4, 4.7p-q). Andesite, flow-banded to brecciated rhyolite and associated volcaniclastic rocks are calc-alkaline (Zr/Y 4.6-22.0, most ~6-15), strongly LILE- and LREE-enriched (Th ~92-465 x chondrite, La/Yb_{CN} 3.4-20.4), and display prominent negative Nb (Th/Nb_{CN} 1.1-11.1) and HFSE anomalies characteristic of formation within an island-arc environment. εNd_t values are strongly

negative. Rhyolite and diorite from the Greencastle have produced εNd_t values of -8.9 and -9.2, respectively (Draut et al. 2009). Andesite and coarse-grained quartzo-feldspathic crystal tuff from Mountfield and Broughderg have produced εNd_t values of -8.0 and -11.6 respectively. τ_{DM} ages are Proterozoic (1.6-2.2 Ga).

4.6 Geochronology

Three samples were selected for U-Pb (zircon) geochronology at the NERC Isotope Geosciences Laboratory. Two samples were analyzed from the Tyrone Volcanic Group, both from within the Greencastle Formation: rhyolite from Cashel Rock (MRC336) and silicified feldspathic tuff from Tullybrick (MRC350). A sample of tonalite from Cashel Rock (MRC337) was also dated. Further analytical information is provided in Chapter 2. Calculated U–Pb ages for samples analyzed herein are presented in Figure 4.8, along with additional information (data in Appendix).

Five zircon fractions (single grains) were analyzed from samples MRC336 (Cashel Rock rhyolite) and MRC337 (Cashel Rock tonalite). Five analyses from each are concordant when their systematic $\lambda^{238}U$ and $\lambda^{235}U$ decay constant errors are considered. Analyses from MRC336 (Cashel Rock rhyolite) form a coherent single population yielding a weighted mean $^{206}Pb/^{238}U$ date of 469.42 ± 0.38 (0.60)[0.79] Ma (MSWD = 2.2). Analyses from sample MRC 337 (Cashel Rock tonalite), form a coherent single population yielding a weighted mean $^{206}Pb/^{238}U$ date of 469.29 ± 0.33 (0.58)[0.77] Ma (MSWD = 1.7).

The calculated U–Pb ages for rhyolite (MRC336: 469.42 ± 0.38 Ma) and tonalite (MRC337: 469.29 ± 0.33) from Cashel Rock are within error at c. 469 Ma, and both are younger than rhyolite along strike at Formil (473.0 ± 0.8 Ma; Cooper et al. 2008), and significantly older than a previously dated sample of tonalite from Cashel Rock (JTP209 465.66 ± 1.1 Ma; Cooper et al. 2011). Field-relations and U-Pb zircon geochronology imply several generations of tonalite occur within the succession. At Cashel Rock at least two generations can be identified; early tonalite (c. 469 Ma) is foliated and present as xenoliths within both a younger unfoliated tonalite (c. 465 Ma) and syndepositional rhyolite (c. 473-469 Ma).

For sample MRC350 (silicified feldspathic tuff from Tullybrick) six fractions (single grains) were analyzed. Each analysis is concordant however there is dispersion with $^{206}Pb/^{238}U$ dates ranging from 469.8 ± 0.9 to 471.9 ± 0.5 Ma. The younger age is defined by a cluster of three equivalent $^{206}Pb/^{238}U$ dates (z6A, z6B and z15) yielding a weighted mean $^{206}Pb/^{238}U$ date of 470.37 ± 0.31 (0.56)[0.76] Ma (MSWD = 1.7) which we

interpret as being the best estimate for the age of sample. As this sample was taken from near the top of the Greencastle Formation, a maximum age of c. 470.37 ± 0.31 Ma is consistent with underlying rhyolites dated at c. 473-469 Ma. No Proterozoic ages were derived from any of the dated zircon fractions, although zircon selection was biased to avoid morphologies that may contain inherited cores.

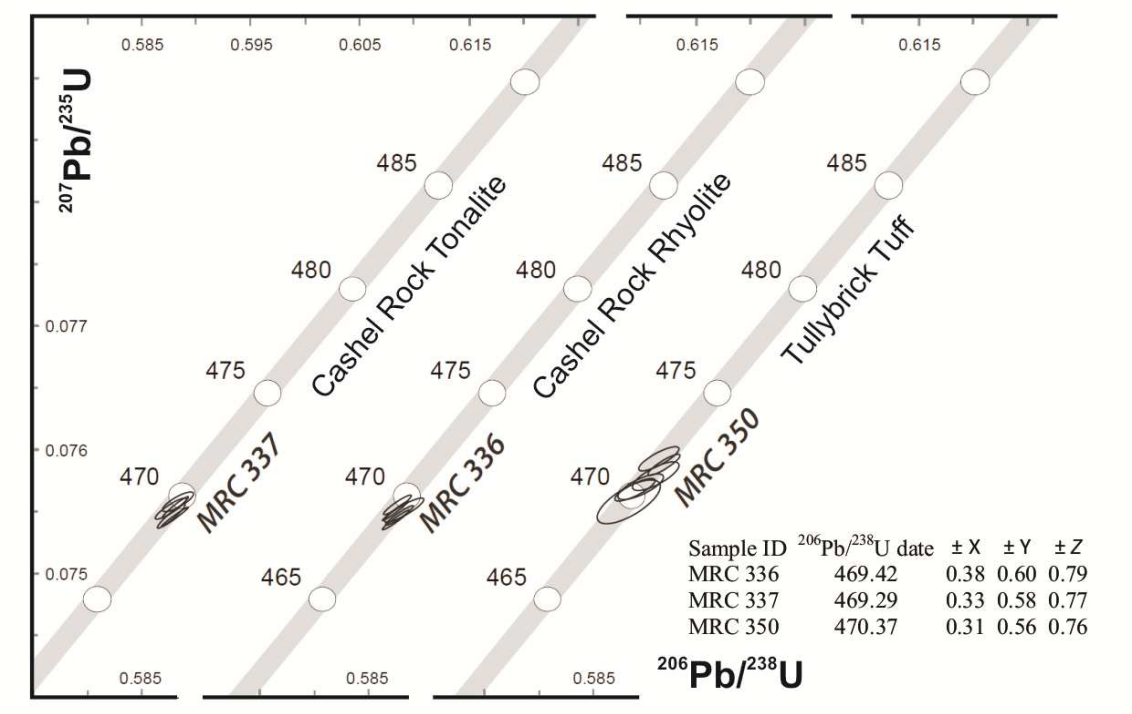

Figure 4.8. U-Pb zircon concordia and summary of interpreted U-Pb zircon dates.

4.7 Discussion

4.7.1 Evolution of the Tyrone arc

The new stratigraphic, geochemical and geochronological data presented here suggest that the evolution of the Tyrone Volcanic Group is more complex than the trifold cyclicity proposed by Cooper and Mitchell (2004), although an apparent cyclicity is recognized in the occurrence of Fe-Ti eMORB at several stratigraphic levels and through the repeated occurrence of ferruginous jasperoid (ironstone). In addition, the stratigraphic chart of Draut et al. (2009) is re-evaluated as this was constructed primarily using geochemical data.

Early magmatism within the lower Tyrone Volcanic Group is characterized by subalkaline (transitional to calc-alkaline) basalt and basaltic andesite with subordinate crystal and lapilli tuff. Cherts associated with pillowed, massive and sheet-flow basalt display geochemical characteristics consistent with both continentally derived and

evolved island-arc components (Fig. 4.7e). High LILE and LREE-enrichment and Proterozoic τ_{DM} ages suggest the lower Tyrone Volcanic Group formed close to the Laurentian margin or upon a fragment of peri-Laurentian microcontinental crust and was contaminated by such material. The presence of mafic breccias that contain rare felsic clasts (and interbedded rhyolite, rhyolitic tuff and breccias, and mafic lavas) indicate effusive mafic volcanism was coeval with silicic activity. Collectively, these data argue for an early history in the Tyrone Volcanic Group characterized by subaqueous arc magmatism in a peri-Laurentian realm.

The evolution of the lower Tyrone Volcanic Group is recorded by the progressive replacement of transitional to calc-alkalic island-arc vesicular basalt (of the Creggan and Loughmacrory formations), by porphyritic-andesite, and finally flow-banded rhyolite and rhyolitic volcaniclastic tuff in the Beaghmore Formation. This evolution was coeval with the replacement of plagioclase-pyroxene crystal tuff (Creggan Formation) by hornblende-bearing and quartzo-feldspathic crystal tuffs (Loughmacrory and Beaghmore formations). This lithostratigraphic evolution is reflected by increasing SiO_2, Zr/TiO_2, Zr/Y, Th_{CN} and La/Yb_{CN} and more negative εNd_t values (Fig. 4.6). However, several returns to more primitive geochemical compositions, associated with episodes of rifting, are evident in Figure 4.6.

The occurrence of interbedded LILE- and LREE-enriched island-arc volcanic rocks, with Fe-Ti eMORB, and LREE-depleted island arc tholeiite (IAT) imply a history of intra-arc rifting within the Tyrone Volcanic Group. Fe-Ti±P enriched lavas of eMORB affinity occur throughout the group at several stratigraphic levels (Figs. 4.4, 4.6-4.7), and are typically interbedded with or overlie island-arc basalt and/or tuff. Primitive εNd_t values and high Nb/Y ratios imply an association with rifting and the upwelling of asthenosphere. Intermittent rifting of the arc-system and the eruption of Fe-Ti eMORB may be due to slab rollback and/or the interaction between the arc system and a propagating rift (see below).

An episode of rifting at c. 475 Ma, represented by the occurrence of tholeiitic rhyolitic agglomerate and tuff with flat REE profiles (TF), Fe-Ti eMORB, and tholeiitic LREE-depleted basalt (IAT) in the Beaghmore formation led to the formation of an intra-arc/backarc basin (Cooper et al. 2011). Early volcanic activity within the Beaghmore Formation, exposed around Teebane, is characterized by LILE- and LREE-enriched tuffs (CA-I) interbedded with vesicular Fe-Ti eMORB. Overlying deposits at Beaghbeg are characterized Fe-Ti eMORB interbedded with ferruginous jasperoids (ironstone) and tholeiitic rhyolite breccias with flat to U-shaped REE profiles (TF). Continued rifting led

to the eruption of further Fe-Ti eMORB and LREE-depleted IAT, capped by LILE- and LREE-enriched tuff (CA-I) and ironstone at Bonnety Bush.

Collision between the Tyrone arc and Tyrone Central Inlier is typically placed at c. 470 Ma (Cooper et al. 2011) during deposition of the Greencastle Formation of the upper Tyrone Volcanic Group (c. 473-469 Ma). At this time an abundance of rhyolite (e.g. Cashel Rock, Fig. 4.2b) and thick quartzofeldspathic crystal tuff dominates the succession. An absence of xenocrystic zircons within a c. 473 Ma rhyolite and their occurrence in c. 470-464 Ma intrusive rocks (Cooper et al. 2011) suggests arc-accretion occurred between c. 473-470 Ma. All lithostratigraphic units sampled within the Greencastle Formation are strongly LILE- and LREE-enriched implying continental material contaminated this phase of volcanism. Increasingly negative εNd_t values suggest the Tyrone Central Inlier occupied a lower plate setting during arc-accretion, due to the progressive underthrusting of Laurentian-affinity continental material and obduction of the Tyrone Volcanic Group.

Normal arc magmatism ceased shortly after collision. Thin rhyolite flows of the Broughderg Formation (e.g. at Crosh, Figs. 4.2b, 4.4) mark this termination and record late ensialic arc rifting (see geochemistry in Chapter 7). The Broughderg Formation is predominantly characterized by tuff, chert and argillaceous sedimentary rocks. A late stage of rifting is recorded by the presence of alkali OIB-like Fe-Ti-P enriched basalts with weakly oceanic εNd_t values (Mountfield Basalts; Fig. 4.4). Late-stage rifting may have formed the deeper water conditions in which layered cherts and argillaceous sedimentary rocks of the upper Broughderg Formation were deposited.

4.7.2 Petrogenesis of Fe-Ti basalts

Fe-Ti basalts are defined by >12 wt.% FeO_T and >2 wt.% TiO_2 (e.g. Sinton et al. 1983), and typically display lower concentrations of MgO, CaO and Al_2O_3 than normal MORB. They are interpreted to form by high degrees of closed-system fractional crystallization maintained by low fO_2 (references in Harper 2003; Raveggi et al. 2007). These conditions are necessary to delay the saturation of Ti-magnetite in the melt and allow Fe-Ti enrichment in the most evolved fractionates. Fe-Ti basalts are confined to extensional settings and have been reported from: continental and oceanic rifts (e.g. Afar Rift of Ethiopia, Red Sea Rift, mid ocean ridges); on tips of propagating rifts; on intersections of mid ocean ridges and transform faults; in triple junctions; and also in ophiolites (references within Raveggi et al. 2007). Propagating spreading centres are common in many backarc basins (references within Harper 2003), with Fe-Ti basalt having been erupted in the tip of the Central Lau Basin Spreading Centre (Pearce et al. 1994).

The repeated occurrence of Fe-Ti±P enriched basalt within the Tyrone Volcanic Group suggests intermittent rifting may have been caused by the propagation of a rift into the Tyrone arc/backarc. High Fe-Ti basaltic rocks from the Paleoproterozoic Broken Hill Block of New South Wales, Australia, show some similarities with samples reported herein. Fe-Ti amphibolites with La/Sm_{CN} ~1.5-3 and Gd/Lu_{CN} ~1 display eMORB-like geochemical compositions (Raveggi et al. 2007). Similarly, Mattsson and Oskarsson (2005) recorded a progression within the Eastern Volcanic Zone of Iceland from tholeiitic basalt, through Fe-Ti rich lavas interlayered with silicic lavas, to alkalic compositions at the southernmost tip of the propagating ridge. Some Fe-Ti enriched basalts from the Heimaey volcanic centre of the Eastern Volcanic Zone have similar La/Sm ratios to eMORB, displaying LREE enrichment and positive Nb anomalies (Mattsson & Oskarsson 2005). Fe-Ti enriched eMORB has also been recognized within the Annieopsquotch Accretionary Tract of Newfoundland (Zagorevski 2008; see below), and the peri-Gondwanan affinity Bathurst Mining Camp of the Tetagouche-Exploits backarc basin (Rogers & van Staal 2004), Port aux Basques Gneiss of Newfoundland (Schofield et al. 1998), and from several peri-Gondwanan ensialic arc sequences of the British and Irish Caledonides (e.g. Leat et al. 1986; McConnell et al. 1991).

4.7.3 Correlations across the Grampian – Taconic event

Direct correlations between Newfoundland Appalachians and the British and Irish Caledonides have previously proven difficult due to poor exposure and the excision of key terranes along strike, such as the Southern Uplands (Colman-Sadd et al. 1992; Winchester & van Staal 1995; van Staal et al. 1998). New and recently published geochronology and geochemistry (Cooper et al. 2008; Draut et al. 2009; Chew et al. 2010; Cooper et al. 2011; Fig. 4.9) allow refinement of previous correlations with the Tyrone Igneous Complex and across the orogen as a whole.

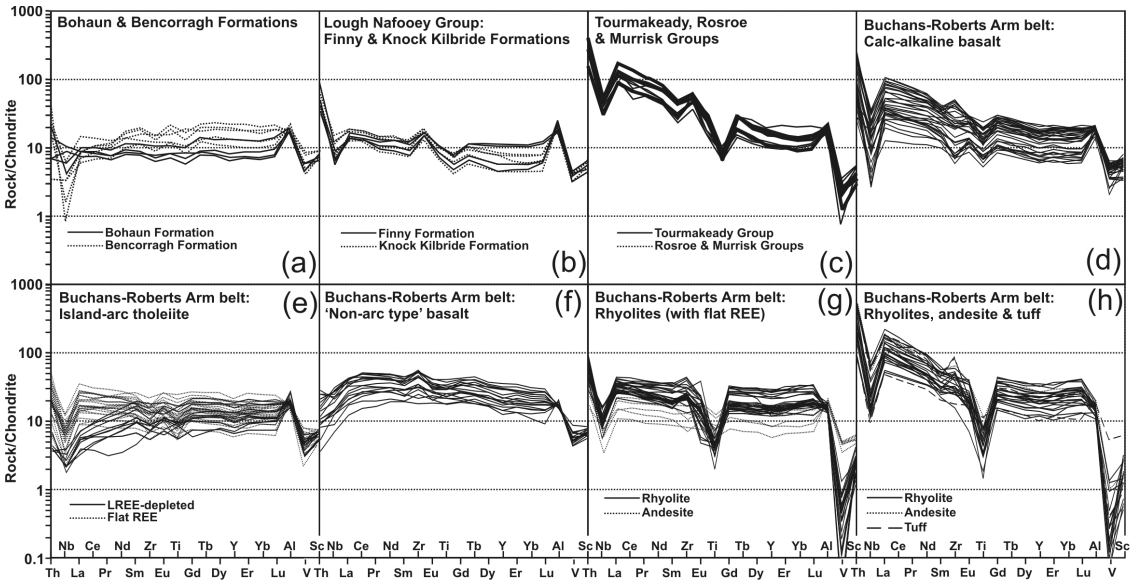

Figure. 4.9. Multi-element variation diagrams for samples from western Ireland (data from Draut et al. 2004) and the Buchans - Robert's Arm Belt (data from Zagorevski 2008). Chondrite normalization values after McDonough and Sun (1995).

Although previous workers have correlated the Tyrone Igneous Complex with the Lough Nafooey arc system of western Ireland (e.g. Draut et al. 2009) the data presented herein demonstrate the Tyrone Igneous Complex represents a distinct arc-ophiolite complex accreted to the composite Laurentian margin during the Grampian orogeny. Consequently, we present a revised model for the evolution of the British and Irish Caledonides where outboard microcontinental blocks play a crucial role (after Chew et al. 2000). Their involvement within the Newfoundland Appalachians helped to explain (i) discrepancies between the timing of syntectonic sedimentation and tectonic loading on the passive continental margin at c. 475 Ma and ophiolite emplacement prior to 488 Ma (see Waldron & van Staal 2001); and (ii) the range of ages for Iapetian ophiolites accreted to the Laurentian margin (see van Staal et al. 2007). Three phases of arc-ophiolite emplacement to the Laurentian margin have been recognized within central Newfoundland during the equivalent Taconic orogeny (van Staal et al. 2007; see Figs. 4.10-4.11). Most of the major terranes recognized in Newfoundland bear strong temporal, lithological and geochemical resemblances to those now identified within the British and Irish Caledondies.

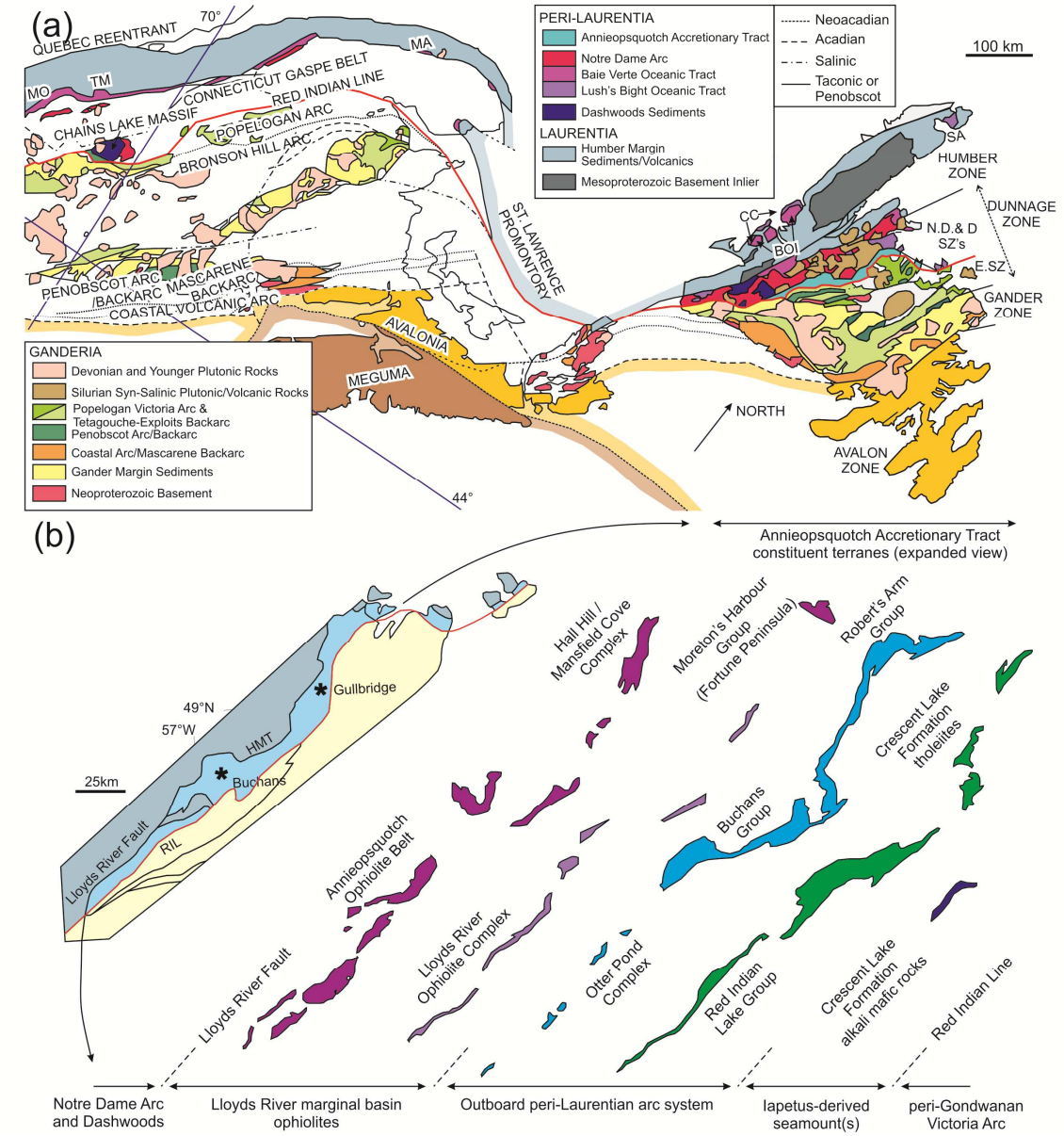

Figure 4.10. (a). Geology of the Canadian and adjacent New England Appalachians with the geographical distribution of the major tectonic elements discussed in text (modified after van Staal et al. 2009). (b) Tectono-stratigraphic subdivisions of the Annieopsquotch Accretionary Tract (expanded view: modified after Zagorevski et al. 2009a, Zagorevski & van Staal 2011). BOI, Bay of Islands; CC, Coastal Complex; E.SZ, Exploits Subzone; HMT, Hungry Mountain Thrust; N.D & D. SZ's, Notre Dame and Dashwoods Subzones; MA, Mont Albert Ophiolite; MO, Mount Orford Ophiolite; RIL, Red Indian Line; SA, St Anthony Complex; TM, Thetford Mines Ophiolite.

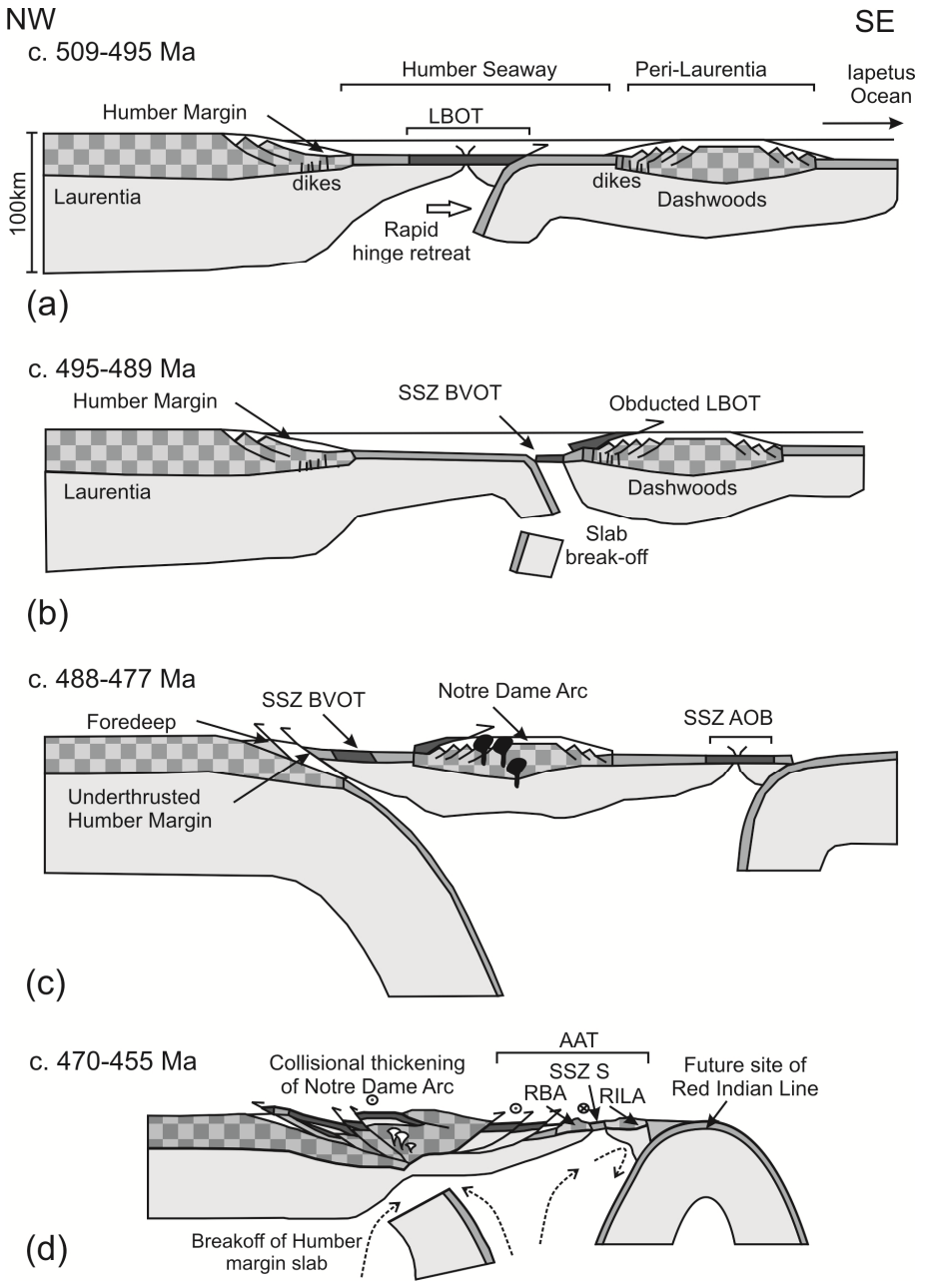

Figure 4.11. Evolution of the Laurentian margin during the Taconic event (after van Staal et al. 2007; Zagorevski & van Staal 2011). (a) formation of the Lushs Bight Oceanic Tract (LBOT) inboard of the Dashwoods microcontinent. (b) development of the Baie Verte Oceanic Tract (BVOT) and the Snooks Arm and Notre Dame arcs (NDA) following collision of the LBOT. (c) Collision between the Humber margin and Dashwoods leads to the initiation of west-dipping subduction and formation of the Anniopsquotch ophiolite belt (AOB). (d) Collisional thickening of the Notre Dame arc, slab-break off, and the accretion of the Annieopsquotch ophiolite belt, remnant Buchans arc (RBA), Skidder basalts (S) and Red Indian Lake arc (RILA) to the Laurentian margin. AAT, Anniopsquotch Accretionary Tract; BOI, Bay of Islands ophiolite; SSZ, suprasubduction zone affinity.

Early ophiolite emplacement

Early obduction in central Newfoundland is recorded by the emplacement of the c. 510-501 Ma Lushs Bight Oceanic Tract (Fig. 4.11a) onto the Dashwoods peri-Laurentian microcontinental block (Waldron & van Staal 2001) between c. 500 and 493 Ma (van Staal et al. 2007; Fig. 4.11b). The Lushs Bight Oceanic Tract comprises an ophiolitic association of pillow basalts, sheeted dykes, gabbro and rare ultramafic rocks (Kean et al. 1995). Abundant boninite, primitive island-arc tholeiite (εNd_t 0 to +2.8) (Swinden 1996; Swinden et al. 1997) and the presence of large intrusions of juvenile trondhjemite and diorite (Fryer et al. 1992), imply the tract represents an infant arc terrane that formed close to Laurentia (van Staal et al. 1998; Fig. 4.11a).

Although the Lushs Bight Oceanic Tract occupied an upper plate setting during its accretion, it is currently unclear whether it formed inboard or outboard of Dashwoods (Zagorevski & van Staal 2011). Recently Zagorevski and van Staal (2011) have suggested the Lushs Bight Oceanic Tract may have developed inboard of Dashwoods and was obducted from the west (as in Fig. 4.11b). This model removes the requirement for the Dashwoods to have been completely subducted under the Lushs Bight Oceanic Tract. Formation inboard of Dashwoods is also supported by the presence of Lushs Bight remnants in a forearc position during the final closure of the Taconic Seaway (references in Zagorevski & van Staal 2011).

Recent work on the Deer Park (514 ± 3 Ma) and Highland Border (499 ± 8 Ma) ophiolites of the British and Irish Caledonides demonstrated that subduction and the onset of obduction occurred at least 15 m.y. before Grampian orogenesis (Chew et al. 2010). Early obduction may have occurred outboard of the Laurentian margin onto ribbon-shaped microcontinental blocks, consistent with the evolution of the Lushs Bight Oceanic Tract (van Staal et al. 2007). Metadolerite blocks that preserve ophitic textures and chilled-margins within the Deer Park Complex, are tholeitiic, juvenile (εNd_t +6) and display similar suprasubduction zone geochemical characteristics (Ryan et al. 1983; Chew et al. 2007).

The Highland Border Ophiolite has produced a U-Pb age of 499 ± 8 Ma from amphibolite (Chew et al. 2010). A garnet-muscovite schist xenolith constrains obduction P-T estimates to 5.3 kbar and 580 ˚C, with metamorphism dated by a 490 ± 4 Ma ^{40}Ar-^{39}Ar hornblende age and a 488 ± 1 Ma ^{40}Ar-^{39}Ar muscovite age (Chew et al. 2010). Mylonitized pillow basalt from Arran, placed in the Trossachs Group (i.e. Dalradian) by Tanner and Sutherland (2007), contains white mica which has yielded a ^{40}Ar-^{39}Ar cooling age of 476 ± 1 Ma (Chew et al. 2010). Mafic rocks within the Highland Border ophiolite also include primitive suprasubduction tholeiites (see

Henderson & Robertson 1982; Robertson & Henderson 1984; Dempster & Bluck 1991). The Mount-Orford ophiolite (504 ± 3 Ma; Fig. 4.10a) of the Quebec Appalachians is of mixed boninitic, tholeiitic and transitional-alkaline affinity (references in Tremblay et al. 2011) and may also be a potential correlative to the Lushs Bight Oceanic Tract.

Possible microcontinental blocks and correlatives to the Dashwoods Block within the British and Irish Caledonides may include the Tyrone Central Inlier (e.g. Chew et al. 2008, 2010), Slishwood Division (Flowerdew et al. 2009) and Connemara (Chew et al. 2010). The Chain Lakes massif of Western Maine may also represent a possible outboard microcontinental block (Waldron & van Staal 2001; Fig. 4.10a), although it has recently been suggested the high grade metasedimentary sequence may have been originally deposited in a fore-arc setting to a peri-Laurentian island arc adjacent to or upon a microcontinental block (Gerbi et al. 2006). Similar metasedimentary rocks are also preserved structurally underneath the c. 480 Ma Thetford Mines ophiolite of the Quebec Appalachians (see Tremblay et al. 2011; Fig. 4.10a).

Early obduction outboard of the Laurentian margin onto microcontinental blocks may explain discrepancies between the timing of obduction in the British and Irish Caledonides and the termination of the Laurentian Cambrian-Ordovician shelf sequences of NW Scotland (see Chew et al. 2010). Deposition of the Ardvewck and Durness Groups of the Hebridean terrane, NW Scotland, were not terminated until at least the Late-Arenig – Early Llanvirn (c. 470-465 Ma: Huselbee & Thomas 1998), yet the onset of obduction and metamorphism in Scotland occurred some c. 15 Myr earlier (Chew et al. 2010). Emplacement of the Deer Park Complex and Highland Border ophiolites outboard of these shelf-sequences may also explain (after Chew et al. 2010) differences in detrital zircon signatures between the Cambrian-Ordovician passive margin of NW Scotland and its temporal equivalents in the Dalradian Supergroup (Cawood et al. 2007); and why there is an absence of Grampian terrane detritus in the Laurentian passive margin (Bluck 2007).

Nafooey – Baie Verte – Notre Dame Arc system

Following the emplacement of the Lushs Bight Oceanic Tract, eastward directed subduction in the Humber Seaway led to the formation and emplacement of the c. 487-489 Ma Baie Verte Oceanic Tract coeval with both, the first phase activity within the continental Notre Dame arc (c. 489–477 Ma), and the development of the c. 476-467 Ma Snooks Arm arc/backarc complex along strike (van Staal et al. 2007; Skulski et al. 2010; Fig. 4.11b). The Baie Verte Oceanic Tract includes low-Ti and intermediate-Ti boninite, and younger island-arc tholeitiic mafic crust that formed between c. 489 and 487 Ma (Skulski et al. 2010). In the Irish Caledonides, the Baie Verte Oceanic Tract is

represented by the c. <490-476 Ma Lough Nafooey Group (Lough Nafooey arc: see Ryan et al. 1980; Fig. 1a) which collided with the Laurentian margin c. 476 Ma (timing after Ryan & Dewey 2011).

The Lough Nafooey Group (c. <490-476 Ma) is of primitive island arc affinity near its base (Ryan et al. 1980; Clift & Ryan 1994), and shows an increasing proportion of Laurentian-derived melt up section (Draut et al. 2004) (Fig. 4.9, 4.12). LREE-depletion and the strongly positive εNd_t values of tholeiitic basalts in the lower Lough Nafooey Group suggest an origin far from Laurentia (Draut et al. 2004). By c. 490 Ma it is likely that the arc was incorporating some crustal material (Chew et al. 2007). Younger volcanic rocks exhibit a trend towards higher SiO_2 and K_2O, increasing LREE enrichment (Ryan et al. 1980), calc-alkaline affinities and lower εNd_t values, associated with continental material entering the subduction channel (Draut et al. 2004; Fig. 4.9, 4.12). Boninitic-affinity rocks recognized by Clift and Ryan (1994) from the Bohaun Volcanic Formation (Fig. 4.9a) are of unknown age but are typically placed below, or at the base of, the Lough Nafooey Group (e.g. Draut et al. 2004; Ryan & Dewey 2011).

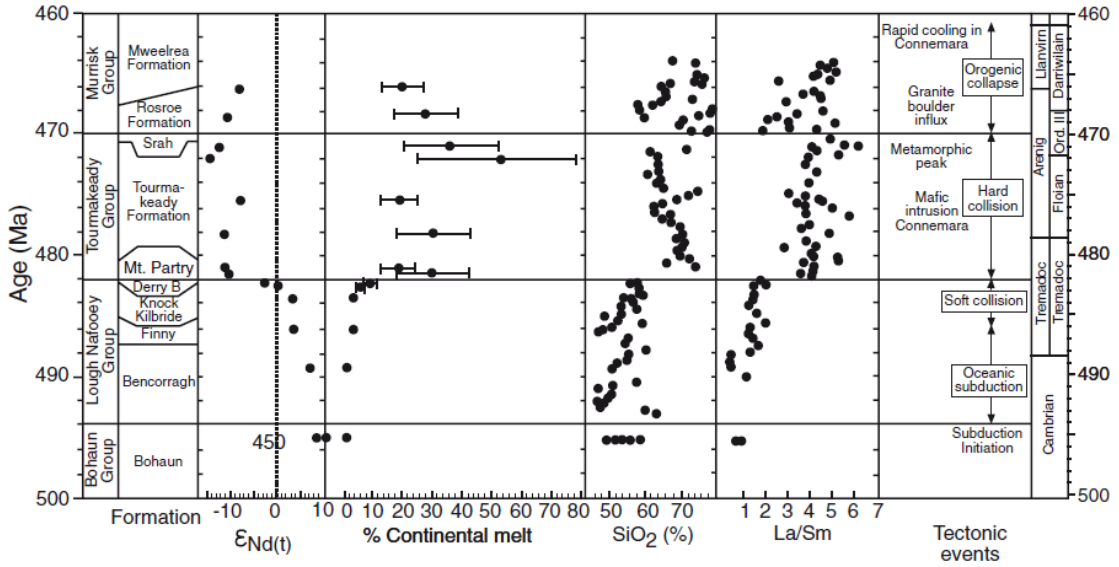

Figure 4.12. Temporal evolution of the Lough Nafooey arc and its proposed link with the orogenic evolution of western Ireland (after Draut et al. 2004). Note: Ryan and Dewey (2011) place the base of the Tourmakeady Group at c. 476 Ma following the timescales of Sadler et al. (2009).

The Tourmakeady Group (c. 476-470 Ma; Ryan & Dewey 2011) of the Irish Caledonides records volcanism during peak deformation and regional metamorphism of the Dalradian Supergroup, and is characterized by a diverse succession of rock types, including: rhyolitic tuffs, breccias and lavas, green and red cherts, graptolitic mudstones, siltstones, limestones and conglomerates (Draut et al. 2004; Graham

2009). SiO_2, LILE- and LREE-enrichment and strongly negative εNd_t values for volcanic rocks imply the assimilation of old continental material associated with the continental margin entering the subduction channel (Draut & Clift 2001; Draut et al. 2004) (Fig. 4.9c, 4.11). The Tourmakeady Group appears to be equivalent to the Snooks Arm arc/backarc complex of Newfoundland which is characterized by similar lithologies (c. 476-467 Ma: Skulski et al. 2010; Zagorevski & van Staal 2011). Both groups formed syn-collisionally, associated with the accretion of a c. 490 Ma oceanic arc which developed above a south-dipping subduction zone (i.e. Lough Nafooey Group and Baie Verte Oceanic Tract) (Draut et al. 2009; Zagorevski & van Staal 2011).

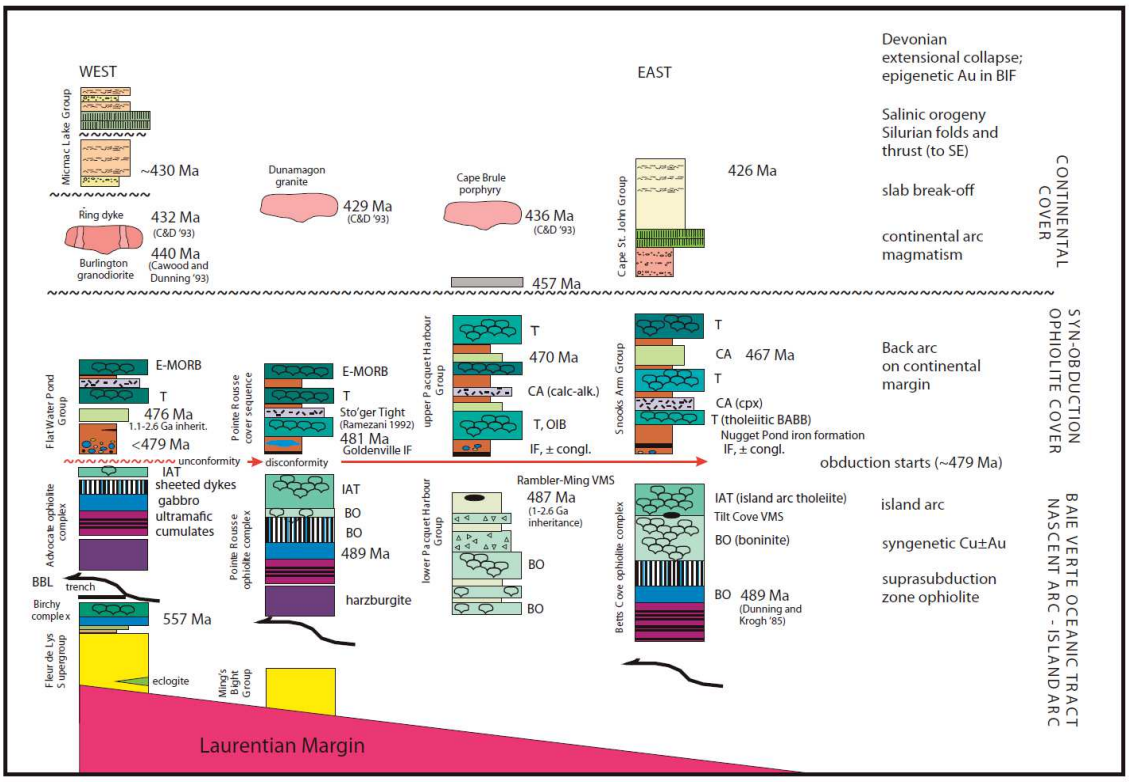

Figure 4.13. Teconostratigraphy of the Baie Verte Oceanic Tract and its cover sequences (diagram from Skulski et al. 2010.

The Snooks Arm Group (c. 476–467 Ma), and its equivalents (e.g upper Pacquet Harbour Group, Flat Water Pond Group, Point Rousse sequence), include a diverse succession of rock types, including many of those described from the Tourmakeady Group (e.g. rhyolitic domes, tuff, tuff breccia, siltstone, chert, conglomerate, mudstone, limestone) (Fig. 4.13). Mafic rocks are dominated by tholeiitic basalt, with calc-alkaline basalt forming a relatively minor component of the Snooks Arm arc (Skulski et al. 2010). Although eMORB and OIB were not described by Skulski et al. (2010) from the Snooks Arm Group *sensu stricto*, these rock types form a relatively minor component in regional equivalents (see Skulski et al. 2010; Fig. 4.13). The

intrusive syntectonic metagabbros and orthogneisses of Connemara (474.5 ± 1 to 467 ± 2 Ma; Friedrich et al, 1999a,b), Ireland, may be correlatives to the continental Notre Dame arc (see Fig. 4.10).

Phase 3: –Development of the Tyrone Igneous Complex?

Using recently published U-Pb zircon geochronology (Cooper et al. 2008, 2011) and the geochemistry and geochronology presented herein we can refine possible correlatives to the Tyrone Igneous Complex.

Correlation of the Tyrone Volcanic Group (c. 475-469 Ma) is inconsistent with both the older Lough Nafooey Group (c. <490-476 Ma) as originally proposed by Draut et al. (2009), and the Baie Verte Oceanic Tract (c. 489-487 Ma), based on the stratigraphy, geochemistry and geochronology presented herein (e.g. Fig. 4.9a-b). LILE- and LREE-enriched island-arc signatures present within the syn-collisional Tourmakeady Group (c. 476-470 Ma; Fig. 7c), and parts of the Snooks Arm Group (c. 476-467 Ma), are comparable to sections of the Tyrone Volcanic Group (also see Cooper et al. 2011), although a direct correlation seems unlikely. The Tourmakeady Group contains no mafic units, which dominate most formations of the Tyrone Volcanic Group; and is characterized by felsic and sedimentary rocks. Sedimentary rocks are scarce within the Tyrone Volcanic Group, restricted to rare beds of siltstone and chert in the lower Tyrone Volcanic Group, and graphitic pelite and layered chert in the uppermost Tyrone Volcanic Group. The Snooks Arm arc is dominated by tholeiitic basalt (Fig. 4.13), which makes up a minor component of one member in the Tyrone Volcanic Group, and similar sedimentary units to the Tourmakedy Group. Furthermore, the Tyrone Volcanic Group is believed to have formed outboard a microcontinental block whereas the Snooks Arm arc formed inboard of Dashwoods (Zagorevski & van Staal 2011).

As there is no evidence for obduction of the Tyrone Volcanic Group onto the Tyrone Central Inlier until c. 470 Ma, correlation to the Tourmakeady Group would require arc-continent collision to be diachronous from c. 476 to 470 Ma across the Irish Caledonides (Draut et al. 2004; Cooper et al. 2011). This scenario predicts a continuation of collision into the Scottish Caledonides associated with a delay in the timing of peak metamorphism and deformation. However, Sm-Nd garnet ages of c. 473-465 Ma for Barrovian metamorphism in the Scottish Highlands (Baxter et al. 2002) are equivalent to U-Pb zircon ages from syn-orogenic intrusives in western Ireland. Syn-D2 to early-D3 basic intrusions from western Ireland give ages of 474.5 ± 1 Ma and 470.1 ± 1.4 (Friedrich et al. 1999a), whereas analysis of late D3 quartz diorite gneisses produced an age of 467 ± 2 Ma (Friedrich et al. 1999b). This demonstrates that Grampian orogenesis was underway by c. 475 Ma across the British and Irish

Caledonides with no clear evidence for diachronous collision along this section of the Laurentian margin. The c. 470 Ma timing in County Tyrone appears to suggest arc-accretion here was associated with an outboard microcontinental block (Tyrone Central Inlier; see Cooper et al. 2011). Although we cannot unequivocally rule out a correlation with the Tourmakedy-Snooks Arm deposits, we believe the Tyrone Igneous Complex more closely correlates with elements incorporated into the Annieopsquotch Accretionary Tract of Newfoundland (see Figs. 4.10, 4.14) in terms of its temporal, geochemical and stratigraphic evolution (see below).

Annieopsquotch Ophiolite Belt: The Annieopsquotch Accretionary Tract of central Newfoundland comprises a thrust stack of Lower to Middle Ordovician arc and backarc terranes accreted to the composite Laurentian margin (van Staal et al. 2009) during the Middle to Upper Ordovician (Zagorevski et al. 2009a) (see Fig. 4.10b). Stratigraphic, geochemical and geochronological similarities have previously been identified between the Annieopsquotch Ophiolite Belt and Tyrone Plutonic Group (Cooper et al. 2011). The c. 480 Ma Annieopsquotch Ophiolite Belt (Dunning & Krogh 1985) comprises several suprasubduction zone ophiolite complexes, which formed during west-directed (=north-dipping in Ireland) subduction outboard of the peri-Laurentian Dashwoods Block (Lissenberg et al. 2005; Zagorevski et al. 2006; Figs. 4.11, 4.14a). Recent geochronology presented by Cooper et al. (2011: 479.6 ± 1.1 Ma) from the Tyrone Plutonic Group, primitive εNd_t values (+4.5 to +7.5; Draut et al. 2009), tholeiitic suprasubduction geochemical characteristics, and its development outboard of a microcontinental block (Tyrone Central Inlier) are all consistent with the correlation to the Annieospquotch Ophiolite Belt (Lissenberg et al. 2004). Xenocrystic Mesoproterozoic zircons present within the Tyrone Plutonic Group are consistent with τ_{DM} ages of 1200-1800 Ma from the Moreton's Harbour Group of Newfoundland (part of the Annieopsquotch Ophiolite Belt; Cutts et al. 2012). The presence of xenocrystic zircons within the Tyrone Plutonic Group suggests it may have formed above a north-dipping subduction zone by the propagation of a spreading centre into a microcontinental block (=Tyrone Central Inlier). A similar tectonic scenario was presented for the formation of the Annieopsquotch Ophiolite Belt by Zagorevski et al. (2006, In Prep; Fig. 4.14a). Fe-Ti-P enriched basalt (to 2.9 wt.% TiO_2) common at propagating rifts also occurs within the Tyrone Plutonic Group (Chapter 5).

Buchans - Robert's Arm Arc: The Buchans Group and correlative Robert's Arm Group of Newfoundland are composed of peri-Laurentian ensialic island-arc volcanics which formed above a west-dipping subduction zone (= north-dipping in Tyrone; Figs. 4.11, 4.14b-d). The Robert's Arm Group (c. 473-464 Ma) includes several imbricated belts of bimodal to mafic, calc-alkaline dominated, arc volcanic rocks (Kerr 1996; O'Brien 2007;

Zagorevski 2008). The Buchans Group (c. 473 Ma) is a bimodal to felsic dominated calc-alkalic succession with strong isotopic and zircon inheritance suggesting interaction with old continental crust (Swinden et al. 1997; Rogers 2004; Zagorevski 2008; Fig. 4.14d); εNd_t values from the Buchans Group range between +1 and -10 (Zagorevski et al. 2006). The geochemistry of the Buchans and Robert's Arm groups is presented within Zagorevski (2008) and summarized in Figure 4.9**.** These data are consistent with correlation to the Tyrone Volcanic Group (Figs. 4.6-4.7) and Fe-Ti enriched non-arc type basalts are also present within the Annieopsquotch Accretionary Tract (to 15.9 wt.% Fe_2O_{3T} and 2.5 wt.% TiO_2) (Fig. 4.7f; Zagorevski 2008). The presence of Fe-Ti enriched non-arc type basalt at many stratigraphic levels within the Tyrone Volcanic Group is consistent with propagation of a rift into the arc/backarc system. A similar situation was invoked to explain how the continental portion of the Robert's Arm -Wiley's Brook arc rifted off Dashwoods leading to the opening the Lloyds River backarc (see Zagorevski et al. 2006). Recently, Zagorevski et al. (2012) have suggested disorganized spreading in the Buchans-Robert's Arm arc may account for the diversity of magma types present (Fig. 4.14d). The Lloyds River ophiolite (c. 473 Ma) is coeval with the oldest members of the Robert's Arm arc and has a chemistry suggesting at this stage the rift had evolved into an oceanic backarc basin (Figs. 4.10b; 4.14b).

Lithologies present within the Robert's Arm (e.g. Kerr 1996; O'Brien 2007) and Buchans Groups (stratigraphy of Zagorevski et al. 2009b; Zagorevski et al. 2010) are also consistent with correlation to the Tyrone Volcanic Group. The Robert's Arm Group includes a diverse succession of calc-alkaline mafic flows, felsic pyroclastic rocks, volcaniclastic turbidites and 'chert-jasperoid' sediments (O'Brien 2007). Massive and pillowed basalt, porphyritic andesite, volcanic breccia (agglomerate) lithic-crystal tuff, argillite, laminated chert, oxide-facies iron formations and tuffaceous sandstone of the Gullbridge tract (see O'Brien 2007; Fig. 4.10b) are all present within the Tyrone Volcanic Group (Fig. 4.4). Within the correlative Buchans Group, the Buchans River Formation is composed mainly of calc-alkaline massive to flow banded rhyolite to rhyodacite, pyroclastic rocks, dacite, volcanogenic conglomerate, granite-bearing conglomerate, sandstone and turbiditic wacke (Zagorevski et al. 2009b), and is similar to the Greencastle Formation of the Tyrone Volcanic Group. By contrast the Ski Hill and Sandy Lake formations of the Buchans Group closely resemble the Creggan, Loughmacrory and Broughderg formations, in that they contain abundant mafic lava, breccias and tuff with subordinate sedimentary rocks, chert, 'jasperoid sediments', rhyolite and felsic tuff (Zagorevski et al. 2009b). The Mary March Brook Formation of the Buchans Group is a tholeiitic bimodal volcanic succession, interpreted to represent

a rifted-arc environment (Zagorevski et al. 2010), which closely resembles the Beaghmore Formation.

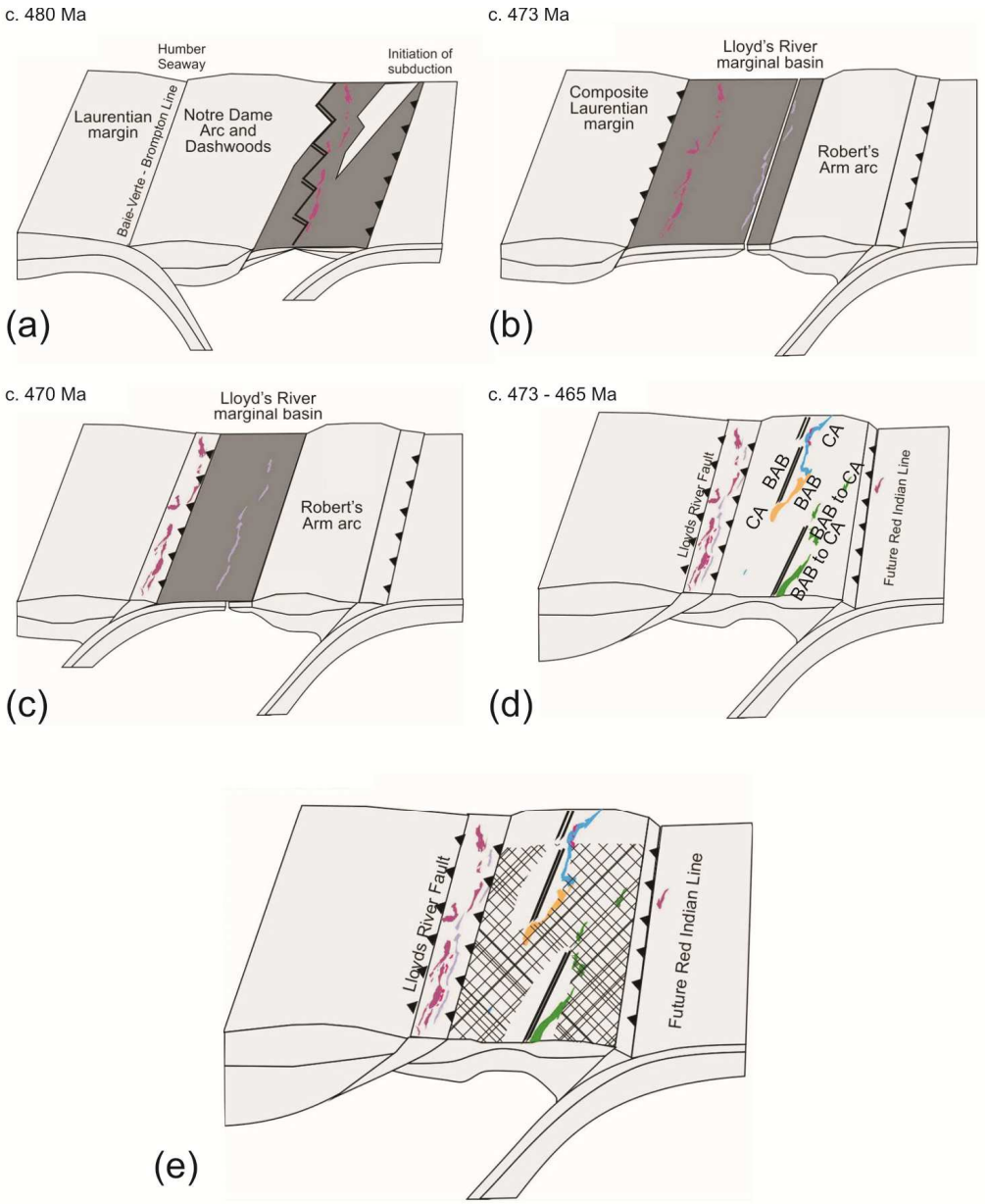

Figure 4.14. Evolution of the Buchans-Robert's Arm arc system (after Zagorevski et al. 2012). (a) Formation of the Anniopsquotch Ophiolite Belt at c. 480 Ma immediately outboard of Dashwoods. The propagation of this spreading centre into the Dashwoods microcontinental block may explain the geochemistry of ophiolites such as the Moreton's Harbour Group and fragments of continental crust under the Buchans-Robert's Arm arc. (b) Formation of the Lloyd's River backarc at c. 473 Ma and the Buchans-Robert's Arm arc. (c) Accretion of the Annioepquotch Ophiolite Belt to the composite Laurentian margin at c. 470 Ma. (d) Disorganised rifting in the Buchans-Robert's Arm belt led to a diversity of magma types. Fe-Ti enriched rift related basalts most likely formed at propagating rifts. (e) Continental inheritance in the Buchans-Robert's Arm Belt.

Accretion to Laurentia: Accretion of the Annieopsquotch Ophiolite Belt, Lloyds River Ophiolite Complex and Buchans-Robert's Arm arc system to the Dashwoods microcontinent occurred between c. 473 and 468 Ma (see Lissenberg et al. 2005; Zagorevski et al. 2006). Similar ages were determined from the c. 470 Ma tonalite suite within the Tyrone Igneous Complex which stitches the Tyrone Plutonic and Tyrone Volcanic Groups to the Tyrone Central Inlier (Cooper et al. 2011). Biotite and hornblende-bearing granitic plutons from the Tyrone Igneous Complex (c. 467 Ma: Cooper et al. 2011) also occur within the central Newfoundland (see Zagorevski et al. 2009b). Following accretion of the c. 465-460 Ma Red Indian Lake Group (Zagorevski et al. 2008), continued closure of Iapetus was accompanied by the accretion of seamount fragments to the Laurentian margin, such as the Crescent Lake Formation (Fig. 4.10b). The South Connemara Group of western Ireland comprises an accretionary volcanic and sedimentary sequence separated from the Dalradian rocks of Connemara by the Skird Rocks Fault, a possible continuation of the Southern Uplands Fault (Hutton & Murphy 1987). Ryan and Dewey (2004) identified part(s) of an accreted seamount within the succession.

4.7.4 Diachronous collision and accretion style

Although we present a model whereby the major terranes and tracts of the Newfoundland Appalachians correlate across the orogen into the British and Irish Caledonides (also see Chew et al. 2010), there are several important differences associated with arc-ophiolite accretion along the Laurentian margin that need to be addressed. Of particular importance is: (i) the diachronous accretion of ophiolites from first-order promontories to adjacent reentrants; (ii) the presence of several terranes that appear to have no direct analogues (e.g. Red Indian Lake Group, Southern Uplands - Longford Down terrane); and (iii) why the arc-ophiolite terranes of the Annieopsquotch Accretionary Tract were underplated to the composite Laurentian margin, whereas in Northern Ireland arc-ophiolite obduction occurred.

Diachronous collision, promontories and reentrants

It has been suggested that first and second order reentrants and promontories along the Laurentian margin may be responsible for the variable preservation of Iapetan ophiolites and their diachronous accretion (Zagorevski & van Staal 2011). Suprasubduction zone ophiolites generated in deep reentrants occur where mainly Mediterranean-style subduction continued as a result of rollback, while convergence slowed significantly at promontories (Zagorevski & van Staal 2011). These peri-collisional ophiolites formed close to the Laurentian margin and were emplaced shortly after formation, occupying an upper plate setting. Most contain well-preserved

metamorphic soles and conform to the classic Penrose stratigraphy (see Zagorevski & van Staal 2011).

In the Quebec Appalachians, the Thetford Mines (479.2 ± 1.6 Ma), Asbestos (478-480 $^{+3}/_{-2}$ Ma) and Lac-Brompton ophiolites (references in Tremblay et al. 2011; Fig. 4.10a) are interpreted to be of similar age to the Annieopsquotch Ophiolite Belt and Tyrone Plutonic Group. However, these ophiolites most likely formed as a result of syn-collisional spreading in reentrants, while obduction of other segments of the Baie Verte Oceanic Tract was ongoing at adjacent promontories (van Staal et al. 2007; Fig. 4.10a). Emplacement of the c. 480 Ma Thetford Mines ophiolite of the Quebec Appalachians onto the Laurentian margin occurred prior to c. 470 Ma (see Tremblay et al. 2011). Younger ages in Quebec for constituents of the Baie Verte Oceanic Tract are consistent with diachronous collision expected when moving from a first order promontory to an adjacent reentrant (Zagorevski & van Staal 2011).

The Ballantrae Ophiolite Complex of Scotland (483 ± 4 Ma U-Pb zircon age: Bluck et al. 1980; Figs. 4.1a, 4.15) is unusual in the British and Irish Caledonides containing a well preserved metamorphic sole which gives a relatively young K-Ar age of 478 ± 8 Ma (Bluck et al. 1980). εNd_t values are between +4.9 and +7.9 and geochemical signatures (including the presence of boninite) are consistent with a suprasubduction zone origin (Smellie & Stone 2001 and references therein). Indication of a suprasubduction zone origin for the Ballantrae ultramafics includes the abundance of harzburgite over lherzolite, wehrlite over troctolite, chrome-spinel chemistry, and Cr-TiO_2 geochemistry of harzburgite (see Oliver et al. 2002).

Evidence supporting a correlation between the Tyrone Igneous Complex and the Ballantrae Ophiolite Complex includes: (i) similar U-Pb zircon ages of c. 484-480 Ma from Ballantrae and the Tyrone Plutonic Group; (ii) their suprasubduction zone characteristics (Cooper et al. 2011); (iii) a close association between ophiolites, island-arc volcanics and within-plate lavas at both; and (iv) the occurrence of Early to Late Arenig graptolitic faunas (Floian to early Darriwilian; Sadler et al. 2009) and tuffs dated at c. 470 Ma (with large analytical errors) from Ballantrae (see Oliver et al. 2002; Sawaki et al. 2010). However, despite these similarities the Ballantrae Ophiolite Complex may also represent a young ophiolite of the Lough Nafooey – Baie Verte arc system associated with a reentrant along the Laurentian margin which was emplaced c. 480 Ma. This could explain the preservation of its metamorphic sole and mantle sequence. Older, albeit unreliable, K-Ar and Sm-Nd ages have also been produced from the Ballantrae Ophiolite Complex for: (i) within-plate affinity gabbro (K-Ar age of 487 ± 8 Ma; Harris et al. 1965), (ii) island-arc lavas (whole-rock Sm-Nd ages of 476 ±

14 Ma and 501 ± 12 Ma; Thirwall & Bluck 1984), and (iii) garnet metapyroxenite (Sm-Nd age of 505 ± 11 Ma; Hamilton et al. 1984). Furthermore, northwestward directed duplexes within the Ballantrae Ophiolite Complex are consistent with southeast directed subduction (Sawaki et al. 2010), whereas the Tyrone Plutonic Group appears to have formed outboard of a peri-Laurentian microcontinetal block above a north-dipping subduction zone.

Obduction or underplating?

Preferential obduction of ophiolites as opposed to their dismemberment and accretion (and possible underplating) is dependent on a number of factors, directly related to tectonic setting and consequently the lithologies involved; these include: (i) the age, hydration and temperature of the crust being emplaced, (ii) the nature of the crust (i.e. type of ophiolite: see Dilek & Furnes 2011), (iii) the presence of topographic highs (e.g. oceanic plateaux or seamounts), (iv) the nature, thickness and effect of the overlying sediment pile, (v) whether the oceanic crust is deformed prior to obduction or accretion, (vi) presence of transform faults; and (vii) the presence and nature of any microcontinental blocks (shape, composition and/or thickness). Underplating of the Annieopsquotch Accretionary Tract to the composite Laurentian margin was associated with the accretion of thin (<5 km) but large slabs of supracrustal arc rocks and ophiolitic crust with high aspect ratios (Zagorevski et al. 2009a). Transfer of these arc-terranes to an upper plate setting was in part controlled by the proximity to the brittle-ductile transition in hydrated crust. Terranes were partially hydrated and cold at the time of their accretion (Zagorevski et al. 2009a). By contrast, the Tyrone Volcanic Group was still hot at the time of its accretion (Cooper et al. 2011) and may have been obducted at the same time as the Tyrone Plutonic Group (see Chapter 5). Other possible explanations for why the obduction of the Tyrone Plutonic and Tyrone Volcanic groups were obducted include: (i) the nature of the microcontinental block onto which they were accreted; and (ii) the arrival of a seamount and temporary jamming of the north-dipping subduction zone, facilitating obduction.

Several lines of evidence now suggest there is basement material underneath the Tyrone Central Inlier: (i) highly magnetic material underlying the Tyrone Central Inlier is clear from Tellus geophysical imagery; (ii) inherited c. 2100 Ma zircons derived from the Tyrone Central Inlier are scarce in peri-Laurentian sources (Cooper et al. 2011); and (iii) extremely negative εHf_{470Ma} values within zircon overgrowths may imply the presence of hidden Archean crust (Flowerdew et al. 2009). An exotic relic of Archean basement material under a consequently thickened microcontinental block may explain why the Tyrone Plutonic Group was obducted rather than underplated.

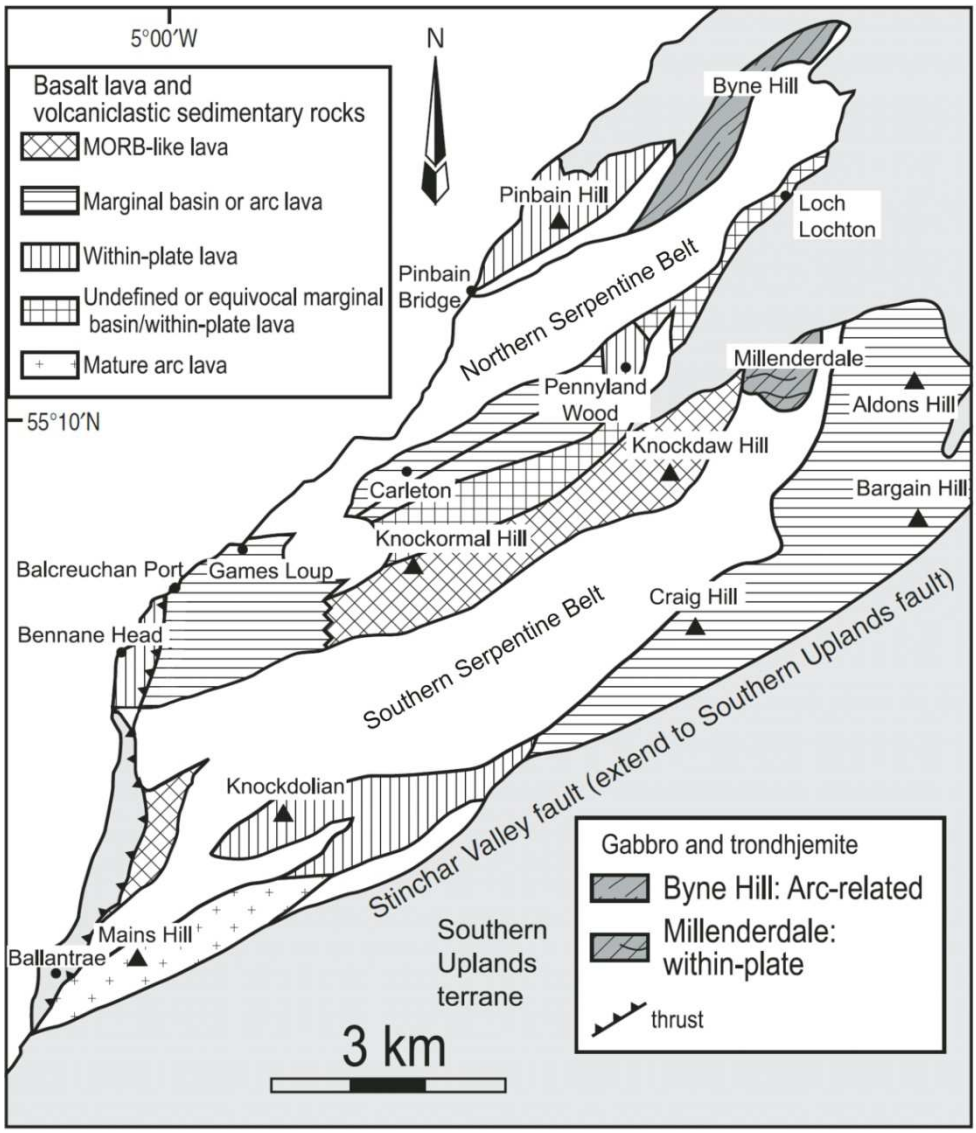

Figure 4.15. Regional geology of the Ballantrae Ophiolite Complex (after Sawaki et al. 2010).

Temporary jamming of the subduction channel may be supported by the presence of the South Connemara Group of western Ireland (Ryan & Dewey 2004). The tectonically disrupted South Connemara Group includes: part(s) of an accreted seamount (Gorumna Formation); oceanic deep sea cherts, with upper levels diluted with distil continentally-derived detritus (Golam Formation); and conglomerate containing abundant detrital almandine from a recycled orogen provenance, and igneous and metamorphic clasts (Lettermullen Formation) (see Dewey & Ryan 2004). Together, with structural data, this argues for formation in a subduction-accretion complex above a north-dipping subduction zone (Ryan & Dewey 2004). Clasts of the Lettermullen Formation imply a post- or syn-Grampian age for the Group. Limited paleontogical constraints place the Golam Formation within the Floian-Darriwilian (Lower-Middle Ordovician; Graham

2009; Sadler et al. 2009). Along the Northern Belt of the Southern Uplands Terrane and along the northern edge of the Longford Down Terrane tectonic slices of alkali and tholeiitic basalt of within-plate affinity occurs; these may be equivalent tectonically accreted fragments of seamount(s) and island-arc volcanoes (Ryan & Dewey 2004). Temporary jamming of the subduction zone by the arrival of a seamount(s) or island-arc volcano may have facilitated obduction at c. 470 Ma. Extensive post-Ordovician cover sequences obscure most of the Midland Valley Terrane SE of the Tyrone Igneous Complex.

The occurrence of the Red Indian Lake Group in the Newfoundland Appalachians and the Southern Uplands – Longford Down accretionary prism in the British and Irish Caledonides may reflect the geometry and along-strike extent of the colliding Red Indian Lake arc system. Although there is evidence for a buried arc terrane within the Southern Uplands – Longford Down terrane, this sector of the Laurentian margin was predominantly characterized by the progressive underplating of Iapetan ocean floor to the composite Laurentian margin throughout the Late Ordovician (Graham 2009).

4.8 Conclusions

The Tyrone Igneous Complex of Northern Ireland is an integral part of the Grampian–Taconic phase of the Caledonian–Appalachian orogen. New geological survey has enabled the Tyrone Volcanic Group to be placed within a detailed structural and stratigraphic context. Extensive new geochemistry details the progressive evolution of a short-lived peri-Laurentian island arc/backarc (c. <475-469 Ma) which developed outboard of a microcontinental block (Tyrone Central Inlier) prior to its accretion at c. 470 Ma. Episodic arc-rifting is recorded by the occurrence of Fe-Ti enriched basalts of eMORB affinity at several stratigraphic levels, alkali basalt, LREE-depleted island-arc tholeiite and tholeiitic rhyolite with flat to U-shaped REE profiles.

Broad correlations can be made across the Grampian–Taconic event. Three major phases of arc-ophiolite accretion identified in the Newfoundland Appalachians are now recognized within the Caledonides. Early ophiolite obduction within the Caledonides is recorded by the emplacement of the Deer Park (c. 514 Ma) and Highland Border (c. 500 Ma) ophiolites onto possible outboard microcontinental blocks, broadly equivalent to the emplacement of the Lushs Bight Oceanic Tract (c. 510-501 Ma) of Newfoundland onto the Dashwoods microcontinental block at c. 500-493 Ma. Continued closure of the Iapetus Ocean led to the formation and accretion of the c. <490-476 Ma Lough Nafooey arc (= buried Midland Valley arc?) to the Laurentian margin. This phase of arc-ophiolite accretion is recorded in Newfoundland by the development and emplacement

of the Baie Verte Oceanic Tract (c. 489-487 Ma). The syn-collisional stage of the Lough Nafooey arc (Tourmakeady Group; c. 476-470 Ma) appears to be broadly equivalent to the development of the Snooks Arm Group (c. 476-467 Ma) of Newfoundland. The Tyrone Igneous Complex (c. 480-464 Ma) closely resembles elements incorporated within the Annieopsquotch Accretionary Tract of Newfoundland, specifically the c. 480 Ma Annieopsquotch Ophiolite Belt and Buchans-Robert's Arm groups (c. 473-464 Ma).

Chapter 5: Evolution and emplacement of the Tyrone ophiolite

This chapter forms the basis of a submitted manuscript: Hollis, S.P., Cooper, M.R., Roberts, S., Earls, G., Herrington, R., & Condon, D.J. (Submitted). *Late obduction of the Northern Irish, Tyrone ophiolite during the Grampian-Taconic orogeny: Links to central Newfoundland?* Journal of the Geological Society, London.

Abstract

The Tyrone Plutonic Group of Northern Ireland represents the upper portions of a tectonically dissected suprasubduction zone ophiolite accreted to the composite Laurentian Margin during the Middle Ordovician. Understanding its development and relationship to the Tyrone Central Inlier, a fragment of relatively high-grade, peri-Laurentian continental crust exposed SE of the Fair Head – Clew Bay Line, is essential for reconstructing the closure of the Iapetus Ocean. The Tyrone Plutonic Group is composed of tectonised and amphibolite-facies, layered, isotropic and pegmatitic gabbros, sheeted dolerite dykes and rare pillow lavas. New U-Pb zircon TIMS geochronology has produced a date of 483.68 ± 0.8 Ma from pegmatitic gabbro, consistent with a previously published age of 479.6 ± 1.1 Ma from the ophiolite. Geochemical characteristics, Nd and Sr isotope systematics, and zircon inheritance indicate the Tyrone Plutonic Group formed above a N-dipping subduction zone, by the propagation of a spreading centre into a microcontinental block. Syn-kinematic, calc-alkaline tonalitic to granitic melt within its contact to the underlying Tyrone Central Inlier suggests it may have been emplaced relatively late within the orogen at c. 470 Ma. Mineral chemical data from syn-kinematic tonalitic material has produced pressure estimates of c. 2.3-4 ± 0.6 kbar and temperatures of 525-610 ˚C. Coeval accretion of a thick, hot, arc-ophiolite complex at this time may explain how sillimanite-grade metamorphic conditions were reached locally in the underlying Tyrone Central Inlier prior to c. 468 Ma. Strong temporal, geochemical and lithological similarities exist with the Annieopsquotch Ophiolite Belt of Newfoundland, indicating these ophiolites may have a shared origin and evolution.

5.1 Introduction

As detailed in Chapter 1, ophiolites represent rare fragments of upper mantle and oceanic crust incorporated into continental margins during continent-continent and arc-continent collisions, ridge-trench interactions and/or subduction-accretion events (references in Dilek & Furnes 2011). Following the Penrose definition (Anonymous 1972) and establishment of the plate tectonic theory, a paradigm shift occurred for ophiolite genesis between the early 1970s and mid 1980s, when it was recognized that most have geochemical similarities to island-arcs (e.g. Miyashiro 1973; Harper 1984). Consequently, the ophiolite concept moved toward a magmatic origin in subduction zone settings (suprasubduction zone ophiolites; e.g. Pearce et al. 1984b). Suprasubduction zone ophiolites are interpreted to form in arc-forearc or backarc settings at convergent margins shortly before orogenesis (Dilek & Furnes 2011). Common within many Early Paleozoic orogens, such as the Caledonian, Appalachian, and Uralian belts, suprasubduction zone ophiolites often mark the location of subduction sutures within short-lived collision zones and can therefore provide essential information on the closure of ancient ocean basins and their temporal evolution (e.g. Dewey 2005).

The Grampian (=Taconic) phase (c. 475-465 Ma) of the Caledonian-Appalachian orogen (Fig. 5.1) resulted from the progressive accretion of a diverse set of arc terranes, ribbon-shaped microcontinental blocks and oceanic tracts to the Laurentian margin during the Early Paleozoic closure of the Iapetus Ocean (Draut et al. 2004; Cooper et al. 2011). In the British and Irish Caledonides, deformed and metamorphosed Neoproterozoic to Early Paleozoic rocks of the Dalradian Supergroup represent cover sequences of the Laurentian margin (Chew 2009). Recent advances, including: new fieldwork, geochemistry, U-Pb zircon and Ar-Ar geochronology (e.g. Chew et al. 2008, 2010; Flowerdew et al. 2009; Cooper et al. 2008, 2011; Hollis et al. 2012), have now revealed the Grampian orogeny was much more complex than previously thought. Three main episodes of arc-ophiolite emplacement are recognized within the Newfoundland Appalachians, during the equivalent Taconic orogeny (van Staal et al. 2007). Although potential correlatives to each of the c. 510-500 Ma Lushs Bight Oceanic Tract, c. 490-470 Ma Baie Verte Oceanic Tract/Snooks Arm arc, and c. 480-460 Ma Annieopsquotch Accretionary Tract of the Newfoundland Appalachians have been identified in the British and Irish Caledonides (Chew et al. 2010; Cooper et al. 2011; Hollis et al. 2012), a number of specific terrane correlations remain contentious. Group and Deer Park Complex.

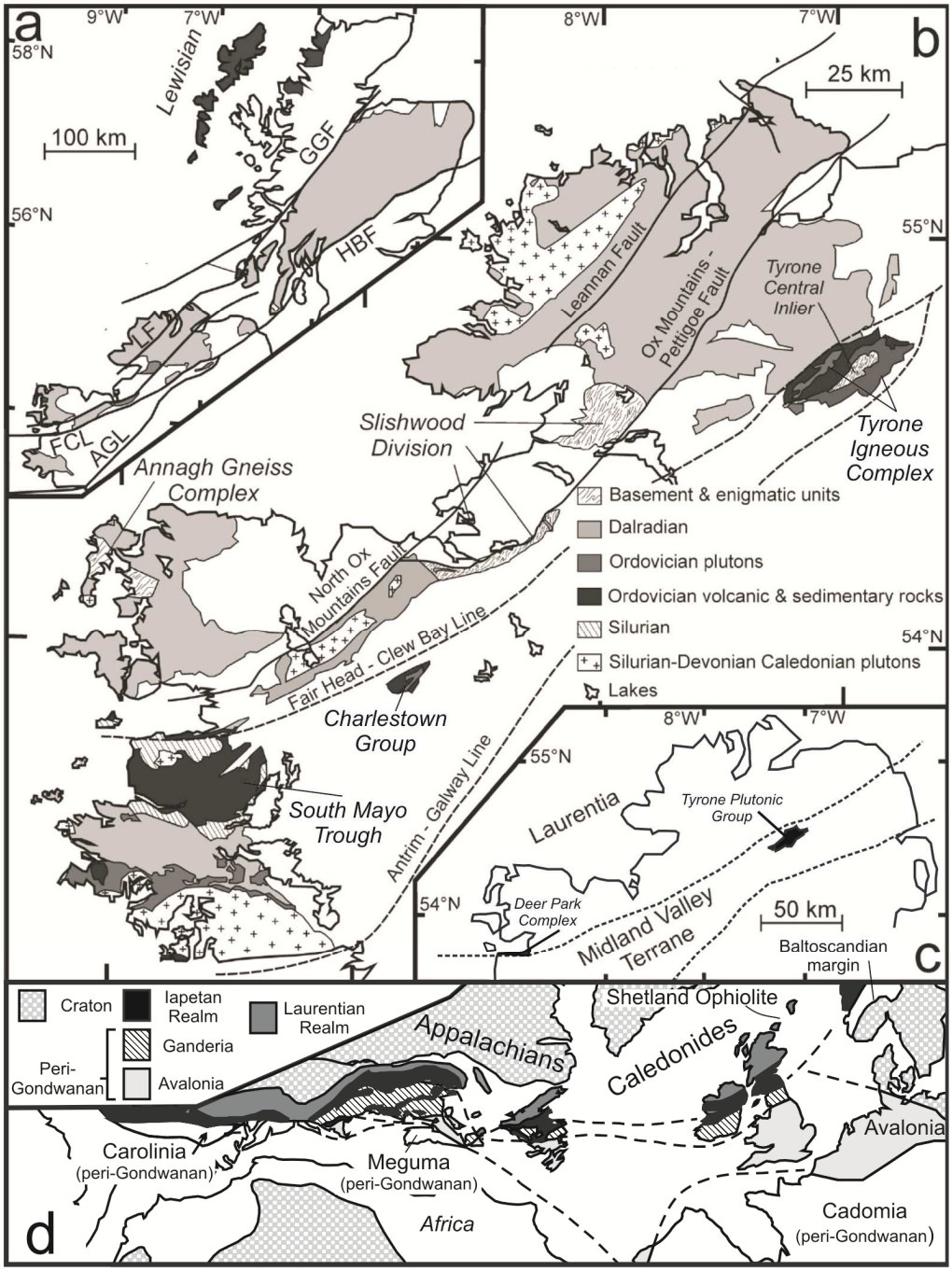

Figure 5.1. (a) Schematic geology of British and Irish Caledonides showing major fault lines (from Flowerdew et al. 2009). Dark shading: Grenvillian and older crystalline basement rocks; medium shading: Slishwood Division and Tyrone Central Inlier; pale shading: Dalradian Supergroup. AGL, Antrim - Galway Line; FCL, Fair Head – Clew Bay Line; GGF, Great Glen Fault; HBF, Highland Boundary Fault; LF, Leannan Fault (b) Schematic geology of NW Ireland. Bold lines refer to major faults; crustal structures inferred from geophysical data are dashed (after Flowerdew et al. 2009). (c) Map showing the distribution of Laurentia and the Midland Valley Terrane in the north of Ireland. Outcrop of ophiolites are shown by shading: Tyrone Plutonic

Group and Deer Park ophiolite. (d) Early Mesozoic restoration of North Atlantic region and Appalachian-Caledonian orogen (after Pollock et al. 2009).

In the Newfoundland Appalachians, the presence of outriding microcontinental blocks was invoked to explain the discrepancies between the timing of syntectonic sedimentation and tectonic loading on the passive continental margin at c. 475 Ma and ophiolite emplacement prior to 488 Ma (see Waldron & van Staal 2001); and the range of ages for Iapetian ophiolites accreted to the Laurentian margin (van Staal et al. 2007). Recent work from the British and Irish Caledonides has similarly demonstrated that subduction and the onset of obduction occurred at least 15 Ma before the Grampian orogeny (Chew et al. 2010). Consequently, understanding the relationship between suprasubduction zone ophiolites and any peri-Laurentian microcontinental blocks within the Caledonides (such as the Tyrone Central Inlier and Slishwood Division; Flowerdew et al. 2009, Chew et al. 2010; Hollis et al. 2012) is vital for reconstructing the progressive closure of the Iapetus Ocean.

The Tyrone Plutonic Group of Northern Ireland (Fig. 5.2) represents the upper parts of a tectonically dissected ophiolite sequence (Hutton et al. 1985) accreted onto an outboard segment of Laurentia, the Tyrone Central Inlier, during the Middle Ordovician (Cooper & Mitchell 2004). Opinions on the timing of its formation, emplacement and relationship to both the Tyrone Volcanic Group (a peri-Laurentian island arc) and the Tyrone Central Inlier (a peri-Laurentian microcontinental block; Chew et al. 2008, 2010) have varied (e.g. Angus 1970; GSNI 1979; Hutton et al. 1985; Cooper & Mitchell 2004; Cooper et al. 2008; Chew et al. 2008; Draut et al. 2009; Cooper et al. 2011). Recent U-Pb zircon geochronology has dated LREE-depleted layered gabbro from the Tyrone Plutonic Group to 479.6 ± 1.1 Ma (Cooper et al. 2011), which is significantly younger than previous geochronology from the ophiolite (493 ± 2 Ma: Draut et al. 2009) and other ophiolites preserved in the British and Irish Caledonides. For example, the Deer Park Complex of western Ireland, the Scottish Highland Border Ophiolite and the Shetland Ophiolite have yielded considerably older ages of 514 ± 3 Ma, 499 ± 8 Ma and 492 ± 3 Ma respectively (Spray & Dunning 1991; Chew et al. 2010). Only the Ballantrae Ophiolite Complex of Scotland has produced a similar U-Pb zircon age of 483 ± 4 Ma (Bluck et al. 1980).

Here we present the interpreted results of high-resolution airborne geophysics, whole rock and mineral geochemistry, and key field relationships across the region, in addition to a new U-Pb zircon age for a pegmatitic gabbro from the Tyrone Plutonic Group. These new data suggest that the c. 484-480 Ma Tyrone Plutonic Group was emplaced relatively late in the Grampian orogeny at c. 470 Ma, coeval with the

accretion of the Tyrone arc (=Tyrone Volcanic Group, see Cooper et al. 2011), and is therefore broadly equivalent to the c. 481-478 Ma Annieopsquotch Ophiolite Belt of Newfoundland. As the Tyrone Plutonic Group lacks an ultramafic section, it is unlikely to have obducted a sufficiently thick and hot ophiolite sequence to account for the sillimanite-grade metamorphic conditions in the underlying Tyrone Central Inlier (c. 670 ± 113 ˚C, 6.8 ± 1.7 kbar; Chew et al. 2008). However, coeval accretion of a hot, thick arc-ophiolite complex may explain how these metamorphic conditions were reached prior to c. 468 Ma.

5.2 Field relationships

The Tyrone Plutonic Group is exposed across approximately 95 km^2 of counties Tyrone and Londonderry, Northern Ireland. It crops out predominantly SE of the Tyrone Central Inlier, and to a lesser extent to the NW around Davagh Forest in faulted contact with the Tyrone Volcanic Group (Fig. 5.2). The Tyrone Plutonic Group consists mainly of variably tectonised and metamorphosed, layered, isotropic and pegmatitic gabbros, sheeted dolerite dykes and rare pillow lavas which were thrust over the Tyrone Central Inlier during the Middle Ordovician (Hartley 1933; GSNI 1979, 1995; Hutton et al. 1985; Cooper & Mitchell 2004) (Fig. 5.2).

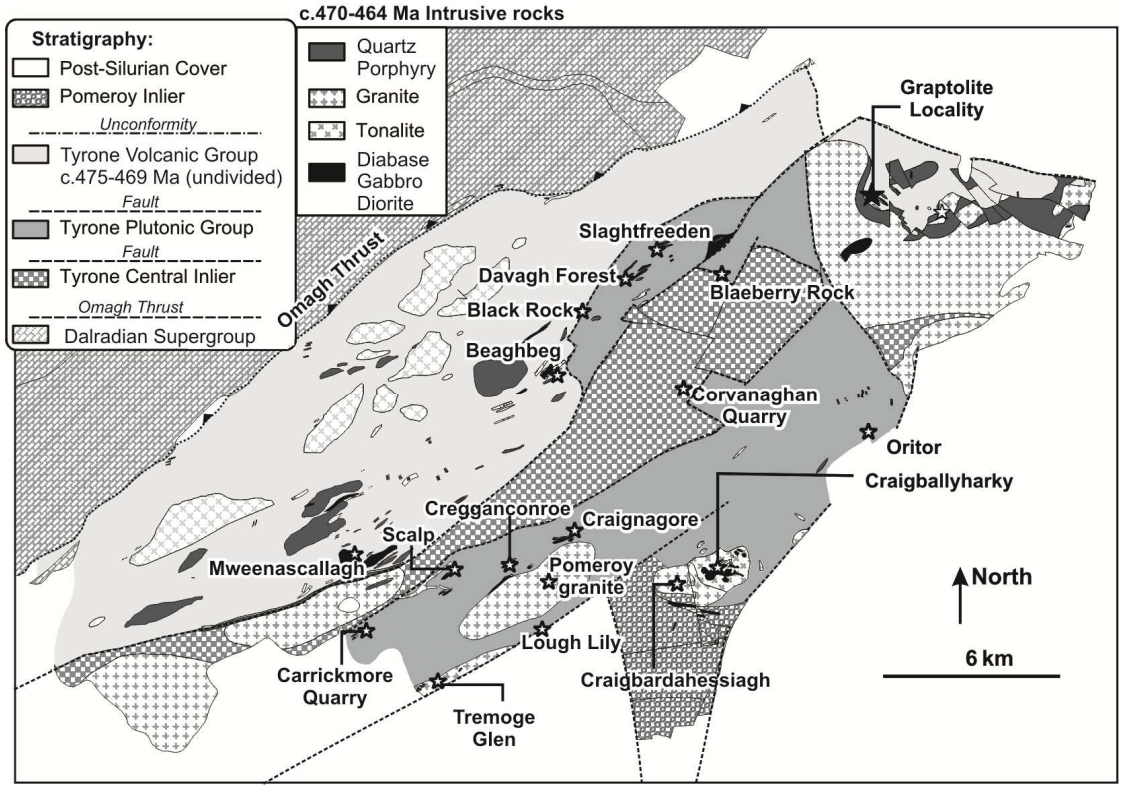

Figure 5.2. Geological map of the Tyrone Igneous Complex (after GSNI 1979, 1983, 1995; Cooper et al. 2011; Hollis et al. 2012). For subdivision of the Tyrone Volcanic Group see Hollis et al. (2012). Stars refer to localities discussed in the text.

Primary mineral assemblages in the Tyrone Plutonic Group have been altered to epidote-amphibolite metamorphic assemblages (Merriman & Hards 2000). Mafic minerals have been replaced by hornblende, epidote, actinolite and/or chlorite, with feldspars variably sericitised. Groundmass often comprises a mixture of quartz, amphibole, actinolite, chlorite and epidote, as well as less abundant zircon, titanite, sericite, biotite, and locally carbonate. Although the Tyrone Plutonic Group is tectonically dissected and poorly exposed, several key localities preserve a relatively complete upper crustal ophiolite sequence (Hutton et al. 1985; Fig. 5.3). The following zones have been recognised (adapted after GSNI 1979; Hutton et al. 1985).

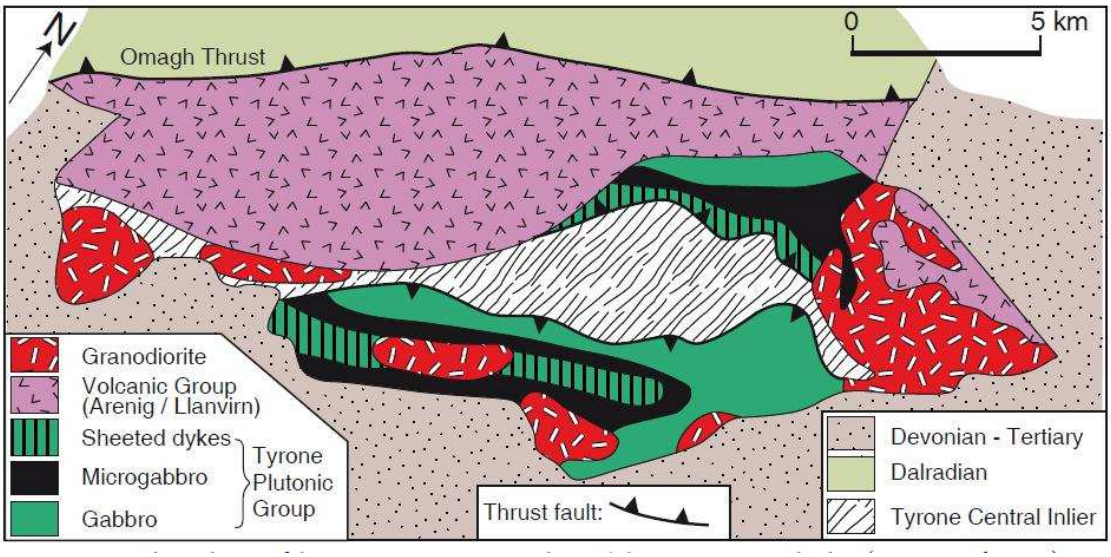

Figure 5.3. Geological map of the Tyrone Igneous Complex and Tyrone Central Inlier with emphasis placed on Tyrone Plutonic Group (after Hutton et al. 1985; Chew 2009).

5.2.1 Layered and isotropic gabbros

Layered and isotropic gabbros comprise the majority of the Tyrone Plutonic Group and are best exposed at Scalp Hill and eastwards through Creggan conroe and Craignagore (Fig. 5.2). Olivine gabbros at Scalp Hill (serpentine after olivine) display cumulate layering, locally differentiated into compositionally distinct bands (cm to m scale) (Cobbing, 1969; GSNI 1979). Locally gabbro may be deformed to resemble hornblende schist, with schistosity parallel to mineral layering in surrounding rocks (Cooper & Mitchell 2004). Cooper et al. (2011) reported a U-Pb zircon age of 479.6 ± 1.1 Ma for layered gabbro from Scalp Hill. Layered magnetite gabbro is common around Scalp and immediately NW of the Craigballyharky Complex (GSNI 1979).

Layered and isotropic gabbros at several localities appear to be younger than an early suite of dolerites (equivalent to 'Early Dolerites and Gabbros': BGS 1986). At Craignagore (Fig. 5.2), a central gabbro is enclosed by fine to medium grained amphibolite-facies dolerite (Angus 1970). The gabbro is largely uniform and porphyritic adjacent to its southern contact, and is cut by a late series of dolerite dykes (equivalent to the 'Ophitic Dolerites of Carrickmore': BGS 1986). Dolerite surrounding the gabbro is generally foliated or schistose; with a finely crystalline relic of pyroxene-hornfels exposed at one locality (Angus 1970).

5.2.2 Transition Zone

At Black Rock (Fig. 5.2), coarse-grained hornblende gabbro intrudes, and contains xenoliths of, an early-formed suite of dolerite ('Early Dolerites and Gabbros': BGS 1986). This sequence is in turn intruded by younger 1-2 m wide, basalt and dolerite dykes (Cooper & Mitchell 2004) (Fig. 5.4a-b). Early basaltic and dolerite dykes are deformed, locally schistose and extensively altered with fine stringers of epidote. Gabbro is extremely coarse grained, ranging from equigranular in nature to pegmatitic. Irregular veins of pegmatitic gabbro contain large hornblende and plagioclase crystals often exceeding 2 cm in diameter (rarely > 8 cm). The youngest suite of basaltic and doleritic dykes at Black Rock (equivalent to the 'Ophitic Dolerites of Carrickmore': BGS 1986) are relatively undeformed and less extensively altered. Porphyritic varieties contain 1-2 mm rounded and angular laths of plagioclase in a fine-grained, ophitic or intergranular matrix.

At Oritor (Fig. 5.2), dolerite dykes intrude gabbro, which contains xenoliths of an earlier foliated dolerite. Dolerite dykes typically trend NW-SE and can be distinguished from Palaeogene olivine-bearing dykes by their composition and state of alteration; the former always being extensive uralitised (Hartley 1933). At Slaghtfreeden (Fig. 5.2), isotropic and pegmatitic gabbro, microgabbro and dolerite also contain xenoliths of foliated basalt. These are intruded by and present as xenoliths in, late intrusives of quartz and hornblende porphyritic diorite (Fig. 5.4c). Late ophitic dolerite dykes are also present at Carrickmore, Creggan conroe and Craignagore (Fig. 5.2) which cut olivine gabbro and/or poikiloblastic hornblende gabbro.

5.2.3 Sheeted Dykes

Although the presence of ophitic dolerite at Carrickmore was recognized by Hartley (1933), it was Hutton et al. (1985) who first reported the presence of parallel sheeted dolerite dykes in Carrickmore Quarry (Fig. 5.2). The sheeted dykes typically average 1 m in thickness, intrude one another forming two-sided chilled margins and more

commonly one sided chilled margins and can locally constitute 100% of the exposure. Dolerite at Carrickmore appears aphanitic in hand specimen, though may be either intergranular or ophitic in thin section. In Craigballyharky Quarry, dolerite dykes display rare chilled margins and are intruded by relatively undeformed plagiogranite and aplite (Fig. 5.4d).

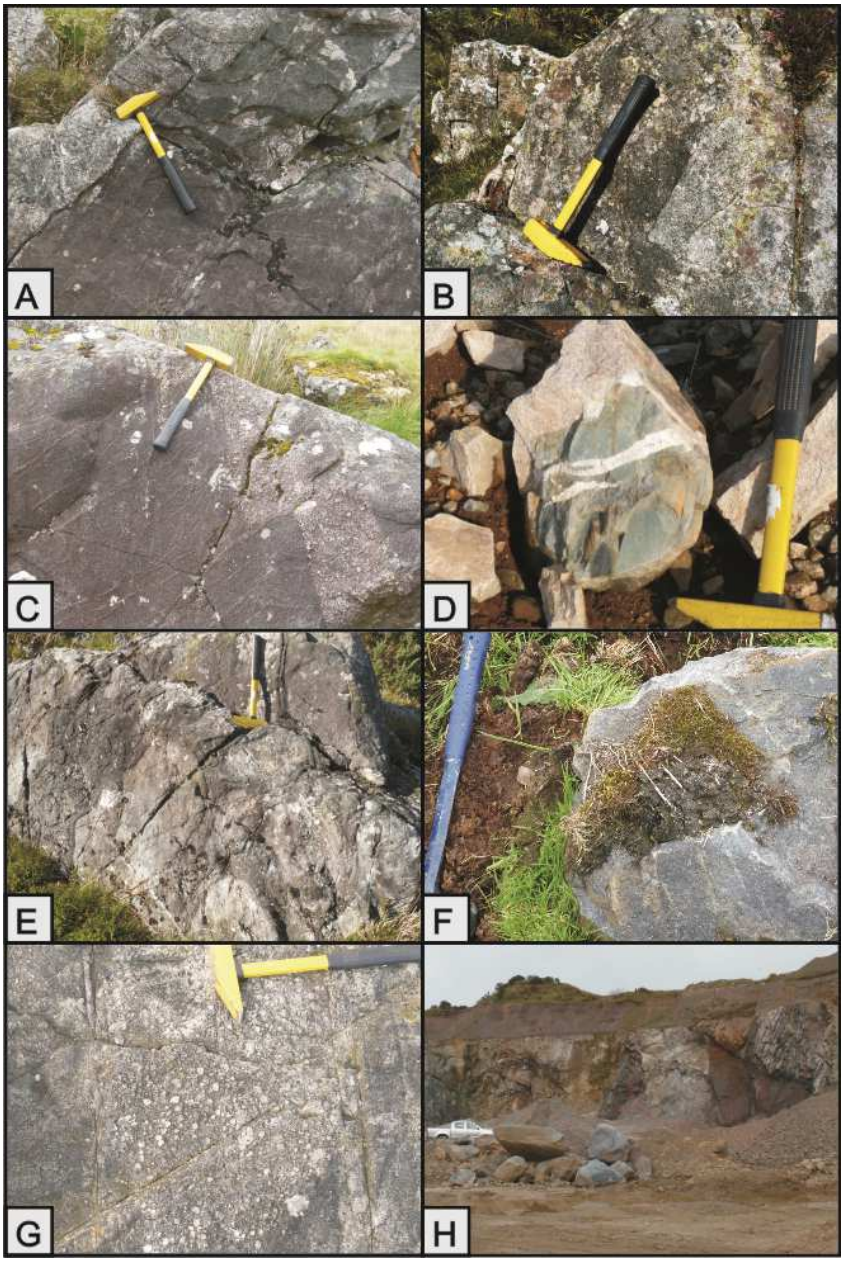

Figure 5.4. Field photographs from across the Tyrone Plutonic Group. (a) Pegmatitic gabbros intruding (and intruded by) dolerite/basaltic dykes at Black Rock. (b) Angular xenoliths of early foliated dolerite/gabbro in hornblende gabbro at Black Rock. (c) Dolerite intruded by a dyke of quartz and hornblende porphyritic diorite at Slaghtfreeden. (d) Dolerite cut by veins of aplite at Craigballyharky Quarry. (e) Pillow basalts at Craigballyharky. (f) Roof pendant of ironstone in biotite granodiorite at Craigbardahessiagh. (g) Quartz ocilli migrating from tonalite into gabbro

at Craigballyharky. (h) Tremoge Glen muscovite granite intruding gabbros of the Tyrone Plutonic Group.

5.2.4 Pillow basalts and volcaniclastic rocks

Pillow lavas are scarce within the Tyrone Plutonic Group, and are best exposed as a series of roof-pendants within the Craigballyharky complex (Cobbing et al. 1965). Pillow structures at Craigballyharky typically range between 30 and 75cm in diameter (Fig. 5.4e). These lavas are aphanitic, subalkaline, tholeiitic, LILE and LREE-depleted and of suprasubduction affinity (Cooper et al. 2011). Intermediate and basic lavas have also been reported to occur at Scalp (Hartley 1933), with amygdaloidal lavas present SW of Scalp Hill. At Slaghtfreeden, Hartley (1933) noted a sheet of gabbro intruding lavas overlain by coarse breccias and tuffs, which are in turn were subsequently intruded by a dolerite dyke.

5.2.5 Craigballyharky complex

The Craigballyharky complex (Cobbing et al. 1965; GSNI 1979) is exposed across approximately 3.5 km^2 (Fig. 5.2) and is composed of three major units: an intrusion of tonalite representing the summit of Craigballyharky (472 $^{+2}/_{-4}$ Ma of Hutton et al. 1985; 470.3 ± 1.9 Ma of Cooper et al. 2011), an intrusion of biotite-granodiorite representing the summit of Craigbardahessiagh (464.9 ±1.5 Ma of Cooper et al. 2011), and quartz-diorite (see Angus 1962, 1977). A series of roof pendants exposed across the complex include siliceous ironstone most likely derived from the Tyrone Volcanic Group, and isotropic gabbros, dolerites and pillow lavas from the Tyrone Plutonic Group (Cobbing et al. 1965). Silicious ironstone has been recorded within both the Craigbardahessiagh granodiorite (Fig. 5.4f) and Craigballyharky tonalite (GSNI, 1979). Together, these roof pendants imply both the Tyrone Volcanic Group and Tyrone Plutonic Group were in their present structural position above the Tyrone Central Inlier prior to c. 470 Ma, as these intusions contain Proterozoic xenocrystic zircons derived from the Tyrone Central Inlier (Cooper et al. 2011). Occurrences of agglomerate, limestone and silicified metasedimentary rocks have also been reported (Cobbing et al. 1965; GSNI 1979) though were not observed during recent fieldwork.

Quartz diorite is widely regarded to be hybrid in origin (Angus 1962, 1977), produced by magma-mixing between arc-related gabbro and c. 470 Ma tonalite at Craigballyharky (Hutton et al. 1985; Cooper et al. 2011). Although recent dating reported an age of 493 ± 2 Ma for Craigballyharky gabbro (Draut et al. 2009), Cooper et al. (2011) presented a recalculated mean $^{206}Pb/^{238}U$ age of 473.2 ±1.6 Ma for this unit, significantly younger and in agreement with field-relations and its relatively unaltered and undeformed nature. Consequently, the Craigballyharky gabbro is

attributed to the younger c. 470-464 Ma arc related intrusive suite, consistent with its LILE and LREE-enriched geochemical characteristics (Cooper et al. 2011). Arc-related gabbro also intrudes the c. 475-469 Ma Tyrone Volcanic Group at Beaghbeg and Mweenascallagh (Fig. 5.2; Hollis et al. 2012), although the latter is of eMORB affinity. At Craigballyharky, magma mixing within a hybrid quartz diorite is seen in outrop where large quartz phenocrysts (oscilli) are observed to have migrated from the tonalite into gabbro through magma mixing-mingling (Hutton et al. 1985). Contacts are typically diffuse and irregular, though may locally be sharp (Fig. 5.4g).

5.2.6 Arc-related intrusive suite

The arc-related intrusive suite includes a series of high-level plutons, sills and dykes of various compositions, which intrude all levels of the Tyrone Igneous Complex (Fig. 5.2). Large intrusions of diorite, granodiorite, tonalite, biotite- and hornblende-bearing granite, and quartz ± feldspar porphyry are the most frequent; although minor occurrences of arc-related gabbro and dolerite also occur (Hollis et al. 2012). Field relationships and published U-Pb geochronology (Cooper et al. 2011) are consistent with the intrusions being significantly younger than the Tyrone Plutonic Group. For example, diorite at Lough Lily (Fig. 5.2) contains angular xenoliths of ophiolite-derived dolerite and intrudes the latter as veins (Hartley 1933). At Scalp, coarsely crystalline, pink and grey hornblende-rich tonalite (equivalent to the Golan Burn tonalite of Cooper et al. 2011: 469.9 ± 2.9 Ma) contains xenoliths of gabbro which show all stages of assimilation and the development of hybrid granite (GSNI 1979). At Black Rock, xenoliths of amphibolite-facies gabbro are present within LREE-enriched arc-related quartz ± biotite ± hornblende porphyry.

5.2.7 Tremoge Glen

Medium to coarse grained and pale-grey to pink granite exposed at Tremoge Glen is unusual within the Tyrone Igneous Complex as it is extensively altered, intensely sheared and muscovite-bearing. Geological mapping reveals the granite intrudes gabbros of the Tyrone Plutonic Group (Fig. 5.4h) and is itself intruded by NE and NW trending late basaltic/doleritic dykes with ophitic textures (GSNI 1979; Fig. 5.2). The Tremoge Glen intrusion occurs as a NE-SW orientated wedge of granite bound on its eastern side by the Tempo – Sixmilecross Fault (Fig. 5.2).

5.3 Ophiolite contact: Blaeberry Rock

A high strain zone of mylonitic meta-igneous rocks E of Davagh Forest was discovered at the mapped contact between the Tyrone Central Inlier and Tyrone Plutonic Group (Fig. 5.2). The exposure, known locally as Blaeberry Rock, consists of a 7 x 6 x 3 m

block and several smaller boulders (Fig. 5.5a). The main exposure comprises cm- to dm-sized blocks of amphibolite-facies gabbroic to doleritic material within a mélange of mm- to cm- scale banded and isoclinally folded syn-kinematic tonalitic to granitic melt product, amphibolite and possible Dalradian metasedimentary rocks (Fig. 5.5b-e). Nearby exposures include smaller angular blocks of gabbro and dolerite which display preserved chilled margins and quartzofeldspathic paragneisses of the Tyrone Central Inlier invaded by tonalitic melt, leucosomes and pegmatite. Younger moderately deformed tonalitic to granitic veins cut the sheared rocks and may themselves be folded and boudinaged.

Preferential localization of strain appears to be confined to the intrusive sheets, with gabbroic inclusions relatively undeformed except for some alignment of amphibole crystals. Amphibole porphyroclasts up to 3.5cm in length occur within the melt network and appear to be derived from brecciated bodies of gabbro cut by thin veins. These amphibole crystals, along with minor drag folds, show evidence for sinistral shearing (Fig. 5.5f). Paler grey tonalitic fragments also contain a well-developed mineral stretching lineation. Narrow shear zones and late veins of epidote cut the exposure.

Gabbroic and doleritic blocks exposed within the Blaeberry Rock contact are petrologically similar to those from the Tyrone Plutonic Group. These ophiolite derived lithologies have experienced amphibolite facies metamorphism and are composed of actinolite (after pyroxene) and plagioclase replaced by white-mica, chlorite and epidote (Fig. 5.5g-j). Synkinematic and late tonalitic veins are dominated by quartz, orthoclase, sericitised labradorite with minor muscovite, trace biotite and accessory phases (fluorapatite and sphene). Plagioclase may be internally altered to chlorite, epidote and muscovite (Fig. 5.5g-j).

5.4 Tellus airborne geophysics

During 2005-2006 the Tellus airborne geophysical survey, part of the Tellus Project (see GSNI 2007), was flown across the entirety of Northern Ireland. Magnetic, radiometric and electromagnetic (EM) data were acquired. Further detail on survey specification and geophysical data processing are summarised within Hollis et al. (2012) and provided in detail within Gunn et al. (2008). Interpreted total magnetic intensity (analytic signal) and EM maps over the Tyrone Plutonic Group are shown in Figure 5.6.

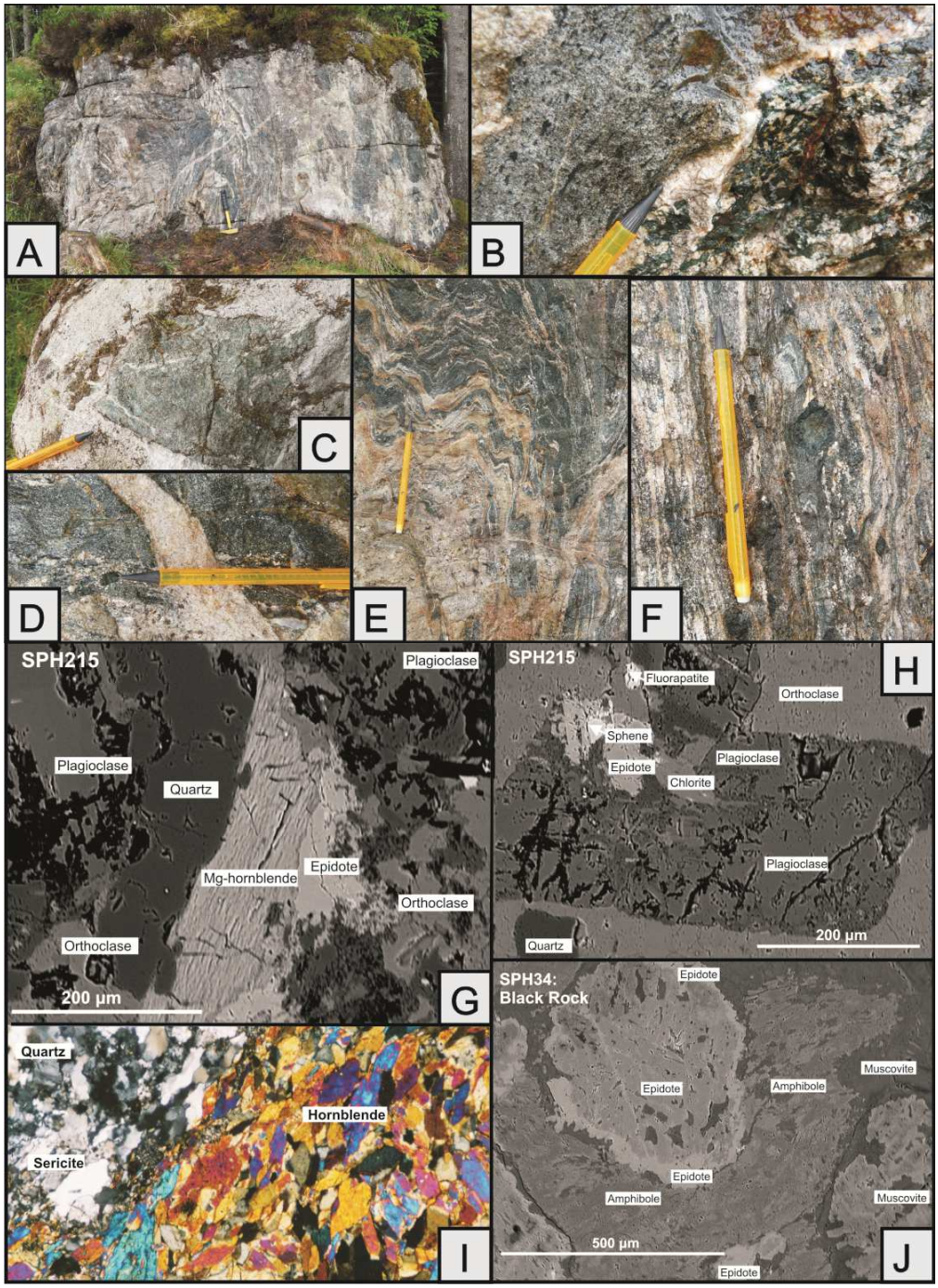

Figure 5.5. Field photographs and petrography from Blaeberry Rock and the Tyrone Plutonic Group. (a) Main Blaeberry Rock exposure. (b) Blocks of amphibolite facies gabbro (right) and andesite (left). (c) Angular block of amphibolite-facies basalt in granitic-tonalitic material. (d) Late stage granitic-tonalitic veins. (e) Isoclinally folded tonalitic to granitic melt and amphibolite. (f) Sinistrally rotated amphibole crystals in melt network. (g-h) SEM microphotographs of from Blaeberry Rock contact. (i) Thin section photograph of contact between amphibolite and tonalitic/granitic material at Blaeberry Rock. (j) SEM microphotograph of Black Rock pegmatitic gabbro from the Tyrone Plutonic Group.

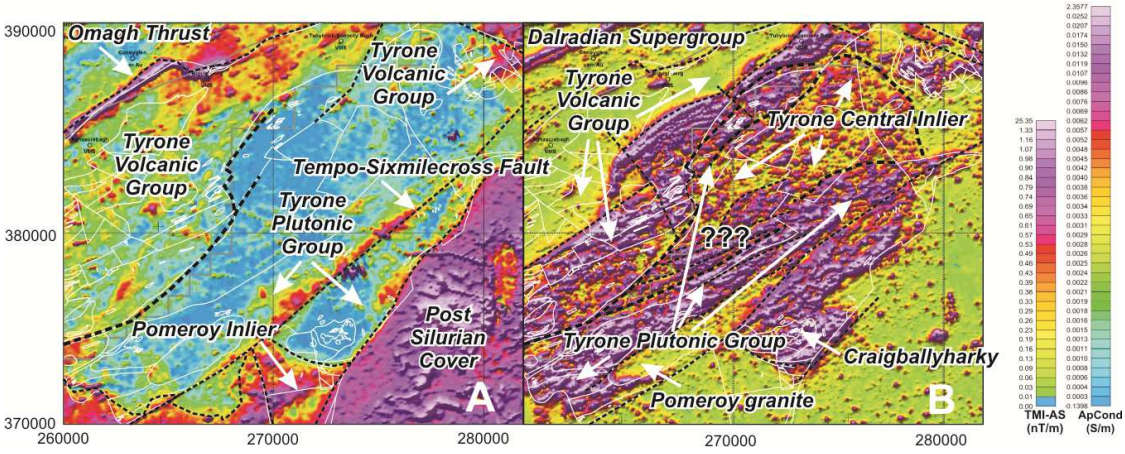

Figure 5.6. Results of the Tellus airborne geophysical survey of Northern Ireland. (a) Total magnetic intensity, analytic signal (TMI-AS). (b) EM low frequency (ApCond). All maps show original GSNI linework (GSNI 1979, 1983 and 1995). Grid references are according to Irish Grid. Dashed lines denote interpreted faults/unconformities. Heavier set lines show the boundaries between the Tyrone Volcanic Group, Tyrone Plutonic Group and Tyrone Central Inlier. Question marks show the position of magnetic material of unknown affinity underlying the Tyrone Central Inlier.

The Tyrone Plutonic Group is characterized by short-wavelength magnetic anomalies (Gunn et al. 2008), with magnetic highs corresponding to areas of magnetite-bearing dolerite and gabbro. Magnetic imagery reveals the Tyrone Plutonic Group to be dissected into thin slices by a series of NE-SW orientated faults. Lithologies of the Tyrone Plutonic Group are clearly distinguishable from the non-magnetic units of the Tyrone Central Inlier. Faulted contacts between the Tyrone Plutonic Group, Tyrone Volcanic Group, Tyrone Central Inlier and post-Ordovician cover sequences are best discriminated by EM imagery, with boundaries corresponding well to previous mapping (GSNI 1979, 1995) (see Hollis et al. 2012).

Along the eastern side of the Tyrone Central Inlier where gneissose psammites and semipelites crop out, highly-magnetic lithologies appear to be present at depth. Although it is possible a portion of the Tyrone Plutonic Group structurally underlies the Tyrone Central Inlier (due to late SE directed 'back thrusting'), these magnetic rocks may also represent mafic volcanics associated with the rifting of the Tyrone Central Inlier from the Laurentian margin or buried basement material. *In situ* Hf isotope analysis of zircon rims from c. 470 Ma granitoid rocks that cut the Tyrone Central Inlier paragneisses yield negative εHf_{470} values of c. -39. This isotopic signature requires an Archaean source, suggesting that rocks similar to the Lewisian Complex of Scotland occur at depth beneath the Tyrone Central Inlier (Flowerdew et al. 2009). Magnetic lows within the Tyrone Plutonic Group are associated with deep seated

granitic plutons of the c. 470-464 Ma arc-related intrusive suite (e.g. Pomeroy granite) and demagnetized zones associated with faulting (e.g. Tempo-Sixmilecross; Fig. 5.2). Tonalitic and granodioritic plutons at Craigballyharky and Craigbardahessiagh, may represent thin laccoliths underlain by highly magnetic material.

5.5 Whole rock geochemistry

5.5.1 Sampling and analytical techniques

Samples were collected from key localities across the Tyrone Plutonic Group and Blaeberry Rock for whole-rock geochemical analysis. Major-elements and trace-elements were determined for powdered whole-rock samples on fused glass beads and powder pellets by X-ray fluorescence at the University of Southampton. Rare earth-elements (plus Nb, Hf, Ta, Th, U) were determined by inductively coupled plasma mass spectrometry on the same samples using HF/HNO_3 digest. Strontium isotopes (n=2) were measured on a VG Micromass Sector 54 thermal ionization mass spectrometer (TIMS) at the University of Southampton. Geochemical analyses of Draut et al. (2009) and Cooper et al. (2011) are also included. Results are presented in the Appendix. Further detail is provided in Chapter 2.

5.5.2 Element mobility

Various studies have demonstrated that most of the major elements (e.g. SiO_2, Na_2O, K_2O, CaO, MgO) and the low field strength elements (LFSE: Cs, Rb, Ba, Sr, U, except Th) are mobile during metamorphism and hydrothermal alteration (references in Dilek & Furnes 2011). The degree of alteration across the Tyrone Plutonic Group can be assessed by a number of indices, including the: (i) Sericite Index (SI) of Saeki and Date (1980; K_2O/K_2O+Na_2O); (ii) the carbonate-chlorite-pyrite index (CCPI) of Large et al. (2001; $100*[FeO_T+MgO]/[FeO_T+MgO+Na_2O+K_2O]$); (iii) Ishikawa alteration index (AI: Ishikawa et al. 1976; $100*[MgO+K_2O]/[MgO+K_2O+CaO+Na_2O]$); and (iv) Al_2O_3/Na_2O ratio of Spitz and Darling (1978); as well as more conventional plots against immobile elements (see Appendix). Breakdown of sodic plagioclase and volcanic glass and their replacement by sericite with quartz, and chlorite are associated with gains in K_2O, MgO and FeO, and losses in Na_2O and CaO. Consequently, increased sericitisation leads to higher Al_2O_3/Na_2O ratios, and higher SI and AI values. High CCPI values document increases in MgO and FeO_T associated with Mg-Fe chlorite development at the expense of albite, K-feldspar or sericite. Mg-Fe carbonate alteration (dolomite, ankerite, or siderite), and pyrite, magnetite, or hematite enrichments may also be associated with high CCPI values (Large et al. 2001).

Comparison of the major and trace element data from the Tyrone Plutonic Group to Zr (assumed immobile) confirms this mobility, with considerable scatter for Na_2O, K_2O, Sr and Ba in particular. TiO_2, MgO, P_2O_5, Th, Nb, V, Cr, Co, Sc Y, U and the REEs appear to have remained immobile. SiO_2 appears to have remained relatively immobile, apart from minor silicification in some samples. Al_2O_3/Na_2O ratios vary between 2.3 and 23.9 (Fig. 5.7a). Element mobility plots are provided in the Appendix. Sampled lithologies show carbonate-chlorite-pyrite index (CCPI: see of Large et al. 2001) values typical of mafic volcanics (41.1-95.4, most >80; Fig. 5.7b) and Ishikawa alteration index (AI: Ishikawa et al. 1976) values (22.6-51.5) typical of weakly altered rocks. Sericite Index values (Saeki & Date 1980; K_2O/K_2O+Na_2O) vary between 0.07 and 0.49. Loss on ignition (LOI) values are <3.2 wt%. Analyses show a weak negative correlation between Na_2O and LOI, suggesting that lower Na_2O contents are due to Na losses associated with alteration (e.g. sericitisation).

5.5.3 Petrochemistry

Tyrone Plutonic Group

As primary mineral assemblages within the Tyrone Plutonic Group have been metamorphosed to amphibolite facies and many of the major and trace elements show evidence for mobility, only elements demonstrated to be immobile are used in this paper to elucidate petrogenesis, tectonic affinities, and chemostratigraphy. In addition to TiO_2, Th, V, Co and Sc, the high-field strength elements (HFSE, e.g. Nb, Hf, Ta, Zr, Y), and rare-earth elements (REE, minus Eu ± Ce) typically remain immobile during metamorphism to amphibolite facies conditions (e.g. Pearce & Cann 1973; MacLean 1990; Jenner 1996). TiO_2 and Fe_2O_{3T} concentrations within the Tyrone Plutonic Group typically range from 0.1 to 0.9 wt% and 3.0 to 12.0 wt% respectively. Higher Fe_2O_{3T} and TiO_2 concentrations occur in layered gabbro from Scalp and gabbro from Carrickmore (1.6-1.8% TiO_2 and 13.1-18.4% Fe_2O_{3T} due to an increased abundance of magnetite.

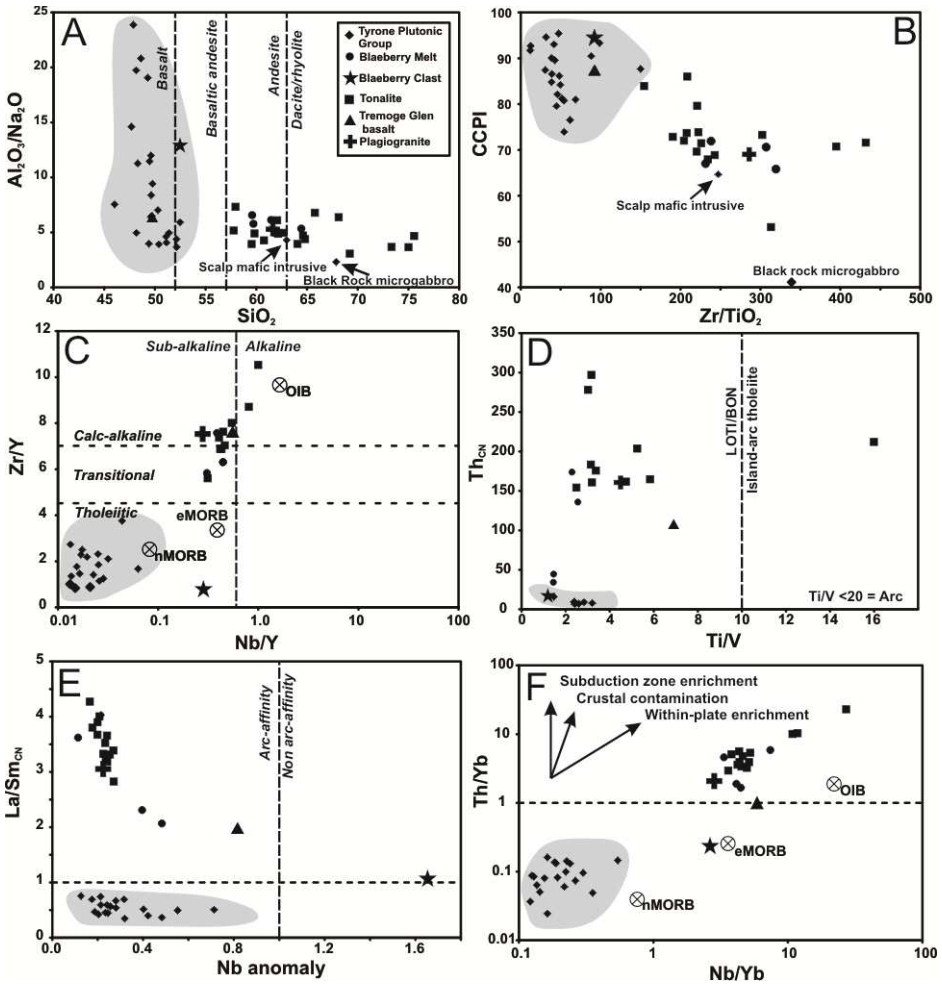

Figure 5.7. Geochemistry of the Tyrone Plutonic Group and associated rocks discussed herein. (a) Al_2O_3/Na_2O ratio of Spitz and Darling (1978) against SiO_2. (b) Carbonate-chlorite-pyrite Index of Large et al. (2001) against Zr/TiO_2. (c) Zr/Y against Nb/Y. (d) Th_{CN} against Ti/V. (e) La/Sm_{CN} against Nb anomaly (calculated from Th and La). (f) Th/Yb against Nb/Yb (after Pearce, 1983). Data of Draut et al. (2009) and Cooper et al. (2011) also included. Grey shading corresponds to tholeiitic rocks of the Tyrone Plutonic Group.

Immobile element ratios within the Tyrone Plutonic Group are predominantly subalkaline (Nb/Y <0.06) and tholeiitic (Zr/Y 0.7-3.8; Fig. 5.7c). On multi-element variation diagrams sampled lithologies display slight LREE depletion (La/Sm 0.6-1.2, Fig. 5.8a) and flat HREE profiles (Gd/Lu 0.7-1.1, most 1.0-1.1). Th (i.e. LILE) concentrations are similarly low (Th_{CN} 0.76-15.88; Fig. 5.7d). HFSE concentrations are generally less than those of nMORB. Aphanitic basaltic rocks classify as island-arc tholeiitic basalts according to Pearce and Cann (1973), Pearce and Norry (1979), Wood (1980), and Meschede (1986). Positive Pb, negative Nb and modest Ti anomalies across the Tyrone Plutonic Group are consistent with formation in a suprasubduction environment (Draut et al. 2009; Cooper et al. 2011) (Fig. 5.7e-f; 5.8a). Gabbro and pegmatitic gabbro from Black Rock, Carrickmore and Bonnety Bush display slightly

lower Th_{CN}, LREE and HREE concentrations than other rocks sampled from the Tyrone Plutonic Group. Plagiogranite that cuts sheeted dykes at Craigballyharky is borderline calc-alkaline, and strongly LILE and LREE-enriched (Zr/Y 7.5, La/Yb 6.8, Th_{CN} 166.55) relative to the HREE (Fig. 5.8).

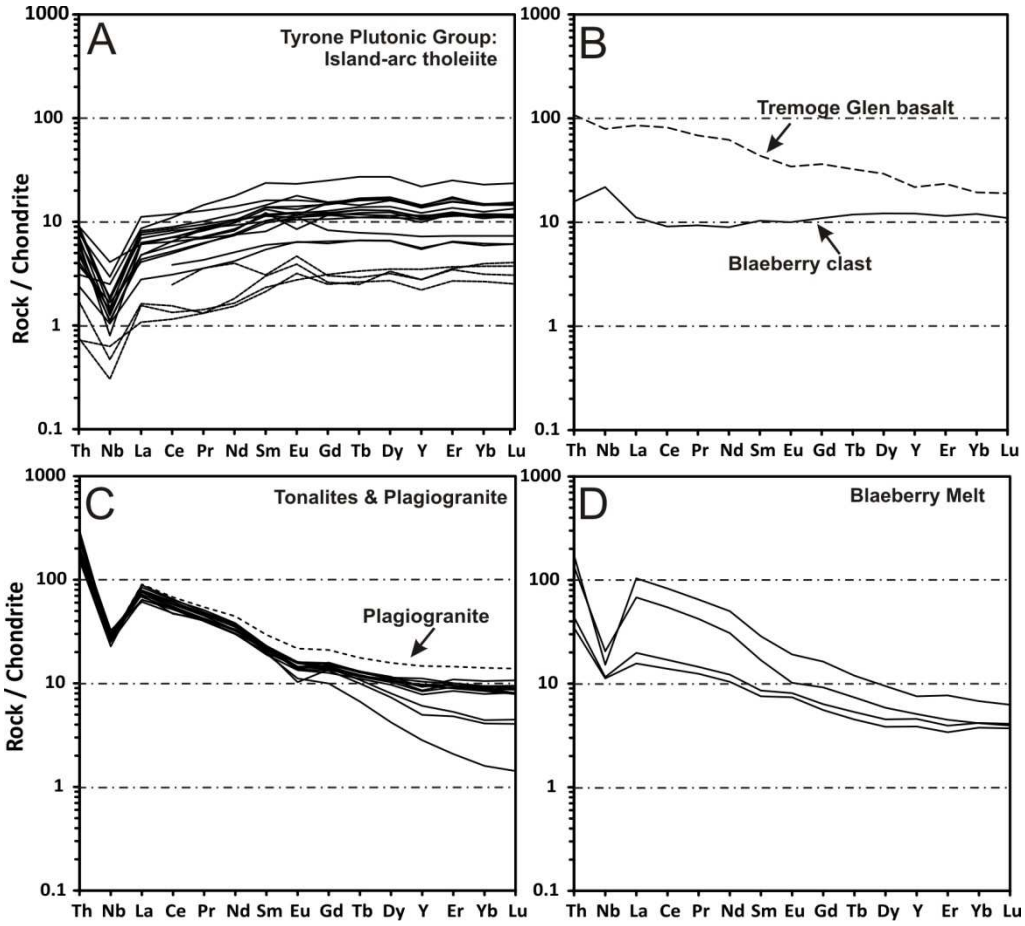

Figure 5.8. Multi-element variation diagrams for samples from the Tyrone Plutonic Group, Blaeberry Rock and arc-related intrusive suite. Chondrite normalization values after McDonough and Sun (1995). Analyses of Draut et al. (2009) and Cooper et al. (2011) are also included.

Initial $^{87}Sr/^{86}Sr$ ratios were calculated for two samples from the Tyrone Plutonic Group at an age of 480 Ma (after Cooper et al. 2011). A late dolerite dyke from Craigballyharky Quarry produced an $^{87}Sr/^{86}Sr_i$ ratio of 0.71019. A similar $^{87}Sr/^{86}Sr_i$ ratio of 0.71064 was produced for a dolerite dyke from Black Rock. Mobility of Rb and Sr is well documented during seafloor hydrothermal alteration, metamorphism and subsequent weathering (e.g. Jacobsen & Wasserburg 1979).

$^{87}Sr/^{86}Sr_i$ ratios of MORB glasses from the tropical East Pacific Rise fall within a narrow range around 0.70250 (0.70235 to 0.70275: Gillis et al. 2005). Sr-isotope characteristics of modern oceanic crust have been reconstructed using data from

Ocean Drilling Program (ODP) holes by Alt & Teagle (2000). $^{87}Sr/^{86}Sr$ ratios vary most within the lava and uppermost part of the sheeted dyke sequence between ~0.7025 (similar to fresh rock) and 0.7085 (close to the composition of modern seawater ~0.7090) (Alt & Teagle 2000). Towards the base of the sheeted dykes and gabbroic sequences, $^{87}Sr/^{86}Sr$ values are slightly more radiogenic than those of fresh rock (Alt & Teagle 2000). Sr isotope profiles through well studied suprasubduction zone, Cretaceous ophiolites such as Troodos or Oman, display similar patterns to those of modern oceanic crust, although are often more radiogenic and show a greater replacement of igneous phases (see Gillis et al. 2005). $^{87}Sr/^{86}Sr_i$ ratios measured throughout the ophiolite at Troodos are again significantly more radiogenic than $^{87}Sr/^{86}Sr_i$ ratios from fresh glasses from the ophiolite (~0.7037). Samples analysed down to the upper gabbros range from ~0.7037 to 0.7072 (see Alt & Teagle 2000; Gillis et al. 2005), with upper values similar to that Cretaceous seawater (~0.7073).

$^{87}Sr/^{86}Sr_i$ ratios obtained from the Tyrone Plutonic Group are comparable to the $^{87}Sr/^{86}Sr$ isotopic composition of Lower to Middle Ordovician seawater (0.7087-0.7090, Young et al. 2009), although slightly more radiogenic. Slightly higher $^{87}Sr/^{86}Sr_i$ values may suggest the incorporation of some continental material into the source region, which is supported by the presence of inherited zircons in layered gabbros from Scalp (Cooper et al. 2011).

Nd isotope geochemistry from the Tyrone Plutonic Group is restricted to that of Draut et al. (2009). Recalculated $\varepsilon Nd_{(t=480\ Ma)}$ values vary between +4.4 and +7.4 and are slightly lower than calculated values from the depleted mantle growth curve at c. 480 Ma (DePaolo 1988), suggesting some contamination from continentally-derived material into the source region consistent with the occurrence of xenocrystic Proterozoic zircons (see section 5.8.2). Wright et al. (2002) report εNd_t values of -13.3 to -14.8 for Iapetus seawater near the Laurentian margin during the Arenig-Llanvirn, which suggests the Nd-isotopic composition of the Tyrone Plutonic Group was largely unaffected by hydrothermal alteration and metamorphism.

Blaeberry Rock

A fine to medium grained doleritic clast collected from Blaeberry Rock is subalkaline (Nb/Y 0.27) and tholeiitic (Zr/Y 0.94, Fig. 5.7c), relatively LILE-depleted (Th_{CN} 15.8) and slightly LREE-depleted relative to the HREE (La/Yb_{CN} 0.93; Fig. 5.7d-e; 5.8b). These geochemical characteristics, in addition to low Ti/V (1.2), and Zr/TiO_2 (91.9), moderate AI (53.2), and high CCPI (94.5), Al_2O_3/Na_2O (12.9) and Gd/Lu ~1 are consistent with derivation from the Tyrone Plutonic Group. Th/Yb-Nb/Yb systematics classifies the clast as similar to eMORB (Fig. 5.7f). This sample displays a positive Nb anomaly

relative to Th and La (Fig. 5.8b), and a higher Nb/Y ratio than samples typical from the Tyrone Plutonic Group (Fig. 5.7c). Nb enrichment may be associated with increased alteration (e.g. CCPI).

Samples of tonalitic to granitic material collected from Blaeberry Rock (SiO_2 59.6-64.4 wt%, Zr/TiO_2 227.9-318.5) are calc-alkaline (Zr/Y 5.8-16.2), strongly LILE-enriched (Th_{CN} 34.7-174.0, Fig. 5.8c), and display steep LREE profiles (La/Sm 3.3-6.5) relative to the HREE (La/Yb 4.2-16.4) and strong negative Nb anomalies (0.11-0.48) on multi-element variation diagrams (Fig. 5.8d). These samples geochemically resemble the c. 470-465 Ma tonalites of the Tyrone Igneous Complex (see Cooper et al. 2011) which are characterized by high Zr/TiO_2 (154.5-583.8), Zr/Y (5.6-10.5) and La/Sm (4.5-6.8) ratios, Th_{CN} values (154.2-297.0) and pronounced -ve Nb anomalies (0.17-0.27, Fig. 5.8c) (values from Cooper et al. 2011; Hollis et al. 2012). Sampled Dalradian-affinity metasedimentary rocks of the Tyrone Central Inlier from Corvanaghan Quarry and Fir Mountain Quarry (adjacent to Blaberry Rock: Fig. 5.2) similarly have steep REE profiles (La/Sm to 7.2, La/Yb to 28.7) and can display pronounced –ve Nb anomalies (often due to the presence of melt), but have significantly higher Zr, Rb, Ba, Th_{CN} and REE_{Total} concentrations, and higher Ti/V and Nb/Y ratios (to 0.9).

Tremoge Glen

S-type muscovite granite from Tremoge Glen shows calc-alkaline characteristics (Zr/Y 13.3) is strongly LREE enriched relative to the HREE (La/Yb 18.2), and strongly LILE enriched (Th_{CN} ~325). Samples analyzed have high $K_2O/(K_2O+Na_2O)$ ratios of ~0.6 and are strongly peraluminous (after Shand 1943). The S-type geochemical characteristics suggest it may have been intruded shortly after the emplacement of the Tyrone Plutonic Group from the melting of metasedimentary material of the Tyrone Central Inlier. This is consistent with its high Th_{CN} and LREE enrichment.

Fe-Ti enriched basaltic-doleritic dykes from Tremoge Glen (Fe_2O_{3T} 15.4, TiO_2 2.7), which intrude the S-type muscovite granite, lack the prominent negative Nb anomalies of island-arc tholeiites (Nb anom 0.82) and are of 'within-plate' or eMORB affinity (e.g. Wood, 1980, Fig. 5.7b). Samples analysed are subalkaline, calc-alkalic, LILE and LREE enriched (Nb/Y 0.55, Zr/Y 7.2, La/Yb 4.7, Th_{CN} 107.83). Ti/V ratios (6.9) are higher than those of the Tyrone Plutonic Group (0.9-4.7, most <3). Low Cr (~50ppm) and Ni (~14ppm) confirms their relatively evolved nature. High LOI (7.06 wt.%), CCPI (87.4), SI (0.31) and AI (50.9) values are consistent with extensive alteration.

5.6 Mineral chemistry

Electron microprobe analyses were completed at the Natural History Museum, London, to determine epidote, amphibole, chlorite, and feldspar mineral compositions, and establish P-T conditions from the Tyrone Plutonic Group and its contact with the underlying Tyrone Central Inlier. Three samples were analysed; one from pegmatitic gabbro from Black Rock within the 'transition zone' of the Tyrone Plutonic Group (SPH34) and two from Blaeberry Rock (SPH210 and SPH215). SPH34 from Black Rock is dominated by plagioclase and amphibole (Fig. 5.5j). Plagioclase is extensively altered along grain boundaries to secondary minerals: epidote, carbonate, white mica, chlorite and residual albite. Amphibole occurs as large anhedral grains of hornblende intergrown with actinolite. Two samples were collected from Blaeberry Rock: SPH210, a gabbroic clast, and SPH215 from tonalitic melt in the contact. Sample SPH210 (gabbroic clast) is similar to SPH34 (collected from Black Rock) and contains amphibole closely associated with epidote and muscovite, and is believed to represent ophiolite derived material. By contrast, sample SPH215 comprises a mixture of hornblende, quartz, orthoclase, plagioclase, chlorite, epidote and accessory phases (sphene and fluorapatite) from tonalitic layers in the contact (Fig. 5.5g-h). Results are presented in the Appendix.

Amphiboles analysed from SPH34 (Black Rock) and SPH210 (Blaeberry Rock clast) chemically classify as tremolitic actinolite and magnesio-hornblende, whereas those analysed from tonalitic material at Blaeberry Rock (SPH215) classify as magnesio-hornblende with significantly lower Mg/(Mg+Fe) ratios and Si contents, and higher Ti, Fe and Mn concentrations (Fig. 5.9a). Low TiO_2 (0-0.45 wt.%) and Al_2O_3 (1.74-4.79 wt.%) in amphiboles from Black Rock (SPH34) and SPH210 (Blaeberry rock ophiolite-derived clast) plot predominantly just off the geothermometer of Ernst and Llu (1998), producing temperature estimates of c. <500 to 570 ˚C. Spot analyses from SPH215 amphiboles (tonalitic material) contain higher TiO_2 (0.35-0.65 wt.%) and Al_2O_3 (6.51-8.54 wt.%) indicating slightly higher temperatures of 525-610 ˚C.

Hammarstrom and Zen (1986) first proposed that solidus pressures of intermediate calc-alkaline plutons can be estimated from the Al content of hornblende. Rocks should be near-solidus with the magmatic assemblage: hornblende + biotite + plagioclase + quartz + orthoclase + sphene + magnetite or ilmenite ± epidote. The Al-in-hornblende geobarometer experimentally calibrated by Schmidt (1992) produces estimates of c. 2.3 to 4 ± 0.6 kbar for tonalitic melt from Blaeberry Rock. The experimentally calibrated geobarometer of Johnson and Rutherford (1989), which used

a mixed CO_2-H_2O fluid phase for calibration, produces lower pressure estimates (1.2-2.8 ± 0.5 kbar).

Epidotes from the Tyrone Plutonic Group typically have lower Fe and Ca, and higher Al, contents than those from Blaeberry Rock. Samples SPH210 and SPH215 are chemically similar, with the exception of epidote from SPH215 that is characterized by higher Si. Alkali feldspar compositions from Blaeberry Rock sample SPH215 are restricted to a relatively narrow range of K-enriched sanidines between $Or_{82.6}Ab_{16.1}An_{1.3}$ and $Or_{96.7}Ab_{3.3}An_{0}$ (Fig. 5.9b). BaO and Ce_2O_3 concentrations range between 0.46 and 1.4 wt% and 0.17 and 0.53 wt% respectively. FeO_T concentrations vary between 0.03 and 0.43 wt%. The composition of plagioclase from SPH215 varies from Ca-rich andesine to labradorite ($Or_{0.9}Ab_{59.6}An_{39.4}$ to $Or_{0.7}Ab_{48.0}An_{51.3}$) (Fig. 5.9b). FeO_T concentrations range between 0.11 and 0.17 wt%.

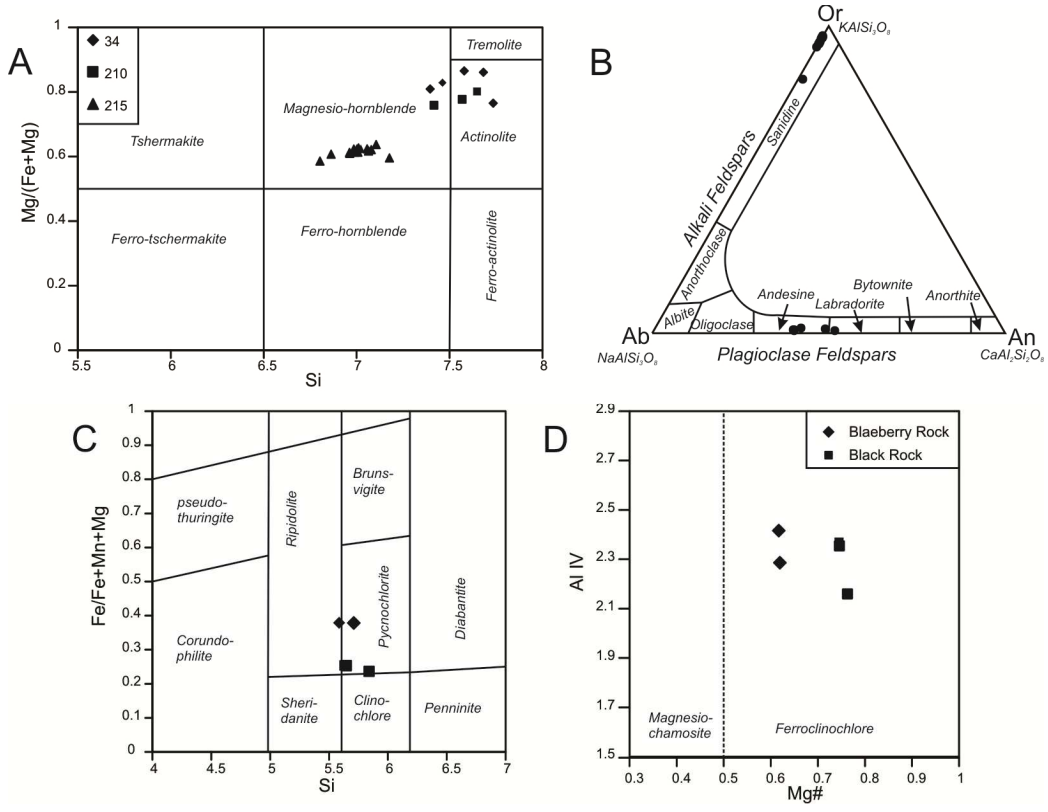

Figure 5.9. Mineral chemistry of samples from Black Rock (SPH34) and Blaeberry Rock (SPH210 and SPH215). (a) Amphibole mineral chemistry. (b) Feldspar mineral chemistry from Blaeberry Rock sample SPH215. (c) and (d) Chlorite mineral chemistry.

Chlorites from the Tyrone Plutonic Group are relatively Mg-rich and classify as pycnochlorite, whereas those analysed from Blaeberry Rock classify as both pycnochlore and ripidolite and have lower Mg# numbers (Fig. 5.9c-d). Si

concentrations are similar and range between 5.6 and 5.8 apfu (based on 22 oxygens). Fe/(Fe+Mg+Mn) ratios are approximately 0.4 from Blaeberry Rock and 0.25 from the Tyrone Plutonic Group. Al_{IV} concentrations vary between 2.15 and 2.41 apfu. Chlorite geothermometers of Zhang and Fyfe (1995) and Kranidiotis and MacLean (1987) produce temperature estimates of c. 261-274˚C and 289-302˚C respectively for chlorites from Blaeberry Rock sample SPH215. Similar temperature estimates were produced from chlorites of Black Rock (261-281˚C and 265-288˚C respectively). Chlorite temperature estimates most likely reflect retrogressive overprint.

5.7 U-Pb geochronology

5.7.1 Analytical methods

A sample of pegmatitic gabbro from Black Rock was selected for U-Pb zircon geochronology at the NERC Isotope Geosciences Laboratory (NIGL). Zircons were isolated using conventional mineral separation techniques. Zircons were examined by NIGL staff to avoid avoid morphologies which may contain inherited cores. Prior to isotope dilution thermal ionization mass spectrometry (ID-TIMS) analyses zircons were subject to a modified version of the chemical abrasion technique (Mattinson 2005). Methods are identical to those reported in Hollis et al. (2012). Data is presented in the Appendix. Errors for U-Pb dates are reported in the following format: ±X(Y)[Z], where X is the internal or analytical uncertainty in the absence of systematic errors (tracer calibration and decay constants), Y includes the quadratic addition of tracer calibration error (using a conservative estimate of the standard deviation of 0.1% for the Pb/U ratio in the tracer), and Z includes the quadratic addition of both the tracer calibration error and additional ^{238}U decay constant errors of Jaffey et al. (1971).

5.7.2 Results

Six fractions (single grains) were analyzed from the Black Rock sample MRC344. All six analyses are concordant when their systematic $\lambda^{238}U$ and $\lambda^{235}U$ decay constant errors are considered with five analyses forming a coherent single population yielding a weighted mean $^{206}Pb/^{238}U$ date of 483.68 ± 0.36 (0.60)[0.81] Ma (MSWD = 1.8) (Fig. 5.10). We interpret this as being the best estimate for the age of this sample. This age is slightly older than that produced for layered gabbro from Scalp (479.6 ± 1.1 Ma: Cooper et al. 2011). No inherited Proterozoic ages were derived from any of the dated zircon fractions as in Cooper et al. (2011), although zircon selection was biased (see above).

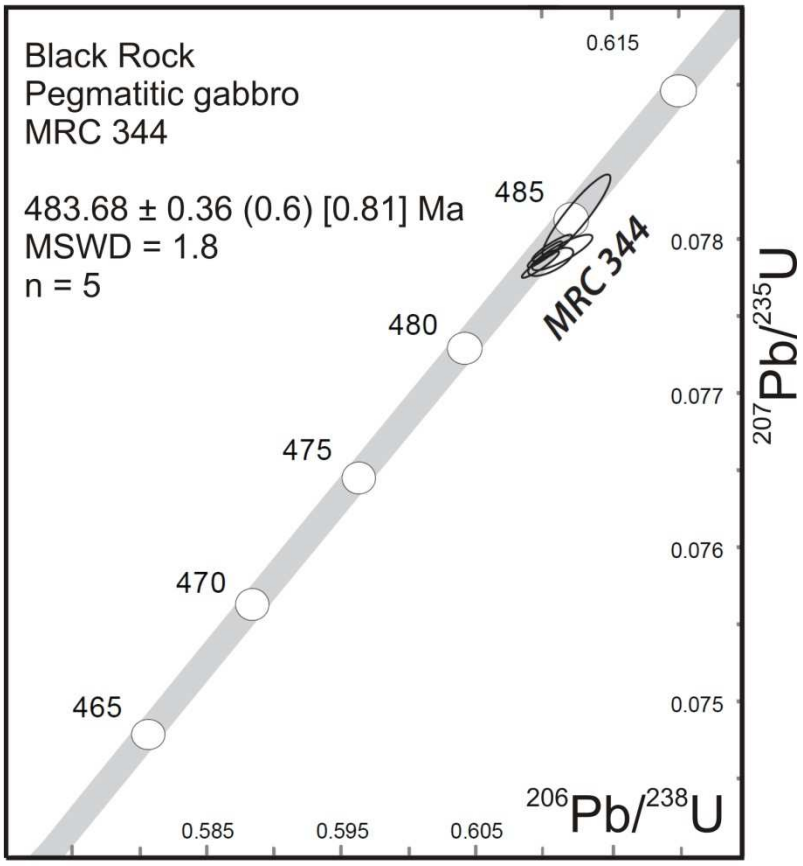

Figure 5.10. U-Pb zircon concordia and summary of interpreted U-Pb zircon date for pegmatitic gabbro from Black Rock.

5.8 Discussion

5.8.1 Evolution of the Tyrone Plutonic Group

The Tyrone Plutonic Group is composed primarily of layered, isotropic and pegmatitic gabbros, sheeted dolerite dykes and rare pillow lavas (Angus 1970; Hutton et al. 1985; Cooper & Mitchell 2004). Geochemical evidence and field relations presented herein are consistent with the Hutton et al. (1985) interpretation that the Tyrone Plutonic Group represents the uppermost portions of a tectonically dissected ophiolite which was accreted to the Laurentian margin during the Grampian phase of the Caledonian orogeny.

Suprasubduction zone ophiolites are characterized by significant LILE (K, Rb, Cs, Th) and LREE enrichment, and HFSE (Ti, Nb, Hf, Ta) depletion relative to typical normal mid-ocean ridge basalt (nMORB). Geochemical signatures across the Tyrone Plutonic Group are similarly characterized by primitive tholeiitic magmas of island arc affinity, which are Th and LREE enriched (and HFSE depleted) compared to nMORB, and LREE

depleted relative to the HREE (also see Draut et al. 2009; Cooper et al. 2011). Multi-element profiles and Nd-isotope compositions are consistent for basalts generated at an oceanic spreading centre above a subduction zone (Draut et al. 2009).

The new U-Pb geochronology presented here (483.68 ± 0.36 Ma) is consistent with that of Cooper et al. (2011: 479.6 ± 1.1 Ma) constraining the formation of the Tyrone Plutonic Group to c. 484-480 Ma. A slightly older age presented here for pegmatitic gabbro from Black Rock is in agreement with its more primitive geochemical characteristics. Pegmatitic gabbro from Black Rock is more LILE, LREE and HREE depleted than layered gabbro from Scalp. It is entirely possible that multiple slices of Iapetan ocean floor of various ages occur within the Tyrone Plutonic Group as the ophiolite is tectonically dissected.

Field relationships across the ophiolite are consistent with several phases of intrusive activity typical of oceanic spreading centres. Poor preservation of the sheeted dyke complex is typical of suprasubduction zone ophiolites in general; with large well-developed complexes requiring an appropriate balance between spreading and magma supply rates (references in Robinson et al. 2008). In contrast to fast-spreading Mid Ocean Ridges, where these conditions are maintained, suprasubduction zone spreading rates are not directly controlled by magma supply but are ultimately dependent on slab rollback, which is related to the angle of subduction (i.e. age and density of subducted lithosphere) and the rate of convergence (Robinson et al. 2008). Magma supply is controlled by the local temperature profile, nature of the subducting crust and mantle wedge, history and degree of mangle melting, and the nature and abundance of fluids (references in Robinson et al. 2008). The absence of a thick ultramafic section within the Tyrone Plutonic Group may be explained by post-tectonic excision or more likely by delamination and subduction of the lower crust during ophiolite emplacement (e.g. Annieopsquotch Ophiolite Belt; Zagorevski et al. 2009a). Limited occurrences of ultramafic material are present around Davagh Forest, where "basic and ultrabasic rocks, often pyroxenitic" have been described (see Gunn et al. 2008).

Fe-Ti enriched basaltic dykes which intrude S-type muscovite granite at Tremoge Glen are of within-plate affinity and lack a distinct island-arc geochemical signature. High LILE and LREE-enrichment, coupled with low Cr and Ni, is indicative of their more evolved nature than other samples from the Tyrone Plutonic Group. Fe-Ti basalts are defined by >12 wt% FeO_T and >2 wt% TiO_2 (e.g. Sinton et al. 1983), and typically display lower concentrations of MgO, CaO and Al_2O_3 than normal MORB. Geochemically identical Fe-Ti basalts of within-plate affinity to those within the Tyrone Plutonic Group

have been described from the Tyrone Volcanic Group, where they were proposed to originate from the interaction between a propagating rift and an island-arc (Hollis et al. 2012).

Fe-Ti basalts have been widely reported from the Galapagos Spreading Centre, which extends eastwards from a triple junction with the East Pacific Rise to the Panama fracture zone, where it separates the Cocos and Nazca plates (Sinton et al. 1983). Fe-Ti basalts are located on the flanks of a high amplitude magnetic zone that is bisected by the E-W orientated Galapagos ridge, and terminated against a fracture zone at 95°W and the Inca transform fault near 85°W. Shallow crustal fractional crystallization has been invoked to explain the presence of Fe-Ti basalt at both 85°W and 95°W (e.g. Christie & Sinton 1986). These ridge-transform intersections have also been interpreted by Hey et al. (1977, 1980) as propagating rifts. Increasing Fe-Ti enrichment, observed towards the tips of propagating rifts (Christie & Sinton 1981, Sinton et al. 1983), suggests that their migration towards older and colder lithosphere led to the development of small and rapidly cooling magma chambers where fractional crystallization dominates over mixing with newly added magma. Consequently, magmas evolve along a trend toward Fe and Ti enrichment in the perturbed geothermal environments associated with propagating rift tips (see Pearce et al. 1994). At 85°W the greatest diversity of lavas and most abundant siliceous compositions are located at the rift tip, whereas fractionated Fe-Ti lavas are erupted some 60 km further back (Fornari et al. 1983; Sinton et al. 1983). At both sites, liquids erupted in front of the rift tip consist of typical primitive MORB.

Incorporation of Palaeoproterozoic and Mesoproterozoic xenocrystic zircons into the Tyrone Plutonic Group (see Cooper et al. 2011) suggests it may have formed above a north-dipping subduction zone by the propagation of a spreading centre into a microcontinental block (=Tyrone Central Inlier, see below) (Fig. 5.11). A similar tectonic scenario was presented for the formation of the c. 480 Ma Annieopsquotch Ophiolite Belt of Newfoundland by Zagorevski et al. (2006; also Cutts et al. 2012). This is consistent with the occurrence of Fe-Ti-P enriched 'within-plate' basalt (to 2.9 wt% TiO_2) within the Tyrone Plutonic Group at Tremoge Glen, the presence of minor continental material according to Nd- and Sr-isotope systematics, and zircon inheritance at Scalp. This tectonic scenario may also explain the strong LILE, LREE and negative εNd_t values in the c. 475-469 Ma Tyrone Volcanic Group, a peri-Laurentian island arc/backarc which was accreted to the Tyrone Central Inlier at c. 470 Ma (Hollis et al. 2012). The Tyrone Volcanic Group is believed to have formed above a N dipping subduction zone immediately outboard of the Tyrone Central Inlier (Hollis et al. 2012). These geochemical characteristics may be explained if the arc was in part founded

upon a fragment of microcontinental crust which was rifted off the Tyrone Central Inlier during the formation of the Tyrone Plutonic Group. A similar situation has been envisaged for the evolution of the analogous Buchans-Robert's Arm arc of Newfoundland (Zagorevski et al. 2006).

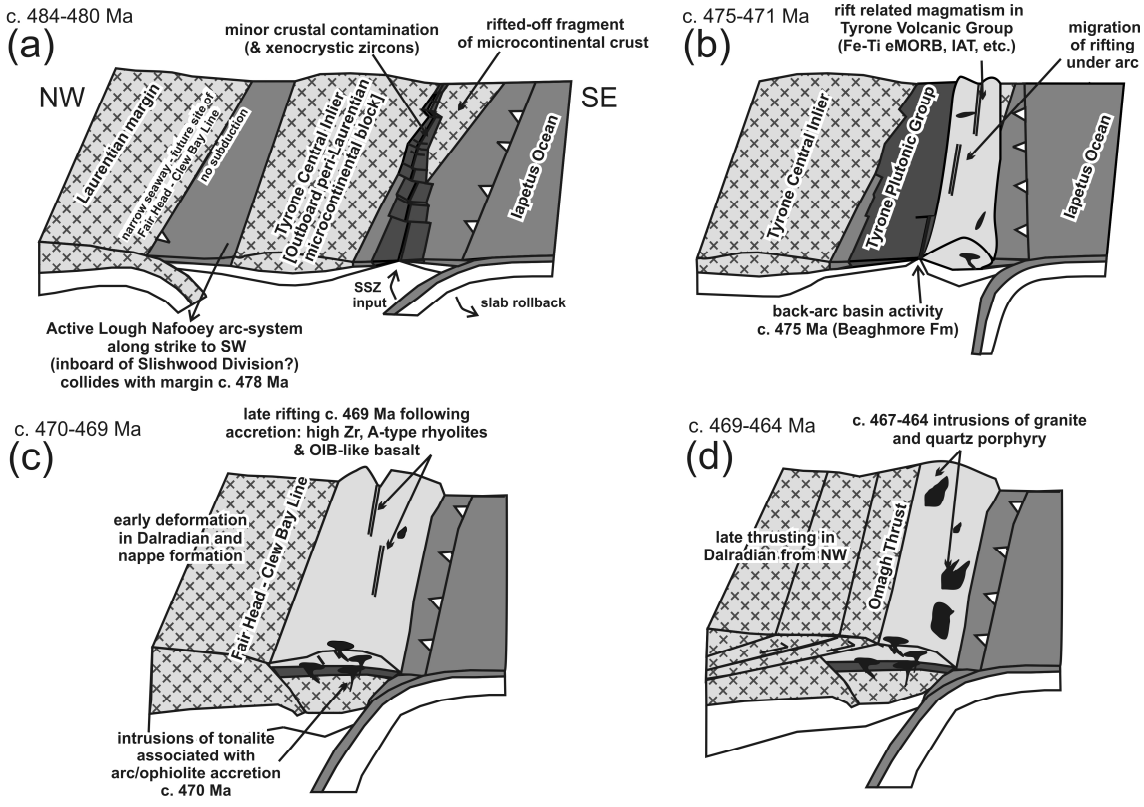

Figure 5.11. Tectonic model for the evolution of the Tyrone Plutonic Group.

5.8.2 Accretion to the Tyrone Central Inlier

The Tyrone Central Inlier is composed of a thick sequence of psammitic and semi-pelitic paragneisses (Hartley 1933) exposed within the central regions of the Tyrone Igneous Complex (Fig. 5.2). The unusual high-grade nature of the Tyrone Central Inlier (up to silimanite grade: c. 670 ± 113 °C, 6.8 ± 1.7 kbar; Chew et al. 2008) and its position SE of the Fair Head - Clew Bay Line (Fig. 5.1) has led recent workers (e.g. Chew et al. 2008; Flowerdew et al. 2009; Chew et al. 2011; Cooper et al. 2011) to suggest the Tyrone Central Inlier may represent part of an outboard segment of Laurentia, which detached as a microcontinent during the opening of Iapetus (c. 570 Ma) and subsequently reattached during the Grampian orogeny (c. 470 Ma). Age dating of syntectonic leucosomes (^{207}Pb-^{206}Pb age of 467 ± 12 Ma) and post-tectonic muscovite-bearing pegmatites (^{40}Ar-^{39}Ar step heating plateaux age of 468 ± 1 Ma) suggest a Grampian age (c. 475-465 Ma) for the deformation and metamorphism of the Tyrone Central Inlier (see Chew et al. 2008).

Obduction of the Tyrone Plutonic Group onto the Tyrone Central Inlier must have occurred prior to the intrusion of the c. 470 Ma Craigballyharky tonalite (470.3 ± 1.9 Ma) which contains inherited Proterozoic zircons and roof pendants of ophiolitic and arc-related material (Cooper et al. 2011). This tonalite is one of several large c. 470-464 Ma calc-alkaline arc related intrusives which stitch the Tyrone Igneous Complex in its present position above the Tyrone Central Inlier (Cooper et al. 2011). All rocks of the arc related intrusive suite are LILE and LREE-enriched with strongly negative εNd_t values (to -11.8: Hollis et al. 2012) implying interaction with continental crust was an integral part of their petrogenesis (Draut et al. 2009). Early intrusions (<470 Ma) overlap in age with the Tyrone Volcanic Group and are synvolcanogenic ± syncollisional. Post-collisional granite from Slieve Gallion (466.5 ± 3.3 Ma) and granodiorite from Craigbardahessiagh (464.9 ± 1.5 Ma) both contain Mesoproterozoic inherited zircons (Cooper et al. 2011). Zircon fractions analysed from quartz porphyritic dacite from Copney (465 ± 1.7 Ma) and tonalite from Craigballyharky (470.3 ± 1.9 Ma) both contain inherited components dated at c. 2100 Ma (Cooper et al. 2011). Xenocrystic zircons are consistent with derivation from the structurally underlying Tyrone Central Inlier (Cooper et al. 2011), although c. 2100 Ma zircons are rare in peri-Laurentian sources including the Tyrone Central Inlier (Chew et al. 2008).

The muscovite granite which cuts layered gabbro at Tremoge Glen is unusual within the arc related intrusive suite; its S-type geochemical characteristics, high Th_{CN} and LREE enrichment suggest it may have been intruded shortly after the emplacement of the Tyrone Plutonic Group from the melting of peri-Laurentian metasedimentary material (probably derived from the Tyrone Central Inlier). Attempts to date the Tremoge Glen muscovite granite using U-Pb zircon were not successful and produced large errors due to organic contamination at the mass spectrometry stage (Noble et al. 2004). Although apparently core-free zircons were picked, two analyses showed very significant inheritance, with upper intercepts of c. 1560 Ma and 2351 Ma (Noble et al. 2004). A second attempt to date this unit is in progress.

Although the Tyrone Plutonic Group was emplaced between c. 480 and 470 Ma, the exact timing of this event has remained elusive. At Blaeberry Rock the presence of ophiolite-derived blocks in abundant synkinematic tonalitic to granitic melt suggests accretion of the Tyrone ophiolite to the Tyrone Central Inlier may have occurred at the same time as the accretion of the Tyrone Volcanic Group at c. 470 Ma. Tonalite intrusions are abundant throughout the Tyrone Igneous Complex and four occurrences have produced U-Pb zircon ages: 470.3 ± 1.9 Ma at Craigballyharky (Cooper et al. 2011), 465.6 ± 1.1. Ma from Laght Hill (Cooper et al. 2011: also 475 ± 10 Ma: Draut et

al. 2009), 469.9 ± 2.9 Ma from Golan Burn (Cooper et al. 2011), and 469.29 ± 0.33 Ma from Cashel Rock (Hollis et al. 2012). Emplacement at c. 470 Ma, synchronous with the Tyrone arc (=Tyrone Volcanic Group), may explain how the metamorphic conditions evident within the Tyrone Central Inlier (c. 670 ± 113 °C, 6.8 ± 1.7 kbar; Chew et al. 2008) were generated prior to c. 468 Ma. Previous work has attributed these conditions solely to the emplacement of the Tyrone Plutonic Group despite it lacking an ultramafic section (Cooper et al. 2011). The emplacement of both the arc and the ophiolite at c. 470 Ma, would provide a c. 10 km thick, hot crustal sequence, enough to produce the required P-T conditions in the Tyrone Central Inlier prior to c. 468 Ma.

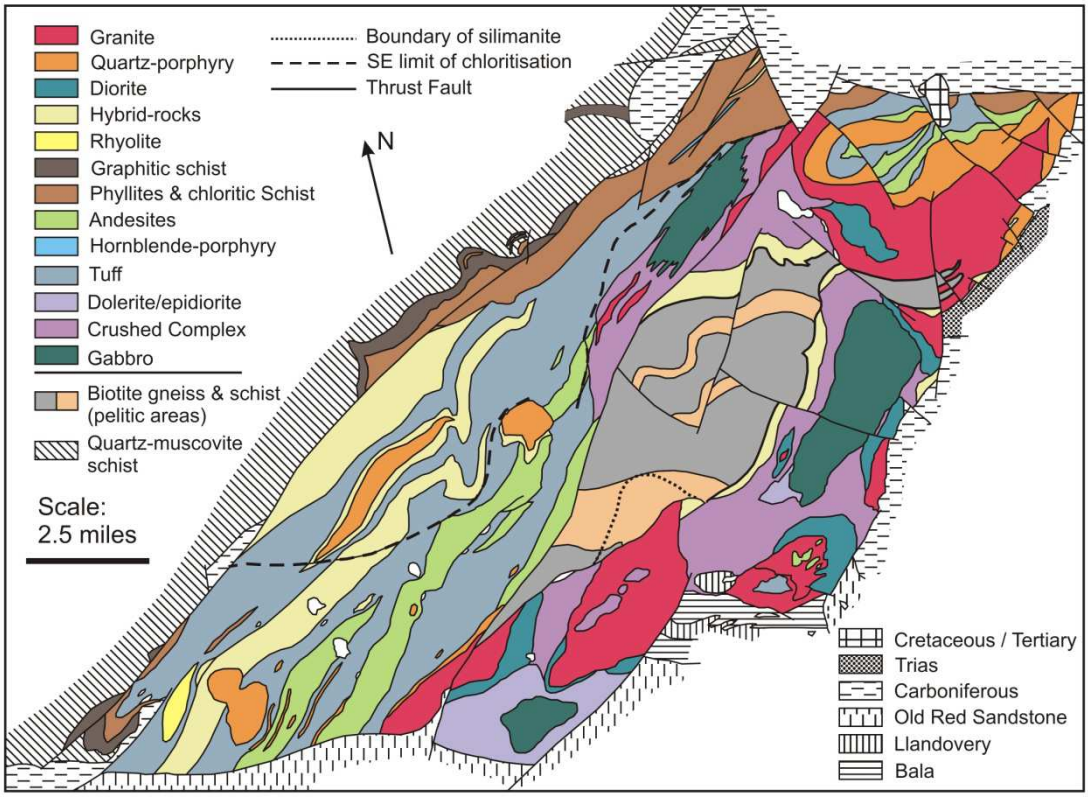

Figure 5.12. Hartley's (1933) original map of the Tyrone Igneous Series (now Tyrone Igneous Complex and Tyrone Central Inlier), with the presence of silimanite restricted to the SE side of the Tyrone Central Inlier.

Amphiboles from synkinematic tonalitic sheets within the Blaeberry contact produced temperature estimates of 525-610 °C, slightly lower (but within error) than those produced by Chew et al. (2008) from the Tyrone Central Inlier. Pressure estimates up to 4 ± 0.6 kbar for tonalitic melt from Blaeberry Rock (after Schmidt, 1992) are again lower than those produced by Chew et al. (2008), however Hartley (1933) noted the presence of silimanite in the Tyrone Central Inlier is restricted to its SE side (Fig. 5.12).

As the Tyrone Igneous Complex was emplaced from this direction, the higher temperatures and pressures of Chew et al. (2008) from Corvanaghan Quarry and further south may be restricted to that region. No sillimanite has been observed in the Fir Mountain Quarry exposures of the Tyrone Central Inlier adjacent to Blaeberry Rock.

5.8.3 Evolution and accretion of the Annieopsquotch Ophiolite Belt

Recent fieldwork, U-Pb zircon geochronology and geochemistry from across the Tyrone Igneous Complex has highlighted the close similarities between: (i) the Tyrone Plutonic Group and the Annieopsquotch Ophiolite Belt of Newfoundland, (ii) Tyrone Volcanic Group and the Buchans and Robert's Arm groups of central Newfoundland; and (iii) a late suite of calc-alkaline stitching arc-related intrusives (see Cooper et al. 2011; Hollis et al. 2012).

The c. 480 Ma Annieopsquotch Ophiolite Belt of central Newfoundland comprises several suprasubduction zone ophiolite complexes (e.g. King George IV, Annieopsquotch, Star Lake), which formed during west-directed subduction outboard of the Dashwoods peri-Laurentian microcontinent at c. 481-478 Ma (Dunning & Krogh 1985; Dunning et al. 1987; Whalen et al. 1997; Lissenberg et al. 2005; Zagorevski et al. 2006). The Annieopsquotch Ophiolite Complex is the largest and most studied; and consists of suprasubduction zone affinity layered to isotropic gabbros, sheeted dykes and pillow basalts (Lissenberg et al. 2005). The lower gabbro zone contains enclaves of troctolite inferred to have formed from boninitic melts (Lissenberg et al. 2004). The youngest basalts are of MORB-type affinity and are cut by sheeted dykes with backarc geochemical characteristics (Lissenberg et al. 2005). εNd_t values within the Anniopsquotch Ophiolite Belt range from +7.6 to +8.4 (Zagorevski et al. 2006). The ophiolite lacks an upper mantle section apart from rare occurrences of dunite and pyroxenite (Lissenberg & van Staal 2006).

The age determination of the Tyrone Plutonic Group presented herein (483.68 ± 0.36 Ma), primitive εNd_t values (+4.5 to +7.5: Draut et al. 2009), tholeiitic suprasubduction geochemical characteristics, preserved ophiolite sequences, and its development outboard of a possible microcontinental block (=Tyrone Central Inlier) are consistent with correlation to the Annieopsquotch Ophiolite Belt of Newfoundland; and formation at an oceanic spreading centre above a subduction zone (Draut et al. 2009; Cooper et al. 2011). Xenocrystic Mesoproterozoic zircons present within the Tyrone Plutonic Group are consistent with T_{DM} ages of 1200-1800 Ma from felsic intrusive rocks of the Moretons Harbour Group (part of the Annieopsquotch Ophiolite Belt of Newfoundland; Cutts et al. 2012) indicating a significant amount of contamination from Mesoproterozoic or older continental crust. Furthermore, the Lloyds River Fault Zone

which separates the Annieopsquotch Ophiolite Belt from the Dashwood microcontinental block bears a striking resemblance to Blaeberry Rock (Lissenberg & van Staal 2002).

The Lloyds River Fault at its type locality is a complex shear zone having a central high-strain zone (mainly characterized by mafic and felsic tectonites), which is bounded by less-strained moderately foliated amphibolite and orthogneiss dissected by narrow shear zones (Lissenberg & van Staal 2002). The central high strain zone is composed of an intimate mixture of banded amphibolite and metapyroxenite (probably of ophiolitic origin) and strongly foliated quartz-diorite and tonalite. Moderately deformed, late-kinematic, folded and boudinaged tonalitic to granodioritic veins that cut sheared rocks suggests these arc magmas were intruded synkinematically (Lissenberg & van Staal 2002). The outer zone of the Loyds River Fault consists of gabbro and diabase cut by diorite and tonalite, with weakly deformed mafic rocks alternating with strongly sheared amphibolite and orthogneiss. Preferential localization of shear zones occurs in intrusive sheets rather than the ophiolite derived gabbro, as at Blaeberry Rock. Shear sense indicators imply both the Lloyds River Fault and Blaeberry Rock contact accommodated oblique motion with a sinsistral component. Abundant metamorphic hornblende at both sites also suggests the fault zones formed at amphibolite facies conditions (with subsequent retrograde overprint) (Lissenberg & van Staal 2002). Abundant tonalitic synkinematic melt at Blaeberry Rock implies the Tyrone Plutonic Group was accreted at the same time as the Tyrone Volcanic Group at c. 470 Ma. This again is remarkably similar to that of the Annieopsquotch Ophiolite Belt which occurred prior to c. 468 Ma (Lissenberg et al. 2005; Zagorevski et al. 2006). Possible reasons for why the accreted tracts of Annieopsquotch were underplated to Dashwoods, whereas the Tyrone Igneous Complex was obducted are outlined in Hollis et al. (2012).

5.9 Conclusions

The Tyrone Plutonic Group of Northern Ireland represents the upper portions of a tectonically dissected suprasubduction zone ophiolite accreted to the Laurentian Margin during the Middle Ordovician. Understanding its development and relationship to the Tyrone Central Inlier, a fragment of relatively high-grade peri-Laurentian continental crust exposed SE of the Fair Head - Clew Bay Line (=Highland Boundary Fault), is essential for reconstructing the closure of the Iapetus Ocean. The Tyrone Plutonic Group is composed of variably tectonised and metamorphosed, layered, isotropic and pegmatitic gabbros, sheeted dolerite dykes and rare pillow lavas. New and previously published geochronology constrains the formation of the Tyrone

Plutonic Group to c. 484-480 Ma, broadly equivalent to the Annieopsquotch Ophiolite Belt of Newfoundland. Sampled lithologies are geochemically consistent with formation at a spreading centre above a subduction zone. S-type, peraluminous muscovite granite contains abundant inherited Proterozoic zircons, and appears to have been intruded shortly after ophiolite emplacement generated from the partial melting of Laurentian-affinity metasedimentary material. Ophiolite obduction onto the Tyrone Central Inlier must have occurred prior to the intrusion of a c. 470 Ma tonalite which contains roof pendants of ophiolitic and arc material. Late Fe-Ti basaltic dykes of eMORB affinity are consistent with formation at a propagating rift following obduction. The presence of syn-kinematic, calc-alkaline tonalitic melt within the contact between the Tyrone Central Inlier and Tyrone Plutonic Group suggests the latter may have been emplaced relatively late within the orogen at c. 470 Ma synchronous with the Tyrone arc. In the absence of an ultramafic section the coeval obduction of the ophiolite and volcanic arc may explain how metamorphic conditions within the sillimanite-grade Tyrone Central Inlier were reached prior to c. 468 Ma.

Chapter 6: Timing of arc evolution in the Irish Caledonides

This chapter forms the basis of a submitted manuscript: Hollis, S.P., Roberts, S., Cooper, M.R., Earls, G., Herrington, R., & Condon, D.J. (Submitted). *New stratigraphic, geochemical and U-Pb zircon constraints from Slieve Gallion, Northern Ireland: A correlation of the Irish Caledonide arcs*. Journal of the Geological Society, London.

Abstract

Recent Ar-Ar and U-Pb zircon geochronology from across the British and Irish Caledonides has revealed a prolonged period of arc/ophiolite formation (c. 514-464 Ma) and accretion (c. 490-470 Ma) to the Laurentian margin during the Grampian orogeny. The Slieve Gallion Inlier of Northern Ireland, an isolated occurrence of the Tyrone Volcanic Group, records the development of a peri-Laurentian island-arc/backarc and its obduction onto an outboard microcontinental block. Although a previous biostratigraphic age constraint provides a firm correlation of at least part of the volcanic succession to the Ca1 Stage of the Arenig (c. 475-474 Ma), there is uncertainty on its exact statigraphic position in the Tyrone Volcanic Group. Earliest magmatism is characterized by light rare earth element (LREE) depleted island-arc tholeiite. Overlying deposits are dominated by large ion lithophile and LREE-enriched, hornblende-phyric and feldspathic calc-alkaline basaltic andesites and andesitic tuffs with strongly-negative εNd_t *values. Previously published biostratigraphic age constraints, combined with recent U-Pb zircon geochronology and new petrochemical correlations, suggest the Slieve Gallion Inlier is equivalent to the lower Tyrone Volcanic Group. Strong temporal and petrochemical correlations between the Slieve Gallion Inlier and Charlestown Group of Ireland suggest they may be part of the same arc-system which was accreted at a late stage (c. 470 Ma) in the Grampian orogeny. A switch from tholeiitic volcanism to calc-alkaline dominated activity within the Lough Nafooey Group of western Ireland occurred prior to c. 490 Ma, approximately 15 to 20 Myr earlier than at Tyrone and Charlestown.*

6.1 Introduction

The Caledonian-Appalachian orogen provides a rare window through the mid to lower crustal levels of an evolving orogenic belt. Early Paleozoic closure of the Iapetus Ocean resulted in extensive arc-ophiolite accretion to the Laurentian margin (=Grampian-Taconic orogeny) prior to continent-continent collision (=Acadian orogeny) (Dewey 2005; van Staal et al. 2007; Chew 2009). Modern subduction systems, such as the W and SW Pacific, reveal complexities during episodes of large-scale ocean closure, including: diachronous and/or oblique arc-continent collision, arc-arc collisions, subduction polarity reversals, subduction rollback, triple junctions, arc-interactions with propagating rifts and spreading centres, and the presence of microcontinental blocks and oceanic plateaus. Despite these complexities, forward modeling of collision between Australia and the Asian continent has produced remarkably linear orogenic belts when associated with sinistral oblique convergence (see van Staal et al. 1998). Pseudo-simplistic linear orogenic zones can conceal complex histories and geometries, especially if poorly exposed and subjected to terrane excision and strike-slip duplication (van Staal et al. 1998). It is only through detailed study of individual terranes, and their inter-relationships, that orogens may be understood

The Grampian-Taconic orogeny resulted from widespread and episodic arc-ophiolite accretion to the Laurentian margin between the Late Cambrian and Middle Ordovician (Dewey & Shackleton 1984; van Staal et al. 2007; Chew et al. 2010). Western Ireland, although not representative of the Grampian orogeny as a whole, was a focus for establishing many of the fundamental processes of arc-continent collision due to its abundant exposure, low metamorphic grade and limited deformation (e.g. Dewey & Shackleton 1984; Dewey & Ryan 1990; Draut et al. 2004; Dewey 2005; Ryan & Dewey 2011). Collision between the Lough Nafooey arc of western Ireland and the passive Laurentian margin was associated with polyphase deformation and metamorphism of thick Neoproterozoic cover sequences such as the Dalradian Supergroup between c. 475-465 Ma. The South Mayo Trough, a thick and relatively undeformed accumulation of lavas and volcaniclastic sedimentary rocks, represents the pre-collisional fore-arc and syn- to post-collisional successor basin to the Lough Nafooey arc (Draut et al. 2004) (Fig. 6.1). Within its sedimentary record, the South Mayo Trough preserves the progressive evolution of the Lough Nafooey arc system, its collision with the Laurentian margin, and the unroofing of the orogen (reviewed in Ryan & Dewey 2011). A younger c. 464 Ma continental arc founded upon the Laurentian margin was associated with subduction polarity reversal following arc-continent collision (Dewey 2005).

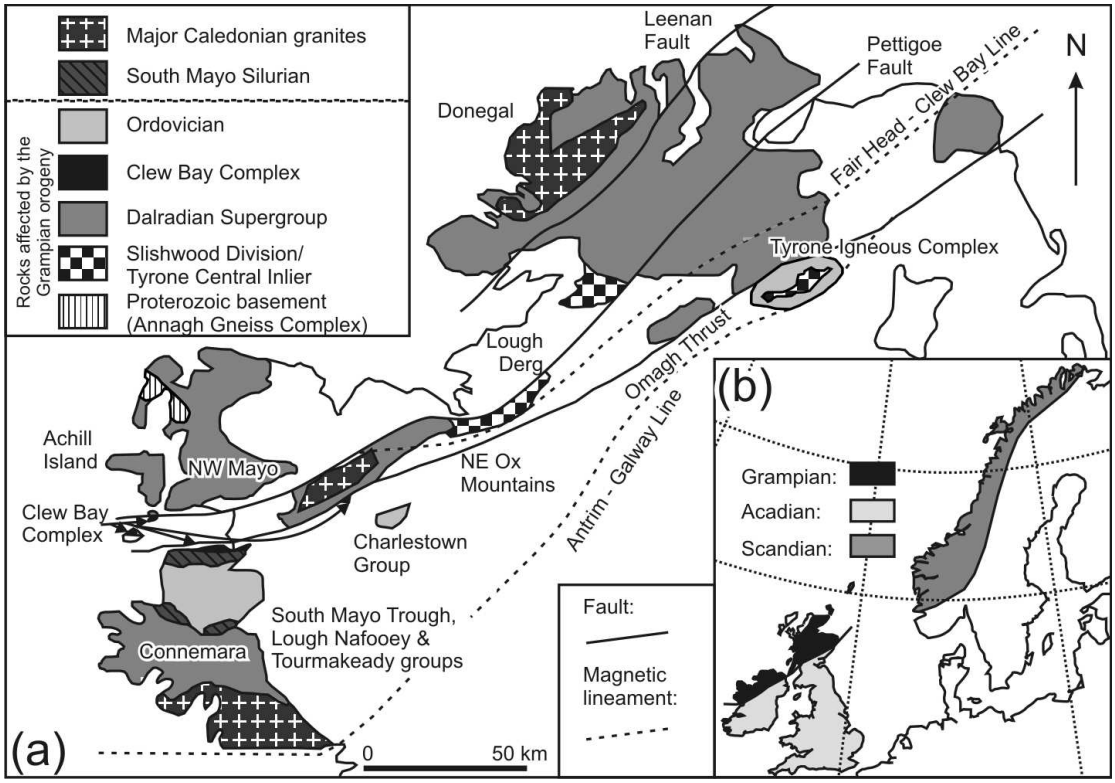

Figure 6.1. (a) Geological map of NW Ireland showing the setting of the Tyrone Igneous Complex and other comparable ophiolite and volcanic arc associations, major structural features and Precambrian and Lower Palaeozoic inliers in the Irish Caledonides. (b) Rocks affected by the Grampian, Acadian and Scandian orogenys. Figure after Chew (2009).

Arc-ophiolite formation is now recognized to span c. 514-464 Ma within the peri-Laurentian British and Irish Caledonides (e.g. Chew et al. 2008, 2010; Cooper et al. 2011; Hollis et al. 2012). Early obduction of some ophiolites onto outboard microcontinental blocks (c. 510-490 Ma) may explain discrepancies in the timing between the termination of Laurentian passive margin sedimentation and ophiolite emplacement (Chew et al. 2010). Remnant slices of the accreted volcanic arcs are exposed across the Midland Valley terrane as the: Bohaun Volcanic Formation, Lough Nafooey Group, Tourmakeady Group and Charlestown Group of Ireland, the Tyrone Volcanic Group of Northern Ireland (Fig. 6.1), and probably the Games Loup and Mains Hill successions of the Ballantrae Ophiolite Complex, Scotland. Abundant arc-related and ophiolitic detritus in sediments of the Southern Uplands terrane and Middle Ordovician sediments of Girvan also indicate the presence of an extensive arc-ophiolite complex(s) buried within the Midland Valley Terrane (Midland Valley arc) (see Oliver et al. 2002).

The Tyrone Volcanic Group of Northern Ireland occupies an important position in the Caledonides between the well documented sectors of western Ireland and Scotland

(Fig. 6.1). It records the formation of a peri-Laurentian island arc/backarc during the Middle Ordovician and its accretion to an outboard microcontinental block at c. 470 Ma (see Cooper et al. 2011; Hollis et al. 2012). However, despite its importance, geochronology from the Tyrone arc is limited to three high resolution U-Pb zircon dates from one formation (Cooper et al. 2008; Hollis et al. 2012). Furthermore, the volcanic succession exposed at Slieve Gallion (herein termed the Slieve Gallion Inlier) provides the only biostratigraphic age constraint for the entire Tyrone Volcanic Group (Cooper et al. 2008). Although the Slieve Gallion Inlier was initially suggested to be within the upper Tyrone Volcanic Group (Cooper et al. 2008), this appears to be unfounded as similar lithologies are now known to occur in the Loughmacrory Formation towards the base of the Tyrone Volcanic Group (Hollis et al. 2012).

This chapter presents the results of new field mapping, complemented by high-resolution airborne geophysics, the first detailed geochemical study of the volcanic succession, and two new U-Pb zircon dates that shed further light on this enigmatic arc-system and the orogen as a whole. Herein it is demonstrated that the Tyrone and Lough Nafooey arcs differ significantly in the timing of their geochemical evolution and accretion. Either arc evolution and accretion was diachronous in the Irish Caledonides, or perhaps more likely the Tyrone and Lough Nafooey arcs represent distinct arc systems accreted to the Laurentian margin during the Grampian orogeny (after Hollis et al. 2012).

6.2 Previous work

The Slieve Gallion Inlier of Northern Ireland is exposed over ~15km^2 directly NE of the ophiolitic Tyrone Plutonic Group (layered gabbro: 479.6 ± 1.1 Ma, Cooper et al. 2011; pegmatitic gabbro: 483.68 ± 0.81 Ma, Chapter 5), which separates this package of rocks from the main occurrence of the c. 475-469 Ma Tyrone Volcanic Group to the SW (Fig. 6.2). The Slieve Gallion Inlier is bounded to the north and east by post-Silurian cover and along its southern margin has been intruded by a large body of biotite/hornblende-bearing granite (Slieve Gallion granite: 466.5 ± 3.3 Ma; Cooper et al. 2011) (Fig. 6.2). The first comprehensive study of the inlier was presented within Hartley's (1933) seminal work on the "Tyrone Igneous Series" (now Tyrone Igneous Complex). Although no stratigraphy was attempted, Hartley's map for the complex divided the volcanic succession at Slieve Gallion into (i) andesites, (ii) tuffs, and (iii) phyllites and chloritic schists. The volcanic rocks have since been resurveyed for the 2nd edition Cookstown and Draperstown sheets (Geological Survey of Northern Ireland: GSNI 1983 & 1995; also see Cameron & Old 1997), which provided the most up to date

map of the inlier. No division within the volcanic succession was presented at 1:50,000, although GSNI field-slips record a variety of lithologies in detail.

Fragmentary graptolites from one locality at Sruhanleanantawey Burn [IGR 27905-38790] have been variably interpreted since their initial discovery by Hartley (1936). A late Llandeilo to early Caradoc age was originally favoured on the presence of specimens identified as Dicranograptus and Climacograptus (Hartley 1936). Re-collection by Hutton and Holland (1992) further identified the presence of Tetragraptus serra (Brongniart) and Sigmagraptus sensu lato, demonstrating an earlier Arenig to Llanvirn age. Most recently Cooper et al. (2008) collected more than 20 graptolites and a lingulate brachiopod, and reexamined the specimens of Hutton and Holland (1992). They concluded through the presence of Isograptus victoriae lunatus, the index fossil of the Isograptus victoriae lunatus Zone of the Australasian graptolite succession, the fauna can be assigned to the lowest Ca1 subdivision of the Castlemainian Stage. This is approximately equivalent to the top of the Whitlandian Stage of the Arenig (c. 475-474 Ma after Sadler et al. 2009).

In addition to their evaluation of the Sruhanleanantawey Burn fauna, Cooper et al. (2008) determined a U-Pb zircon date for a flow-banded rhyolite from Formil Hill from the main outcrop of the Tyrone Volcanic Group to the SW (473 ± 0.8 Ma). Rhyolites are common across the upper Tyrone Volcanic Group, exposed from Racolpa through Cashel Rock to Formil (Fig. 6.2) within the Greencastle Formation (c.473-469 Ma), and structurally and stratigraphically below the graphitic pelite and chert bearing localities around Mountfield and Broughderg (e.g. Crosh; c.469 Ma Broughderg Formation; Hollis et al. 2012). Cooper et al. (2008) suggested that the chert, thinly-bedded tuffaceous siltstone and pyritic mudstones, with greenish-grey tuffs and lavas at Slieve Gallion formed synchronously with the succession at Broughderg. At this time, U-Pb geochronology from the Tyrone Volcanic Group sensu stricto was restricted to their one high-resolution age from Formil Hill and no detailed stratigraphic or petrochemical account of the Tyrone Volcanic Group existed. Two similar, albeit slightly younger, U-Pb zircon TIMS dates have subsequently been obtained from the Greencastle Formation (469.42 ± 0.38 and 470.37 ± 0.31 Ma; Hollis et al. 2012).

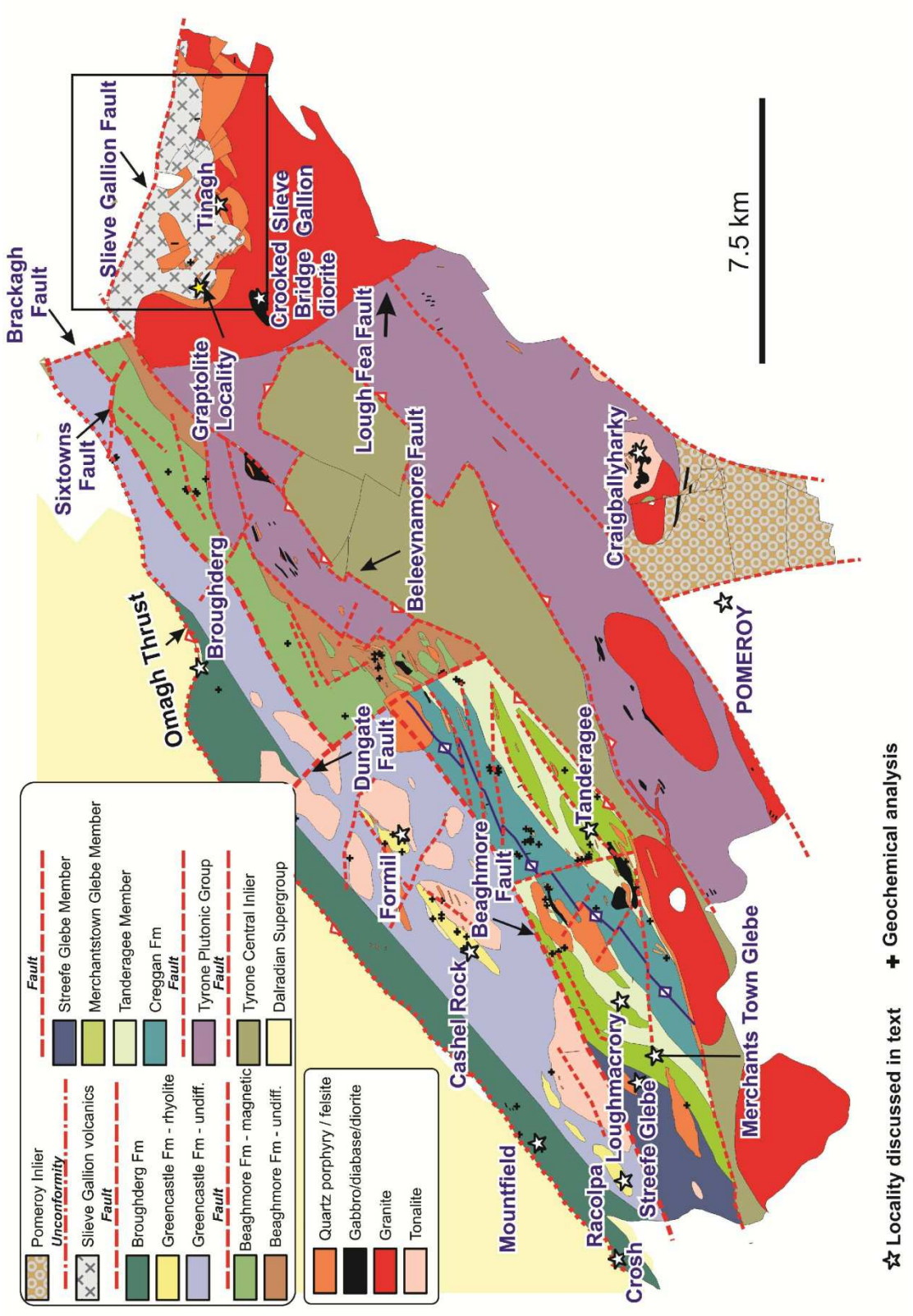

Figure 6.2. Geological map of the Tyrone Igneous Complex (after Hollis et al. 2012).

6.3 Stratigraphy

The Slieve Gallion Inlier has been re-mapped through the integration of previous geological survey data and new fieldwork, geochemistry (see following) and the Tellus airborne geophysical survey of Northern Ireland. A new map is presented in Figure 6.3. Magnetic, radiometric and electromagnetic (EM) data were acquired as part of the Tellus Project in 2005-2006 (see GSNI 2007). Details on survey specification and geophysical data processing are summarised within Beamish et al. (2007). The volcanic succession at Slieve Gallion is hereby divided into three formations: Tinagh, Tawey, and Whitewater (Figs. 6.3-4). Each is described below. Major ESE-WNW orientated faults divide the volcanic succession into three stratigraphic packages. South of the Tirgan Fault, the Tinagh and Tawey formations are exposed; the latter is restricted to the W side of Slieve Gallion. North of the Tirgan Fault the structurally overlying Whitewater Formation is exposed. An older set of NW-SE striking faults cut the formations and are offset by the Tirgan Fault. Several of these NW-SE striking faults, which are clear from regional magnetics (Fig. 6.3) are directly mapable (e.g. NE of Tinagh; GSNI 1983, 1995). Ordovician intrusive rocks of quartz-porphyry, hornblende- and biotite-granodiorite, aplite and diorite cut the volcanic succession. Units have been metamorphosed to subgreenschist facies conditions and consequently the prefix meta- is omitted from all lithologies.

6.3.1 Tinagh Formation

The Tinagh Formation crops out extensively across the southern side of the Slieve Gallion Inlier and includes the following informal stratigraphic units: Derryganard Lavas, Windy Castle Lavas, Letteran Volcanics, Torys Hole Ironstone, and the Mobuy Wood Basalts, each named after their type localities. The Tinagh Formation is dominated by calc-alkaline hornblende porphyritic tuffs and lavas, and non-arc type Fe-Ti enriched basalt of e-MORB affinity (see following sections). Lesser amounts of calc-alkaline, feldspar porphyritic andesite, mafic crystal tuff, ferruginous jasperoid (ironstone), mafic agglomerate (interpreted as interpillow breccias), tholeiitic pillow lavas, and rhyodacite are also present. The formation has a maximum exposed thickness of 1.2 km, although the rift-related Mobuy Wood Basalts appear have been erupted locally at different times (Fig. 6.4) and packages of the Windy Castle Lavas vary considerably in thickness along strike.

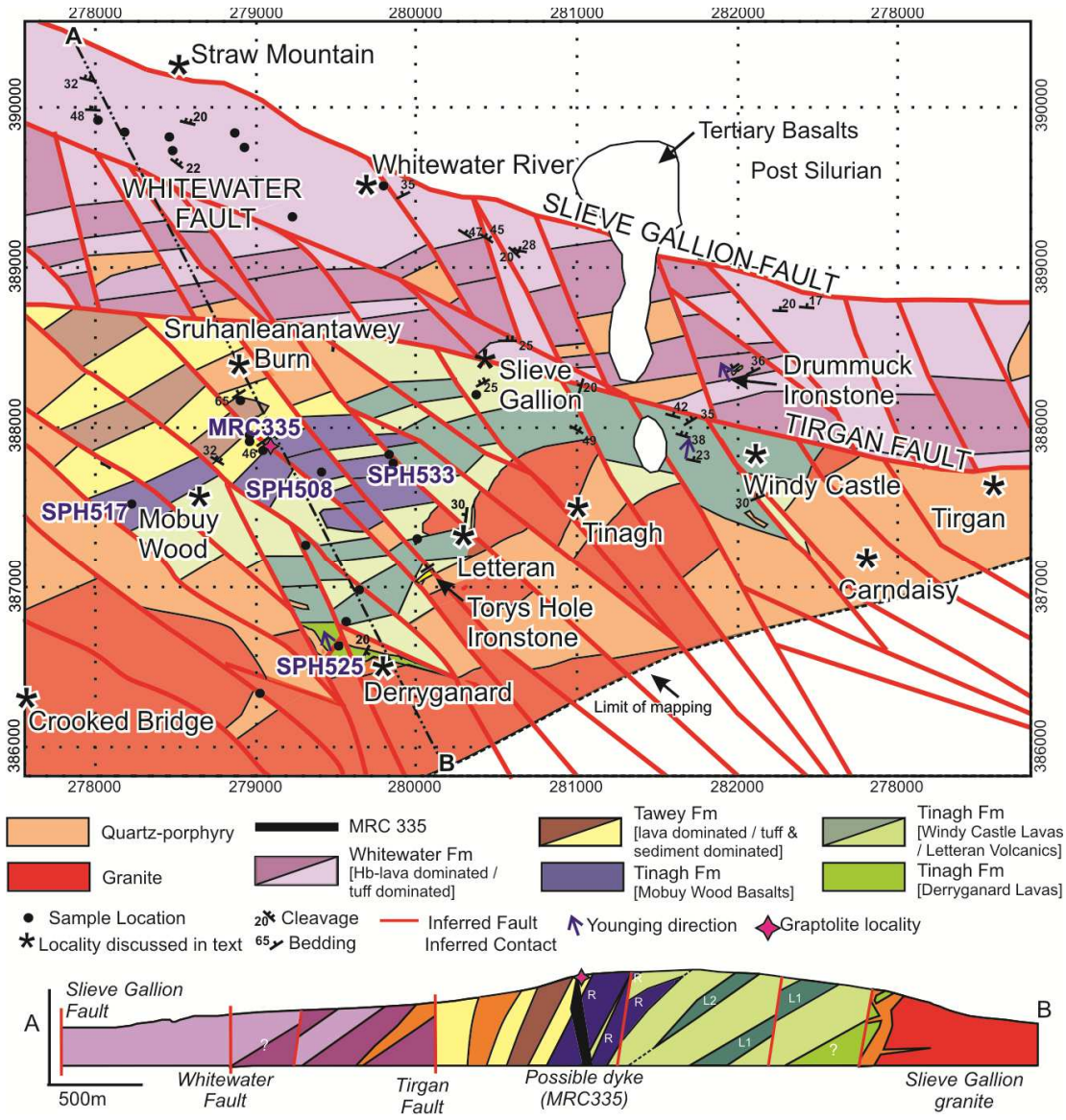

Figure 6.3. (a) Geological map of the Slieve Gallion Inlier.

Pillow lavas exposed at Derryganard (=Derryganard Lavas) are believed to represent the oldest stage of volcanism within the Slieve Gallion Inlier and are restricted to this area. The succession is at least 130 m thick with pillow structures younging north towards the Windy Castle Lavas. The succession is bounded to the south and east by younger intrusions of c.465-464 Ma quartz-porphyry and a large body of biotite granite and succeeded in the northwest by the Windy Castle Lavas which dip NW to NE (Fig. 6.3). Pillows are generally aphanitic, highly vesicular and range between 8 and 35 cm in diameter (Fig. 6.5a,h). Flows become more massive up section, and rare augite phenocrysts occur in some near the base of the sequence. No interpillow chert or sediment was observed. The Derryganard Lavas are non-magnetic and are geochemically distinct from all other units present in the Slieve Gallion Inlier,

displaying tholeiitic and LREE-depleted geochemical characteristics (see petrochemistry).

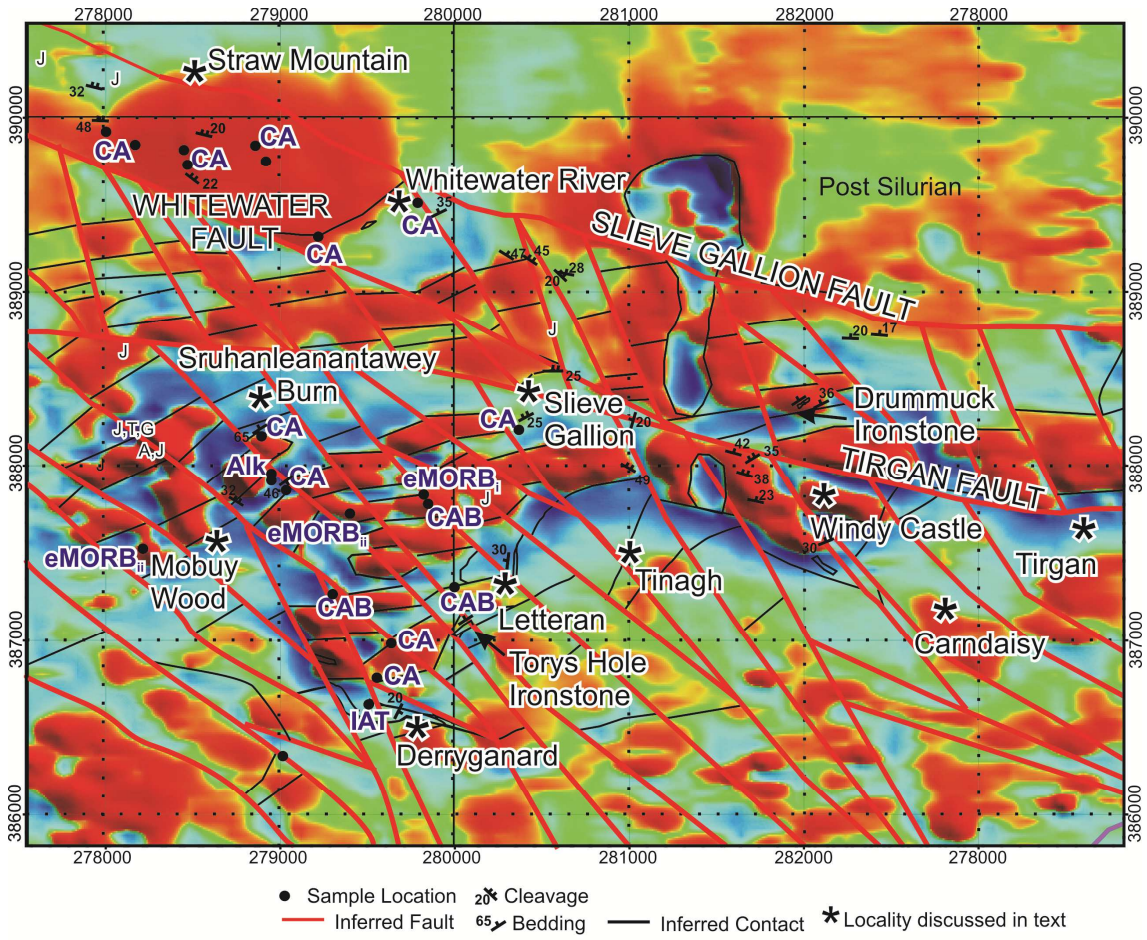

Figure 6.3. (b) Interpreted total magnetic intensity map (reduced to pole) over the Slieve Gallion Inlier including the affinity of sampled rocks. CA, calc-alkalic undifferentiated; CAB, calc-alkaline basalt; IAT, island arc tholeiite; eMORB, enriched mid ocean ridge basalt; Alk, alkali basalt. Faults and Boundaries are as in figure 6.3a. A, T, J and G refer to areas of significant agglomerate, tuff, jasper and granite float in areas of poor exposure. Red to blue shows decreasing total magnetic intensity.

Immediately overlying the Derryganard Lavas, the Tinagh Formation is dominated by calc-alkaline tuffs and andesites, with flows becoming increasingly pillowed and associated with agglomerate up section. This sequence, has been divided into the Windy Castle Lavas and Letteran Volcanics on the basis of the dominant phenocryst type in flows, intensity of magnetic response, and type of associated tuff (i.e. mafic or hornblende-phyric). The contact with the underlying Derryganard Lavas was placed at the first occurrence of hornblende-phyric basaltic andesite/andesite or tuff (Fig. 6.5b-c). The Windy Castle Lavas are characterized by vesicular hornblende-phyric andesites with lesser mafic crystal tuff; type localities occur at Windy Castle and W of Letteran.

Locally the Windy Castle Lavas reaches a thickness of 275 m. The Letteran Volcanics are characterized by non-magnetic, calc-alkaline, and feldspar-phyric, massive and pillowed andesites (which lack abundant hornblende phenocrysts) and sheared hornblende-bearing crystal tuffs (Figs. 6.3-4). The Letteran Volcanics locally vary in thickness between ~275 to 340 m. Packages of the Windy Castle Lavas alternate with the Letteran Volcanics both up sequence and along strike (Fig. 6.3). This suggests different areas experienced pyroclastic and effusive activity at different times, most likely associated with rifting (see following). This is further supported by the geochemistry of the closely associated Mobuy Wood Basalts (see petrochemistry) and the occurrence of ironstone at Torys Hole, where a 1 m thick bed is exposed towards the base of the Tinagh Formation. This unit is characterized by a mosaic of quartz and haematite (petrography in Cameron & Old 1997).

Non-arc type basalts of eMORB affinity are restricted to the SW side of the Slieve Gallion Inlier, exposed between Sruhanleanatawey Burn and Letteran (Fig. 6.2b), and around Mobuy Wood. These lavas are geochemically distinct to all others analysed from the Slieve Gallion Inlier, having rift-related characteristics (see petrochemistry). They are herein termed the Mobuy Wood Basalts. Flows are often highly vesicular, and either massive or display well developed pillow structures with radial fractures. Basaltic agglomerates, interpreted as interpillow breccias (Fig. 6.5d), are commonly associated with the latter. Although the Mobuy Wood Basalts are largely aphanitic, some flows contain rare augite phenocrysts, which can display evidence for rounding (Fig. 6.5g). This suggests these may be xenocrysts derived from the underlying Derryganard Lavas. The Mobuy Wood Basalts can be distinguished based on their geochemistry and high total magnetic intensity (see Supplementary Information), and from underlying flows of the Windy Castle Lavas and Letteran Volcanics by a lack of hornblende phenocrysts. It is not known if the Mobuy Wood Basalts are present on the E side of Slieve Gallion as these lavas were not sampled for geochemistry, although augite bearing andesites have been reported on GSNI fieldsheets north of Tirgan suggesting a slice of the Tinagh Formation may exist in this area. A single unit of rhyodacite also occurs at Mobuy Wood near the base of the overlying Tawey Formation. This rhyodacite is extensively sheared and is associated with rare hornblende-phyric lava, tuff and small intrusions of quartz diorite.

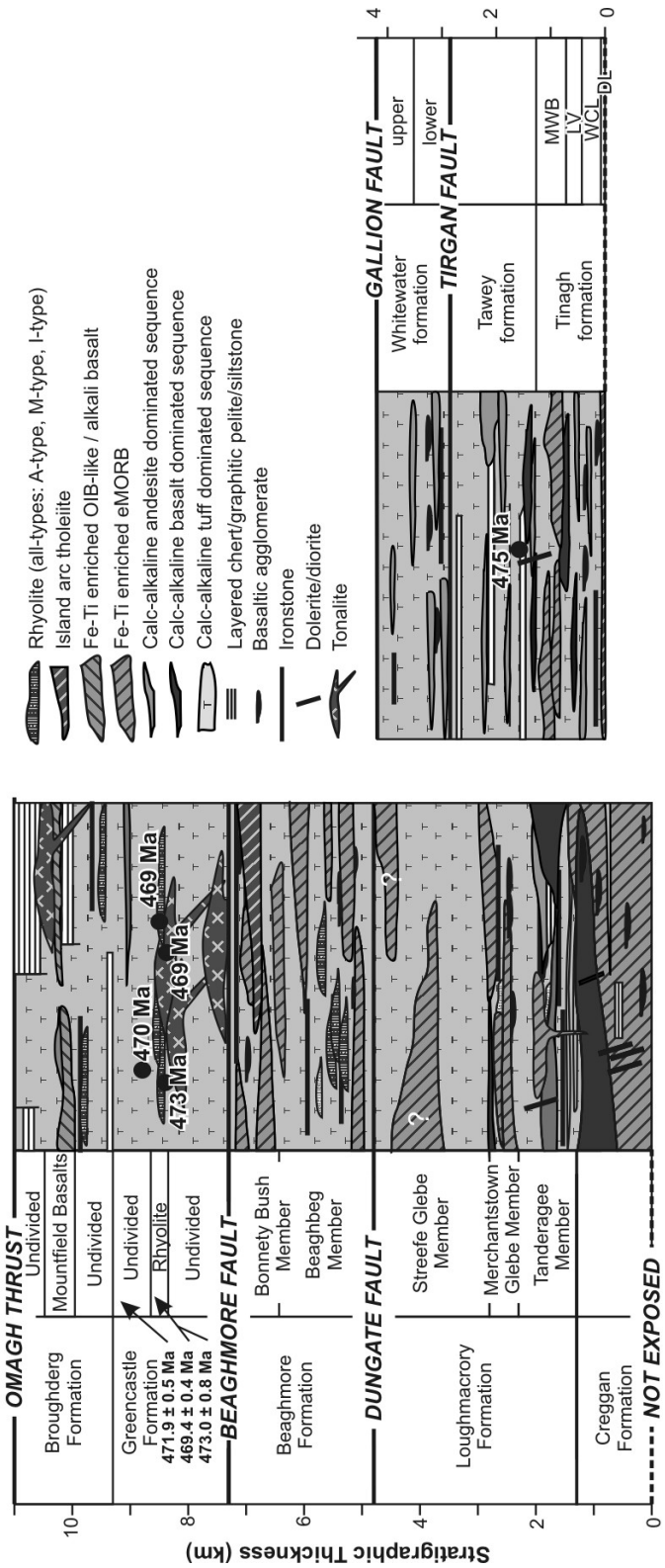

Figure 6.4. Simplified stratigraphy of the Slieve Gallion Inlier and Tyrone Volcanic Group including the petrochemical affinities of mafic to felsic units within each formation (after Hollis *et al.* 2012 and unpublished data). DL, Derryganard Lavas; LV, Letteran Volcanics; MWB, Mobuy Wood Basalts; WCL, Windy Castle Lavas.

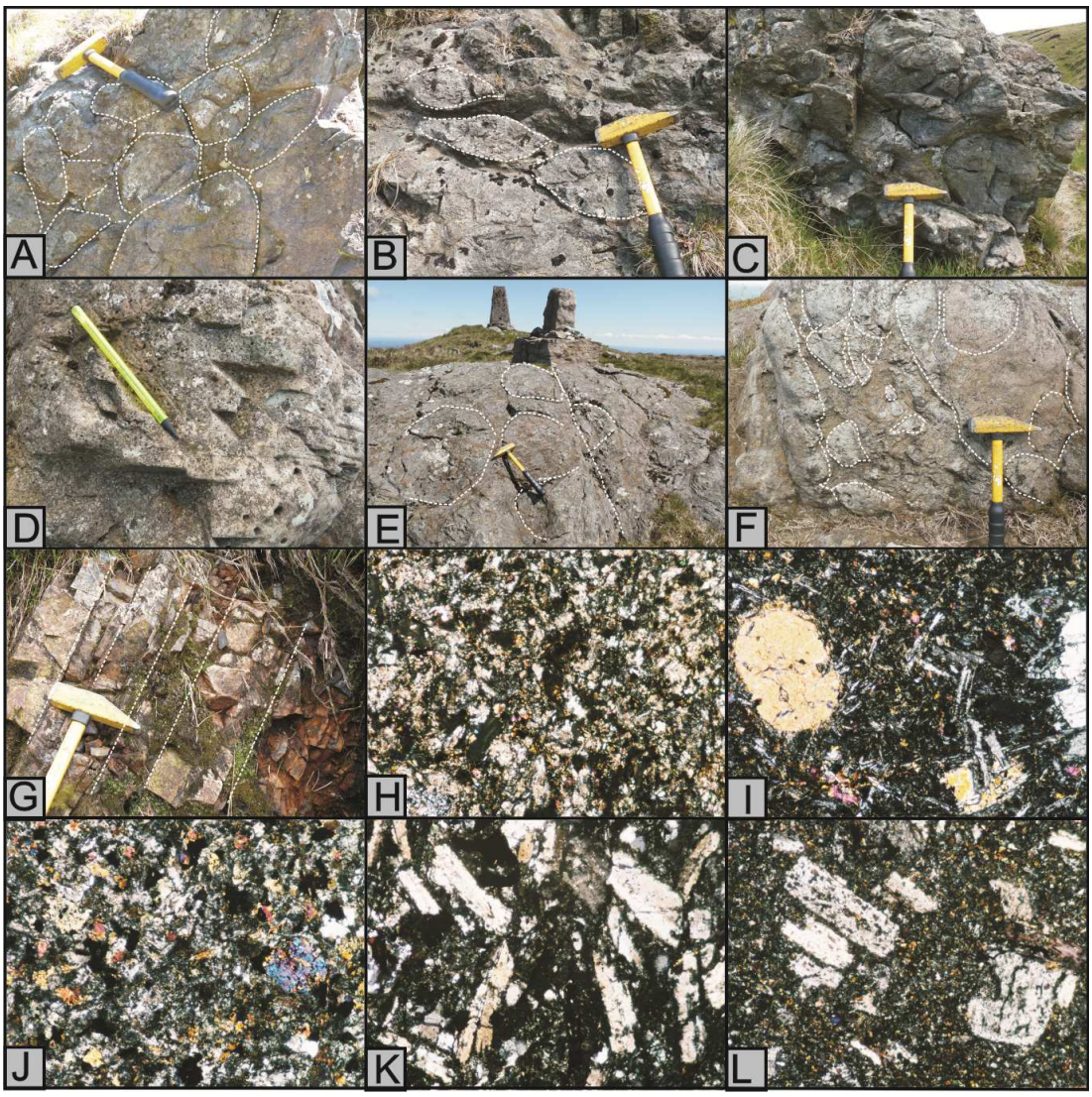

Figure 6.5. Field and thin section photographs from across the Slieve Gallion Inlier. (a) Tholeiitic basaltic pillow basalt from Derryganard (Tinagh Formation). (b-c) Sheared, pillowed and brecciated lava near Tinagh. (d) Vesicular eMORB at top of Slieve Gallion dipping under pillowed calc-alkaline basalt seen in (e). (f) Younger pillow breccias at top of Slieve Gallion. (g) Graptolite bearing succession at Sruhanleanantawey Burn. (h) Extensively altered tholeiitic basalt from Derryganard (SPH525). (i) Vesicular pillowed Fe-Ti eMORB from Slieve Gallion with pyroxene and feldspar phenocrysts (SPH533). (j) Fe-Ti enriched eMORB from Mobuy Wood (SPH517). (k) Feldspathic alkali basaltic intrusive from Sruhanleanantawey Burn (MRC334). (l) Calc-alkaline hornblende- and feldspar-phyric andesite (SPH534) from Letteran. Field of view is approximately 3mm across.

6.3.2 Tawey Formation

The overlying Tawey Formation is at least 1.45 km thick (discounting intrusive units) and is dominated by crystal and lithic tuffs, hornblende-phyric lavas with lesser fine-grained sedimentary rocks (banded chert, pyritic mudstone, banded siltstone and

phyllite) (Fig. 6.4). Poorly exposed, the Tawey Formation is restricted to the western side of Slieve Gallion. It has been broadly divided into sequences dominated by lava (associated with high total magnetic intensity due to the presence of Fe-oxides; Fig. 6.3) and those dominated by tuff and sedimentary rocks. The base of the Tinagh Formation was placed at the first occurrence of sedimentary rocks or layered chert, as crystal tuffs and hornblende-phyric lavas occur in both formations. No evidence for faulting between these formations is apparent from field relationships or geophysics. No pillowed or vesicular flows have been recognized in the Tawey Formation, unlike the underlying Tinagh Formation. Way up criteria in the Formation is scarce due to patchy outcrop. Bedding towards the base of the Sruhanleanantawey Burn, the formations type locality, dips steeply NW, whereas towards the top bedding dips moderately SE (Fig. 6.3). It is believed this variation in the SE is due to localized doming associated with intrusive activity. Intrusions are abundant in the stream section and include quartz-porphyry, a >35 m thick unit of hornblende-rich diorite and alkali-basalt (see MRC335 discussion). A large NW-SE orientated fault also cuts the upper part of the stream, perpendicular to bedding below the SE dipping graptolite-bearing succession. Due to poor exposure combined with structural complications the succession is described as a transverse up Sruhanleanantawey Burn, the type locality for the formation, as in Cameron and Old (1997).

Near the base of the Sruhanleanantawey Burn section the formation is characterized by greenish-grey hornblende and feldspar phyric tuff and lava, which have been intruded by sills of reddish and pink weathered quartz porphyritic dacite common throughout the Tyrone Igneous Complex (see Fig. 6.3). Euhedral quartz, plagioclase feldspar and occasional greenish mica phenocrysts occur in a fine-grained pink dacitic matrix (Cameron & Old 1997). Quartz-porphyritic dacite that intrudes the lower Tyrone Volcanic Group has been dated at 465 ± 1.7 Ma (Cooper et al. 2011). Contacts of alternating exposures between quartz-porphyritic dacite and greenish-grey tuff and lava, which contain hornblende and feldspar phenocrysts, are not well exposed, although at Torys Hole and Tinagh quartz-porphyry is chilled against tuffs and dark greenish-grey dacite respectively. Bedding is clear in coarse tuffs and banded phyllites, although extensive shearing often makes it difficult to distinguish between units of hornblende-bearing crystal tuffs and lavas.

The upper reaches of Sruhanleanantawey Burn have been mapped and logged in detail by the GSNI (Cameron & Old 1997) which is summarized here. Pale grey, chert-like phyllites display faintly visible bedding and are composed of very fine-grained quartz, schistose sericite with weathered-out pyrite porphyoblasts surrounded by limonite haloes (Cameron & Old 1997). Further upstream, phyllites are interbedded with coarse

tuffs and dark grey coarse-grained crystal tuff. A horizon of pale grey tuffaceous chert also occurs with bands of crystal-rich material and light grey thinly bedded tuffaceous siltstone. Some tuffs pass laterally into siltstone (Cameron & Old 1997). Towards the top of the Sruhanleanantawey Burn section, dark blue-grey pyritiferous mudstones and thin coarse tuff bands are overlain by strongly banded blue-grey siltstones. Cooper et al. (2008) obtained a Ca1 Whitlandian age from a sparse graptolite fauna from this part of the sequence (Fig. 6.5g). Coarse crystal tuff further up Sruhanleanantawey Burn is associated with blocks of chert. A thick (>30 m) feldspar-phyric silicified basaltic rock is also present in Sruhanleanantawey Burn downstream from the graptolite bearing horizon. This unit is non vesicular, massive and appears to contain small angular xenoliths of aphanitic basalt or fine-grained silicified sediment. Its contacts with adjacent units are not exposed although due to U-Pb zircon geochronology and its unique geochemical characteristics (see following) it is interpreted as intrusive.

6.3.3 Whitewater Formation

Whitewater River and its tributaries provide the most complete section through the Whitewater Formation. The lower part of this formation (>650 m thick) is characterized by thick accumulations of interbedded hornblende-phyric andesite and tuff, and is in faulted contact with the Tinagh and Tawey formations (Fig. 6.3). Tuffs are often schistose on the northern side of Slieve Gallion and are often chloritic and/or silicified. Lithic and crystal varieties occur with broken crystals of hornblende, augite, epidote, orthoclase and plagioclase set in a feldspathic groundmass with quartz, chlorite and epidote (Hartley 1933). Augite and plagioclase would suggest a mafic source and glass fragments can display a devitrified perlitic structure (Hartley 1933). Rare agglomerate containing chert fragments crops out SE of Windy Castle, whilst at Tirgan a 30 cm thick bed of layered chert occurs which contains intercalated tuff bands (Cameron & Old 1997; Fig. 6.3). Some of the andesites NE of Slieve Gallion and N of Tirgan display pillow structures with a consistent orientation suggesting younging towards the north. No evidence for overturned stratigraphy was observed in the formation, consistent with observations in the Tyrone Volcanic Group as a whole. A rare horizon of ironstone (quartz-hematite) crops out at Drummuck (=Drummuck Ironstone: Fig. 6.3), with float exposed along strike to the N of Slieve Gallion. The upper part of the formation is best exposed around Straw Mountain and is composed of a >750 m thick sequence of chloritic and silicified lithic and crystal tuff with rare andesite. Locally tuffs in Whitewater River (S of Straw Mountain) are extensively sericitised and pyritic. Ironstone (quartz-hematite) float is also common around Straw Mountain, suggesting a second stratigraphically higher unit may be present in the Whitewater Formation above the Drummuck Ironstone (Fig. 6.3).

6.3 Petrochemistry

Volcanic rocks from all major stratigraphic horizons within the Slieve Gallion Inlier were sampled for whole-rock geochemical analysis. All signs of weathering, alteration and veining were removed prior to powdering in a Cr-steel TEMA. Major-elements and trace-elements were determined for whole-rock samples on fused glass beads and powder-pellets, respectively, by X-ray fluorescence (Philips® MagiX-Pro 4kW Rh x-ray tube) at the University of Southampton. Rare earth-elements (REE; plus Nb, Hf, Ta, Th, U) were determined by inductively coupled plasma mass spectrometry (Thermo Scientific Xseries 2) on the same powders following an HF/HNO_3 digest. Accuracy (%RD) and Precision (%RSD) was typically <3 % for ICP-MS analyses and <5 % for XRF analyses based on replicate analyses of a range of international standards (XRF: JR-1, JR-2, JG-3, JB-1a, JA-a; ICP-MS: BHVO-2, JB-1a, JB-3, JGB-1, JR-1). Elements with accuracy and precision >10% (ICP-MS: Ta, Hf; XRF: Cu, Co) are considered poor (Jenner, 1996) and were not used. Nd isotope ratios were measured using a VGMicromass Sector 54 thermal ionization mass spectrometer at the University of Southampton. Further detail on methods is reported in Chapter 3. All results are presented in Appendix 6.1. Geochemical analyses of Cooper et al. (2011; MRC prefixes) are also included where appropriate. Due to the extensive hydrothermal alteration and metamorphism across the Tyrone Volcanic Group, only elements demonstrated to be immobile are used to elucidate petrogenesis, tectonic affinities and chemostratigraphy (after Cooper et al. 2011; Hollis et al. 2012). These include: TiO_2, Th, V, Sc, high field strength elements (HFSE: e.g. Nb, Zr, Y), and the rare-earth elements (REE).

6.3.1 Tinagh Formation

A single sample was analysed from the Derryganard Lavas. This sample (SPH525) is unusual within the Slieve Gallion Inlier displaying low Th (Th_{CN} 8.21) and LREE depletion relative to the HREE (La/Yb_{CN} 0.7). Low Zr/Y (2.24), Zr/TiO_2 and Nb/Y (0.03) ratios suggest these lavas are primitive subalkaline basalts of tholeiitic affinity (Figs. 6.6, 6.7a). Pronounced negative Nb and Ti anomalies are consistent with Formation in an island-arc setting. Sample SPH525 is characterized by high MgO (9.71 wt.%), Cr (650 ppm), Ni (247 ppm) and low SiO_2 (47.1 wt.%).

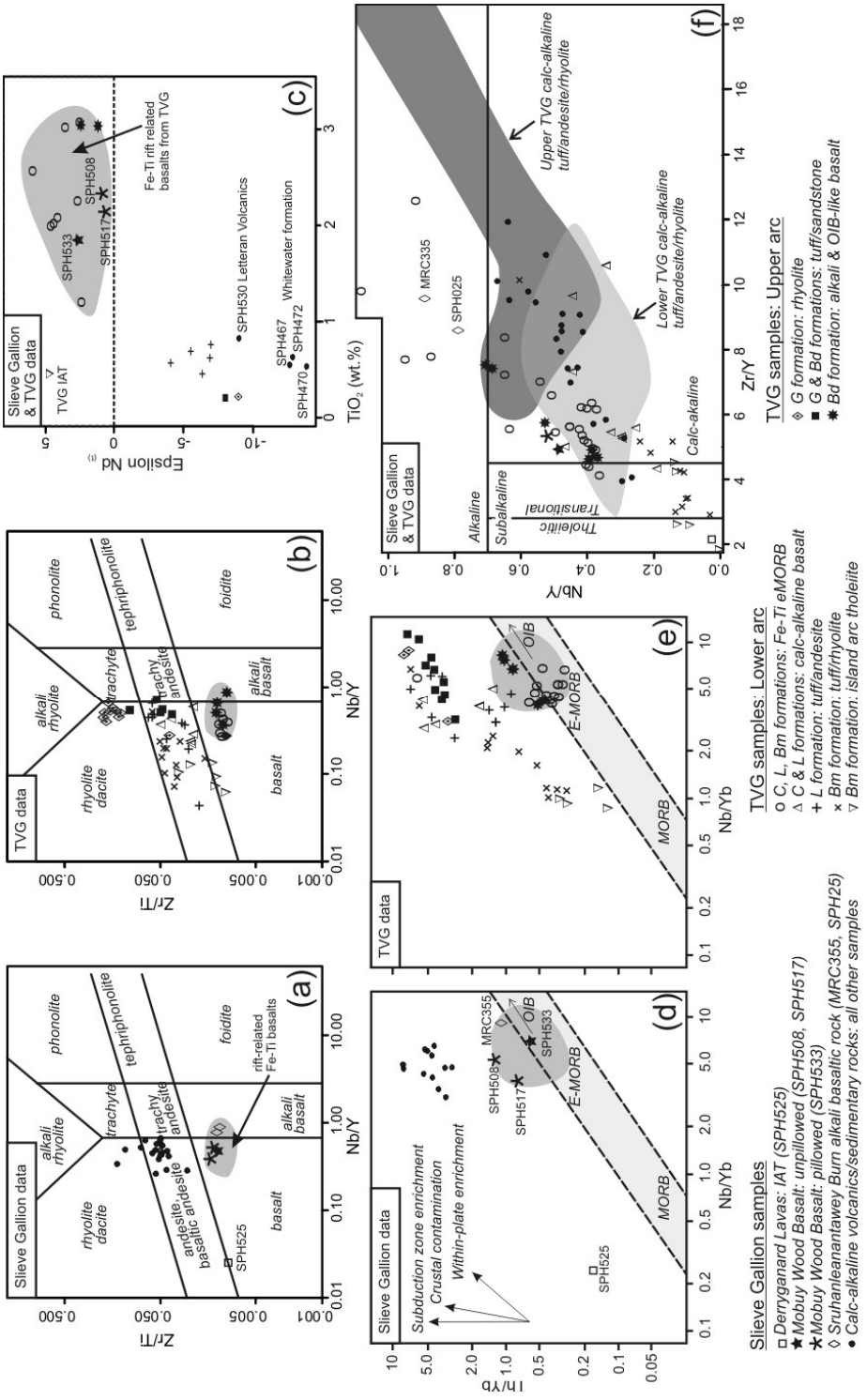

Figure 6.6. Geochemistry of the Slieve Gallion Inlier and Tyrone Volcanic Group (stratigraphy after Hollis et al. 2012). (a-b) Zr-Ti against Nb-Y (after Winchester & Floyd 1977; modified after Pearce 1996); (c) εNd_t against TiO_2; (d-e) Th-Yb against Nb/Yb diagram (after Pearce 1983); (f) Nb/Y against Zr/Y diagram (Zr/Y ratio cut off values from Ross & Bédard 2009). Grey shading in a-e represents the field of Fe-Ti enriched lavas. Grey shading in f represents samples of calc-alkaline affinity from the lower and upper Tyrone Volcanic Group. Data from Draut et al. (2009), Cooper et al. (2011) and Hollis et al. (2012).

Non-pillowed hornblende-phyric lavas of the Windy Castle Lavas were sampled between Derryganard and Slieve Gallion (=SPH506, SPH511, SPH528 and SPH534). These units are strongly calc-alkaline (Zr/Y 6.45-12.1), LILE enriched (Th_{CN} 201.8-458.6) and display high LREE enrichment relative to the HREE (La/Yb_{CN} 9.52-14.00) (Figs. 6.6, 6.7b). TiO_2 (0.48-0.61 wt.%) and Cr (59-173) contents are low, and Nb/Y values range between 0.35 and 0.65. Sample SPH532 was collected from pillow lavas NE of Letteran, and is subalkaline (Nb/Y 0.47) and calc-alkaline (Zr/Y 7.93). It also displays extreme LILE enrichment (Th_{CN} 600) and low MgO (1.06 wt.%), TiO_2 (0.24 wt.%), Cr (99 ppm) and V (34 ppm). All units from the Windy Castle Lavas display island-arc geochemical characteristics including pronounced negative Nb anomalies (Figs. 6.6, 6.7b). Feldspathic andesites (SPH530) analysed from the Letteran Volcanics is also strongly calc-alkaline (Zr/Y 10.37), LILE and LREE enriched (Th_{CN} 237.4, La/Yb_{CN} 12.69) (Figs. 6.6, 6.7b). This sample has a strongly negative εNd_t value of -9.02 (Fig. 6.6c) and displays strong island-arc geochemical characteristics (e.g. negative Nb anomalies).

The Mobuy Wood Basalts are geochemically distinct to all other mafic rocks in the Slieve Gallion Inlier and resemble rift-related lavas of the Tyrone Volcanic Group (Hollis et al. 2012; see following). Low Zr-Ti and high Nb/Y (0.36-0.64) classify these lavas as sub-alkaline basalts, whilst Zr/Y ratios (3.82-6.46) locate them within the calc-alkaline field of Ross and Bédard (2009) (Figs. 6.6a,d,f). All of the samples analysed are characterized by high Fe_2O_{3T} (11.56-13.07 wt.%) and TiO_2 (1.83-2.33 wt.%). εNd_t values are the most primitive of all samples analysed within the Slieve Gallion Inlier (+0.6 to +2.5: Fig. 6.6c). Th/Yb-Nb/Yb systematics and various discrimination diagrams (e.g. Pearce & Cann 1973; Pearce & Norry 1979; Wood 1980; Meschede 1986) suggest these lavas are of eMORB affinity and slightly enriched in subduction zone components (Fig. 6.7c-d). On multi-element variation diagrams all three samples analysed from the Mobury Wood Basalts show high LILE (Th_{CN} 38.8-155.3) and REE enrichment, and LREE enrichment relative to the HREE (La/Yb_{CN} 3.44-4.82) (Fig. 6.7c-d). Sample SPH533 (vesicular pillowed basalt) displays a small positive Nb anomaly and minor negative Ti anomaly (Fig. 6.7c), whereas samples SPH508 and SPH517 (unpillowed basalt) show negative Nb and Ti anomalies (Fig. 6.7d). Sample SPH533 is characterized by slightly lower TiO_2, Th, REE, HFSE, higher Zr/Y, Cr and MgO, and a more primitive εNd_t value than samples SPH508 and SPH517 (Fig. 6.7c).

6.3.2 Tawey Formation

Four samples have been analysed from the Tawey Formation: lithic tuff (SPH493), tuff associated with chert (SPH494), chert (SPH52) and siltstone (SPH496). The volcanic samples are subalkaline, transitional to calc-alkaline (Zr/Y 3.94-8.57) and display high

Th_{CN} (172.4-275.8) (Fig. 6.6). Chert contains high Th_{CN} (343.5), K_2O+Na_2O and Al_2O_3 (11.16 wt.%) which is consistent with both continentally- and arc-derived components.

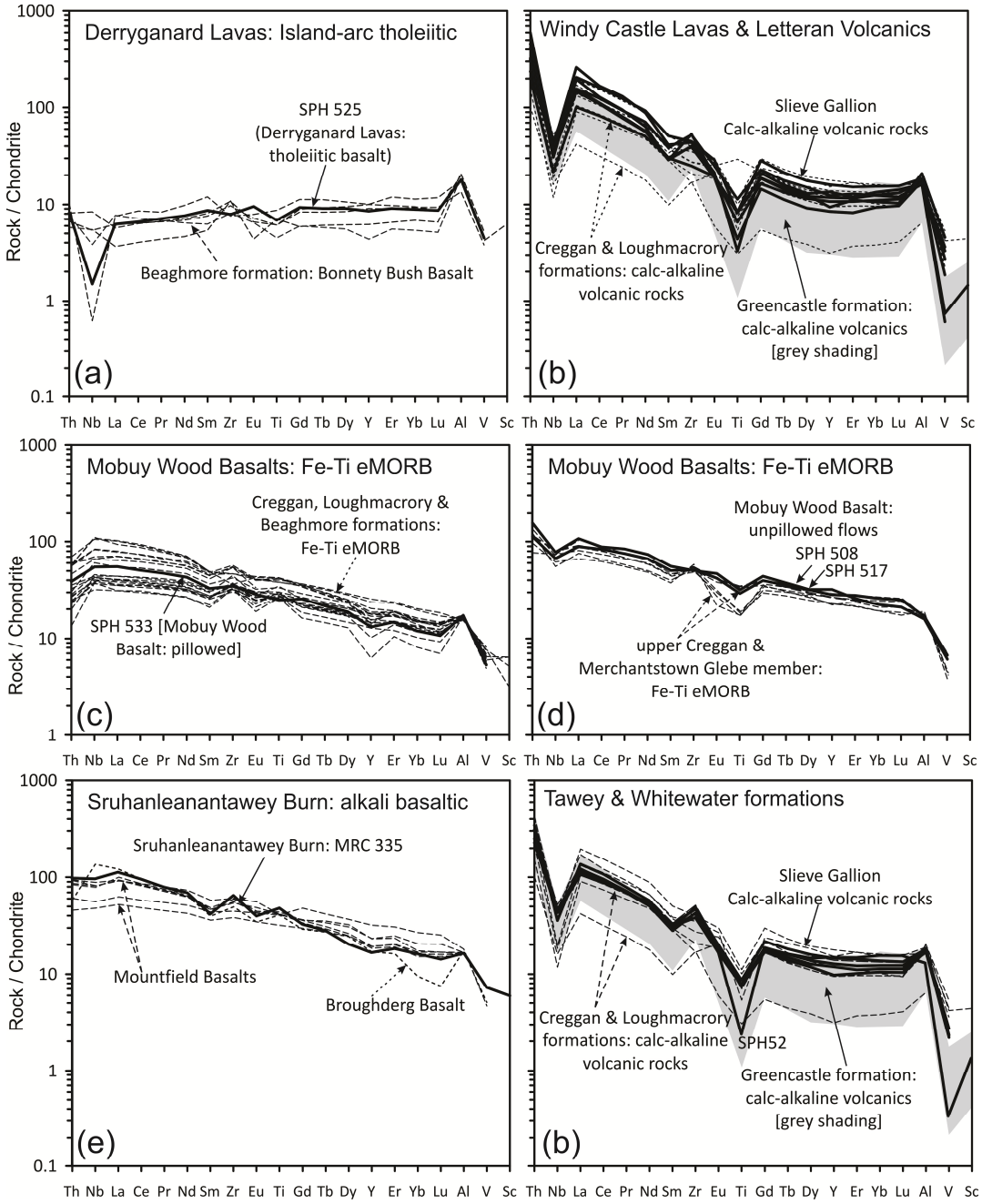

Figure 6.7. Multi-element variation diagrams for samples analysed from Slieve Gallion. Samples from equivalent units in the Tyrone Volcanic Group (after Draut et al. 2009; Cooper et al. 2011; Hollis et al. 2012) are also shown. Multi-element profiles of samples from Slieve Gallion are shown in bold. Chondrite normalization values after McDonough & Sun (1995).

6.3.3 Whitewater Formation

All samples analysed from the Whitewater Formation (SPH467 to SPH488, and SPH502) are basaltic andesitic or andesitic in composition. These rocks are subalkaline (0.45-0.7), strongly calc-alkaline (Zr/Y 5.69-10.57), LILE (Th_{CN} 227.72-310.41) and LREE enriched relative to the HREE (La/Yb_{CN} 7.88-10.91) and HFSE, and are characterized by strongly negative εNd_t values (-12.68 to -13.86) (Fig. 6.6, 6.7f). Cr contents are high (282-405 ppm). All samples show pronounced negative Nb and HFSE anomalies, and positive Zr anomalies, on multi-element variation diagrams (Fig. 6.7f).

6.3.4 Sruhanleanantawey Burn alkali basaltic rock

An extensively altered feldspar-phyric basaltic rock from the upper portions of Sruhanleanantawey Burn (MRC335 and SPH25) was sampled for geochemistry and U-Pb geochronology (see following) downstream of the c.475-474 Ma graptolite bearing rocks analysed by Cooper et al. (2008) and previous workers. This unit is characterized by high TiO_2 (3.53-3.84 wt.%), Fe_2O_{3T} (17.82-18.28 wt.%), P_2O_5 (0.56-0.62 wt.%), LOI (4.51-4.85 %), V (403-463 ppm), Zr (249-283 ppm), and low Cr (4-19 ppm), and Th (2-4 ppm). Sample MRC335 is alkalic (Nb/Y 0.89), of eMORB to OIB affinity (Nb/Yb 8.96) and displays positive Ti and Zr anomalies and weakly negative Nb and Y anomalies (Fig. 6.7e).

6.5 U-Pb geochronology

Two samples were dated by U–Pb thermal ionization mass spectrometry (TIMS) geochronology at the NERC Isotope Geoscience Laboratory (NIGL): (i) MRC335, a silicified Fe-Ti enriched alkali basaltic rock collected from Sruhanleanantawey Burn [IGR 27895-38795], and (ii) MRC351, diorite from Crooked Bridge [IGR 27755-38630]. Zircons were isolated using conventional mineral separation techniques. Prior to isotope dilution thermal ionization mass spectrometry (ID-TIMS) analysis, zircons were subject to a modified version of the chemical abrasion technique (Mattinson 2005). Methods are identical to those reported in Hollis et al. (2012). Errors for U-Pb dates are reported in the following format: ±X(Y)[Z], where X is the internal or analytical uncertainty in the absence of systematic errors (tracer calibration and decay constants), Y includes the quadratic addition of tracer calibration error (using a conservative estimate of the standard deviation of 0.1% for the Pb/U ratio in the tracer), and Z includes the quadratic addition of both the tracer calibration error and additional ^{238}U decay constant errors of Jaffey et al. (1971). All analytical uncertainties are calculated at the 95% confidence interval. Data is presented in Appendix 6.2.

Sample MRC351 was collected from the Crooked Bridge diorite, a 1km long by 400 m wide body exposed within the Slieve Gallion granite (Fig. 6.2). At its northern margin, approximately 400 m N of Crooked Bridge [2750 3859], the transition from granite to diorite is observed over less than 5 m. In places, the granite includes irregular patches of hornblende-rich diorite that are sometimes diffuse, suggestive of magma mingling and mixing. In thin section, diorite from this marginal location contains mainly early euhedral hornblende and plagioclase crystals with late interstitial quartz that encloses smaller sub-anhedral plagioclase. The texture is that of a granite-diorite hybrid and indicates syn-magmatic crystallisation. Seven zircon fractions (single grains) were analyzed from MRC351. All seven analyses are concordant when the systematic $\lambda^{238}U$ and $\lambda^{235}U$ decay constant errors are considered. Six form a coherent single population yielding a weighted mean $^{206}Pb/^{238}U$ date of 469.58 ± 0.32 (0.57)[0.77] Ma (MSWD = 1.4) which we interpret as being the age of sample (Fig. 6.8). One older analysis (z7) is considered to reflect incorporation of older material (c.473 Ma) derived from the Tyrone Volcanic Group into the magmatic system.

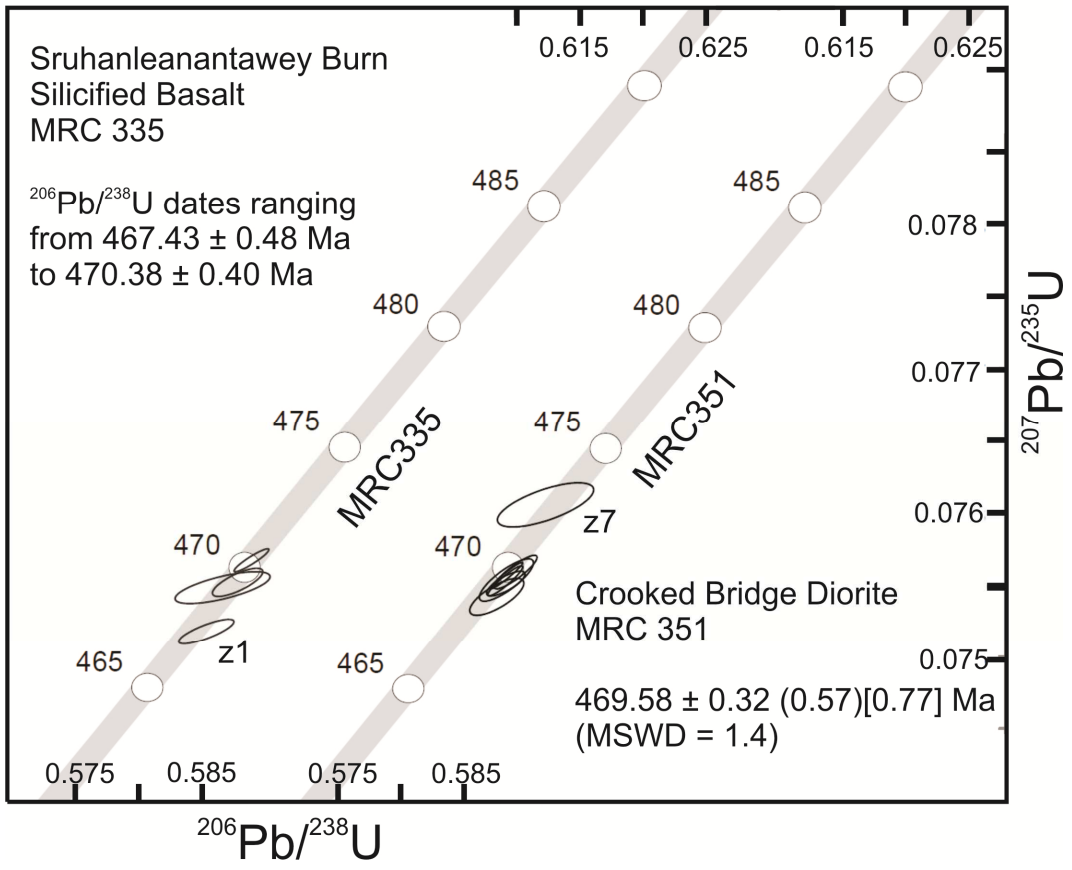

Figure 6.8. U-Pb zircon concordia for samples analysed from the Slieve Gallion Inlier and arc-related intrusive suite.

Sample MRC335 represents a silicified, feldspar porphyritic Fe-Ti enriched alkali basaltic rock which crops out towards the top of Sruhanleanantawey Burn. As detailed above, this unit is non vesicular, massive and appears to contain angular xenoliths of aphanitic basalt or silicified sediment. Its contacts with adjacent units are not exposed. Five zircon fractions (single grains) were analyzed from MRC335. One analyses yielded a Proterozoic age (c.1033 Ma) indicating incorporation of older basement material. Within the remaining population each of the analyses are concordant however there is dispersion with $^{206}Pb/^{238}U$ dates ranging from 467.43 ± 0.48 to 470.38 ± 0.40 Ma (Fig. 6.8). The youngest $^{206}Pb/^{238}U$ date (z1) appears to reflect minor Pb-loss. The age of the sample is approximated by the population of three equivalent $^{206}Pb/^{238}U$ dates (z6, z11 and z14) to 469.36 ± 0.34 Ma (MSWD 0.42).

6.6 Discussion

6.6.1 Petrochemical evolution

Earliest magmatism within the Slieve Gallion Inlier (Tinagh Formation) is characterized by the eruption of tholeiitic pillow basalt of island-arc affinity (=Derryganard Basalts). These lavas are the most primitive of all samples analysed (low SiO_2 and Zr/Y, high MgO). Low La/Yb_{CN} and Th_{CN} suggest magmatism at this stage was not contaminated by continental material. Overlying deposits within the Tinagh Formation (= Letteran Volcanics & Windy Castle Lavas) are dominated by LILE and LREE-enriched hornblende-phyric and feldspathic calc-alkaline basaltic andesites and andesitic tuffs. Strongly-negative $\varepsilon Nd_{(t)}$ values, high Th_{CN} and La/Yb_{CN} suggest a sudden and significant input of continental crust and/or detritus occurred at this time into the arc system; or the Derryganard Basalts represent an episode of volcanism associated with extensive back-arc rifting, such as the Beaghmore Formation of the lower Tyrone Volcanic Group (see Hollis et al. 2012). Mafic tuffs and lavas become increasingly replaced by those of andesitic composition up sequence. The proportion of agglomerates (inter-pillow breccias) and pyroclastic deposits also increases towards the top of the Tinagh Formation.

Primitive, non-arc type Fe-Ti-P enriched basalt of e-MORB affinity recognized around Mobuy Wood (=Mobuy Wood Basalts) are typical of rift related lavas present within the Tyrone Volcanic Group (references within Hollis et al. 2012). Although εNd_t values of Fe-Ti eMORB are the most primitive of all samples analysed within the Slieve Gallion Inlier (+0.6 to +2.5), they are less primitive than those described in Hollis et al. (2012) from main exposures of the lower Tyrone Volcanic Group to the SW (+2.4 to +5.9). Hollis (2012 unpublished PhD thesis) noted systematic geochemical variation in Fe-Ti

enriched basalts of the Tyrone Volcanic Group. Increasing Fe and Ti contents are associated with: increasing Zr, Th, V, La and Nb; decreasing MgO, CaO, Al_2O_3, Ni and Cr; and more negative εNd_t values. These lavas may have formed through the interaction between an island arc and a propagating rift (Hollis et al. 2012).

The occurrence of 1-5 m thick beds of ironstone (or ironstone float) within all formations of the Slieve Gallion Inlier also suggests rifting was episodic during the evolution of the Tyrone arc. Ironstones are common within Tyrone Volcanic Group, where they occur as laterally continuous beds in the Loughmacrory, Beaghmore and Broughderg formations (Fig. 6.2a) and often occur as clasts in overlying tuffs (Hollis et al. 2012). Clasts of ironstone are also found in some basaltic agglomerates of the Creggan Formation (Hollis et al. 2012). Ironstones are temporally and spatially associated with rift-related lavas (e.g. Fe-Ti enriched eMORB, OIB-like, island-arc tholeiite), synvolcanogenic faults, hydrothermal alteration and base-metal mineralization in the Tyrone Volcanic Group (Hollis 2012). Whole rock geochemical ratios and positive Eu anomalies at Torys Hole (and Tanderagee of the Loughmacrory Formation) are comparable to volcanogenic massive sulphide proximal ironstones which form during rift-related hydrothermal activity (Hollis 2012).

The overlying Tawey and Whitewater formations are dominated by calc-alkaline lavas and volcaniclastics with minor sedimentary rocks. This reflects a switch of the arc system from effusive dominated activity (in the Tinagh Formation), through intermittent extrusive and pyroclastic activity (Tawey Formation, lower Whitewater Formation) to pyroclastic dominated activity (upper Whitewater Formation). εNd_t values become progressively more negative up sequence, discounting the Mobuy Wood rift-related lavas (-9.0 Letteran Volcanics; -12.9 lower Whitewater Formation; -12.7 to -13.9 top of Whitewater Formation), suggesting an increased involvement of continentally derived material during petrogenesis associated with arc-accretion. However, this may be an artifact of limited sampling. The presence of thick packages of metasedimentary rocks in the Tawey Formation and the repeated occurrence of ironstone suggests volcanic activity was interrupted by periods of quiescence at several times.

6.5.2 Correlations with the Tyrone Volcanic Group

Using recently published U-Pb zircon geochronology and geochemistry (Cooper et al. 2008, 2011; Draut et al. 2010; Hollis et al. 2012) and the work presented herein, we can refine possible correlations across the Tyrone Volcanic Group. Stratigraphic divisions established within the main occurrence of the Tyrone Volcanic Group, exposed to the SW of the Slieve Gallion Inlier, are presented in Hollis et al. (2012) and summarized in Figure 6.9. Although the volcanic succession at Slieve Gallion was

initially suggested to correlate with the Broughderg Formation of the upper Tyrone Volcanic Group (Cooper et al. 2008), recent geological mapping (Hollis et al. 2012) has identified the presence of similar lithologies (e.g. hornblende-phyric lavas, thinly-bedded argillaceous sedimentary rocks, sheared-rhyolitic tuff, layered chert and greenish-grey tuffs) within the Loughmacrory Formation (Fig. 6.2) of the lower Tyrone Volcanic Group (Fig. 6.9). In addition, the occurrence of ferruginous jasper (ironstone) at Slieve Gallion would argue against a correlation with the Broughderg Formation (c.469 Ma), where ironstones are characterized by magnetite-silica-pyrite and graphitic pelite is abundant (Hollis et al. 2012). Only at Crosh in the Broughderg Formation has quartz-hematite ironstone been recognized (Fig. 6.2), where it replaces a tuffaceous horizon in a thick sequence of graphitic-pelite (Hollis 2012). Pillow lavas and basalt of calc-alkaline affinity are also absent within the upper Tyrone Volcanic Group, but are present in the Creggan, Loughmacrory and Beaghmore formations of the lower Tyrone Volcanic Group (Hollis et al. 2012).

The Loughmacrory Formation is amongst the most diverse succession in the Tyrone Volcanic Group and was divided by Hollis et al. (2012) into three members (Figs. 6.4 & 6.9). The oldest, the Tanderagee Member, is characterized by a thick succession of crystal and lithic tuff, pillowed calc-alkaline basalt/ basaltic-andesite, hornblende and feldspar phyric andesites, and agglomerate, associated with lesser ironstone, Fe-Ti eMORB, layered chert and sedimentary rocks (including siltstone and rare mudstone). The overlying Merchantstown Glebe Member is characterized by pillowed, massive and sheet-flow Fe-Ti enriched basalt/basaltic andesite of eMORB affinity associated with lesser crystal tuff and agglomerate. The youngest, the Streefe Glebe Member, is characterized by a thick sequence of calc-alkaline LILE and LREE enriched crystal tuff with rare occurrences of lava (of unknown affinity). The Loughmacrory Formation bears a striking resemblance to the volcanic succession exposed in the Slieve Gallion Inlier, with the Tinagh and Tawey formations equivalent to the Tanderagee Member, and the Whitewater Formation broadly equivalent to the Streefe Glebe Member (Fig. 6.9). Fe-Ti eMORB lavas of the Mobuy Wood Basalts are present both in the Tanderagee and Merchantstown Glebe members, and the underlying Creggan Formation (associated with lesser calc-alkaline basalt/basaltic andesite, minor agglomerate and layered chert) (Figs. 6.4, 6.9). Although a number of these lithologies can also be found in the Beaghmore Formation of the lower Tyrone Volcanic Group, which is restricted to the E of the Dungate Fault (Fig. 6.2), this backarc assemblage is dominated by bimodal tholeiitic volcanism and Fe-Ti eMORB, with few deposits of calc-alkaline affinity (Hollis et al. 2012).

Geochemical data from both the Slieve Gallion Inlier and all formations of the Tyrone Volcanic Group are plotted together in Figures 6.6-6.7. Multi-element variation profiles allow little distinction between calc-alkaline tuffs of the Tyrone Volcanic Group (Fig. 6.7b,f). Although samples analysed herein of calc-alkaline affinity overlap with lavas and tuffs from both the lower and upper arc, the most evolved samples from the latter are characterized by much higher Zr/Y contents, and Nb/Y ratios toward strongly alkalic compositions (Fig. 6.6f). For example, c. 469 Ma rhyolites of the Broughderg Formation display A-type affinities and are characterized by high Nb and Zr (Hollis 2012 and unpublished data) which have not been recognized at Slieve Gallion.

Mafic lavas of the Tyrone Volcanic Group provide further discrimination between formations, as many units are geochemically distinct. In the lower Tyrone Volcanic Group mafic flows are characterized by calc-alkaline basalt, Fe-Ti enriched eMORB and island-arc tholeiite. In the upper Tyrone Volcanic Group mafic units are restricted to the Broughderg Formation where they are borderline to strongly alkalic and display OIB-like characteristics (Hollis et al. 2012). Pillowed lava sampled from the Mobuy Wood Basalts (SPH533) has an identical multi-element variation profile to Fe-Ti pillowed lavas from the lower Creggan, Loughmacrory (Tanderagee Member) and Beaghmore formations of the lower Tyrone Volcanic Group, with positive Nb anomalies, and similar LILE and REE concentrations (Fig 6.7c). Similarly, massive and vesicular, non-pillowed flows of the Mobuy Wood Basalts (SPH508, SPH517) display slight negative Nb anomalies, and Ti anomalies. These flows are geochemically identical to Fe-Ti lavas from the upper Creggan Formation and Merchantstown Glebe members of the lower Tyrone Volcanic Group (Fig. 6.7d; see Hollis et al. 2012).

Island arc tholeiite, exposed at Derryganard, is only present in the lower Tyrone Volcanic Group in the Beaghmore Formation (eastern block of the lower Tyrone Volcanic Group) (Hollis et al. 2012). Although these lavas display similar multi-element profiles to sample SPH525 (Derryganard Lavas: Fig. 6.7a), they contain higher Nb/Yb, Zr/Y and Nb/Y (Fig. 6.4a-b, d-e) consistent with backarc volcanism in the Beaghmore Formation following intra-arc rifting (Hollis et al. 2012). Tholeiitic tuffs and rhyolitic agglomerates of the Beaghmore Formation which display flat REE profiles and low Zr/Y and Nb/Yb also appear to be unrepresented in the Slieve Gallion Inlier, although rhyodacite from Mobuy Wood was not analysed.

Nd-isotope constraints of samples from Slieve Gallion are shown together with samples from the Tyrone Volcanic Group in Figure 6.4c. Tuffs and lavas of the Loughmacrory Formation are slightly more primitive (εNd_t -4.1 to -7.0) than the Tinagh Formation (Letteran Volcanics: εNd_t -9.0), although chert from the underlying Creggan Formation

has produced a similar value (εNd_t -8.0) (Hollis et al. 2012). No Nd-isotope constrains have been carried out on tuffs of the Streefe Glebe Member, which would equate to the Whitewater Formation (εNd_t -12.7 to -13.9). It is possible the upper part of the Whitewater Formation records the onset of arc-accretion (= lower Greencastle Formation), as similar εNd_t values have also been produced from the syncollisional upper Tyrone Volcanic Group (e.g. rhyolite from Greencastle -8.9, tuff associated with graphitic pelite at Broughderg -11.6). An alternate explanation is the Slieve Gallion volcanics may have been founded upon a portion of thicker continental crust and experienced a greater degree of crustal contamination. This latter scenario is consistent with the geochemistry of the Mobuy Wood Basalts, which display less primitive εNd_t and higher Th/Yb values (Fig 6.6d-e) than associated units in the lower Tyrone Volcanic Group.

In summary, new stratigraphic and petrochemical data from Slieve Gallion suggests the succession at Slieve Gallion is more analogous to the lowermost parts of the Tyrone Volcanic Group, specifically the Loughmacrory Formation (Figs. 6.6-6.7). This is also consistent with U-Pb zircon dating of the upper Tyrone Volcanic Group at c. 473-469 Ma (Cooper et al. 2008; Hollis et al. 2012), and a an age of c. 475-474 Ma from the graptolite bearing succession of Sruhanleanantawey Burn (Cooper et al. 2008).

The Fe-Ti enriched alkali basaltic rock of eMORB to OIB-like affinity from Sruhanleanantawey Burn dated herein to c. 469 Ma is geochemically similar to the Fe-Ti enriched basalts exposed at Mountfield Quarry (Fig. 6.5c) and Broughderg, both of which sit stratigraphically above c. 473-469 Ma rhyolites of the Greencastle Formation. The Sruhanleanantawey Burn and Broughderg Formation basalts plot in similar positions along the mantle array, at higher Nb/Yb than eMORB (Fig. 6.6d-e). Zr/Y ratios are slightly lower in the Mountfield Basalts, although the Sruhanleanantawey Burn samples follow the same trend of increasing alkalinity with Zr/Y (Fig. 6.4f). Sample MRC335 also shows a similar slight negative Nb anomaly, and positive Zr and Ti anomalies (Fig. 6.7e). We interpret the Sruhanleanantawey Burn alkali basaltic rock as a late intrusive and representative of a suite which fed the rift related lavas of the uppermost Tyrone arc. The inherited zircon fraction dated at c. 1033 Ma is consistent with the assimilation of continental material into the magmatic arc at this time. Accretion of the Tyrone arc onto the peri-Laurentian, Dalradian-affinity, Tyrone Central Inlier (Chew et al. 2008) is placed at c. 470 Ma coeval with widespread tonalite emplacement across the Tyrone Igneous Complex (Cooper et al. 2011; also Hollis et al. 2012). Undated Fe-Ti enriched dykes similar to MRC335 also intrude S-type muscovite granite at Tremoge Glen (SPH129: Hollis et al. Chapter 5).

The Crooked Bridge diorite, dated herein to 469.58 ± 0.32 (0.57)[0.77] Ma, displays a clear magma mixing-mingling relationship with hornblende-granite. Biotite-granite dated by Cooper et al. (2011) from the eastern side of Slieve Gallion produced a similar U-Pb zircon age of 466.5 ± 3.3 Ma, within error of that presented here for the Crooked Bridge diorite. Although the biotite- and hornblende-bearing granites of Slieve Gallion may represent distinct magmas, the latter may have been simply contaminated from the underlying Tyrone Plutonic Group as, highly magnetic material of the Tyrone Plutonic Group to be restricted to the southwestern side of Slieve Gallion where hornblende-bearing granite crops out. Both the Slieve Gallion granite and Crooked Bridge diorite belong to the c. 470-464 Ma arc-related intrusive suite of Cooper et al. (2011), which stitches the Tyrone Volcanic Group in its present structural position following arc-accretion.

6.5.3 A correlation for the Irish Caledonide arcs: a link to Charlestown?

Through the study of fossil and modern orogens, and the use of geodynamic models (e.g. Afonso & Zlotnik 2011; Boutelier & Chemenda 2011; Gerya 2011), it is evident that there is not a paradigm that uniquely defines arc-continent collision (reviewed in Brown et al. 2011). Natural complexities in key first order parameters such as the nature of the continental margin (e.g. shape, thickness, presence of re-entrants, hydration, composition) and arc-trench complex (e.g. shape of trench, arc thickness, nature of the basement), result in considerable variation between and within orogens (see Brown et al. 2011), along with their interactions with spreading centres, oceanic plateaus and microcontinental blocks. Arc and ophiolite complexes may be obducted (e.g. Lushs Bight, Bay of Islands: van Staal et al. 2007) or underplated to continental margins (e.g. Annieopsquotch Accretionary Tract: Zagorevski et al. 2009) depending on their relative age at the time of accretion and tectonic position. Fore-arcs may be preserved or completely lost due to the location of failures in the overriding plate, which are determined by sites of lithospheric weakness (Boutelier & Chemenda 2011). Accretion may also be diachronous across the margin, with implications for the timing of subduction reversal (Brown et al. 2011).

Using recently presented stratigraphic, geochemical and U-Pb zircon constraints from the Tyrone Volcanic Group (Cooper et al. 2011; Hollis et al. 2012; and those herein) we can refine possible correlations between the Irish Caledonide arcs which were accreted to the Laurentian margin during the Grampian orogeny. Petrochemical correlations are presented in Figure 6.9 (modified after Ryan & Dewey 2011) according to the timescale of Sadler et al. (2009). Whilst previous work has suggested arc-continent collision during the Grampian orogeny was short-lived and not markedly diachronous (Soper et al. 1999; Dewey 2005), the data presented herein along with recently published

geochronology from the Tyrone Igneous Complex (Cooper et al. 2011; Hollis et al. 2012) clearly demonstrate that either: (i) the evolution of arc volcanism and to some extent arc-accretion was diachronous in the peri-Laurentian Irish Caledonides; or (ii) multiple arc-systems of different age are preserved (e.g. Hollis et al. 2012).

In western Ireland, the generation of suprasubduction zone affinity oceanic crust began prior to c. 514 Ma, the age of high-grade metamorphism and deformation of the Deer Park ophiolitic mélange (514 ± 3 Ma ^{40}Ar-^{39} hornblende: Chew et al. 2010). Early obduction may have occurred to an outboard block of peri-Laurentian affinity microcontinental crust (Chew et al. 2010) as in the Newfoundland Appalachians (=Taconic phase 1: van Staal et al. 2007). Blocks of muscovite-bearing schist within the Deer Park mélange contain detrital zircon spectra similar to the Dalradian Supergroup and have produced a ^{40}Ar-^{39} age of 482 ± 1 Ma (Chew et al. 2010). An age of c. 482 Ma for ophiolite exhumation is consistent with heavy mineral studies from western Ireland which record significant quantities of ophiolite-derived sediment entering the fore-arc (South Mayo Trough) of the Lough Nafooey arc from c. 478-476 Ma (Dewey & Mange 1999; Letterbrock Formation: Fig. 6.9). Together, the South Mayo Trough, Lough Nafooey Group and Tourmakeady Group record the development of the colliding Lough Nafooey arc prior to and during its collision with Laurentia (Ryan et al. 1980; Clift & Ryan, 1994; Dewey & Mange, 1999; Draut & Clift, 2001; Draut et al. 2004; Fig. 6.9). LREE-depletion and the strongly positive εNd_t values of tholeiitic basalts in the lower Lough Nafooey Group suggest an origin far from Laurentia. A switch from the eruption of island-arc tholeiites (and boninitic lavas of the Bohaun Volcanic Formation) to calc-alkaline lavas occurs prior to c. 490 Ma (Fig. 6.9). Increasing SiO_2, LILE and LREE enrichment and more negative εNd_t values with stratigraphic height in the Lough Nafooey arc, reflect an increasing contribution of subducted metasedimentary material into the arc system as it approached the Laurentian margin (Draut et al. 2004; Chew et al. 2007). The overlying syn-collisional Tourmakeady Group (c. 476-470 Ma, Fig. 6.9) formed synchronously with peak metamorphism and regional deformation within the Dalradian Supergroup associated with arc-continent collision. The timing of 'hard' collision in western Ireland (= base of the Tourmakeady Group: Draut et al. 2004) occurred between c. 484 Ma (=graptolite contraint on Lough Nafooey Group) and c. 476 Ma (=age of the Mt. Partry Formation) (Fig. 6.9). This phase of arc-accretion is equivalent to Taconic phase 2 of the Newfoundland Appalachians (van Staal et al. 2007).

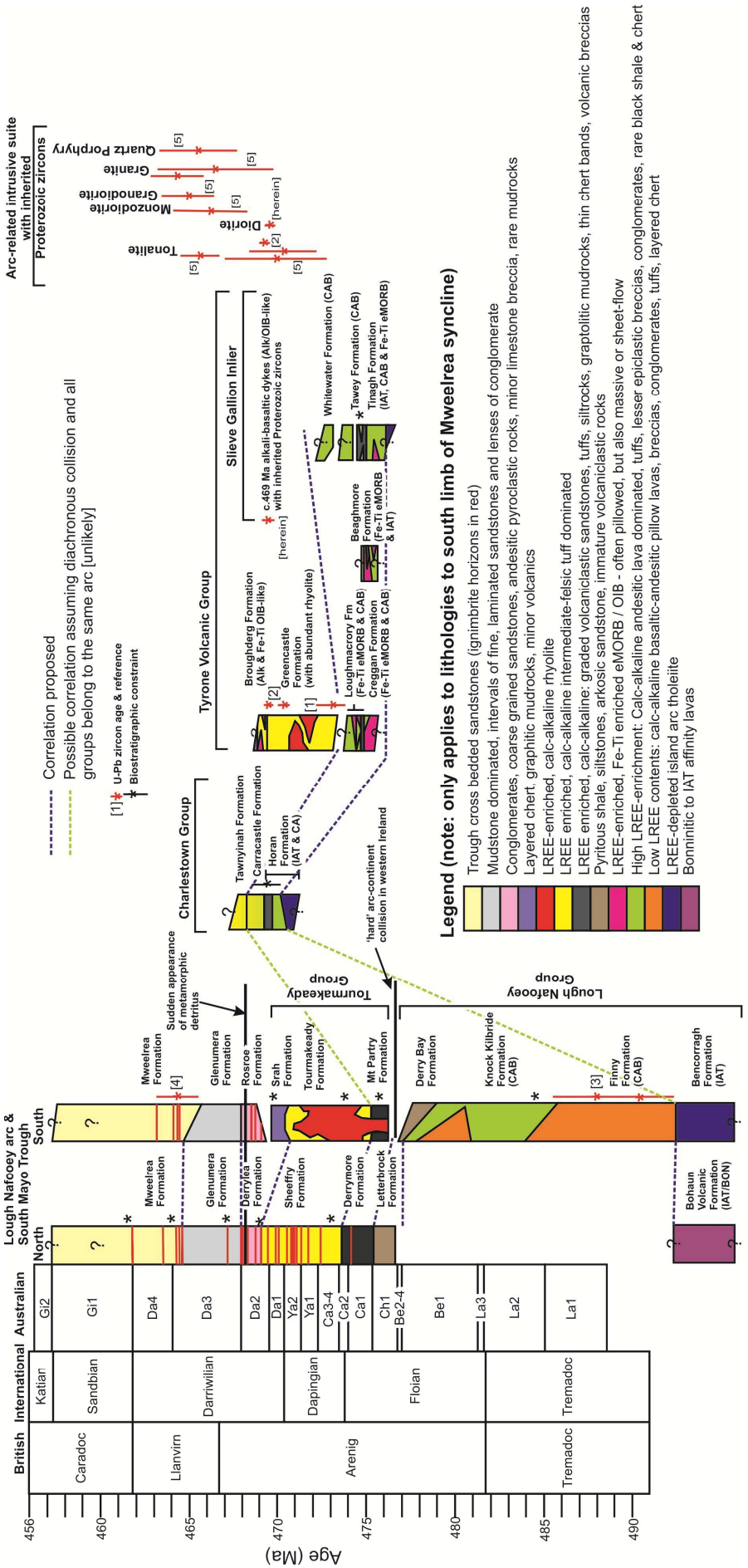
Arc-related intrusive suite with inherited Proterozoic zircons
Quartz Porphyry
Granite
Granodiorite
Monzodiorite
Diorite
Tonalite
[herein]
[1] U-Pb zircon age & reference
Biostratigraphic constraint
Correlation proposed
Possible correlation assuming diachronous collision and all groups belong to the same arc [unlikely]
Tyrone Volcanic Group
Slieve Gallion Inlier
c.469 Ma alkali-basaltic dykes (Alk/OIB-like) with inherited Proterozoic zircons
Broughderg Formation (Alk & Fe-Ti OIB-like)
Greencastle Formation (with abundant rhyolite)
Whitewater Formation (CAB)
Tawey Formation (CAB)
Tinagh Formation (IAT, CAB & Fe-Ti eMORB)
Beaghmore Formation (Fe-Ti eMORB & IAT)
Loughmacrory Fm (Fe-Ti eMORB & CAB)
Creggan Formation (Fe-Ti eMORB & CAB)
Charlestown Group
Tawnyinah Formation
Carracastle Formation
Horan Formation (IAT & CA)
'hard' arc-continent collision in western Ireland
Legend (note: only applies to lithologies to south limb of Mweelrea syncline)
Trough cross bedded sandstones (ignimbrite horizons in red)
Mudstone dominated, intervals of fine, laminated sandstones and lenses of conglomerate
Conglomerates, coarse grained sandstones, andesitic pyroclastic rocks, minor limestone breccia, rare mudrocks
Layered chert, graphitic mudrocks, minor volcanics
LREE-enriched, calc-alkaline rhyolite
LREE enriched, calc-alkaline intermediate-felsic tuff dominated
LREE enriched, calc-alkaline: graded volcaniclastic sandstones, tuffs, siltrocks, graptolitic mudrocks, thin chert bands, volcanic breccias
Pyritous shale, siltstones, arkosic sandstone, immature volcaniclastic rocks
LREE-enriched, Fe-Ti enriched eMORB / OIB - often pillowed, but also massive or sheet-flow
High LREE-enrichment: Calc-alkaline andesitic lava dominated, tuffs, lesser epiclastic breccias, conglomerates, rare black shale & chert
Low LREE contents: calc-alkaline basaltic-andesitic pillow lavas, breccias, conglomerates, tuffs, layered chert
LREE-depleted island arc tholeiite
Bonninitic to IAT affinity lavas
Sudden appearance of metamorphic detritus
Tourmakeady Group
Lough Nafooey Group
Mweelrea Formation
Glenumera Formation
Rosroe Formation
Srah Formation
Tourmakeady Formation
Mt Partry Formation
Derry Bay Formation
Knock Kilbride Formation (CAB)
Finny Formation (CAB)
Bencorragh Formation (IAT)
Derrylea Formation
Sheeffry Formation
Derrymore Formation
Letterbrock Formation
Bohaun Volcanic Formation (IAT/BON)
Lough Nafooey arc & South Mayo Trough
North
South
British
International
Australian
Caradoc
Llanvirn
Arenig
Tremadoc
Katian
Sandbian
Darriwilian
Dapingian
Floian
Tremadoc
Gi2
Gi1
Da4
Da3
Da2
Da1
Ya2
Ya1
Ca3-4
Ca2
Ca1
Ch1
Be2-4
Be1
La3
La2
La1
Age (Ma)
456
460
465
470
475
480
485
490

Fig. 6.9. (previous page) Stratigraphy, petrochemistry and absolute ages for the Ordovician succession of South Mayo, Charlestown and the Tyrone Igneous Complex. Diagram after Ryan and Dewey (2011). The standard British Ordovician stages, those of the IUGS and the Australian Ordovician graptolite zones are assigned to absolute ages after Sadler *et al.* (2009). Absolute ages for events are represented by red stars with error bars. References: 1=Formil rhyolite (Cooper et al. 2008); 2=Tullybrick tuff and Cashel Rock rhyolite of Greencastle Formation, and Cashel Rock tonalite (Hollis *et al.* 2012); 3= clasts in Silurian conglomerate derived from Finny Formation (Chew *et al.* 2007); 4=Ignimbrite of Mweelrea Formation (Dewey & Mange 1999); 5= Arc related intrusive rocks of Cooper et al. (2011). Stratigraphy of the Tyrone Volcanic Group from (Hollis *et al.* 2012 and unpublished data). North and south limbs refer to the Mweelrea syncline (South Mayo Trough).

While the Lough Nafooey arc clearly shows an increasing contribution of subducted metasedimentary material into the arc system as it approached the Laurentian margin (Draut et al. 2004), no such systematic trend is evident in the Tyrone Volcanic Group (Hollis et al. 2012). Both the syn-collisional upper Tyrone Volcanic Group and the pre-collisional basal formations of the lower Tyrone Volcanic Group display strongly negative εNd_t values and strong LILE- and LREE-enrichment (Fig. 6.6c,f, Fig. 6.7b,f; Hollis et al. 2012) indicative of extensive contamination (Draut et al. 2009; Cooper et al. 2011). Two possible scenarios may explain these geochemical characteristics. In the first scenario, the Tyrone Igneous Complex may have developed above a SE-dipping subduction zone and is part of the Lough Nafooey arc system (e.g. Draut et al. 2009). In this instance, extensive crustal contamination would result from subducted sediment derived from the Laurentian margin. Increased contamination may have also occurred if the Tyrone arc was founded upon a segment of peri-Laurentian outriding continental crust. Arc-continent collision would have been diachronous from c. 480-476 Ma in western Ireland to c.470 Ma in Co. Tyrone. Similarly, the geochemical evolution of the arc must have also been strongly diachronous (Fig. 6.9), with a switch from tholeiitic volcanism from <490 Ma in western Ireland (Draut et al. 2004) to c. 475 Ma in the Tyrone Volcanic Group (Cooper et al. 2011). In the second scenario, the Tyrone Igneous Complex may have developed above a N-dipping subduction zone in a manner similar to the Annieopsquotch Accretionary Tract of Newfoundland (Zagorevski et al. 2009; Hollis et al. 2012; Chapter 5), and records the evolution of a younger, separate arc system which collided with the composite Laurentian margin at c. 470 Ma. In this model, the Tyrone Igneous Complex formed immediately outboard of the Tyrone Central Inlier, a peri-Laurentian microcontinental block (Chew et al. 2008). At c. 484-479 Ma the propagation of a spreading centre into this microcontinental block led to the formation of the ophiolitic Tyrone Plutonic Group (Chapter 5). Continental contamination of the Tyrone arc would in this scenario result from the arc being constructed upon the rifted-off fragment of microcontinental crust.

The Charlestown Group, exposed across approximately 45 km^2 of Co. Mayo, is an important link between western Ireland and the Tyrone Volcanic Group of Northern Ireland. Although it is typically attributed to the syn-collisional stage of the Lough Nafooey arc system and is believed to broadly correlate with the Tourmakedy Group (e.g. Chew 2009), it remains one of the most understudied components of the orogen. Charlesworth (1960) provided the first detailed structure and stratigraphy of the Charlestown Group. New exposure allowed O'Connor (1987) to reassess the stratigraphy and re-divide the succession into three formations, renamed by Long et al. (2005) as; (i) Horan Formation, around 630 m thick, characterized by minor sediments, extrusive basalts, spillites and mixed tuffs; (ii) Carracastle Formation, around 290 m thick, dominated by andesitic tuffs and flows, with coarse volcanic breccias; and (iii) Tawnyinah Formation, around 300 m thick, dominated by more silicic lithologies. A gradual change was noted from tholeiitic island-arc spillites at the base with associated tuffs, into calc-alkaline tuffs and resedimented tuffs of the Carracastle Formation, passing into more felsic tuffs with accompanying intrusions of rhyolite and dacite near the top (O'Connor & Poutsie 1986; also O'Connor 1987).

This lithological and petrochemical change is similar to that observed from both the Tyrone Volcanic Group (e.g. IAT into CAB of the Tinagh Formation to syndepositional rhyolites of the upper Tyrone arc) and the Lough Nafooey arc (e.g. Draut et al. 2004), although the timing differs significantly from the latter (Fig. 6.9). In the Charlestown Group, Cummins (1954) obtained an Arenig age from a graptolite bearing sequence near the top of the Horan Formation. This was later verified by Dewey et al. (1970) specifically to British Didymograptus hirundo biozone and Isograptus caduceus biozone of North America. Cooper and Lindholm (1990) equated the Didymograptus hirundo biozone with the Da1 zone of the Darriwilian Australasian stage. The Didymograptus hirundo biozone was subsequently renamed to the Aulograptus cucullus biozone and suggested to correlate with both the Undulograptus austrodentatus biozone (=Da1) and lower part of the Undulograptus intersitus biozone (=lower Da2) (see Zalasiewicz et al. 2009). The Da1 stage has been calculated by Sadler et al. (2009) to 470.54-469.57 Ma, and the upper boundary of Da2 to 467.94 Ma.

Although further work is needed on the Charlestown Group, particularly high-resolution U-Pb zircon geochronology, trace geochemistry and Nd-isotope constraints, it shares strong temporal, lithological and geochemical similarities with the Tyrone Volcanic Group (Fig. 6.9) despite being separated by some distance. We suggest they may belong to the same arc-system (possibly different eruptive centres) which was subsequently juxtaposed with the Lough Nafooey arc during during dextral (Harris

1993) or later sinistral strike-slip activity (Dewey & Strachan 2003). Pb isotope work on galenas from Charlestown and mineral deposits directly NW of (and structurally overlying) the Tyrone Volcanic Group has also suggested a correlation between the two arc terranes (Parnell et al. 2000).

In summary, if the Lough Nafooey, Tourmakeady, Charlestown and Tyrone Volcanic groups are part of the same arc system and represent distinct eruptive centres, the geochemical evolution of this arc must have been strongly diachronous within the Irish Caledonides (Fig. 6.9) from c. <490 to 475 Ma, with diachronous accretion to Laurentia from c. 480-478 Ma to c. 470 Ma. However, primitive Tremadocian to early Arenig (c. 490-480 Ma) arc rocks have also been recognized from the Scottish Caledonides. For example, Chew et al. (2010) obtained a U-Pb zircon age of 490 ± 4 Ma from a mica-schist (interpreted as a volcaniclastic rock) intercalated within the c. 499 ± 8 Ma (U-Pb zircon) Highland Border Ophiolite (an along-strike equivalent of the Deer Park Complex). Similar ages have also been obtained from Ballantrae, Scotland (Sm-Nd 501 ± 12 Ma, 476 ± 14 Ma: Thirlwall & Bluck 1984; K-Ar 487 ± 8 Ma: Harris et al. 1965) suggesting a volcanic arc may have been associated with the Ballantrae ophiolite (483 ± 4 Ma U-Pb zircon; Bluck et al. 1980) at this time. The absence of a volcanic arc in Co. Tyrone prior to c. 475 Ma, combined with strong temporal, petrochemical, and stratigraphic correlations to ophiolites and arc-successions in the Newfoundland Appalachians along strike (Cooper et al. 2011; Hollis et al. 2012; Chapter 5); and the development of the Tyrone Igneous Complex outboard of the Tyrone Central Inlier; together suggest the complex formed within a separate arc-system to the Lough Nafooey Group.

6.6 Conclusions

The Slieve Gallion Inlier of Northern Ireland, an isolated fragment of the Tyrone Volcanic Group, records the development of a peri-Laurentian island-arc/backarc and its obduction onto an outboard microcontinental block (=Tyrone Central Inlier) c. 470 Ma. Earliest magmatism is characterized by LREE-depleted island-arc tholeiite. Overlying deposits are dominated by LILE and LREE-enriched, hornblende-phyric and feldspathic calc-alkaline basaltic andesites and andesitic tuffs with strongly-negative εNd_t values implying substantial contamination by continental crust and/or detritus. Fe-Ti enriched rift related basalts of eMORB affinity may be associated with propagation of a rift into the island-arc. Biostratigraphic age constraints and petrochemical correlations suggest the Slieve Gallion Inlier formed c. <475-473 Ma and is equivalent to the lower Tyrone Volcanic Group. Late c. 469 Ma intrusive rocks of Fe-Ti-P enriched alkali basalt appear to have fed the post-collisional rift-related lavas of

the uppermost Tyrone Arc (=Broughderg Formation). Strong temporal, geochemical and stratigraphic correlations between the Slieve Gallion Inlier (Tyrone Volcanic Group) and Charlestown Group of Ireland suggest they may be part of the same island arc subjected to post-accretion strike-slip faulting. A switch from tholeiitic volcanism to calc-alkaline dominated activity within the Lough Nafooey arc occurred prior to c. 490 Ma approximately ~15 to 20 Myr earlier than at Charlestown (c. 470 Ma) and Tyrone (c. 475 Ma).

Chapter 7: Implications for VMS mineralization in Co. Tyrone

This chapter forms the basis of a manuscript to be submitted to Mineralium Deposita: Hollis, S.P., Roberts, Earls, G., Herrington, R., S., Cooper, M.R. & Piercey, S.J. *Petrochemistry and hydrothermal alteration within the Tyrone Arc: Targeting VMS mineralization in Northern Ireland.* Some sections have been considerably expanded.

Abstract

Although volcanogenic massive sulphide (VMS) deposits can form within a wide variety of rift-related tectonic environments, most are preserved within suprasubduction affinity oceanic and ensialic tracts associated with episodes of ocean-closure. In stark contrast to the VMS rich Appalachian sector of the Grampian-Taconic orogeny, VMS deposits at first glance appear absent in the peri-Laurentian sector of the British and Irish Caledonides. The Tyrone Igneous Complex of Northern Ireland represents a c. 484-464 Ma peri-Laurentian affinity arc-ophiolite complex and an along strike continuation of the Buchans-Roberts arc system of Newfoundland which is host to significant high-grade VMS mineralization. Through a combination of extensive field mapping and petrochemistry, several stratigraphic horizons have been identified which were favourable for the formation and preservation of VMS deposits in the Tyrone Igneous Complex. Each is closely associated with extensive hydrothermal alteration, synvolcanogenic faults and high-level synvolcanogenic intrusions (dolerite, gabbro, diorite and/or tonalite). Episodic rifting is recorded by the eruption of: abundant non-arc type Fe-Ti enriched eMORB ('icelandite'), island-arc tholeiite, OIB-like and alkali basalt, high-temperature M-type tholeiitic rhyolites, and A-type high Zr rhyolites, within the calc-alkaline dominated sequence. Rift-related mafic lavas occur in the hangingwall to VMS-style mineralized showings and are closely associated with ironstones (occasionally Au bearing) and/or argillaceous sedimentary rocks representing volcanic quiescence. Extensive hydrothermal alteration, characterized by Na-depletion, high Ba/Sr, Bi, Sb and variable MgO and CaO contents, allows specific target areas to be identified (along with mineral chemical vectors and ironstone geochemistry). In the lower bimodal-mafic Tyrone arc and backarc, hydrothermal alteration is associated with Zn-Cu mineralized float. Pb-Zn-Cu-Au mineralization occurs in crackle-brecciated and silicified auriferous FII-type rhyolite domes/flows and/or volcaniclastic rocks of the syncollisional bimodal-felsic upper Tyrone arc. Rare

ophiolite hosted Cu mineralization is characterized by chalcopyrite stringers hosted in sheeted dyke sequences.

7.1 Introduction

Although the vast majority of VMS deposits forming on the present day seafloor have been found at plate boundaries in both spreading-ridge and arc environments (Herzig & Hannington 1995), most of those formed in mid ocean ridge settings are typically lost with oceanic crust through subduction processes (Galley et al. 2007a). Consequently, VMS deposits preserved in the rock record predominantly formed in oceanic and continental nascent-arc, rifted-arc, and backarc settings (e.g. Franklin et al. 1998; Barrie & Hannington 1999; Allen et al. 2002) which were accreted to / formed on continental margins during episodes of large-scale ocean closure (e.g. Urals: Herrington et al. 2005; Appalachians: van Staal 2007).

Despite being a desirable deposit type due to their polymetallic nature and Au credits, ancient VMS deposits remain challenging exploration targets due to their relatively small sizes, deformed natures, and associated large scale alteration systems. However, it is also well established that within individual terranes VMS deposits are not distributed evenly, either spatially or temporally, but are typically clustered at specific stratigraphic horizons in arc successions (Sangster 1972), associated with episodes of extension (e.g. calderas and linear rifts), synvolcanogenic faults and intrusions (Sangster 1980). Many camps have specific stratigraphic marker horizons which are actively targeted for further mineralization along strike or down-dip, such as 'mine rhyolites' (e.g. Flin Flon), and/or local/laterally-extensive sulphidic, waterlain tuff, and/or chemical sedimentary units (i.e. tuffite or exhalite horizons: Knuckey et al. 1982; Kalogeropoulos & Scott 1983, 1989; Liaghat & MacLean 1992; Spry et al. 2000; Peter 2003). Locating these stratigraphic horizons and targets areas along each, which were favourable for the formation and preservation of VMS deposits, is a logical approach in greenfield terranes where limited resources are available.

The c. 484-464 Ma Tyrone Igneous Complex of Northern Ireland has been a target for base metal exploration since the early 1970s. Although previous work highlighted a number of Au and Cu targets, no occurrences of any size were identified (Leyshon & Cazalet 1978; Clifford et al. 1992). Advances in our understanding of how VMS deposits form and their common petrochemical associations provide an opportunity to identify VMS prospective areas in the complex. We demonstrate how specific stratigraphic horizons and target areas along each favourable for VMS mineralization have been identified through a combination of extensive field mapping and

petrochemistry. Consideration of element mobility data, mass change, and various 'vectors towards mineralization' (e.g. Ba/Sr, Sb, Tl, Na-depletion, Carbonate-chlorite-pyrite Index, Alteration Index, etc.) within the volcanic stratigraphy allowed specific areas along each to be identified for further exploration. Known showings of VMS-style mineralization in the arc-related sequence (e.g. Leyshon & Cazalet 1978; Clifford et al. 1992; Gunn et al. 2008, unpublished Ennex International reports) fall on these stratigraphic horizons, many of which are coincident with untested geophysical and geochemical (e.g. soil, base of till) anomalies. Furthermore, we provide new geochemical data from drillcore within the Tyrone Volcanic Group. Mineral chemical data and ironstone geochemistry are also presented in the Appendix.

7.2 VMS deposits in the Caledonian-Appalachian orogen

The Caledonian-Appalachian orogenic belt resulted from closure of the Iapetus Ocean and Tornquist's Sea during the early Palaeozoic. Widespread plate reorganization resulted in the progressive accretion of oceanic tracts, arc-related terranes and ribbon shaped microcontinental blocks to the Laurentian margin during the Late Cambrian – Middle Ordovician (Grampian-Taconic orogeny, e.g. van Staal et al. 2007), prior to the arrival of Baltica (=Scandian orogeny) and peri-Gondwanan microcontinents, such as Ganderia (=Salinic orogeny) and Avalonia (=Acadian orogeny) (van Staal et al. 2007).

The Dunnage zone ('Central Mobile Belt') of Newfoundland, Canada, represents a tectonic collage of oceanic and ensialic arc-related terranes which formed in the Iapetus Ocean. VMS bearing vestiges of Iapetus of peri-Laurentian affinity (= Notre Dame subzone) are separated from those of peri-Gondwanan affinity (= Exploits subzone) by the Red Indian Line. VMS deposits are abundant in the Dunnage zone, with over 40 deposits greater than 0.1 Mt massive sulphide for an aggregate total resource of approximately 112 Mt (geological resource), and production and reserves of ~46 Mt (Piercey 2007a; see Fig. 7.1). Several significant new discoveries have been made in recent years, including Lemarchant (1.24 Mt at 5.38% Zn, 1.19% Pb, 59.17 g/t Ag and 1.01 g/t Au) and Boomerang (1.36 Mt at 7.1% Zn, 3.0% Pb, 0.5% Cu, 110 g/t Ag and 1.7 g/t Au) (Piercey & Hinchey 2012, Messina Minerals 2012). Both the Duck Pond (4.08 Mt at 5.68% Zn, 3.29% Cu, 0.9% Pb, 59.3 g/t Ag and 0.9 g/t Au) and Ming deposits (3.65 Mt at 2.26% Cu, 0.32% Zn, 6.78 g/t Ag and 1.13 g/t Au) are currently in production (references in Piercey & Hinchey 2012).

Figure 7.1.

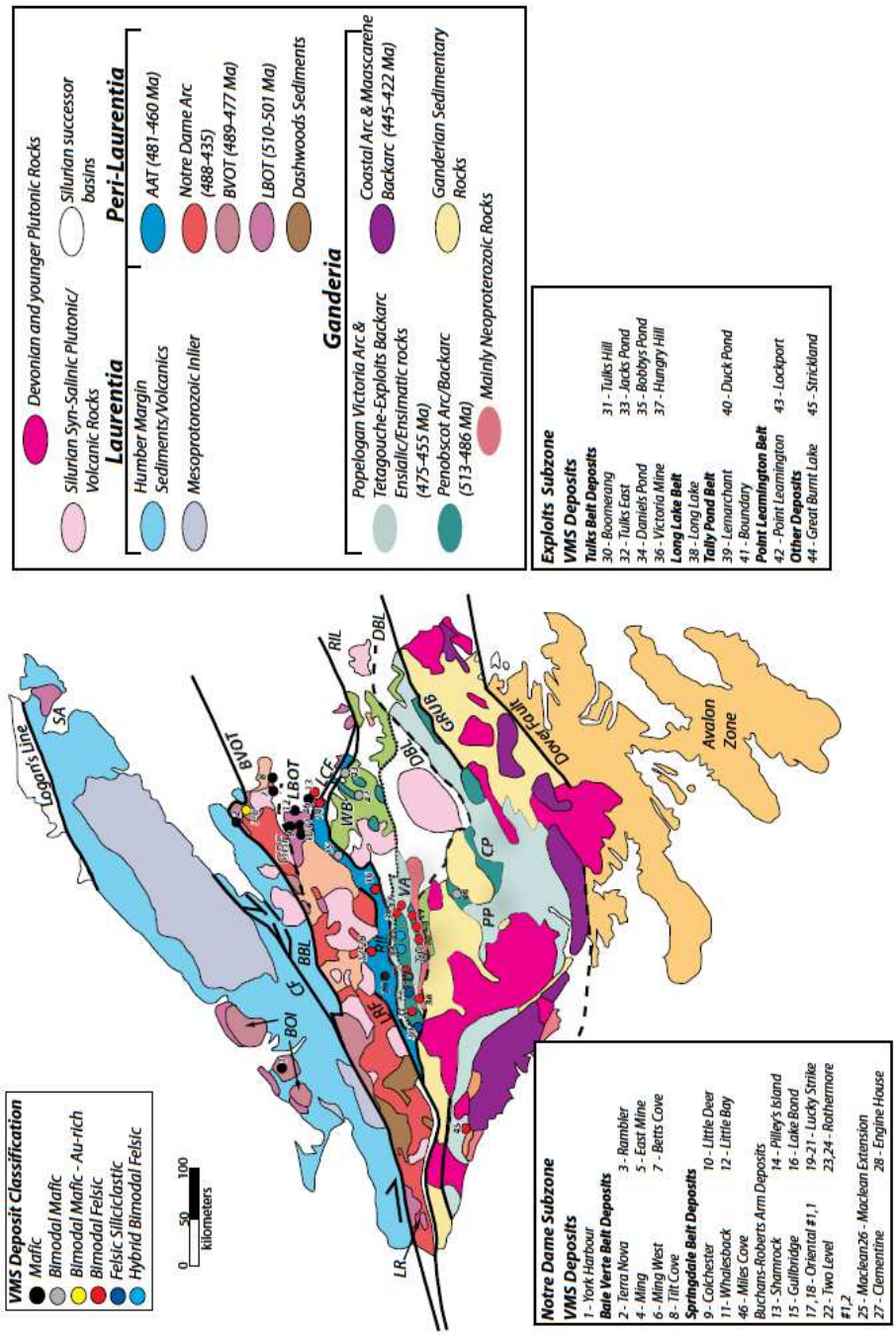

Geological map of the Newfoundland Appalachians with tectonostratigraphic zones, accretionary tracts, VMS deposits, their classifications and associated belts (from Piercey & Hinchey 2012, after van Staal 2007). BBL, Baie Verte - Brompton Line; BOI, Bay of Islands; BVOT, Baie Verte Oceanic Tract; CF, Cabot Fault; CP, Coy Pond Complex; DBL, Dog Bay Line; GBF, Green Bay Fault; GRUB, Gander River Ultramafic Belt; LBOT, Lushs Bight Oceanic Tract; LCF, Lobster Cove Fault; LR, Long Range; LRF, Lloyds River Fault; PP, Pipestone Pond Complex; RIL, Red Indian Line; SA, St. Anthony; TP, Tally Pond Belt; TU, Tulks Volcanic Belt; VA, Victoria Arc; WB, Wild Bight Group.

The scarcity of both peri-Gondwanan and peri-Laurentian affinity VMS deposits in the British and Irish Caledondies is striking. Discovered peri-Gondwanan VMS deposits to

the south of the Iapetus Suture (equivalent to the Red Indian Line) include Parys Mountain, Wales (drill-indicated reserves of 4.8 Mt at 6.0% Zn, 3.0% Pb, 1.5% Cu, 57 g/t Ag and 0.4 g/t Au: Colman & Cooper 2000), and Avoca, Ireland (production from 1720-1982: ~12 Mt at 0.75 % Cu: Bayswater Uranium 2012). Although, the Avoca deposit was mined for Cu, significant Zn-Pb resources remain in the district (West Avoca: ~6 Mt at 5.3% Zn and 1.9% Pb; Bayswater Uranium 2012). Drilling in the 1980's obtained significant intersections of Zn-Pb-Cu-Ag-Au in the Kimacoo zone (8.3m at 10.1% Zn, 5.7% Pb, 0.48% Cu, 284 g/t Ag and 4.52 g/t Au: Bayswater Uranium 2012), confirmed by recent exploration (Bayswater Uranium news release 10 June 2009).

North of the Iapetus Suture, the Vidlin VMS deposit has been recognized in the Dalradian Supergroup on the Shetland Islands (=Laurentian rift and passive margin sequences), where stratabound sulphides reach 10m in thickness and grade up to 1.19% Cu and 1.27% Zn (Colman & Cooper 2000). In the Midland Valley Terrane (equivalent to the Notre Dame Subzone) no peri-Laurentian arc-hosted VMS deposits have been recognized, except possibly the Charlestown Cu deposit of County Mayo (3Mt at 0.6% Cu; O'Connor & Poustie 1986). Although the Charlestown deposit was historically considered to be a porphyry Cu deposit, brecciation textures and alteration assemblages appear to be more consistent with a stockwork zone to a VMS deposit. Mineralization (pyrite-chalcopyrite-sphalerite-galena-barite) is confined to a central silicified zone, which is enveloped in turn by sericitic, sericitic/chloritic and chloritic zones (O'Connor & Poustie 1986).

The c. 480-464 Ma Tyrone Igneous Complex of Northern Ireland is a c. 350km^2 peri-Laurentian arc-ophiolite sequence accreted to the composite Laurentian margin during the Middle Ordovician (Cooper et al. 2012; Hollis et al. 2012). It represents an along strike continuation of the VMS rich Buchans-Robert's Arm arc sequence of Newfoundland (see Hollis et al. 2012) host to the high-grade Kuroko-type Buchans deposits (16.2 Mt mined between 1928 and 1984: 14.51% Zn, 7.56% Pb, 1.33% Cu, 126g/t Ag and 1.37g/t Au: Thurlow 1990), as well as lesser Cyprus-type mineralization (e.g. Skidder deposit 0.2Mt at 2% Cu, 2% Zn) and Noranda-type mineralization (e.g. Gullbridge 3 Mt at 1.1% Cu) (van Staal 2007; also see Piercey & Hinchey 2012).

7.3 Petrochemistry: VMS favourable associations

Understanding why some accreted arc terranes are barren of VMS deposits, whilst others are VMS rich has been the focus of detailed research for some time (Lesher et al. 1986; Lentz 1998; Wyman 2000; Hart et al. 2004). VMS deposits form within volcanic successions due to focused heat flow associated with hydrothermal

convection, which is the result of tectonic extension (i.e. rifting, subsidence), mantle depressurization, and the formation of high temperature mantle melts and crustal partial melts (e.g. Franklin et al. 2005; Galley et al. 2007a). Consequently there is a common association of bimodal volcanism in many VMS mining districts with deposits associated with felsic strata even in bimodal-mafic environments where these rocks make up a minor contribution of the volcanic succession. Petrochemistry of mafic and felsic rocks associated with VMS deposits allow genetic exploration models to be developed to identify VMS prospective areas in underexplored terranes (see Piercey 2007b; Fig. 7.2). Ultimately, petrochemical assemblages of mafic and felsic rocks should be sought that indicate an extensional tectonic setting and high-temperature heat flow (e.g. Campbell et al. 1981; Lesher et al. 1986; Kerrich & Wyman, 1996; Lentz 1998; Wyman 2000; Hart et al. 2004; Fig. 7.2).

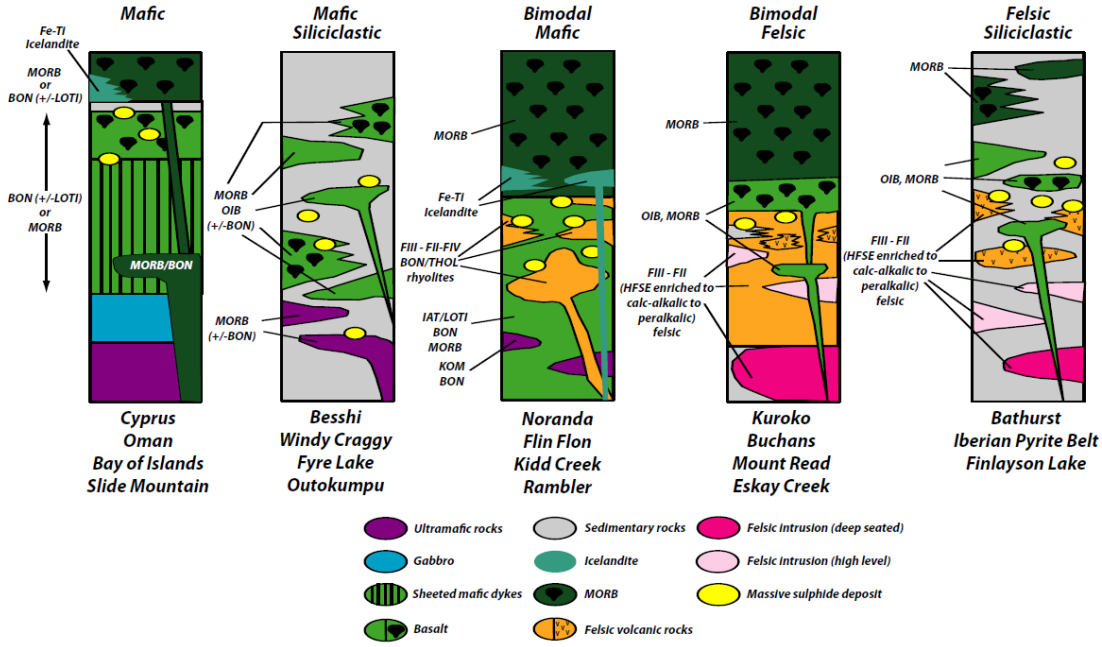

Figure 7.2. Petrochemical assemblage for different mineral-deposit environments which host VMS deposits (from Piercey 2007, 2010).

Systematic changes in the metal content of different VMS deposit types are associated with different host rocks, both of which are a direct function of tectonic setting (reviewed in Piercey 2007). Mafic and bimodal-mafic deposits are Cu-dominated due to higher heat-flow and Cu contents of host strata in oceanic crust and primitive arc sequences. Higher Pb, Zn, Ba, and Ag reflect an increasing proportion of felsic (and continentally derived) material in the host sequence (see Table 7.1). Additional elements may also be present in significant quantities due to the local footwall compositions. For example, the presence of immature sediments (i.e. black shale) has been postulated to account for the Se-rich Wolverine and KZK deposits of the Finlayson

Lake Camp (see Bradshaw et al. 2003). Ultramafic-mafic hosted deposits such as those in the Urals (e.g. Herrington et al. 2005) can contain significant Se, Co and Ni (Galley et al. 2007a). Magmatic contributions from devolatizing subvolcanic intrusions may account for anomalous levels of Se, Sn, In, Bi, Te, and possibly Au and Sb contents (references in Galley et al. 2007a).

Au grade is unrelated to base-metal content, with Au-rich deposits occupying specific stratigraphic positions in many camps reflecting a change in the geodynamic environment and magmatic evolution of local volcanic complexes (Mercier-Langevin et al. 2011). In many instances Au-rich deposits are associated with transitional to calc-alkaline intermediate to felsic volcanic rocks, which may represent a particularly fertile geodynamic setting and/or timing (Mercier-Langevin et al. 2011). Many Au-rich VMS deposits appear to be linked to changes from arc volcanism to arc rifting to backarc volcanism (e.g. Eskay Creek, British Columbia). A magmatic input may be required to explain the common association between these rocks (which often show advanced argillic, aluminous, strongly siliceous, or K-feldspar alteration) and high Au-Ag-As-Bi-Sb ± Bi-Hg-Te (Mercier-Langevin et al. 2011).

Geometric mean	Mafic	Mafic-siliciclastic	Bimodal-mafic	Bimodal-felsic	Felsic-siliciclastic
Cu (%)	1.82	1.23	1.24	1.04	0.62
Pb (%)	0.02	0.68	0.30	1.14	1.09
Zn (%)	0.84	1.58	2.32	4.36	2.70
Au (g/t)	1.40	0.75	0.81	1.06	0.59
Ag (g/t)	10.62	19.29	21.14	56.35	38.54
Total sulphide ore (t)	2,699,466	4,721,093	3,421,075	3,320,784	7,139,305
Total metal (t)	63,035	132,968	128,515	198,461	324,748
N	76	90	291	241	106

Table 7.1. Geometric means of metal contents of the main principle types of VMS deposits (from Franklin et al. 2005). Note: Hybrid bimodal-felsic VMS deposits not included.

7.3.1 Mafic geochemistry

It is well established that the composition of mafic rocks offers a useful discriminant towards identifying tectonic setting (e.g. Pearce & Cann 1973; Pearce & Norry 1979; Pearce 1983). Furthermore, it is well recognized that in many primitive arc terranes the location of VMS deposits corresponds with a shift from basalt of normal arc affinity (e.g. IAT, CAB) to that more typical of rift-related magmatism (see Franklin et al. 2005; Piercey 2010). Mafic magmas indicative of high temperature magmatism and/or

rifting in arc-successions include: boninite, komatiite, low-Ti island arc tholeiite (LOTI), backarc basin basalt (BABB), mid-ocean ridge basalt (n-type and eMORB), Fe-Ti enriched basalt (often referred to as 'icelandite' in VMS-related literature) and ocean-island basalt (OIB) (see Piercey 2010; Fig. 7.2, Table 7.2). Essentially, these magmas provide evidence for a sudden change in the geodynamic environment to one associated with rifting and high-temperature heat flow favourable for the formation of VMS deposits.

In juvenile mafic-dominated environments (i.e. mafic, bimodal-mafic, mafic-siliciclastic) VMS deposits are associated with boninite, LOTI, MORB and BABB, with magmas sourced from either the depleted arc mantle wedge (e.g. boninite, LOTI) or upwelling depleted, mid-ocean ridge or backarc asthenospheric mantle (e.g. MORB, BABB) (see Piercey 2010). By contrast, in evolved (e.g. bimodal-felsic and felsic-siliciclastic) environments mafic rocks associated with VMS deposits have alkalic signatures (e.g. OIB, alkali basalt) or are characterized by MORB and/or BABB, in the hangingwall of deposits (Piercey 2010). In some environments alkali basalt cross-cuts and overies the main VMS hosting horizon and shows a stratigraphic progression to MORB, reflecting a shift from rifting to true spreading (e.g. Rogers & van Staal 2004). In calc-alkaline dominated arc environments IAT may also be indicative of a change in the geodynamic environment towards rift related magmatism and/or backarc spreading.

VMS deposit type	Mafic	Felsic
Mafic	Boninite, low-Ti tholeiite, MORB	-
Mafic-siliciclastic	MORB, EMORB, alkalic, boninite (rare)	-
Bimodal-mafic	MORB, boninite, low-Ti tholeiite (calc-alkalic and island arc tholeiites present but rarer), icelandite	Archean – FIII rhyolites. Proterozoic-Phanerozoic - tholeiitic rhyolites, boninitic rhyolites (M-type)
Bimodal-felsic	MORB, OIB-alkalic, IAT	HFSE-enriched rhyolites (A-type), peralkaline and calc-alkalic rhyolites (rarer)
Felsic-siliciclastic	MORB, OIB-alkalic	HFSE-enriched rhyolites, peralkaline, and calc-alkalic rhyolites (rarer)

Table 7.2. Petrochemical assemblages of mafic and felsic rocks commonly associated with different VMS deposit types (modified after Piercey 2007b).

Fe-Ti enriched basalt ('icelandite') typically occurs as late intrusives and extrusive sequences in the hangingwall of many VMS deposits of bimodal-mafic systems. These basalts often lack an island-arc signature (nMORB or eMORB affinity: e.g. Leat et al. 1986) but may also be of IAT affinity (e.g. DeWolfe et al. 2009). Fe-Ti enriched basalt has been recognized in the hangingwall of the Triple 7 and Callinan deposits of the

Flin Flon mining district (DeWolfe et al. 2009), as well as at Kidd Creek (Wyman et al. 1999), Kam-Kotia (Barrie & Pattison 1999), Galapagos (Embly et al. 1988; Perfit et al. 1999), in the Buchans-Roberts Arm and Tally Pond belts of Newfoundland (Zagorevski 2008; Gerry Squires, personal communication 2012), the Bathurst Mining Camp (Rogers and van Staal 2004), and peri-Gondwanan affinity arc volcanics of the British and Irish Caledonides (e.g. Parys Mountain, Avoca: Leat et al. 1986; McConnell et al 1991).

7.3.2 Felsic geochemistry

Felsic volcanic suites have been used for some time to distinguish VMS-prospective from VMS-barren systems (e.g. Lesher et al. 1986; Barrie et al. 1993; Barrett and MacLean 1994; Lentz 1998; Hart 2004; Fig. 7.11 & 1.12, Table 7.2). Lesher et al. (1986) identified three types of rhyolite (FI to FIII), with FIII rhyolites (considered the most VMS prospective) characterized by low Zr/Y and La/Yb with flat and tholeiitic, chondrite-normalized REE patterns and high HFSE contents (Zr >200 ppm) (reviewed in Piercey 2010). FI rhyolites are typically calc-alkalic (high Zr/Y and La/Yb), with lower HFSE contents and LREE enriched chondrite-normalized REE profiles (Fig. 7.3 & 7.4). FII represents an intermediate stage between FI and FIII. Hart et al. (2004) proposed a fourth grouping (FIV), which characterizes juvenile arc terranes of the Archean, with extremely low La/Yb_{CN} ratios.

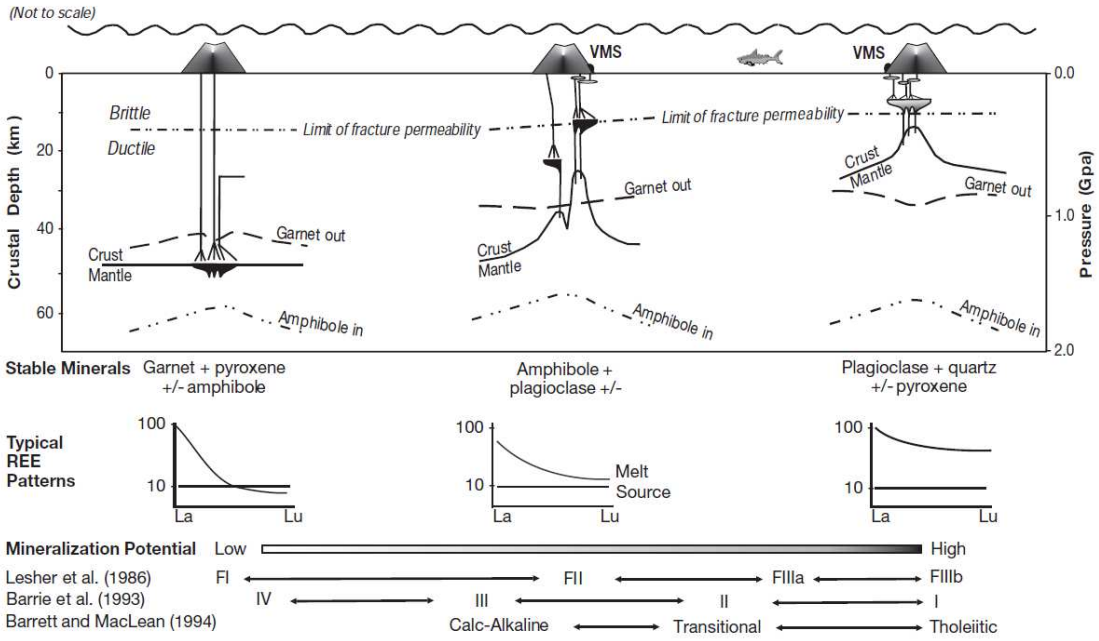

Figure 7.3. Conceptual petrogenetic model of Hart et al. (2004) for the formation of FII (left) to FIV (right) felsic volcanic rocks formed by partial melting at progressively shallower crustal depths. FII rhyolites were considered less VMS prospective in post-Archean primitive

environments due to higher-temperature heat flow and lower-pressures associated with shallower FIII and FIV felsic volcanics. FIII rhyolites were noted to host many of the larger tonnage and higher grade VMS deposits (e.g. Kidd Creek, Neves Corvo, United Verde, Eskay Creek).

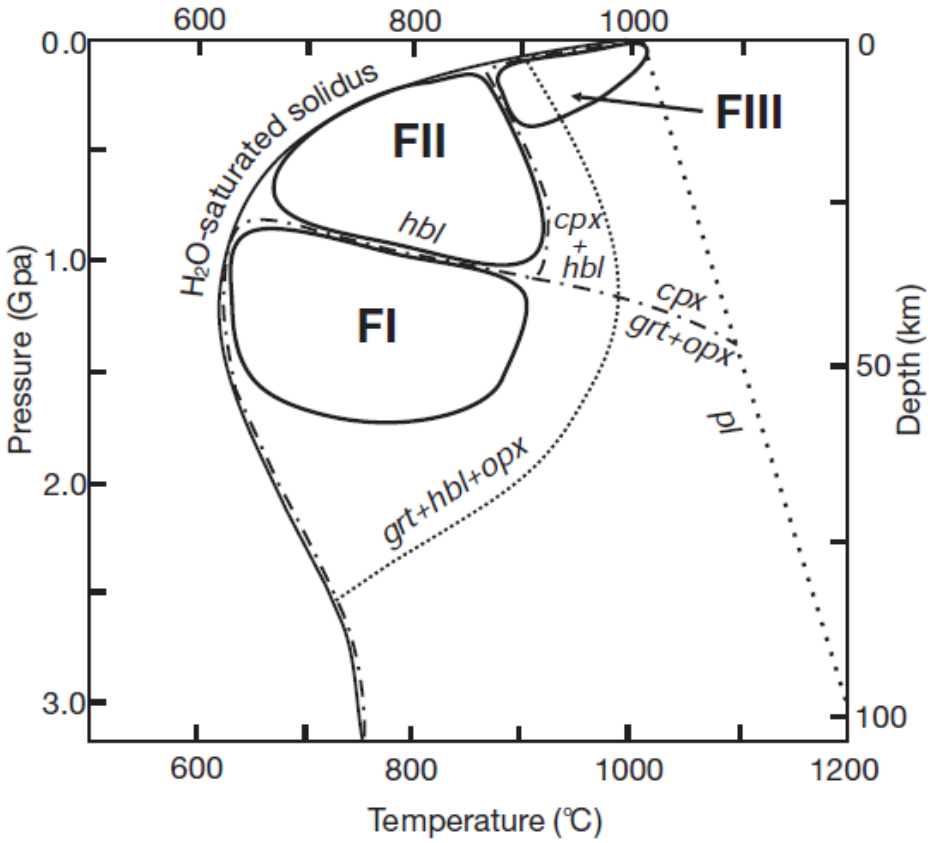

Figure 7.4. Approximate fields for FI, FII and FIII felsic volcanic rocks based on phase relationships from melting experiments using dry basalt, basalt-H_2O and amphibolite (from Hart et al. 2004). Stable minerals with high partition coefficients for HREE and HFSE are displayed with the abbreviations: cpx, clinopyroxene; gr, garnet; hbl, hornblende; opx, orthopyroxene.

In post-Archean, mafic-dominated juvenile settings, felsic rocks associated with VMS deposits have tholeiitic to boninite-like affinities. These tholeiitic rhyolites are characterized by low Zr/Y, flat REE profiles and primitive-mantle normalized patterns, with negative Nb anomalies, HFSE and REE (Zr <50-100 pm) depletion, and display M-type affinities on Nb-Y diagrams and FIV-type characteristics (Piercey 2010; Fig. 7. 5). 'Boninitic rhyolites' are similar but have U shaped REE profiles. They have been attributed to the melting of "mafic (to andesitic) substrates often associated with forearc rifting, intra-arc rifting, or rifting during the initiation of backarc basin activity" (Piercey 2010 p.10). Rhyolites which host the giant VMS deposits of the Urals (e.g. tholeiitic Karamalytash rhyolites) were demonstrated by Herrington et al. (2005) to plot

closer to the FIII field of Lesher et al. (1986) than those which host the smaller VMS deposits (predominantly FII type).

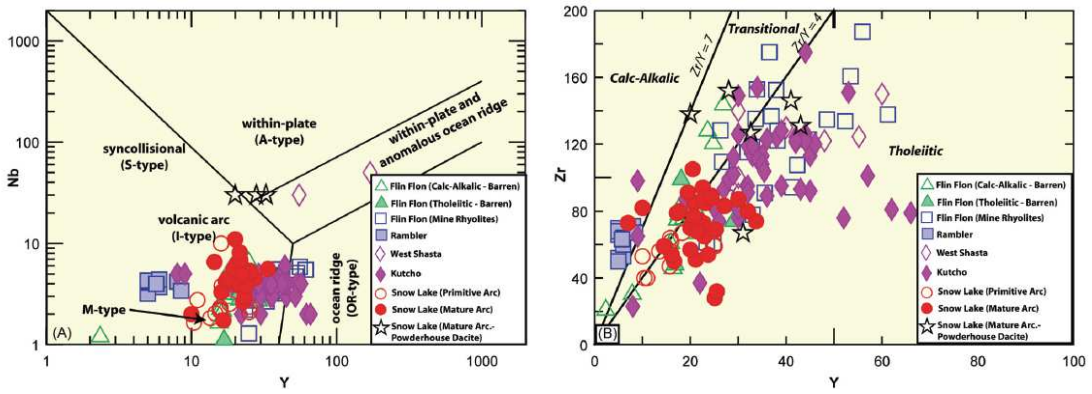

Figure 7.5. Discrimination diagrams for post-Archean rhyolites from juvenile arc environments. Those associated with VMS deposits are M-type and have tholeiitic affinities (from Piercey 2007b).

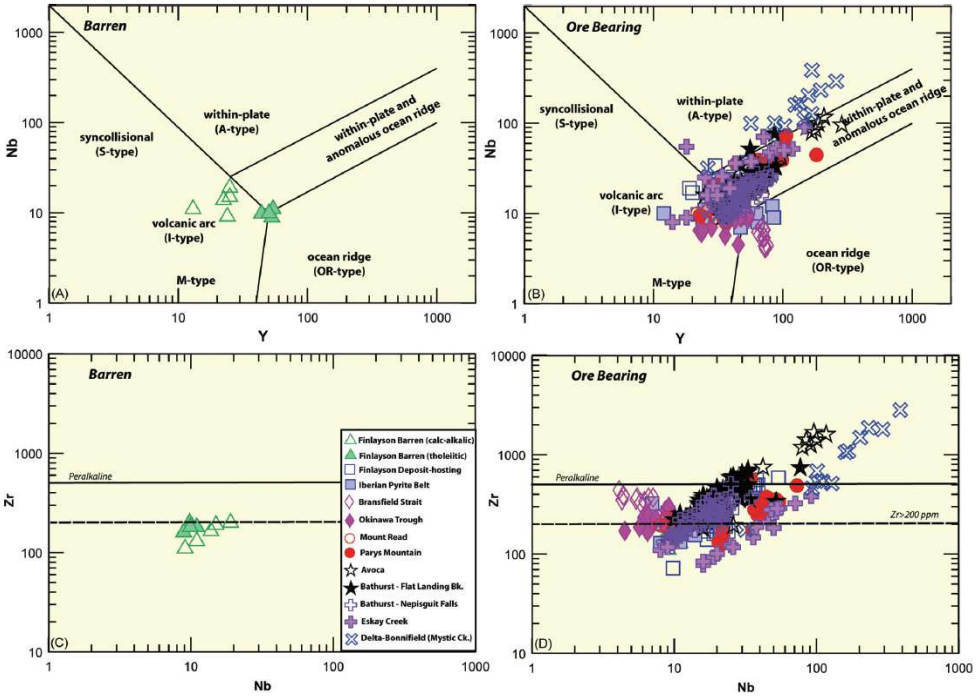

Figure 7.6. Tectonic distribution diagrams for rhyolites in post-Archean evolved arc settings. Those associated with VMS deposits have A-type, high Zr and peralkaline affinities (from Piercey 2007b).

In post-Archean evolved settings felsic rocks associated with VMS deposits are typically HFSE and REE enriched, have within-plate (A-type) characteristics, are calc-alkaline to peralkaline in composition, and dominantly FII-type (although some FIII, and lesser FI-types occur) (Piercey 2010; also see Shukuno et al. 2006; Fig. 7.6). Rhyolites associated with continental rifts or continental backarc rifting can display extreme

HFSE concentrations. High Zr rhyolites (Zr > 500 ppm) were recognized at Snowdonia and Avoca by Leat et al. (1986; also in McConnell et al. 1991). These HFSE-enriched, high-temperature (> 900 °C) and high-silica rhyolites have geochemical signatures consistent with low to moderate degrees of partial melting of crust in continental rifts, intracontinental rifts, and continental backarc rifts (Piercey 2007).

7.4 Petrochemistry of the Tyrone Igneous Complex: identifying VMS prospective horizons

The Tyrone Igneous Complex of Northern Ireland is broadly divisible into a structurally lower dismembered suprasubduction zone ophiolite (= c. 484-480 Ma Tyrone Plutonic Group), and an overlying, relatively complete (though poorly exposed) arc-related sequence (= c. 475-469 Ma Tyrone Volcanic Group) (Cooper et al. 2008, 2011; Hollis et al. 2012). Both were accreted to an outboard peri-Laurentian microcontinental block (=Tyrone Central Inlier, c. 600 Ma) at c. 470 Ma; and intruded by a suite of syn- to post-collisional arc plutons between c. 470 and 464 Ma. The petrochemical evolution of Tyrone Igneous Complex has only recently been documented (Draut et al. 2009; Cooper et al. 2011; Hollis et al. 2012; Chapters 5 & 6), on which this account is based. Previously unpublished information is also provided including new drillcore XRF geochemistry from across the upper Tyrone Volcanic Group. Methods are outlined in Chapter 2. Data is presented in the Appendix (7.2).

7.4.1 Tyrone Plutonic Group: a dismembered suprasubduction zone ophiolite

The c. 484-480 Ma Tyrone Plutonic Group is composed predominantly of layered and isotropic gabbros typical of the lower portions of suprasubduction zone oceanic crust. Scarce outcrops of sheeted dykes and pillow lavas are present, although these are laterally restricted due to widespread faulting within the ophiolite (see Chapter 5). All lithologies are characterized by primitive island arc tholeiite, which is LREE and HFSE depleted relative to the HREE (Draut et al. 2009; Cooper et al. 2011). Nd-isotope constraints and inherited zircons in dated layered gabbros are consistent with a minor crustal component (see Draut et al. 2009; Cooper et al. 2011; Chapter 5). The lack of a significant portion of the upper oceanic crust suggests large areas of the Tyrone Plutonic Group are not favourable for VMS mineralization, which is typically associated with lava and sheeted dyke sequences in ophiolitic successions. Areas where extensive exposures of the sheeted dyke complex crop out (e.g. Carrickmore) are the most favourable, although areas where pillow lavas have been reported (e.g. Oritor, Craigballyharky: Hartley 1933) should also be targeted. Soil survey results reveal large Cu-Pb-Zn anomalies near Carrickmore (660, 930 & 260 ppm respectively) associated

with localized occurrences of Cu mineralization. As the Tyrone Plutonic Group lacks a significant upper crustal section and is poorly preserved, it's potential to host significant mineralization is not discussed further. No VMS deposits are known in the correlative c. 480 Ma Annieopsquotch Ophiolite Belt of Newfoundland (Rogers et al. 2007).

7.4.2 Lower Tyrone Volcanic Group: a bimodal-mafic oceanic arc

The lower Tyrone Volcanic Group, exposed south of the Beaghmore Fault, is a bimodal-mafic assemblage divided into three formations: the Creggan, Loughmacrory and Beaghmore formations. No U-Pb zircon geochronology exists for the lower Tyrone Volcanic Group; its age is constrained by petrochemical correlations to the adjacent c. 475-474 Ma Slieve Gallion Inlier which represents an isolated package of the Tyrone Volcanic Group with its own stratigraphy (Chapter 6). Although the Creggan Formation is known to be stratigraphically younger than the Loughmacrory Formation, their relationship with the Beaghmore Formation (exposed E of the Dungate Fault) is unknown. The Beaghmore Formation has petrochemical assemblages consistent with intra-arc rifting and the formation of a young backarc basin. Due to the presence of evolved volcaniclastic rocks in the Beaghmore Formation and the geochemistry of associated Fe-Ti basalts ('icelandite'), it was placed stratigraphically above the Loughmacrory Formation by Hollis et al. (2012), although it may be coeval (see below).

The Creggan Formation is a flow-dominated lithofacies characterized by Fe-Ti enriched, pillowed (with lesser massive and sheet-flow) rift-related Fe-Ti eMORB associated with interpillow breccias (basaltic agglomerate), and rare volcaniclastic crystal tuff and layered chert (Fig. 7.7a-b). This sequence is in turn overlain by more massive calc-alkaline affinity basalt (with minor pillowed flows) associated with basaltic agglomerate near the top of the formation (Fig. 7.7c). Minor fragments of ironstones in some agglomerates suggest these areas experienced hydrothermal activity at this time. Synvolcanogenic intrusives of calc-alkaline affinity occur as small dykes of basalt, dolerite and diorite.

The overlying Loughmacrory Formation is a diverse assemblage predominantly composed of calc-alkaline volcaniclastic rocks with thick accumulations of mafic flows of both calc-alkaline and Fe-Ti eMORB affinity at several stratigraphic horizons (Fig. 7.7d-e). These units are typically interlayered with porphyritic andesites, with lesser layered chert and argillaceous sedimentary rocks representing episodes of volcanic quiescence. Areas associated with rift-related Fe-Ti eMORB such as Tanderagee, Loughmacrory, Merchantstown Glebe and S of Creggan, are also characterized by laterally extensive ironstones that display geochemical signatures suggesting some are

vent proximal (Appendix 7). The close association between Fe-Ti eMORB flows, ironstones, synvolcanogenic intrusions (e.g. Fe-Ti enriched gabbros of eMORB affinity at Tanderagee and Mweenascallgh; Fig. 7.7d) and possible synvolcanogenic faults (associated with large changes in the thickness of volcaniclastic rocks, and sudden lithology changes) suggests these areas experienced significant rifting, magmatism and hydrothermal alteration. Consequently, these areas of the Tanderagee Member (and lower Merchantstown Glebe Member) appear to be favourable for VMS mineralization. As felsic flows and domes are rare in the Loughmacrory Formation any potential deposits may be replacive and associated with felsic volcaniclastic strata or FII affinity silicified rhyolitic agglomerates (petrochemically unfavourable).

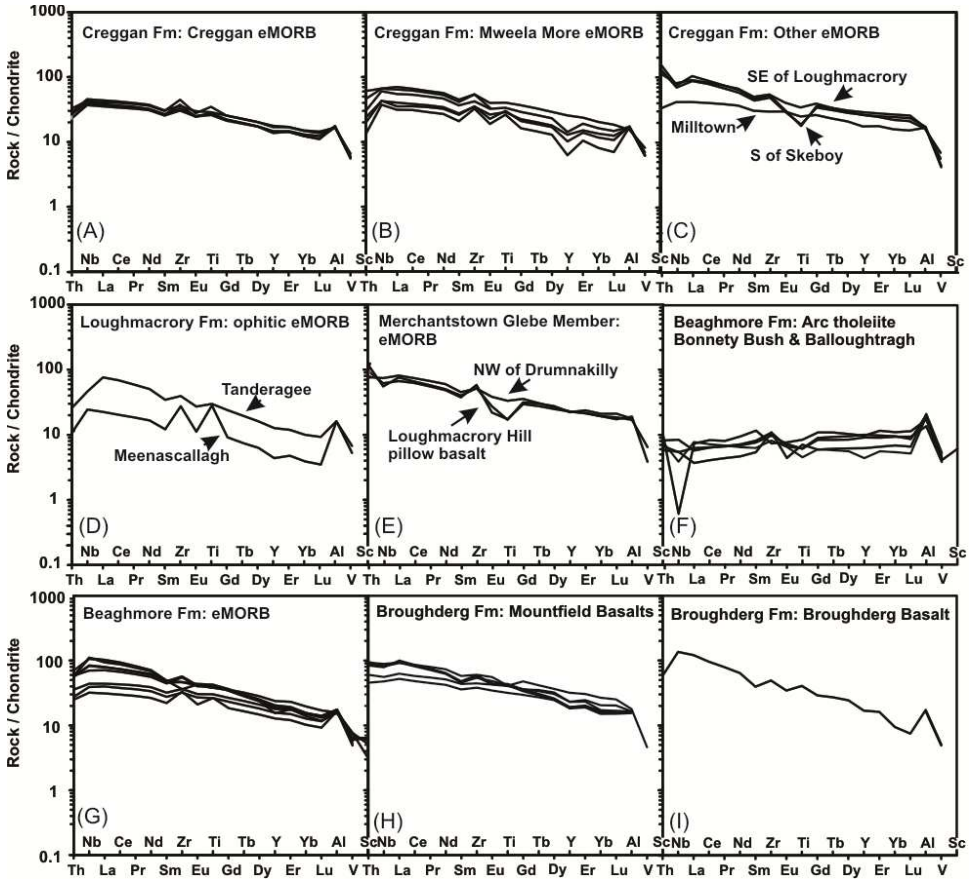

Figure 7.7. Rift-related mafic lavas of the Tyrone Volcanic Group after Hollis et al. (2012). Chondrite normalization values after McDonough and Sun (1995).

In the upper Beaghbeg Member (lower Beaghmore Formation) there is a close association between tholeiitic to boninitic rhyolite agglomerates (Figs. 7.8 & 7.9a), Fe-Ti eMORB affinity lavas (Fig. 7.7g), iron formations (Appendix) and synvolcanogenic intrusions of gabbro (of unknown affinity) between Beaghbeg and Evishessan Bridge. Normal arc magmatism is characterized by LILE and LREE enriched volcaniclastic rocks

and rare calc alkaline basalt, best preserved in the southernmost deposits of the formation (around Teebane and Dungate). Tholeiitic to boninitic rhyolitic agglomerates display M-type and FIV affinities and are characterized by low Zr and Zr/Y. These M-Type and FIV affinity rhyolites are preferentially associated with VMS deposits in post-Archean, bimodal-mafic juvenile settings (Fig. 7.5). The Beaghbeg agglomerates are consistent with rhyolitic debris flows developed off the flanks of high-temperature rhyolite domes. The eruption of these high-temperature lavas was coeval with the eruption of Fe-Ti eMORB on the paleoseafloor, most likely associated with the onset of backarc basin formation (intra-arc rifting) in the bimodal-mafic succession (e.g. Piercey 2007).

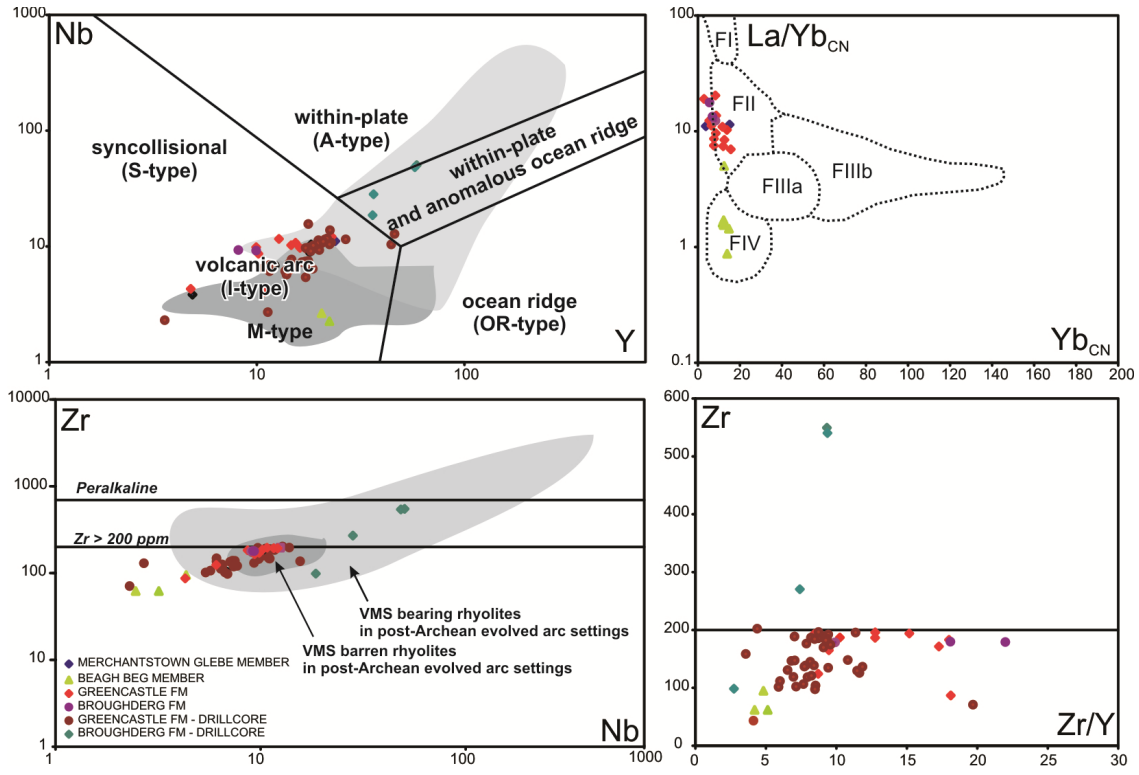

Figure 7.8. Petrochemical affinity of felsic volcanic rocks from the Tyrone Volcanic Group. Those of the Beaghmore Formation are associated with M-type and FIV affinities and low Zr/Y ratios. By contrast, rhyolite flows of the Greencastle Formation are calc-alkaline, I-type and FII type with high (and variable) Zr/Y ratios. Felsic rocks from Broughderg are A-type and borderline peralkaline associated with higher Zr contents. Data from Hollis et al. (2012) and drillcore analyses herein (Appedix 7.2).

Large stratigraphic changes associated with the NW-SE orientated Dungate, Evishessan, Brackagh and nearby faults may suggest these were originally large synvolcanogenic normal faults associated with a backarc basin and/or any potential caldera related structures, and were subsequently reactivated. Features useful in identifying

synvolcanogenic faults include (after Franklin et al. 2005): (i) debris flows, particularly those that thicken or terminate over a short lateral distances; (ii) synvolcanogenic dyke/sill swarms, particularly those that terminate in either cryptodomes or at intra-volcanic sedimentary horizons; (iii) the location of felsic flows, domes and cryptodomes; (iv) transgressive alteration zones, commonly silicified, intense phyllic alteration, vein and disseminated sulphides; (v) preferential alignment of volcanic vents; (vi) local discontinuities in the stratigraphy where footwall, but not hangingwall strata may be displaced; and (vii) diachronous wedges of talus. The first three are recognized around Beaghbeg, as well as silicification and/or patchy sericitic alteration in some tuffs/flows, and elevated base metal contents in showings. A synvolcanogenic intrusion of gabbro near Beaghbeg terminates at the Dungate fault and may have been sourced at depth along this structure or is simply cut by it. Other highly magnetic mafic flows revealed from regional geophysics (Hollis et al. 2012) which are not exposed show a similar relationship to the Dungate and nearby Evishessan faults. U-Pb zircon geochronology is in progress to constrain the relative ages of units across the Dungate and Brackagh faults.

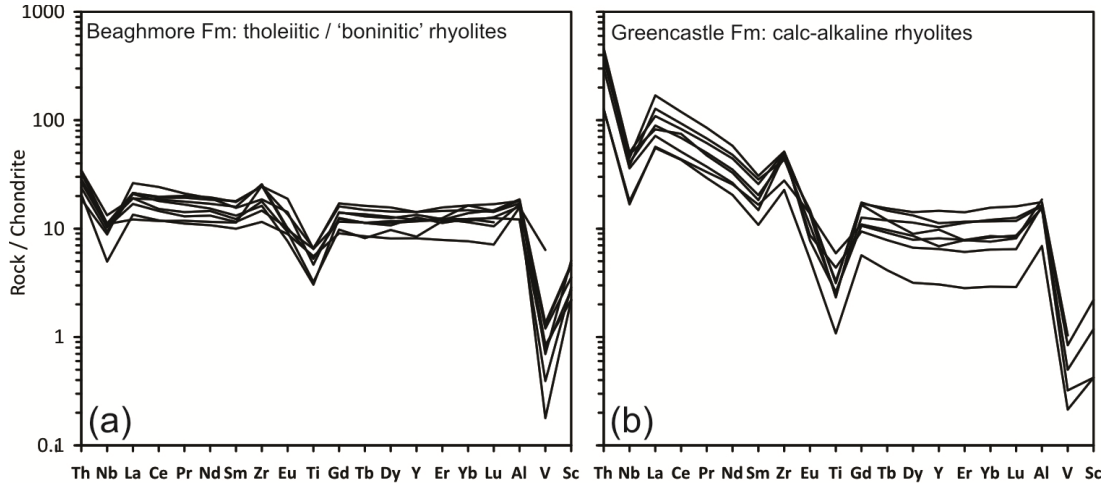

Figure 7.9. Chondrite normalized multi-element profiles for felsic volcanic rocks of the Beaghmore and Greencastle formations. (a) M- and FIV-type tholeiitic felsic rocks of the Beaghmore Formation characterized by flat and U-shaped REE profiles. (b) I- and FII-type, calc-alkaline and LREE-enriched felsic rocks of the Greencastle Formation characterized by steep REE profiles and LILE enrichment. Chondrite normalization values after McDonough and Sun (1995).

In the uppermost Beaghmore Formation (upper Bonnety Bush Member), there is a similar close association of eMORB (Fig. 7.7g), laterally extensive ironstones, hydrothermally altered volcaniclastic rocks, M-type and FIV affinity felsic volcanic rocks with flat to U-shaped REE profiles (e.g. Cooper et al. 2011) and LREE-depleted island arc tholeiite (Fig. 7.7f-g). The latter appears to reflect the eruption of primitive basalt in a newly formed backarc basin. Both the Beaghbeg and Bonnety Bush areas and their

along strike equivalents are considered highly prospective for Cu-Zn Noranda-type VMS mineralization. At Bonnety Bush, island arc tholeiites are characterized by intense silica-epidote alteration and variable LREE-mobility (Fig. 7.7) characteristic of extensive hydrothermal circulation.

7.4.3 Upper Tyrone Volcanic Group: a bimodal-felsic syncollisional arc

The upper Tyrone Volcanic Group (c. 473-469 Ma), exposed north of the Beaghmore Fault, comprises two formations (Greencastle and Broughderg) and is a bimodal-felsic succession. This volcanic-dominated sequence is composed predominantly of calc-alkaline volcaniclastic rocks, with syndepositional rhyolite flows, domes and associated deposits (autobreccias) (lower Greencastle Formation), overlain by a diverse succession which includes: thick accumulations of crystal and lithic tuff, lesser arkosic sandstone, porphyritic andesite, OIB-like basalt (Mountfield Basalts), alkali basalt (Broughderg Basalts), graphitic pelite, layered chert, ironstone, and thin rhyolite flows and sills (upper Greencastle and Broughderg formations).

Basalts in the upper Tyrone Volcanic Group are confined to the Broughderg Formation and are borderline-alkalic to alkalic in composition, typical of mafic rocks associated with VMS deposits in post-Archean evolved arc settings (e.g. Piercey 2007). Those exposed around Mountfield are more OIB-like (e.g. higher LILE and REE enrichment) than those of the lower Tyrone Volcanic Group, and are similarly Fe-Ti enriched (Fig. 7.7h). Basalt analysed from Broughderg is alkalic and displays strong Fe-Ti, LILE and LREE enrichement, a +ve Nb anomaly and steep REE profile (Fig. 7.7i). All of these lavas are indicative of rift related magmatism following arc-continent collision (c. 470 Ma: Greencastle Formation; see Hollis et al. 2012).

Felsic flows and intrusive rocks of the upper Tyrone Volcanic Group can be divided into two groups: (i) I-type and FII-type, strongly LILE and LREE enriched calc-alkaline rhyolites with strongly -ve εNd_t values and Zr contents < 200ppm typical of the Greencastle Formation, as recognized in Hollis et al. (2012) (Figs. 7.8 & 7.9b); and (ii) within-plate, A-type rhyolites with higher Zr (to 550 ppm), Nb (to 50 ppm) and Y (to 59 ppm) and high La_{CN} values (to ~200), recognized from XRF analysis of historic drillcore from the lower Broughderg Formation (Fig. 7.8). Rhyolites at Crosh are of unknown affinity but are along strike equivalents of the Broughderg rhyolites. FII-type (e.g. Cashel Rock) and A-type (e.g. Broughderg) rhyolites were considered the most VMS prospective types in evolved post-Archean settings by Piercey (2007), which contain alkalic or MORB affinity mafic rocks in their hangingwall successions (Figs. 7.2 & 7.6). Consequently, stratigraphic horizons associated with rhyolite domes and flows (and autobreccias) in the upper Tyrone Volcanic Group which contain alkalic mafic rocks in

their hangingwall sequences are considered the most prospective in this bimodal-felsic sequence. These include the: (i) FII-type and calc-alkaline Formil, Cashel Rock and Racolpa rhyolite domes and flows (and autobreccias), and any unexposed along strike equivalents in the Murrins area; (ii) sheared Cashel Burn, and Tullybrick felsic units of the uppermost Greencastle Formation, and their along strike volcaniclastic equivalents around Greencastle, Crouck and Aghascrebagh; and (iii) felsic lithologies of the Broughderg Formation (e.g. A-type rhyolites at Broughderg, and Crosh rhyolites) and their along strike equivalents (e.g. Cashel Bridge). All of these areas are characterized by extensive hydrothermal alteration, base-metal and Au mineralization (see below), and / or occur in close proximity to synvolcanogenic intrusions.

7.5 Synvolcanogenic intrusions of the upper Tyrone Volcanic Group

In effusive, flow-dominated environments exploration for VMS deposits should be focused up to 3 km upsection in the coeval volcanic rocks in the hangingwall of large subvolcanic intrusions, as these bodies have been suggested to provide the necessary heat to drive long-lived hydrothermal circulation (Galley et al. 2007a). Intrusions of tonalite ± diorite are spatially associated with c. 473-469 Ma rhyolite domes and flows of the Greencastle Formation and lower Broughderg Formation, occurring in close proximity to VMS-prospective assemblages at Racolpa, Cashel Rock, Formil, Crouck, Aghascrebagh, Broughderg (drillcore) and Tullybrick (drillcore). Similar deformational histories to their host strata, a lack of contact metamorphic aureoles, field relations and U-Pb zircon geochronology (Cooper et al. 2011; Hollis et al. 2012) indicate these intrusives were high-level, composite and synvolcanogenic.

Synvolcanogenic suites of gabbro-diorite-tonalite-trondhjemite have been recognized from a number of VMS mining camps worldwide, occurring in close proximity to VMS deposits in arc environments (e.g. Archaean Panorama, Noranda, Sturgeon Lake, Snow Lake, Skellefte, Mount Read: references in Franklin et al. 2005). Galley (2003) noted that diorite-tonalite-trondhjemite composite intrusions are associated with 80 % of Precambrian VMS camps. This association is typical of either nascent arc or primitive arc rifts, where these intrusions are emplaced into thin crust at high levels (2-3 km of the sea floor), due to crustal thinning, mantle decompression, basaltic underplating and resultant crustal melting (Galley 2003). In primitive arc successions, composite synvolcanogenic intrusions commonly have a tholeiitic character (and are associated with Cu-(Au) or Cu(Zn) VMS deposits). By contrast, the rifting of thicker arc crust in more evolved successions results in partial melting at higher levels and calc-alkalic

composite intrusions (Galley 2003), typical of those in the upper Tyrone Volcanic Group.

Late intrusions of quartz ± feldspar porphyritic dacite cut all levels of the upper Tyrone Volcanic Group (c. 464 Ma), occurring in close proximity to VMS-prospective mineralized assemblages at Cashel Rock, Cashel Bridge, Formil, Racolpa and Tullybrick (drillcore). Although these intrusions of quartz ± feldspar porphry are too young and would have contained too little heat to have driven high temperature hydrothermal convection, they are likely to have exploited the same deep seated crustal pathways which focused hydrothermal alteration. They are therefore still indicative of the 'thermal corridor' in the camp, along with the presence of synvolcanogenic intrusions of gabbro, tonalite and diorite (e.g. Galley 2003).

7.6 Preservation potential

Three principle mechanisms are favourable for the preservation of VMS deposits on the seafloor:

(I) Anoxic seawater will not only provide an unlimited supply of reduced sulphur to fix metals during the formation of VMS deposits, but will present sulphide oxidation. Most of the giant Phanerozoic VMS deposits (e.g. Bathurst Mining Camp, Iberian Pyrite Belt, Mount Read Belt) and SEDEX deposits (e.g. Red Dog, Howards Pass, Anvil District) formed during periods of global anoxia in the Late Cambrian, Middle Ordovician, Late Ordovician-Early Silurian, and Late Devonian-Early Mississippian (Goodfellow 2007). A clear exception to this is in the Urals (Herrington et al. 2005).

(ii) Formation of VMS deposits in siliciclastic environments as replacive orebodies will immediately protect sulphides from any potential oxygenated bottom waters (e.g. Duck Pond). Large VMS deposits such as Bathurst are typically associated with siliciclastic/volcaniclastic units of high initial porosity.

(iii) Rapid burial will similarly provide protection from erosion or oxygenated waters. However, typically a period of volcanic quiescence is required to form large orebodies in effusive settings or large hydrothermal systems.

In the lower Tyrone Volcanic Group, VMS prospective horizons identified include areas of the Tanderagee Member and lower Merchantstown Glebe Member of the Loughmacrory Formation; and the upper Beaghbeg and uppermost Bonnety Bush Members of the Beaghmore Formation (e.g. Fig. 7.14). All of these successions contain units indicative of volcanic quiescence (e.g. ironstones, layered chert, siltstone) closely

associated with rift-related mafic lavas. VMS prospective assemblages (such as those already described) should be targeted stratigraphically below these units.

In the upper Tyrone Volcanic Group, a similar situation occurs where VMS prospective stratigraphic horizons contain strata indicative of volcanic quiescence immediately in their hangingwall sequences. In the Greencastle Formation, a small body of poorly exposed arkosic sandstone which contains elevated base-metal and Ba concentrations directly overlies the Cashel Rock rhyolite along part of its length. A similar unit overlies the c. 473 Ma correlative VMS-hosting rhyolites of Buchans, central Newfoundland (Thurlow 2010). The base of the Broughderg Formation was placed by Hollis et al. (2012) at the first occurrence of chert, argillaceous sedimentary rocks or basalt north of the Beaghmore Fault. This regionally extensive episode of volcanic quiescence is characterized by thin horizons of layered chert to the SW of the Dungate Fault (e.g. Carnaransy Burn, Mountfield) and thick accumulations of graphitic pelite and layered chert to the NE (e.g. between Broughderg and Tullybrick and around Crosh). A >70m thick sequence of pyrite-bearing graphitic pelite at Broughderg suggests (at least locally) parts of the Tyrone arc were anoxic at this time. At Crosh (SW corner of Broughderg Formation), Au-bearing silicified rhyolites are similarly associated with ironstone (hematite-quartz, replacive) and contain thick accumulations of graphitic pelite in their hangingwall sequences. Thin horizons of layered chert also occur at Crosh and above VMS prospective felsic units of the upper Greencastle Formation (e.g Cashel Burn, Tullybrick, Aghascrebagh, Crouck).

7.7 Element mobility in the upper Tyrone Volcanic Group

As detailed in Piercey (2007; also see Appendix), characterising hydrothermal alteration within a VMS prospective terrane is a useful tool for both distinguishing between zones of regional semiconformable alteration, regional metamorphism, and pipe-like footwall alteration; and for vectoring towards VMS mineralization. Due to the extensive hydrothermal alteration and metamorphism across the Tyrone Volcanic Group, a number of elements, such as Si, Na, K, Ca, Mg and Fe, and the low-field strength elements (LFSE: Cs, Rb, Ba, Sr, U), may have been mobile since the rocks formed (e.g. MacLean 1990). Furthermore, the absolute concentrations of immobile elements may have been affected by mass change. Element mobility was checked for each of the petrochemical suites identified in the Tyrone Volcanic Group (after Hollis et al. 2012), against Zr, TiO_2 and a range of other elements/ratios often considered immobile in greenschist facies terranes (e.g. Al, Cr, Y, La, Zr/TiO_2). Little element mobility occurs in the lower Tyrone Volcanic Group, except in areas associated with petrochemically favourable successions (e.g. Merchantstown Glebe, Beaghbeg, etc.).

Consequently, this section focuses on the extensive hydrothermal alteration across the upper Tyrone Volcanic Group. Further detail on element mobility and hydrothermal alteration across the lower Tyrone Volcanic Group is presented in the Appendix.

7.7.1 Element mobility in the upper Tyrone Volcanic Group

The upper Tyrone Volcanic Group is characterized by subgreenschist to greenschist facies metamorphism, and various types and intensities of hydrothermal alteration. Chlorite-grade greenschist facies metamorphism is restricted to ~2km from the Omagh Thrust. Prehnite is common further south around NE Formil. Both regionally extensive, weak hydrothermal alteration and more intense, laterally-restricted, pipe-like 'footwall' alteration occur. The latter is restricted to petrochemically favourable horizons identified in section 7.4. (e.g. around Cashel Rock, Formil, Aghascrebagh-Crouck, Cashel Burn, Tullybrick, etc.). Primary rock textures have largely been obliterated as seen in both outcrop (Fig. 7.10) and drillcore (Fig. 7.11). Rare plagioclase and/or alkali feldspar phenocrysts are preserved in some samples characterized by weaker regional hydrothermal alteration along non-petrochemically favourable horizons (e.g. around Mountfield, see SPH139, SPH457: Fig. 7.10) and areas more distil to mineralization (e.g. NE Formil: 106-211-6: Fig. 7.11). Quartz phenocrysts typically show pressure shadows associated with the overthrusting of the Dalradian Supergroup along the Omagh Thrust (e.g. SPH444), with groundmass minerals often segregated into compositionally distinct bands of quartz-albite, chlorite and sericite (e.g. SPH187: Fig 7.10). Individial lithostratigraphic units can show a wide variety of alteration types and intensities (e.g. Cashel Rock and Formil rhyolites: Figs. 7.10 & 7.11). At Cashel Rock and Formil several distinct types of hydrothermal alteration occur (e.g. silicified, chlorite-sericite(pyrite), advanced argillic, sericitic) which change with distance from mineralized showings. Further from mineralization, these areas are characterized by weak chloritization and/or sericitization best seen NE of Formil and at NE of Cashel Rock. Most rocks associated with mineralization are either strongly silicified, strongly sericitized and/or strongly chloritized, with or without carbonate-alteration (e.g. DDH 106-200).

Element mobility diagrams demonstrate that despite the hydrothermal alteration and metamorphism across the upper Tyrone Volcanic Group a number of elements have remained largely immobile (Fig. 7.12 & 7.13). Most of these elements (e.g. Al, Fe, V, Sc, Co, Ni, Y, Nb) retain trends of differentiation in the rocks analysed against Zr/TiO_2, with hydrothermal alteration associated with variable Si, Mg, Fe, Na, K and Ca, low Sr, and high Ba, Ba/Sr, AI, CCPI and LOI. Variations in immobile element concentrations away from these trends at a given Zr/TiO_2 ratio are associated with large mass gains and losses in the most hydrothermally altered and/or mineralized samples. Extreme

depletion of Al, V, Th and Y in the Cashel Rock rhyolites (e.g. SPH7: Fig. 7.12 & 7.13) is often due to large gains in SiO_2 and Fe_2O_{3T} (=silicification and mineralization). By contrast, other samples of rhyolite from Cashel Rock (e.g. 106-223-7), are strongly enriched in MgO (to 14.89 wt%), CaO (11.19 wt%) and contain low SiO_2 (31.74 wt%). Higher Th and Nb, and high Cu+Pb+Zn (2384 ppm) suggest this sample was extensively chloritized and mineralized but also strongly leached of Si (=mass loss, resulting in Nb and Th gains).

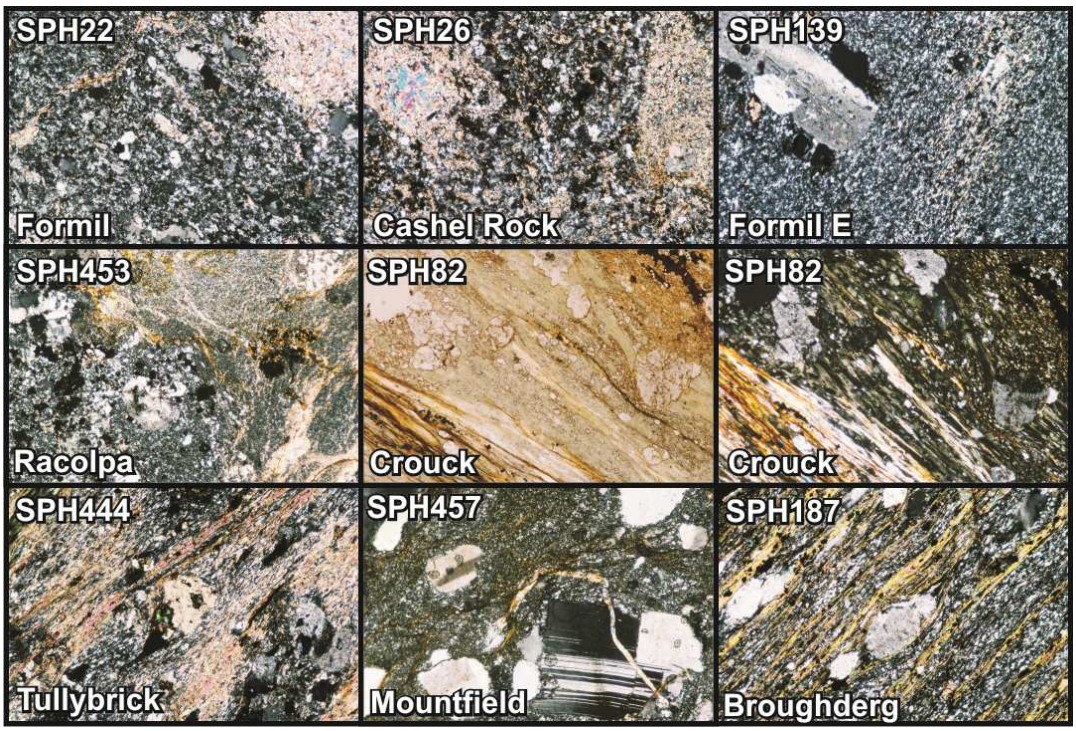

Figure 7.10. Representative thin section photographs from the upper Tyrone Volcanic Group. Field of view is approximately 3mm.

In general, mineralized samples (e.g. Cashel Rock rhyolites, Formil rhyolites, DDH-106-200) are characterized by higher Fe_2O_3 (=sulphides, chlorite), MgO (=chloritization), SiO_2 (=silicification), Cu+Pb+Zn (=sulphides), variable CaO (=carbonate and/or epidote), low Al_2O_3 (=dilution from mass gain), and significant Na_2O and Sr depletion (=sericitization) at a given Zr/TiO_2 ratio. For example, samples of rhyolite from Cashel Rock have Na_2O contents between 0.40 and 5.43 wt%, and MgO contents between 0.11 and 14.89 wt%. Unpublished drilling results from Cashel Rock (11-CR-01) show a systematic decrease in Na_2O (to values ~0.03 wt%) with proximity to mineralization (with increasing AI to 93.2). Hydrothermally altered rhyolites in close proximity to mineralization are also characterized by high Cr, Co, Sb, Bi, Ni, Ba/Sr (Fig. 7.14), used elsewhere to vector towards mineralization (e.g. Flin Flon; Gale 2003). High Cr (to 775 ppm = 106-209-1) is clear in hand specimen by the presence of apple-green Cr-mica

(fuchsite) at Cashel Bridge, Cashel Burn, Cashel Bridge, Tullybrick, Broughderg (drillcore), Crosh, and Racolpa.

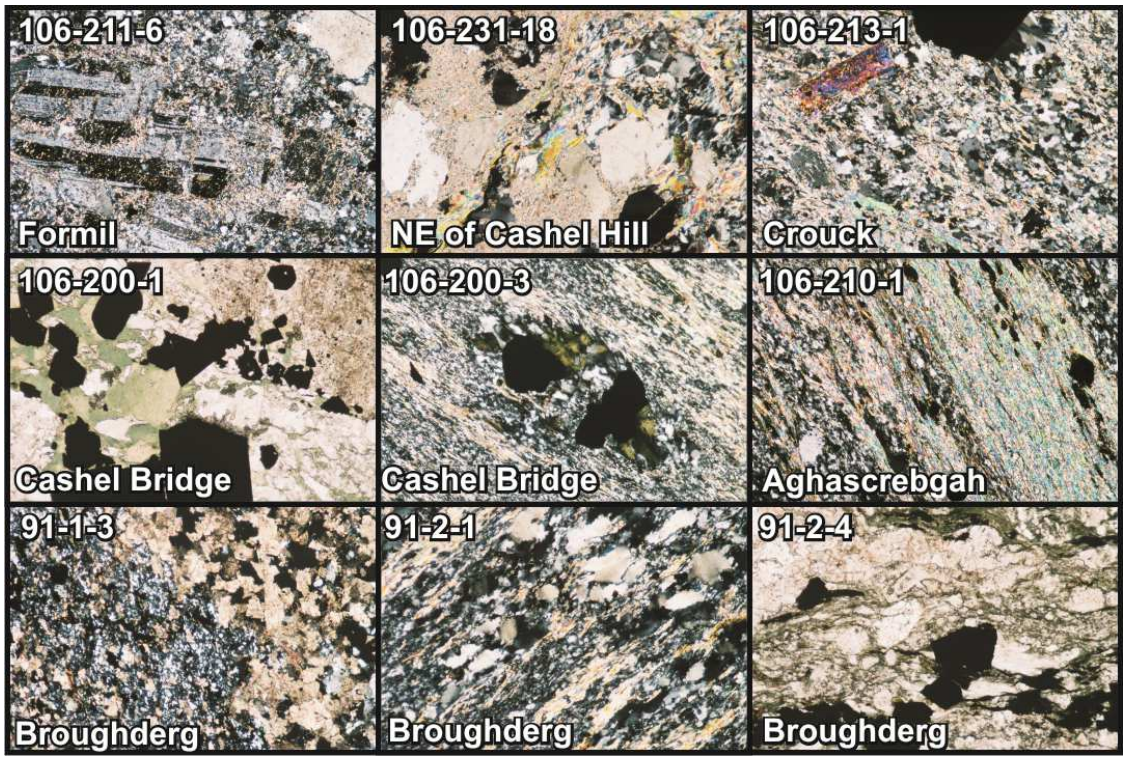

Figure 7.11. Representative thin section photographs from drillcore of the upper Tyrone Volcanic Group. Hydrothermal alteration is intense with most original rock textures replaced by sericite, chlorite, opaque oxides, epidote and albite. Field of view is approximately 3mm.

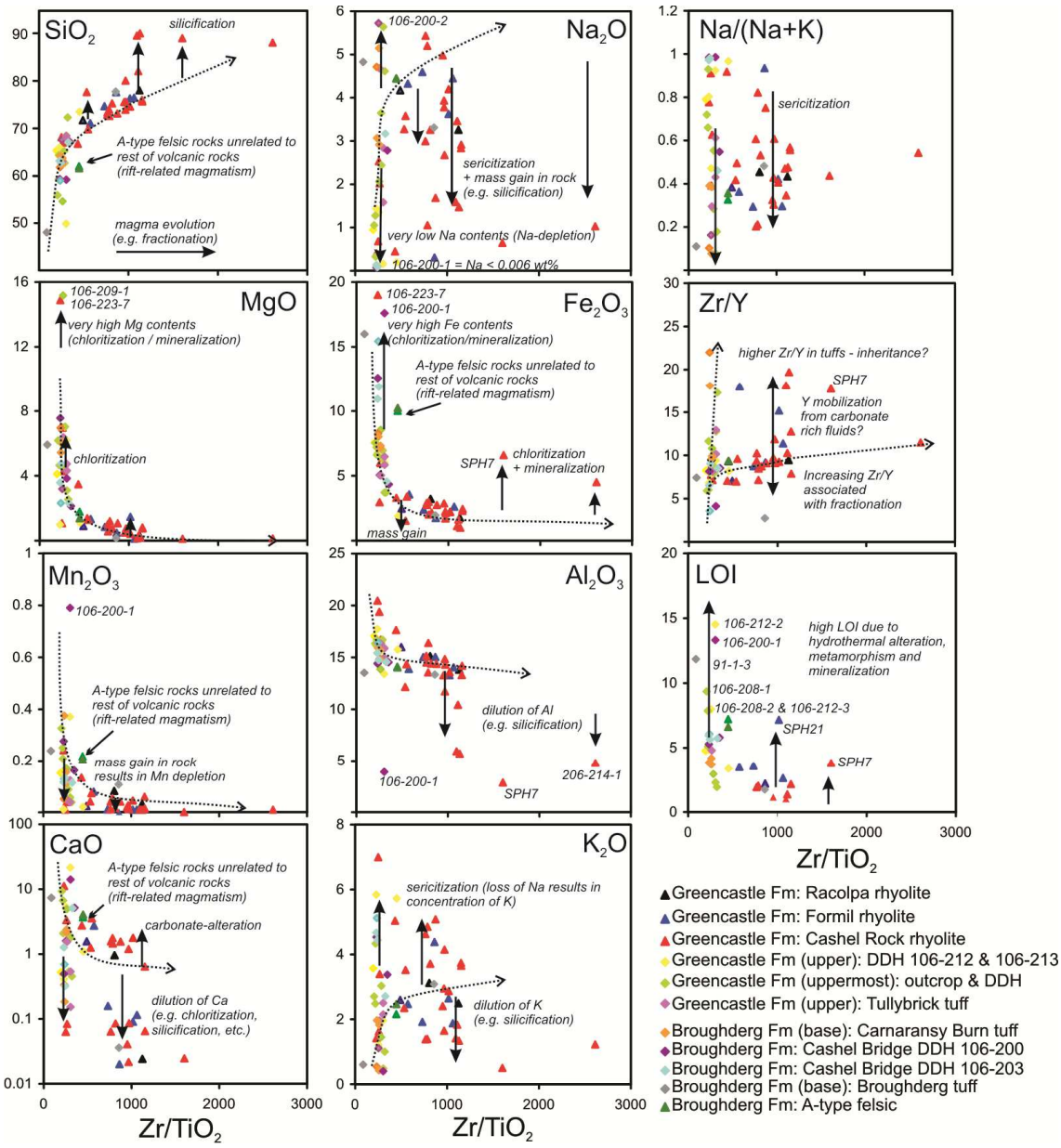

Figure 7.12. Element mobility diagrams for rocks from the upper Tyrone Volcanic Group (not including Fe-Ti enriched lavas). Dashed arrows indicate possible primary differentiation trends. Solid arrows indicate variations likely to be associated with element mobility (e.g. chloritization, sericitization, mass gain, mass loss).

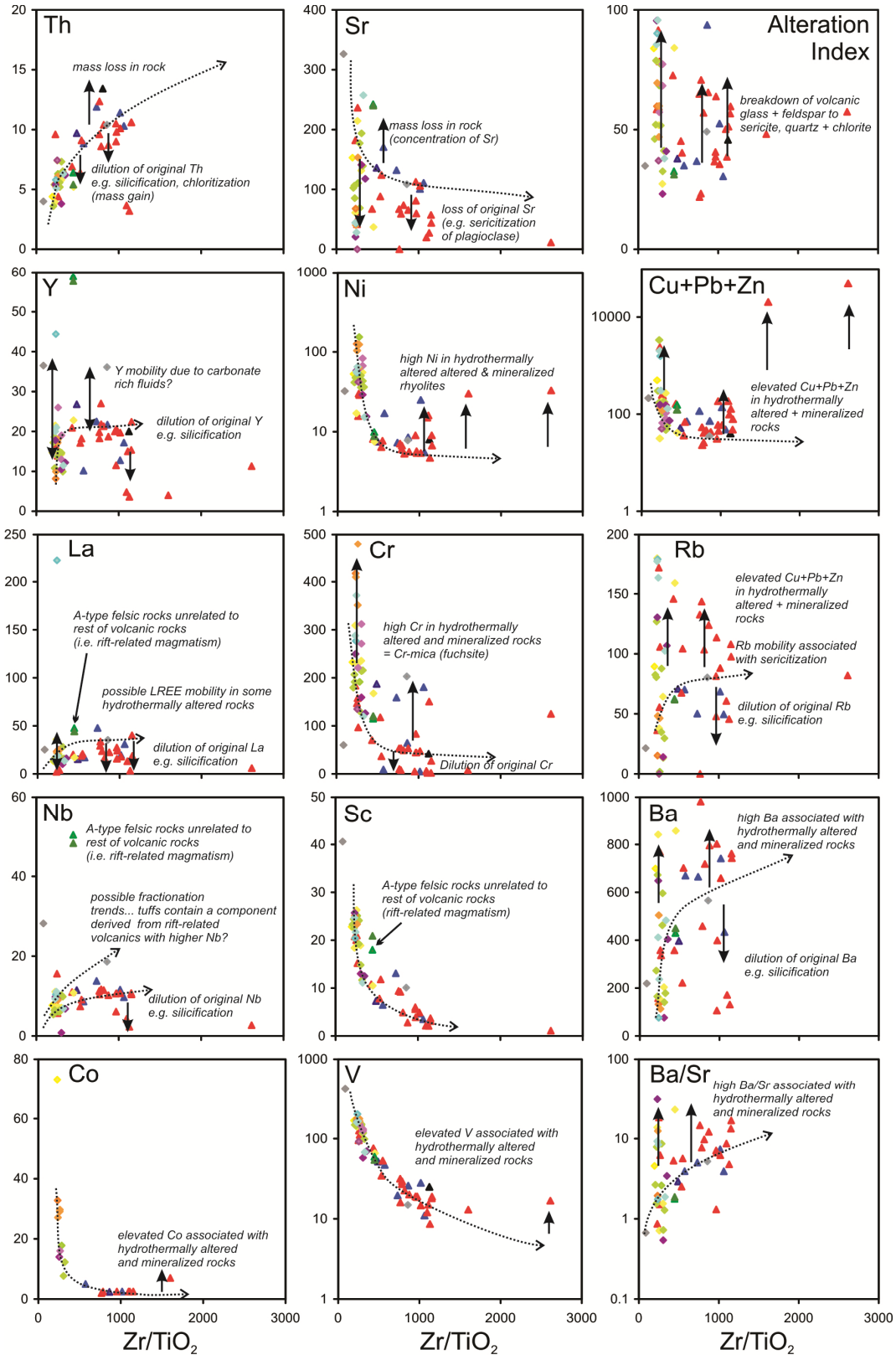

Figure 7.13. Element mobility diagrams for rocks from the upper Tyrone Volcanic Group (not including Fe-Ti enriched lavas). Dashed arrows indicate possible primary differentiation trends. Solid arrows indicate variations likely to be associated with element mobility (e.g. chloritization, sericitization, mass gain, mass loss). Symbols as in Figure 7.12.

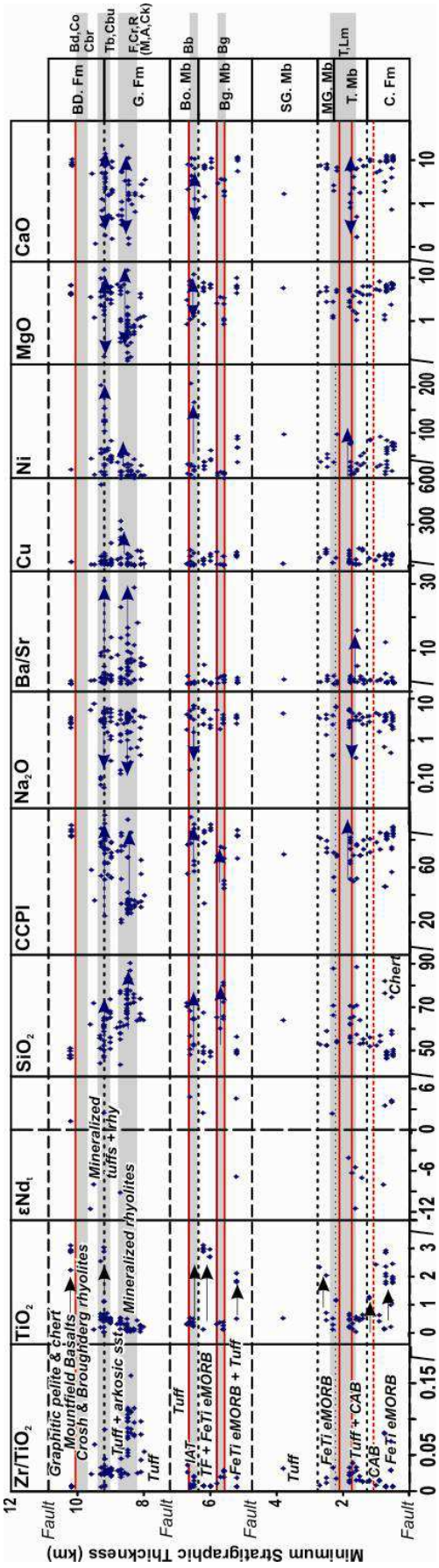

Figure 7.14. Mobile and immobile elements/ratios plotted against stratigraphic height. Petrochemically favourable stratigraphic horizons (marked by grey shading) show the largest variation in SiO_2, CCPI, Na_2O, CaO and MgO, Ba/Sr, Ni, CCPI and Cu associated with hydrothermal alteration. Red lines indicate stratigraphic position of ironstones (dashed red lines indicate ironstone fragments in agglomerate). Most contain ironstones (and rift-related lavas) in their hangingwall sequences. A, Aghascrebagh; Bb, Bonnety Bush; Bd, Broughderg; Bg, Beaghbeg; Cbi, Cashel Bridge; Cbu, Cashel Burn; Ck, Crouck; Co, Crosh; Cr, Cashel Rock; F, Formil; Lm, Loughmacrory; M, Murrins; R, Racolpa; T, Tanderagee; Tb, Tullybrick.

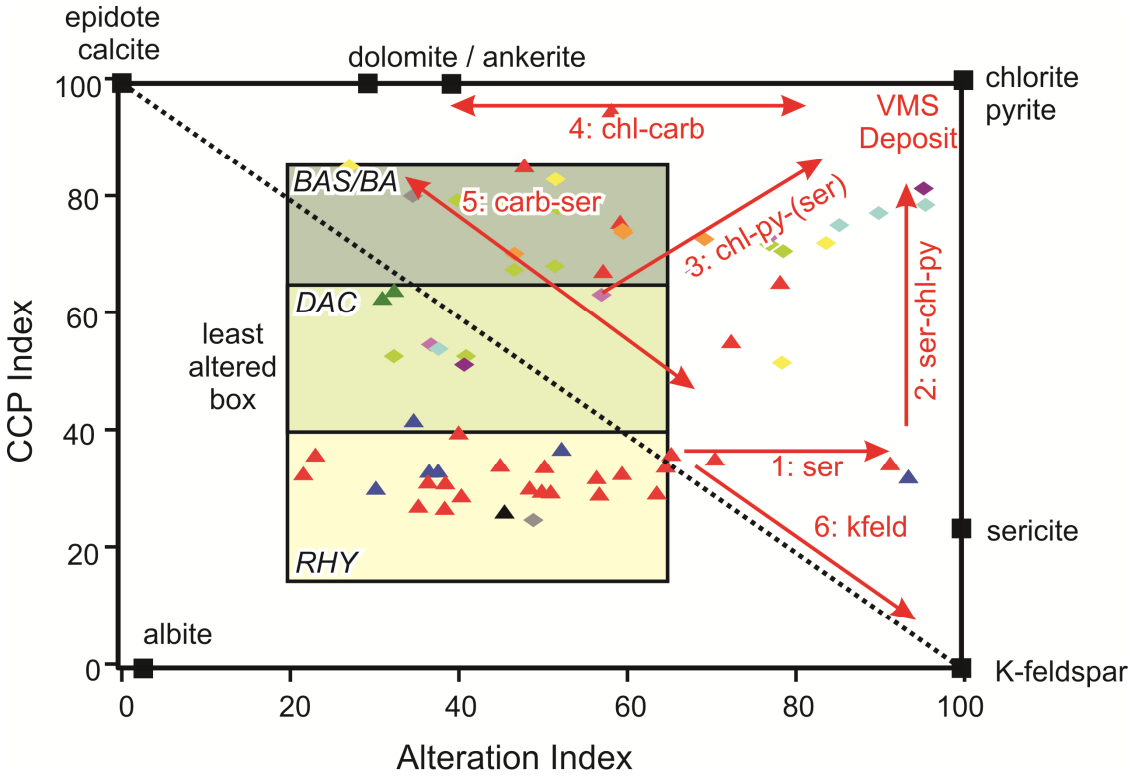

Figure 7.15. Box plot of major-element mobility in the upper Tyrone Volcanic Group (not including Fe-Ti enriched lavas). Arrows show 6 common trends during hydrothermal alteration. *Least altered box*: BA, basaltic andesite; BAS, basalt; DAC, dacite; RHY, rhyolite. *Alteration mineralogy:* carb, carbonate; chl, chlorite; kfeld, K-feldspar; py, pyrite; ser, sericite. After Box Plot of Large et al. (2001).

Samples from drillholes DDH 106-200 and DDH 106-203 at Cashel Bridge are amoung the most hydrothermally altered of all those analysed. Although these drillholes were sited close to the Omagh Thrust and suffered greenschist facies metamorphism, some samples show relatively low MgO contents suggesting chloritization associated with metamorphism was relatively weak in comparison to hydrothermal alteration (or at least locally variable in its intensity). Chloritization is relatively weak in drillhole DDH 106-200, with MgO between 2.1 and 7.6 wt% increasing systematically downhole. Sample 106-200-1 contains high Fe_2O_{3T} (17.6 wt%), CaO (14.1 wt%), Mn_3O_4 (0.8 wt%) and LOI (13.3 wt%), low SiO_2 (59.2 wt%), and extreme Na-depletion (Na_2O 0.006 wt %), consistent with extensive sericitization, carbonate alteration and pyrite mineralization (Cu+Pb+Zn 153 ppm). Samples from Cashel Bridge drillhole DDH 106-203 contain significantly higher base metal contents (to 2010 ppm), higher LOI contents (5.64-6.08 wt%), variable Na_2O (0.09-3.2 wt%), MgO (2.3-4.7 wt%) and moderately high Fe_2O_3 contents. Together these samples from Cashel Bridge show a systematic trend of

increasing AI and CCPI (to 95.5 and 81.4 = 106-200-3) from the 'least altered' field of Large et al. (2001) towards an 'ore centre' (Fig. 7.15). Samples from Tullybrick, Cashel Rock, the uppermost Greencastle Formation (i.e. Aghascrebagh, N of Crouck, Crouck) and Broughderg (unpublished drilling results) follow similar trends, although have lower AI and CCPI values (Fig. 7.15). Other samples from Cashel Rock and Formil follow a trend from 'least altered' compositions towards extensive sericitization (trend 1, Fig. 7.15). Unpublished drilling results show similar variations with distance from Pb-Cu-(Zn)-Ag-Au mineralization at Cashel Rock.

A-type felsic rocks from Broughderg drillcore are characterized by lower SiO_2 and CaO, higher Fe_2O_3, Mn_2O_3, Sc, Nb, La, Sr, Cu+Pb+Zn, and very high Nb and Y contents at a given Zr/TiO_2. Both samples analysed plot within the unaltered dacite field of Large et al. (2001; Fig. 7.15) and contain moderately high LOI values (4.5-4.8 wt%), and low AI and CCPI values (~32 and ~63 respectively). Major element concentrations are consistent with minimal hydrothermal alteration in these samples (SiO_2 61.6-62.0 wt%, MgO 1.4-1.8 wt%, Na_2O 4.4 wt%). Associated tuffs by contrast can be associated with high LOI values (to 11.9 wt%), high CCPI (80.1), MgO (5.9 wt%) and CaO (7.4 wt%).

7.8 Mineralization, geophysics and soil anomalies

As demonstrated in section 7.7, stratigraphic horizons favourable for the formation of VMS mineralization in the Tyrone Volcanic Group (Fig. 7.16) are characterized by weak and regionally extensive, or locally intense and laterally restricted hydrothermal alteration. Target areas of interest along these petrochemically favourable horizons (e.g. Formil, Cashel Rock, Cashel Bridge, Tullybrick, Broughderg etc.) have geochemical signatures consistent with intense VMS proximal, 'footwall' hydrothermal alteration (i.e. significant Mg-gains, Na-depletion, high Ni and Ba/Sr). Several episodes of base-metal (and Au) exploration have been undertaken in the Tyrone Volcanic Group since the 1970s. Work completed during these phases of exploration is reviewed in Leyshon & Cazalet (1978; Riofinex exploration program), Clifford et al. (1992; Ennex exploration program), Peatfield (2004 = post-Ennex exploration), and Hollis (2012).

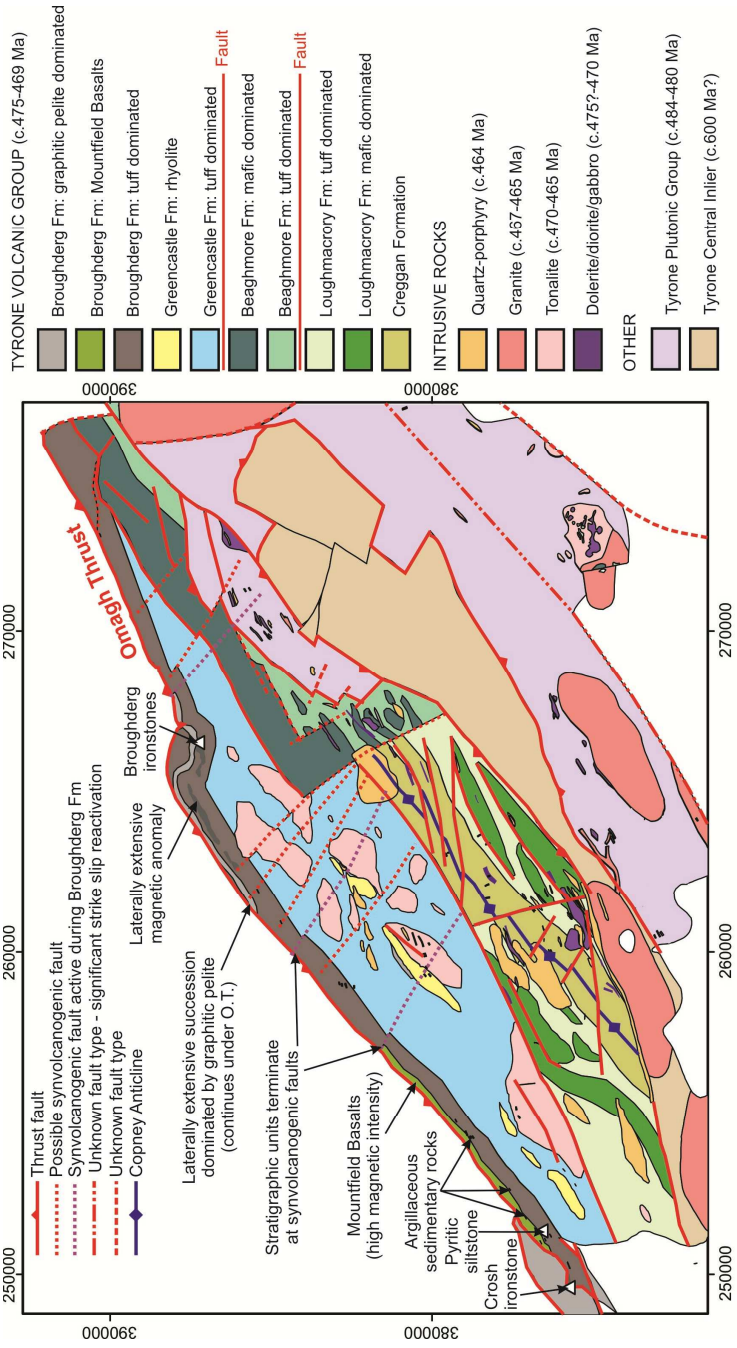

Figure 7.16. Geological map over the Tyrone Igneous Complex, adapted after Hollis et al. (2011). The base of the Broughderg Formation (solid black line) has been repositioned to account for late 2011 drilling results around Broughderg and Tullybrick, the recognition of a significant strike swing at Broughderg, and access to historic drillcore previously drilled around Cashel Bridge and Crouck/Aghascrebagh. New stratigraphic units not previously shown include: Mountfield Basalts, thick accumulations of graphitic pelite at Crosh (associated with rare thin tuff beds) and a laterally extensive unit of graphitic pelite at Broughderg. Possible synvolcanogenic faults are identified (based on the termination of stratrigraphic units along strike). Petrochemically favourable horizons (identified in section 5.5) are marked by grey stipple. Other units as in Figure 4.2b.

Stratigraphic horizons favourable for VMS mineralization and specific target areas along these in the upper Tyrone Volcanic Group occur in the middle Greencastle Formation (e.g. Racolpa, Murrins, Cashel Rock, Formil), the uppermost Greencastle Formation (e.g. Cashel Burn, Aghascrebagh, Crouck, Tullybrick), and middle Broughderg Formation (e.g. Broughderg, Cashel Bridge, Crosh). Each horizon is characterized by high Au, Pb+Cu+Zn, Pb/(Cu+Pb+Zn) in base of till (pionjar) samples, high base metal and/or Au values in prospecting samples, and geophysical anomalies (e.g. EM, IP, magnetics and/or gravity; see Figs. 7.17-7.24). By contrast, petrochemically favourable horizons of lower Tyrone Volcanic Group are associated with higher Zn/(Cu+Pb+Zn) (Fig. 7.20), consistent with a more primitive oceanic affinity for this part of the arc sequence. Prospecting samples are similarly Pb-Zn-Cu-Au rich in the upper Tyrone Volcanic Group (e.g. 3.48% Pb, 2.05% Zn, 0.53% Cu and 2.41 g/t Au, Aghascrebagh float), and are Zn-Cu rich in the lower Tyrone Volcanic Group (e.g. 2.98% Zn Bonnety Bush, float). Several of these areas, which contain high base metal and/or Au values in prospecting samples, have been partially tested by shallow drilling (e.g. Cashel Rock, Broughderg). Other areas contain abundant mineralized float and no mineralized showings (e.g. Aghascrebagh, 4% Pb, 1.22% Zn & 5.94 g/t Au in siliceous tuff). Shallow drilling and trenching of IP and soil anomalies by Ennex in these areas had limited success (e.g. Aghascrebagh, Cashel Bridge), which is summarised below.

Significant historic drilling results in the upper Tyrone Volcanic Group.

Aghascrebagh:		
DDH 106-205	25.70 to 26.22m	52cm at 1.9% Pb+Zn, 0.48 g/t Au
	31.27 to 31.33m	6cm at 1.7% Pb+Zn, 20.5 g/t Au
DDH 106-210	50.25 to 50.75m	50cm at 3.5% Pb (drillhole ends at 50.95m)
Broughderg:		
DDH 91-1	5.53m to 6.15m	0.62m at 1.68 g/t Au
Cashel Bridge:		
DDH 106-201	22.03 to 22.43m	40 cm at 3.36% Pb+Zn,
DDH 106-202	84.25 to 84.44m	19cm at 1.05% Cu, 2.24 g/t Au
	87.41 to 87.55m	14cm at 0.91% Pb, 4.97% Zn
Cashel Rock (best intercepts):		
DDH 106-232	35.9 to 36.46m	0.56m at 11.97 g/t Au, 28.1 g/t Ag, 4.24% Pb
	72.5 to 77.5 m	5.0m at 0.48g/t Au, 12.3 g/t Ag
DDH 106-217	12.3 to 15.93m	3.63m at 30.12 g/t Au, 44.31 g/t Ag; includes 1.23m at 1.14% Cu, 1.85% Pb

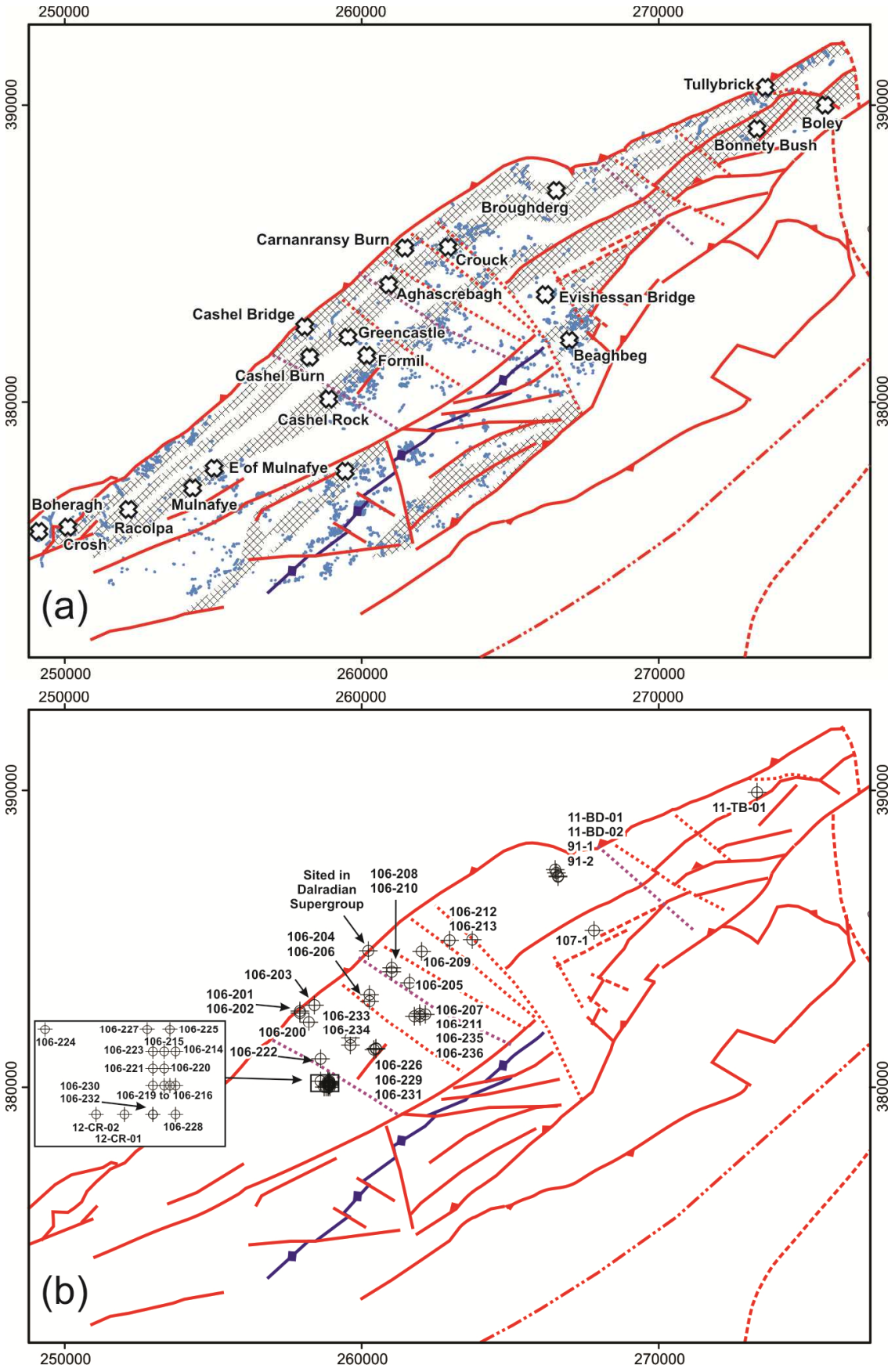

Figure 7.17. (a) Outcrop (blue), petrochemically favourable horizons (grey stipple) and key localities in the Tyrone Volcanic Group. (b) Drillhole locations. Faults as in Figure 7.16.

Mineralization in the upper Tyrone Volcanic Group is broadly divisible into five types:

(i) Au-bearing silicified ± sericitized ± chloritized rhyolites with or without base metal mineralization (e.g. Cashel Rock, Crosh, Racolpa, Formil). Samples can be extremely Au rich (e.g. 65.95 g/t Au, Cashel Rock), especially late quartz veins associated with areas of intense silicification (e.g. 112.7g/t Au at Cashel Rock). The Cashel Rock Au prospect was identified through geochemical surveying, and is hosted in fine grained flow-banded rhyolite. Subsequent trenching and drilling identifying a zone of silica flooding and crackle brecciation that averages 2 m in thickness and dips ~30 °W. The Au mineralized zone was traced for a strike length of 200 m and depth of ~70 m and is open down-dip and along strike to the south. The most encouraging result came from the deepest vertical hole on the most southerly section, where a > 10 m section of rhyolite that exhibited a stockwork system with extensive chloritic and silicic alteration was intercepted. This suggests massive sulphide mineralization may be present at depth. Recent drilling extended the mineralized zone down dip and identified several zones of intense hydrothermal alteration (associated with Au and Pb-Cu mineralization). At Crosh and Racolpa, Au mineralization is similarly associated with silicified rhyolites and tuffs which often host base-metal mineralization (e.g. 18m @ 0.42 g/t Au in channel sampling at Crosh). No drilling has been carried in these areas, where mineralized outcrops are coincident with VLF/EM-R and magnetic anomalies, and high Au and/or base metal values in base of till samples.

(ii) Bands of pyrite ± galena ± sphalerite ± chalcopyrite in extensively chloritized, sericitized and/or silicified felsic tuffs (e.g. Crouck, Aghascrebagh, Cashel Burn, Cashel Bridge, Tullybrick). These areas are often extensively sheared and associated with fuchsite. Talc and chloritic altered felsic tuffs around Greencastle contain bands of pyrite-galena-sphalerite-chalcopyrite and assay up to 10% Zn, 2.83 % Pb and 1.23 % Cu. At Tullybrick Au bearing quartz veins occur in intensely chloritized and/or quartz-sericite±fuchsite altered fine-grained felsic to intermediate crystal tuffs. These rocks can contain significant Au (to 2.78g/t Au). Simiarly at Cashel Burn, an outcrop of sericitic and fuchsite bearing tuff contains bands of galena and sphalerite (1.63 g/t Au and 4.3 % Cu+Pb+Zn).

(iii) White quartz float with visible gold, chalcopyrite and malachite staining occurs around Mulnafye. This quartz vein material cuts tonalite in float and assays up to 71.5g/t Au.

(iv) Au rich ironstones. Auriferous samples of ironstone have been found as float at Broughderg, S of Creggan (3.0 & 5.6 g/t Au), Boley-Bonnety Bush (2.98 & 4.54 g/t Au) and Tanderagee (1.3 & 1.39 g/t Au).

(vi) Weak Cu mineralization (and malachite staining on shear surfaces) associated with sericitized, silicified ± chloritized volcanic rocks and intrusives at Formil. Abundant Cu mineralization is common around Formil, both in tonalite, rhyolite and associated tuffs. Various alteration types occur around Formil, including silicification, massive pyrite mineralization associated with silicification and magnetite stringers, argillic alteration, sericitization and patchy chloritization. On the west side of Slievemenagh (Formil) Ennex drillhole DDH 106-207 encountered 70 m of kaolinised quartz-porphyry with disseminated (c. 2-5 %) fine grained pyrite with no silicification. Low assays of Cu, and low Au and Ag (below detection, <20 ppb) were recorded. Previous drilling by Riofinex around Formil intersected subeconomic Cu mineralization (131 ft at 0.27% Cu).

(vi) Au-bearing quartz veins, hosted by graphitic pelite. At Boheragh (W of Crosh) a stream section exposes a 1.5m thick quartz vein which contains pyrite, galena, sphalerite and arsenopyrite and assayed 9.34 g/t Au. Pyrite rich quartz veins were intersected by recent drilling at Broughderg in graphitic pelite, although none hosted Au mineralization. Similar units occur in the working Mountfield Quarry, directly along strike.

During 2011-2012 targeted prospecting along these petrochemical 'fairways' for mineralization identified several new mineralized showings including: the discovery of mineralization at Cashel Burn (1.63 g/t Au and 4.3 % Cu+Pb+Zn in outcrop), and new showings around Crosh (to 2.99% Cu+Pb+Zn), Racolpa (to 2.19g/t Au), and E of Mulnafye (1.33% Cu+Pb+Zn, 0.3g/t Au), in addition to outcropping massive pyrite at Formil (Dalradian Resources News Release 2011). This demonstrates this technique not only correctly identified areas of known mineralization, but also new areas of mineralization for subsequent exploration. Reccommendations for exploration are discussed in section 7.9.

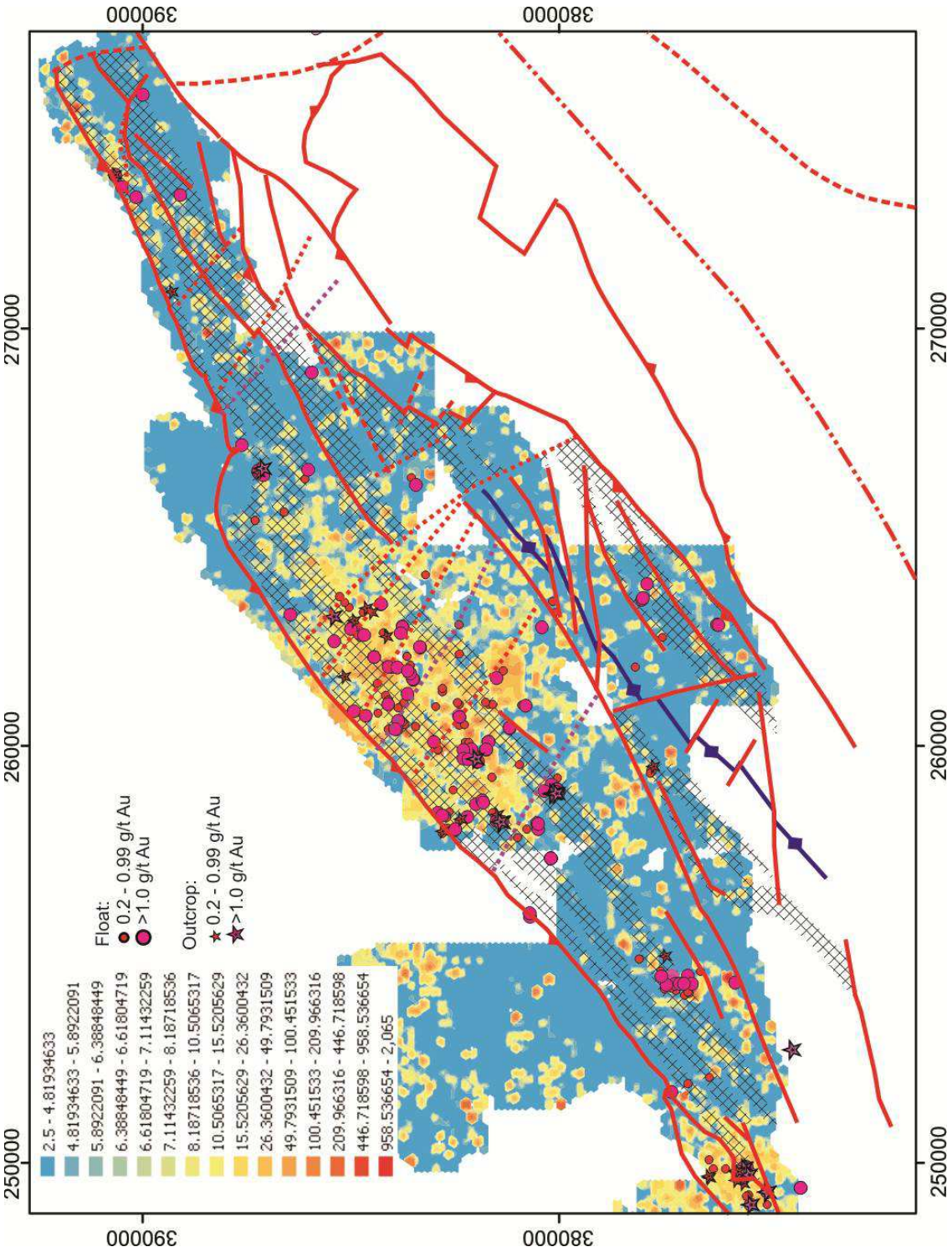

Figure 7.18. Au base of till (pionjar) geochemical map (inverse distance weighting, in ppb) and historic prospecting results (in g/t Au) showing a close spatial association with petrochemically favourable horizons (grey stipple). Faults as in Figure 7.16. Au values in base of till samples are highest around Crosh, between Cashel Rock and Broughderg, E of Racolpa (i.e. Mulnafye – associated with visible Au in bucky white quartz float), and near Tullybrick.

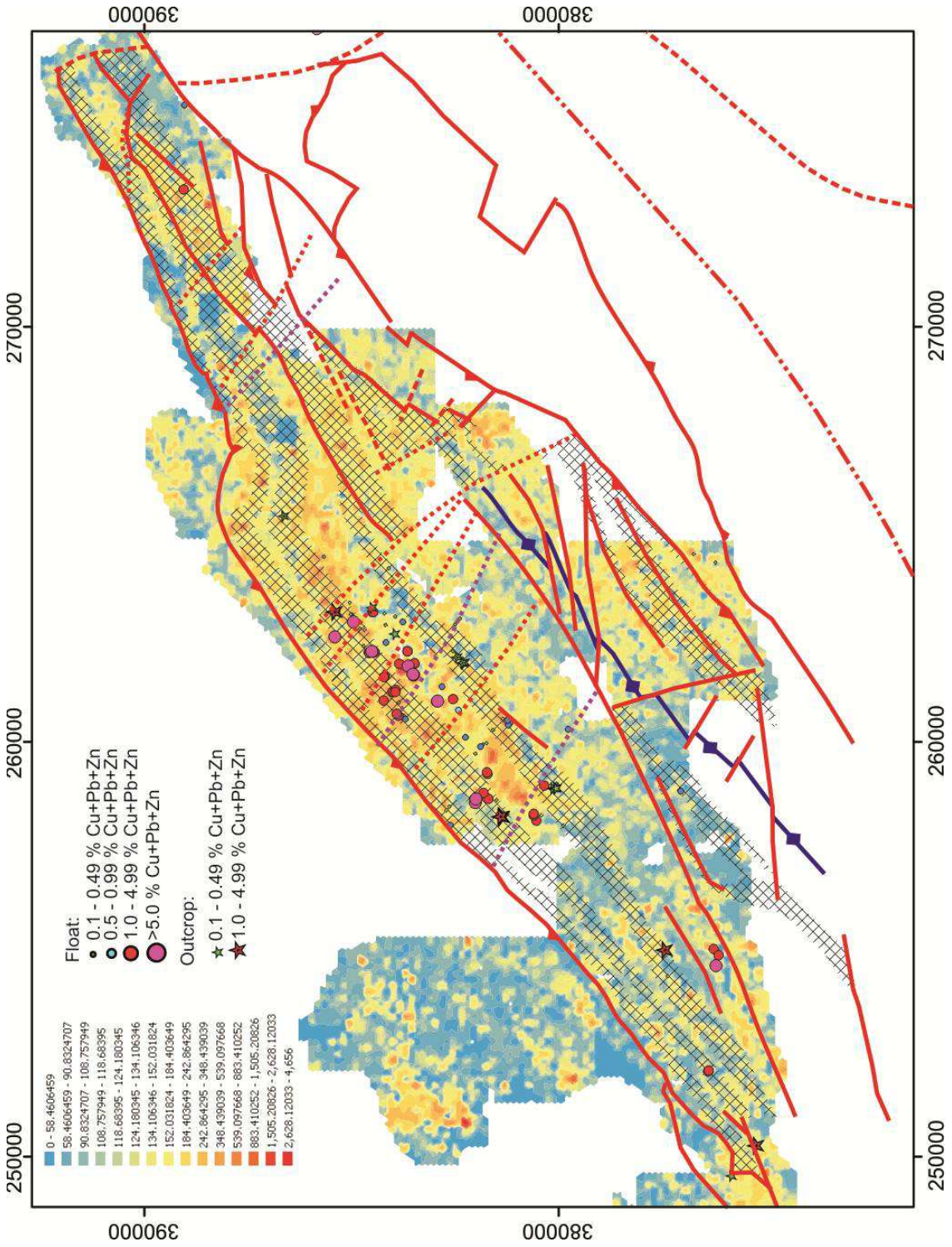

Figure 7.19. Cu+Pb+Zn base of till (pionjar) geochemical map (inverse distance weighting, in ppm) and historic prospecting results (% Cu+Pb+Zn) showing a close spatial association of both with petrochemically favourable horizons (grey stipple) and target areas characterized by extensive hydrothermal alteration. Faults as in Figure 7.16. Petrochemically favourable horizons are associated with high Cu+Pb+Zn in base of till and in prospecting samples particularly between Cashel Rock and Broughderg.

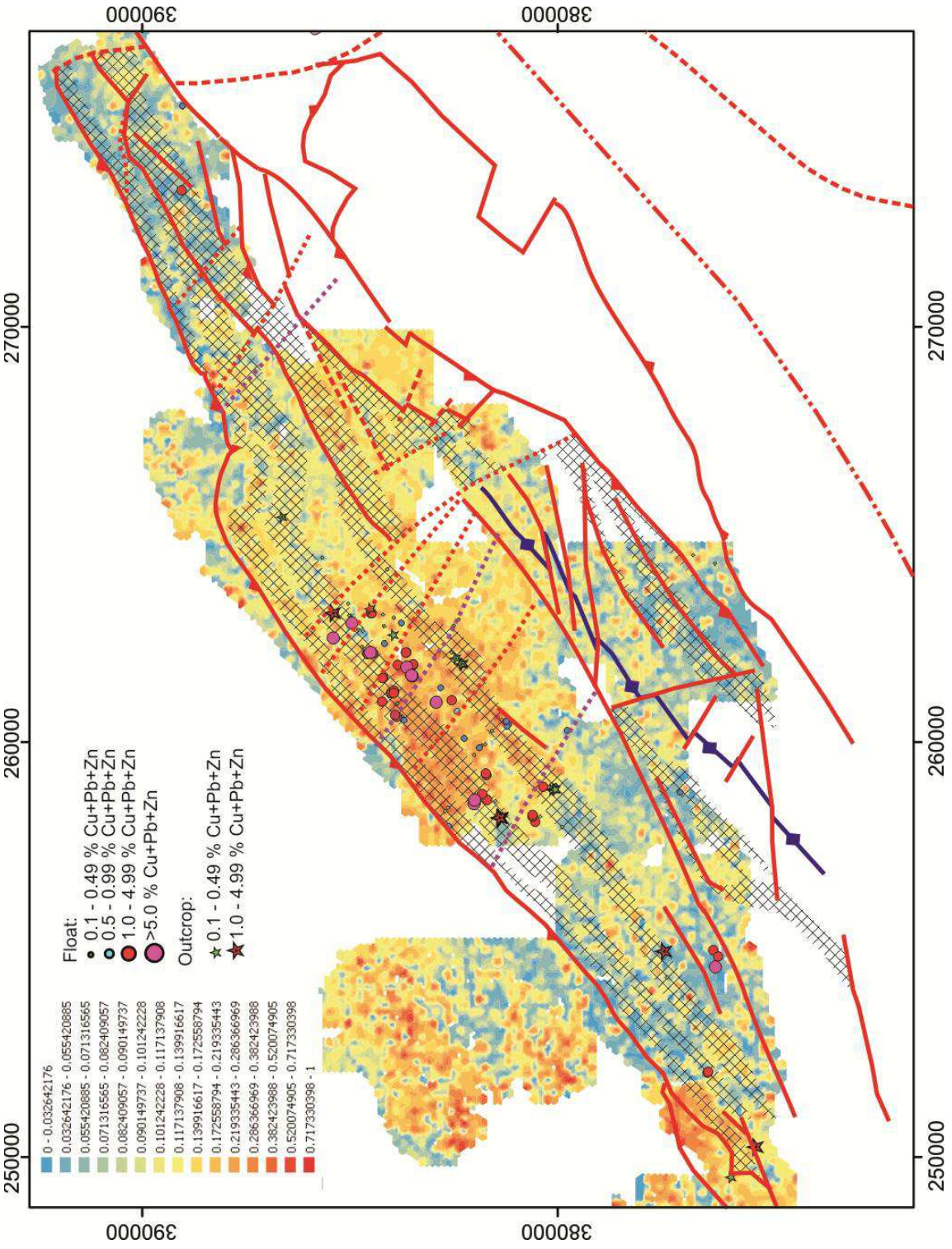

Figure 7.20. Pb/(Cu+Pb+Zn) base of till (pionjar) geochemical map (inverse distance weighting) and historic prospecting results (% Cu+Pb+Zn) showing a close spatial association of both with petrochemically favourable horizons (grey stipple) and target areas characterized by extensive hydrothermal alteration. Faults as in Figure 7.16. Petrochemically favourable horizons in the upper TVG are characterized by high Pb/(Cu+Pb+Zn), whereas those of the lower TVG are characterized by high Zn/(Cu+Pb+Zn) (e.g. Bonnety Bush area).

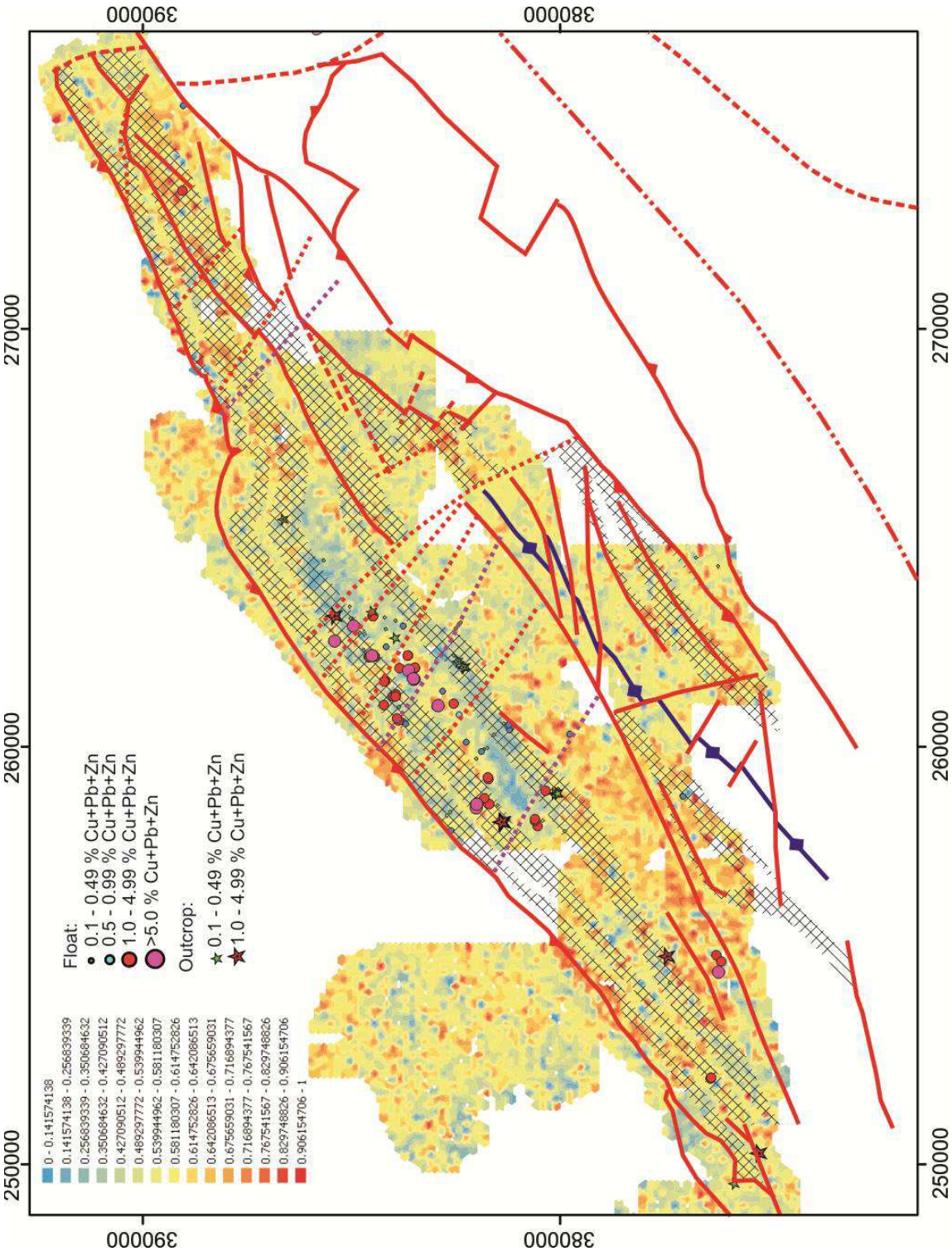

Figure 7.21. Zn/(Cu+Pb+Zn) base of till (pionjar) geochemical map (inverse distance weighting) and historic prospecting results (% Cu+Pb+Zn) showing a close spatial association of both with petrochemically favourable horizons (grey stipple) and target areas characterized by extensive hydrothermal alteration. Faults as in Figure 7.16. Petrochemically favourable horizons in the upper TVG are characterized by low Zn/(Cu+Pb+Zn) (due to high Pb), whereas those of the lower TVG are characterized by high Zn/(Cu+Pb+Zn) (e.g. Bonnety Bush area).

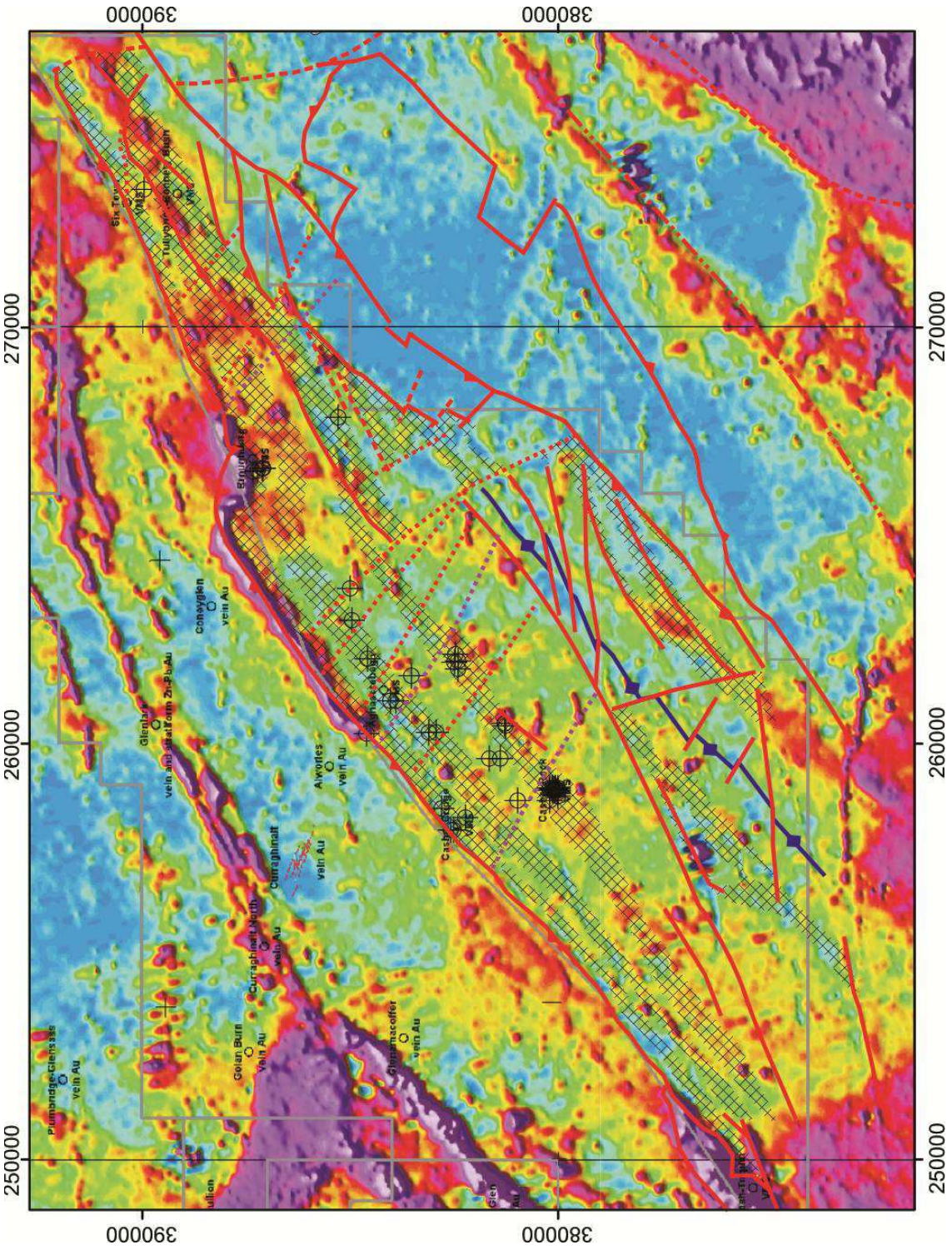

Figure 7.22. Tellus EM apparent conductivity map, with petrochemically favourable horizons and historic drillholes. Faults as in Figure 7.16. A number of large untested geophysical anomalies (high conductivity) are apparent along these horizons, particularly in the Greencastle Formation. Other areas of high conductivity are associated with graphitic pelites around Crosh and between NW of Aghascrebagh and Broughderg.

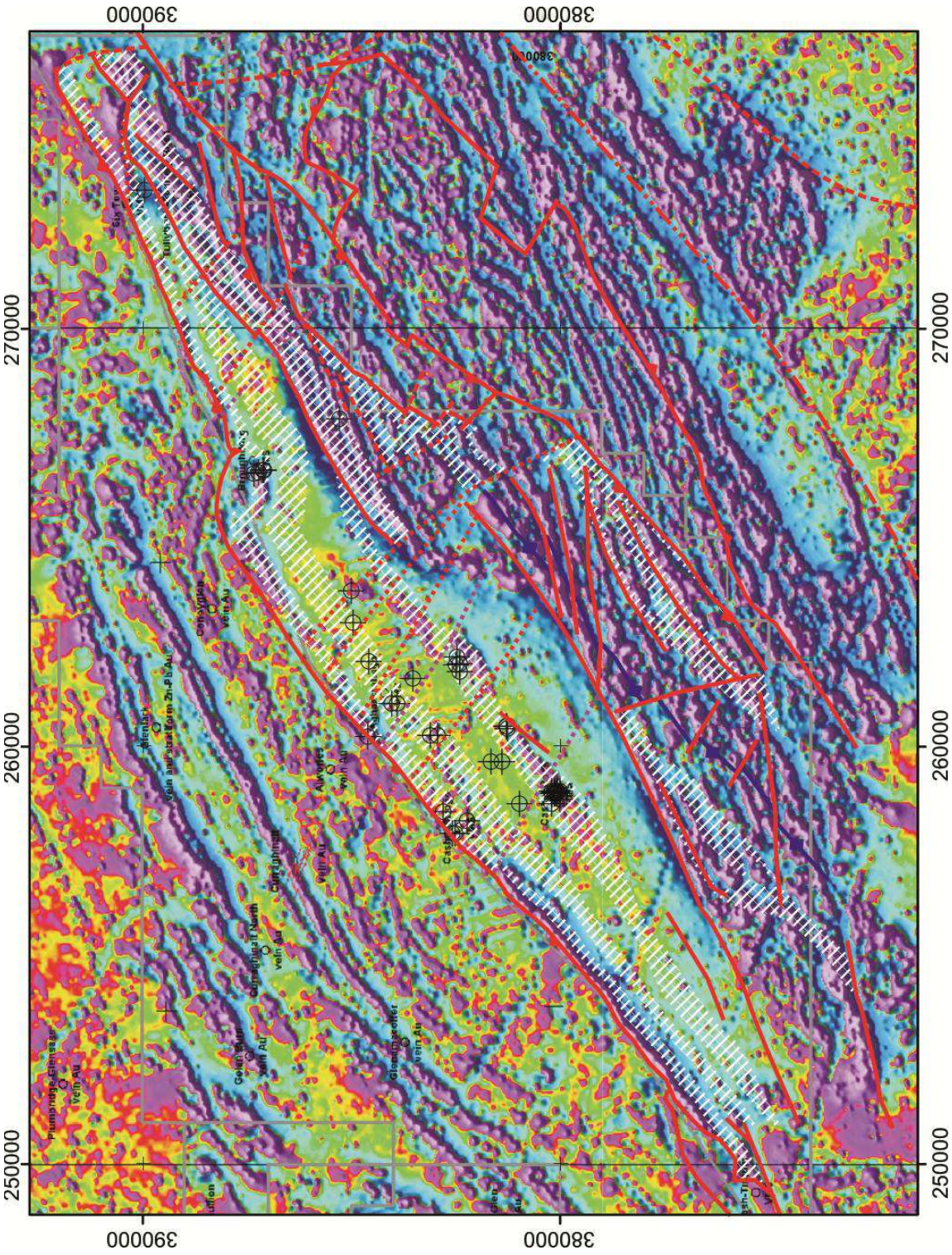

Figure 7.23. Tellus total magnetic intensity (1st vertical derivative) map, with petrochemically favourable horizons and historic drillholes. Faults as in Figure 7.16. A number of large untested geophysical anomalies (high magnetic intensity) are apparent along these horizons, particularly in the Greencastle Formation at Cashel Rock, Formil, and along strike; and in the Broughderg Formation at Crosh, Cashel Bridge and Broughderg. The lower TVG is characterized by high total magnetic intensity.

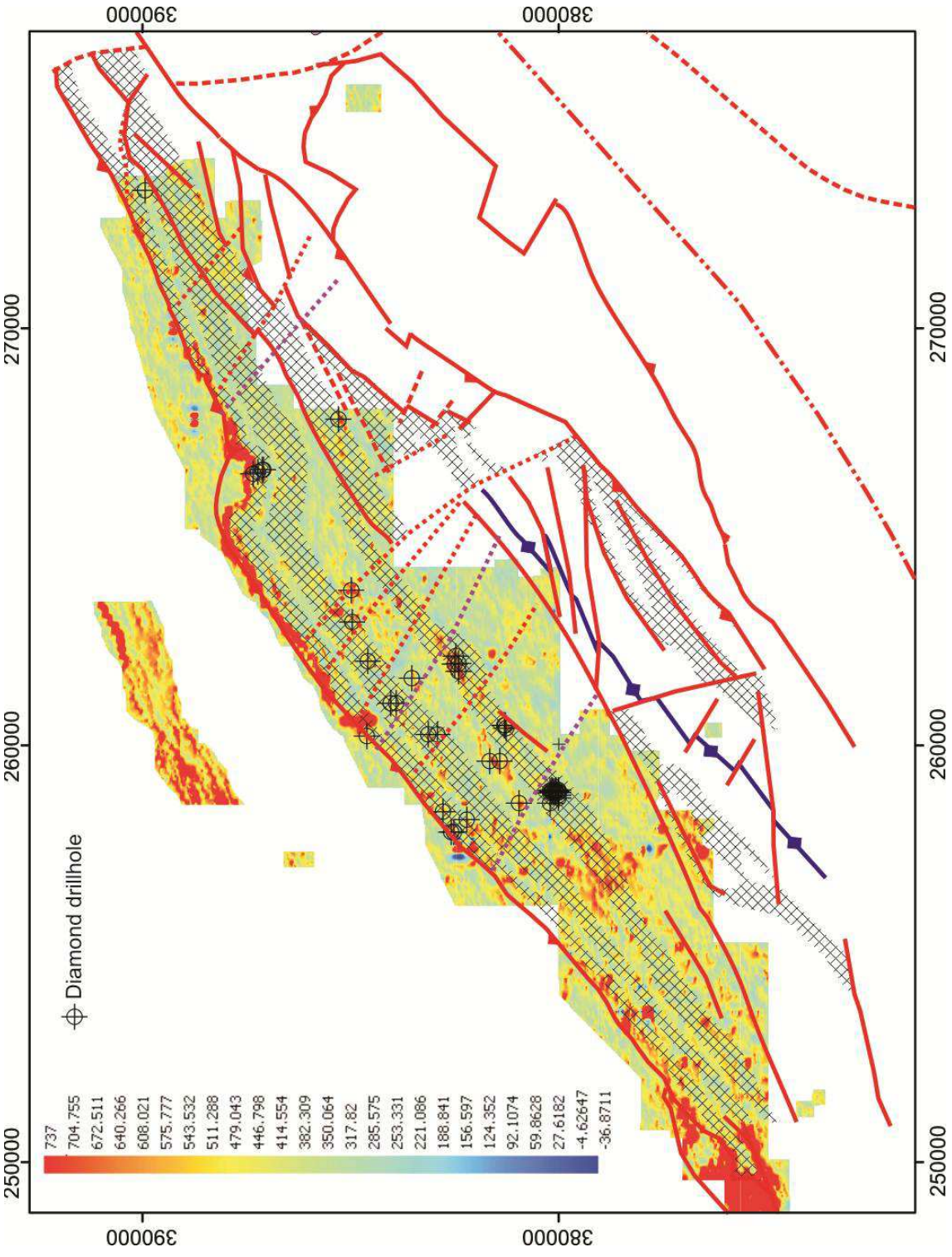

Figure 7.24. Ground IP (induced polarization) chargeability map, with petrochemically favourable horizons and historic drillholes. Faults as in Figure 7.16. A number of areas characterized by high chargeability are apparent along these horizons, some of which were tested by Ennex through shallow drilling (<100m-150m). Most were associated with disseminated pyrite. Other areas of high chargeability are associated with graphitic pelites around Crosh and between NW of Aghascrebagh and Broughderg. Data processed by PGW (2011).

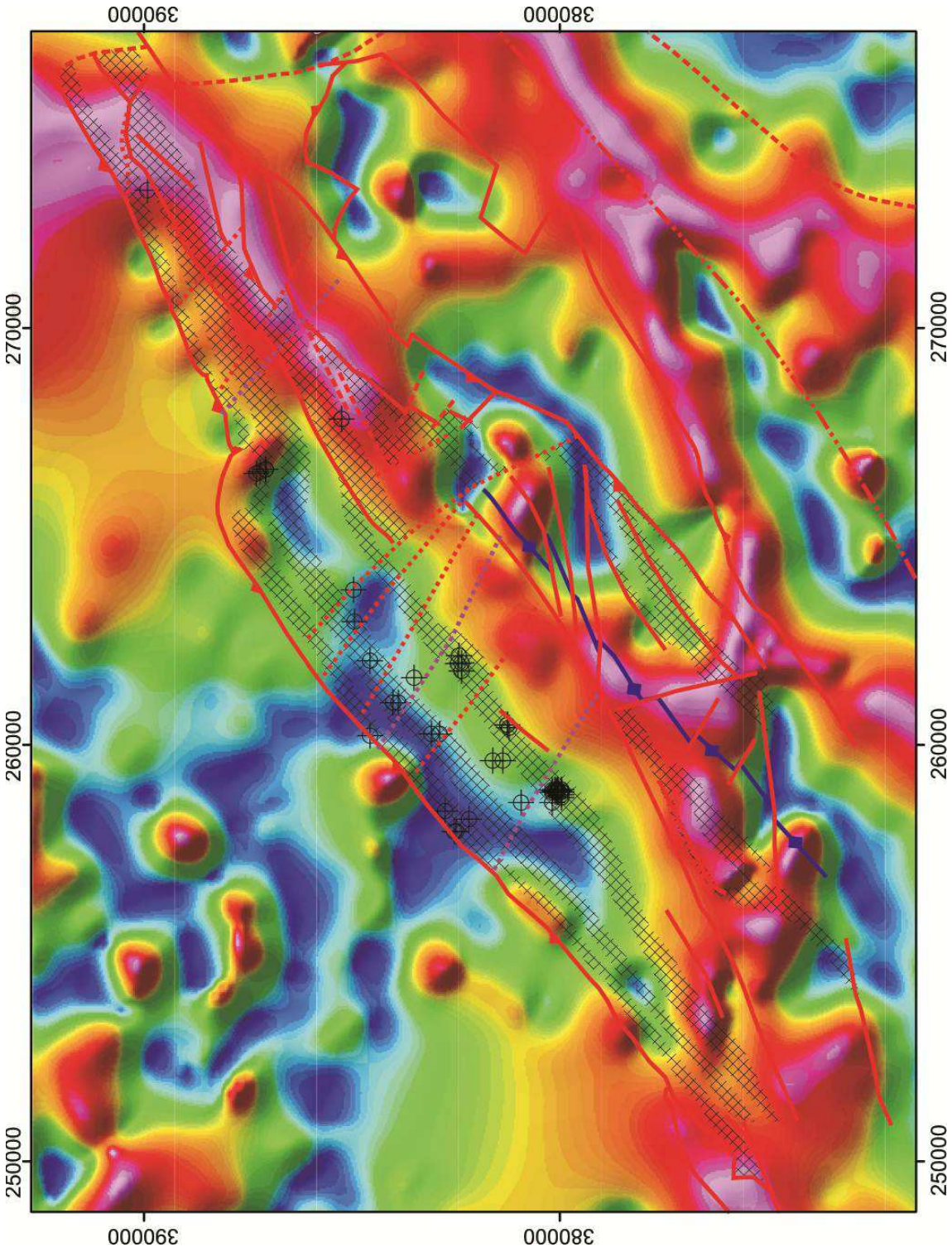

Figure 7.25. BGS regional gravity map, with petrochemically favourable horizons and historic drillholes. Faults as in Figure 7.16. A large magnetic anomaly associated with an ironstone and magnetite-bearing chlorite tuffs at Broughderg is coincident with a large gravity anomaly. The lower TVG is characterized by a higher gravity response.

7.9 Reccomendations for exploration

7.9.1 VMS Prospective horizons

With the arrival of a new phase of VMS exploration in Northern Ireland an opportunity now exists to utilize modern geochemical techniques and established 'geochemical pathfinders' for VMS mineralization within the Tyrone Volcanic Group. Specific stratigraphic horizons suitable for VMS mineralization have now been identified and several areas appear to be prospective for VMS deposits coincident with base metal showings, base of till geochemical anomalies, and geophysical anomalies. Geochemical indices and ratios such as CCPI, AI, Ba/Sr, Na-depletion, Sb and Tl provide useful and cost-effective vectors towards mineralization along with the less routine vectors such as oxygen isotopes, LREE mobility, mineral chemistry (chlorite, epidote, muscovite – see Appendix), and ironstones (Appendix). Many of these (e.g. CCPI, AI, Na depletion) provide a useful quantitative way to characterize the hydrothermal alteration observed (Section 7.7) and plan for further drilling. The completion of new deep diamond drillholes in the Tyrone Volcanic Group provides a unique opportunity to link lithologies and hydrothermal alteration from outcrop to depth at these sites. Further drilling is scheduled to take place following the completion of a high-resolution VTEM survey (www.dalradian.com) covering Cashel Rock, Formil and Cashel Burn. Drilling should target geophysical anomalies associated with hydrothermally altered, petrochemically favourable units (e.g. Cashel, Broughderg and Crosh rhyolites). Particular attention should be given to the identification of synvolcanogenic faults (i.e. changes in facies type and/or thickness) and synvolcanogenic intrusions.

7.9.2 A 3D framework for geochemical vectoring

Establishing a 3D geochemical framework of hydrothermal alteration at Cashel Rock using completed drillholes should be a top priority at this showing. Cashel Rock is also the best example of stockwork mineralization in the Tyrone Volcanic Group. Recent drilling in late 2011 intercepted several zones of hydrothermal alteration (silicified, carbonate-altered, sericitic, chloritic), hydraulic crackle-brecciated rhyolite, Bi-sulfosalts, and base-metal and Au mineralization which show systematic trends in AI, CCPI, Ba/Sr, CaO, MgO, Co, Bi, etc., downhole, with sudden shifts at the sites of Au and Cu-Pb mineralization (Hollis 2012 unpublished report). Sixteen diamond drillholes have been completed over this target across five fences, allowing a 3D geological model of the lithologies, mineralization and hydrothermal alteration to be created providing geochemistry is available. Historic Ennex drillcore should be relogged for hydrothermal alteration and resampled as a top priority for multi-element analysis to provide petrochemical and lithogeochemical constraints in the third dimension.

Analysis of Tl, Sb and the REE is essential at low detection limits to identify 'geochemical haloes' which surround deposits.

7.9.3 Mineral chemistry

Establishing whether Fe- or Mg-enrichement in chlorites occurs in proximity to mineralization at Cashel Rock may provide a potentially powerful vector to ore. This is relatively cost effective and provides large, statistically robust datasets. Unpublished microprobe analyses from historic Riofinex drillcore around Cashel Rock (not the target itself but IP anomalies in the viscinity) show systematic trends in Fe-enrichment downhole, although the original core is not available (Weir 1986 unpublished). Spot analyses downhole (e.g. sampling every ~25 to 50m) would compliment the existing geochemical dataset. Any future analysis (whole rock or mineral chemistry) could be tied to this one DDH, which intersects all main alteration zones. Analyses herein demonstrate Cashel Rock and Formil chlorites formed at high temperature and may be VMS proximal (Appendix).

7.9.4 Ironstones

Ironstones show significant variability in terms of their petrography, major, trace and REE geochemistry at each site in the Tyrone Volcanic Group (Appendix). Laterally extensive float trains linked to linear ground magnetic anomalies suggest these units can be used as marker horizons. A detailed mineralogical or geochemical study of ironstones (including float trains) in the Tyrone Volcanic Group should be carried out to vector in towards VMS mineralization. Some samples analysed herein, from Tanderagee and Slieve Gallion, appear to be VMS proximal (Appendix). A geochemical study of quartz-hematite lenses (red jaspers) was carried out in the Mount Windsor Volcanics, Australia, by Miller et al. (2001) to recognize potential 'near misses' in exploration drilling in and around the Thalanga VMS mine. The realization that elevated Ba, S and Pb (along with positive Eu anomalies) were associated with VMS proximal jaspers, coincident with a $\delta^{18}O$ 'hot spot', directly led to the discovery of the West 45 VMS deposit (see Miller et al. 2001). A number of stable isotopes have also been applied to iron formations, some of which demonstrate they may be useful tools to explore for concealed mineralization. Whole rock O-isotope work on the Japanese Kuroko deposits demonstrated that $\delta^{18}O_{SMOW}$ values decreased from 9 ‰ for the ore horizon tuff to 5.1 ‰ in 'tetsusekiei' (red chert) over a distance of 0.5km from ore, and whole-rock $\delta^{18}O$ values also decrease with proximity to massive sulphides (Scott et al. 1983). $\delta^{34}S$ values in sulphide minerals and $\delta^{13}C$ values in carbonate minerals have also been shown to be higher in iron formations overlying the Brunswick No. 12 deposit compared to distil samples (references in Peter 2003). Variations in the abundance of certain minerals also reflect proximity to VMS at Bathurst (see Spry et al. 2000).

7.10 Conclusions

Through a combination of extensive field mapping and petrochemistry, several stratigraphic horizons have been identified in the Tyrone Igneous Complex which were favourable for the formation and preservation of VMS deposits (e.g. Cashel Bridge, Broughderg, Crosh, etc.). Each is closely associated with rift-related and high-temperature petrochemical associations, extensive hydrothermal alteration, synvolcanogenic faults and high-level synvolcanogenic intrusions (dolerite, gabbro, diorite and tonalite). Rift related magmatism is characterized by the eruption of abundant non-arc type Fe-Ti enriched eMORB ('icelandite'), island-arc tholeiite, OIB-like and alkali basalt, high-temperature, M-type and FIV affinity tholeiitic rhyolites with flat to U-shaped REE profiles, and A-type high Zr rhyolites within the calc-alkaline dominated sequence. Rift related mafic lavas occur in the hangingwall to VMS-style mineralization and are closely associated with ironstones (occassionally Au bearing) and/or argillaceous sedimentary rocks representing volcanic quiescence. Extensive hydrothermal alteration, characterized by Na-depletion, high Ba/Sr, Bi, Sb, Ni, CCPI, AI and variable MgO and CaO contents, allows specific target areas to be identified. In the lower bimodal-mafic Tyrone arc and backarc, hydrothermal alteration is associated with Zn-Cu mineralized float (e.g. Bonnety Bush). Pb-Zn-Cu-Au mineralization occurs in crackle-brecciated and silicified auriferous FII-type rhyolite domes/flows and/or volcaniclastic rocks of the syncollisional bimodal-felsic upper Tyrone arc (e.g. Cashel Rock, Crosh, Broughderg). Rare ophiolite hosted Cu mineralization is characterized by chalcopyrite stringers hosted in sheeted dyke sequences. Petrochemically favourable horizons are characterized by high Au and/or base metal values in prospecting samples and base of till samples, and abundant untested geophysical anomalies (e.g. IP, EM, magnetics, gravity). Preliminary mineral and ironstone geochemistry suggests both may act as vectors to mineralization, along with more standard whole rock geochemical techniques (e.g. Ba/Sr, Na-depletion), to identify VMS mineralization in each target area.

Chapter 8: Conclusions and future work

8.1 Conclusions

This thesis presents the first detailed temporal, stratigraphic, geochemical and structural study of the Tyrone Igneous Complex of Northern Ireland. Results presented herein have important implications for both the evolution of the Grampian-Taconic orogen and VMS mineralization in Northern Ireland. Main conclusions are summarised below.

8.1.1 Evolution of the Tyrone Igneous Complex

- The Tyrone Igneous Complex is broadly divisible into a structurally lower dismembered suprasubduction zone ophiolite (=Tyrone Plutonic Group), and an overlying, relatively complete (though poorly exposed) arc-related sequence (=Tyrone Volcanic Group).
- Both were accreted to an outboard peri-Laurentian microcontinental block (=Tyrone Central Inlier, c. 600 Ma) prior to c. 470 Ma; and intruded by a suite of syn-collisional to post-collisional arc plutons between c. 470 and 464 Ma.
- A mélange, exposed at the contact between the Tyrone Plutonic Group and peri-Laurentian Dalradian-affinity Tyrone Central Inlier comprises blocks of ophiolite derived amphibolite-facies gabbroic to doleritic material within banded and isoclinally folded synkinematic tonalitic to granitic melt and amphibolite, closely associated with Dalradian-affinity metasedimentary rocks.
- Synkinematic, calc-alkaline tonalitic melt within the contact suggests the Tyrone Plutonic Group may have been emplaced relatively late within the orogen at c. 470 Ma synchronous with the Tyrone Volcanic Group. Coeval accretion of a c. 10km thick, hot, arc-ophiolite complex may explain how sillimanite-grade metamorphic conditions were reached in the underlying Tyrone Central Inlier prior to c. 468 Ma.

Tyrone Plutonic Group

- The Tyrone Plutonic Group (c. 484-480 Ma) preserves the upper portions of a tectonically dissected suprasubduction zone ophiolite, characterized by amphibolite-facies, layered, isotropic and pegmatitic gabbros, sheeted dolerite dykes and rare pillow lavas. A cross-cutting S-type and peraluminous intrusion of muscovite granite contains abundant inherited Proterozoic zircons, and appears to be associated with ophiolite emplacement and the melting of underlying metasedimentary material.

- Tholeiitic suprasubduction affinity LREE-depleted geochemical characteristics, zircon inheritance in layered gabbros, and the presence of late Fe-Ti enriched post-obduction dykes suggest the Tyrone Plutonic Group formed above a north-dipping subduction zone by the propagation of a spreading centre into a microcontinental block. This is consistent with εNd_t values (+4.4 and +7.4) slightly lower than calculated values from the depleted mantle growth curve at c. 480 Ma (DePaolo 1988); and $^{87}Sr/^{86}Sr_i$ ratios more radiogenic than the $^{87}Sr/^{86}Sr$ isotopic composition of Lower to Middle Ordovician seawater.

Tyrone Volcanic Group

- The Tyrone Volcanic Group (c. 475-469 Ma) is characterized by mafic to intermediate lavas, tuffs, rhyolite, banded chert, ferruginous jasperoid and argillaceous sedimentary rocks cut by numerous high-level synvolcanogenic intrusive rocks (e.g. tonalite, gabbro, diorite).
- Geochemical signatures are consistent with formation within an evolving peri-Laurentian island-arc/backarc which underwent several episodes of intra-arc rifting prior to its accretion at c. 470 Ma to an outboard peri-Laurentian microcontinental block.
- High LILE and LREE enrichment, calc-alkaline geochemical signatures and strongly negative εNd_t values suggest the Tyrone arc was at least partially founded on a fragment of continental crust, which may have rifted off the Tyrone Central Inlier during the formation of the Tyrone Plutonic Group.
- The lower c. 475-474 Ma Tyrone Volcanic Group, exposed south of the Beaghmore Fault, is a bimodal-mafic assemblage divided into three formations: the Creggan, Loughmacrory and Beaghmore formations. No U-Pb geochronology exists for this part of the sequence; its age is established from petrochemical correlations to graptolite-bearing Slieve Gallion Inlier (an isolated occurrence of the Tyrone Volcanic Group with its own stratigraphy). The lower Tyrone Volcanic Group records the evolution of an intraoceanic island arc, intra-arc rifting and the formation of a backarc basin.
- The upper Tyrone Volcanic Group (c. 473-469 Ma), exposed north of the Beaghmore Fault, comprises two formations (Greencastle and Broughderg) and is a bimodal-felsic succession. This volcanic-dominated sequence records the accretion of the Tyrone arc to the Tyrone Central Inlier (between c. 473-470 Ma) and late post-obduction ensialic arc rifting (associated with c. 469 Ma alkali basalts and high Zr A-type rhyolites).

8.1.2 Implications for the Grampian-Taconic orogen

Irish Caledonides

- Strong temporal and petrochemical correlations between the Slieve Gallion Inlier (part of the Tyrone Volcanic Group) and Charlestown Group of Co. Mayo suggest they may be part of the same island arc subjected to post-accretion, strike-slip faulting.
- A switch from tholeiitic volcanism to calc-alkaline dominated activity within the Lough Nafooey Group of western Ireland occurred prior to c. 490 Ma, approximately ~15 to 20 Myr earlier than at Tyrone (c. 475 Ma) and Charlestown (c. 470 Ma).
- This suggests arc evolution (and arc-continent collision) was either strongly diachronous across the Irish Caledonides, or the Tyrone and Charlestown volcanics were formed in a younger and distinct arc, and are not part of the Lough Nafooey arc (model favoured below).

Wider context

- Broad correlations can be made across the Grampian–Taconic event. Three major phases of arc-ophiolite accretion identified in the Newfoundland Appalachians are now recognized within the Caledonides.
- Early ophiolite obduction within the Caledonides is recorded by the emplacement of the Deer Park (c. 514 Ma) and Highland Border (c. 500 Ma) ophiolites onto possible outboard microcontinental blocks, broadly equivalent to the emplacement of the Lushs Bight Oceanic Tract (c. 510-501 Ma) of Newfoundland onto the Dashwoods microcontinental block at c. 500-493 Ma (Chew et al. 2010).
- Continued closure of the Iapetus Ocean led to the formation and accretion of the c. <490-476 Ma Lough Nafooey arc (= buried Midland Valley arc?) to the Laurentian margin. This phase of arc-ophiolite accretion is recorded in Newfoundland by the development and emplacement of the Baie Verte Oceanic Tract (c. 489-487 Ma). The syn-collisional stage of the Lough Nafooey arc (Tourmakeady Group; c. 476-470 Ma) appears to be broadly equivalent to the development of the Snooks Arm Group (c. 476-467 Ma) of Newfoundland (Chew et al. 2010).
- The Tyrone Igneous Complex (c. 480-464 Ma) closely resembles elements incorporated within the Annieopsquotch Accretionary Tract of Newfoundland, specifically the c. 480 Ma Annieopsquotch Ophiolite Belt and c. 473-464 Ma Buchans-Robert's Arm groups.
- Strong temporal, structural, geochemical and lithological similarities exist between the Tyrone Plutonic Group and the c. 480 Ma Annieopsquotch Ophiolite Belt of Newfoundland suggesting these complexes have a shared origin and evolution.

- Strong lithological, geochemical and temporal similarities exist between the Tyrone Volcanic Group and the Buchans and Robert's Arm groups of central Newfoundland. Both were also intruded by a late suite of calc-alkaline stitching arc-related intrusives associated with their accretion to outboard microcontinental blocks. This suggests Northern Ireland has the potential to host significant VMS mineralization, common within the Buchans-Robert's arc system.

8.1.3 Implications for VMS mineralization in Northern Ireland

- Through a combination of extensive field mapping and petrochemistry, several stratigraphic horizons have been identified in the Tyrone Igneous Complex which were favourable for the formation and preservation of VMS deposits. Each is closely associated with rift-related and high-temperature petrochemical associations, extensive hydrothermal alteration, synvolcanogenic faults and high-level synvolcanogenic intrusions (dolerite, gabbro, diorite and tonalite).
- Rift-related magmatism is characterized by the eruption of abundant non-arc type Fe-Ti enriched eMORB ('icelandite'), island-arc tholeiite, OIB-like and alkali basalt, high-temperature, M-type and FIV affinity tholeiitic rhyolites with flat to U-shaped REE profiles, and A-type high Zr rhyolites within the calc-alkaline dominated sequence.
- Rift-related mafic lavas occur in the hangingwall to VMS-style mineralization and are closely associated with ironstones (occassionally Au bearing) and/or argillaceous sedimentary rocks representing volcanic quiescence. Extensive hydrothermal alteration, characterized by Na-depletion, high Ba/Sr, Bi, Sb, Ni, CCPI, AI and variable MgO and CaO contents, allows specific target areas to be identified.
- In the lower bimodal-mafic Tyrone arc and backarc, hydrothermal alteration is associated with Zn-Cu mineralization (e.g. Bonnety Bush). Pb-Zn-Cu-Au (Kuroko-type) mineralization occurs in crackle-brecciated and silicified auriferous FII-type rhyolite domes/flows and/or volcaniclastic rocks of the syncollisional bimodal-felsic upper Tyrone arc (e.g. Cashel Rock, Crosh, Broughderg). Rare ophiolite hosted Cu mineralization is characterized by chalcopyrite stringers hosted in sheeted dyke sequences.
- Petrochemically favourable horizons are characterized by high Au and/or high base metal values in prospecting samples and base of till samples (Dalradian Resources Ltd), and abundant untested geophysical anomalies (e.g. IP, EM, magnetics, gravity).
- Preliminary mineral chemistry and ironstone geochemistry studies suggests both may act as vectors to mineralization, along with more standard whole rock

geochemical techniques (e.g. Ba/Sr, Na-depletion), may be used to identify VMS mineralization in each target area.

8.2 Future Work

To further improve our understanding of the Grampian-Taconic orogen and identify areas of VMS mineralization, suggestions for future work are presented below.

8.2.1 Tyrone Igneous Complex: additional geochronology

During the course of this PhD, funding was secured through the NERC Isotope Geosciences Facilities Steering Committee (NIGFSC) to carry out additional U-Pb zircon TIMS and Ar-Ar geochronology at the NERC Isotope Geosciences Laboratory (NIGL) and Scottish Universities Environmental Research Centre (SUERC). Funding is to constrain the age of several key lithologies across the Tyrone Igneous Complex to help resolve unanswered questions regarding the progressive evolution of this arc-ophiolite system and its accretion to the Tyrone Central Inlier. Specific questions which still need to be resolved include:

1. What was the duration of magmatism within the Tyrone Plutonic Group and were amphibolite-facies conditions reached prior to emplacement? Recent U-Pb zircon dating by Draut et al. (2009) has produced a controversially old age for the Tyrone ophiolite (c. 493 Ma). The c. 493 Ma age of Draut et al. appears to be an analytical artefact of the SIMS data (see Cooper et al. 2011 - Chapter 3). Subsequent U-Pb zircon dating by Cooper et al. (2011 – Chapter 3) and Hollis et al. (Submitted – Chapter 5) has suggested the ophiolite formed around c. 484-480 Ma. U-Pb zircon dating of a newly discovered occurrence of plagiogranite (associated with sheeted dykes), will further constrain the timing of its formation.

2. When did the Tyrone Volcanic Group form and how long did magmatism last? Recent U-Pb zircon geochronology from the Tyrone Volcanic Group has constrained the development of the Greencastle Formation of the upper Tyrone arc to c. 473-469 Ma (Cooper et al. 2008; Hollis et al. 2012 – Chapter 4). Arc-emplacement onto the Tyrone Central Inlier has been constrained to c. 470 Ma (Cooper et al. 2011). No geochronology exists for the lower Tyrone Volcanic Group or the uppermost deposits (Broughderg Formation) which post-date arc obduction. U-Pb zircon dating of rhyolite/rhyolitic tuff near the base and top of the volcanic succession will establish the duration of magmatism within the arc and the timing of a recently developed stratigraphy (Hollis et al. 2012). Recent work from the Slieve Gallion Inlier and

petrochemical correlations to the lower Tyrone Volcanic Group suggest the latter may have formed at c. 475 Ma (Chapter 6).

3. Did ophiolite- or arc-emplacement (or both) cause the deformation and metamorphism of the underlying Tyrone Central Inlier? Metamorphic conditions within the Tyrone Central Inlier (c. 670 ± 113 °C, 6.8 ± 1.7 kbar) were reached prior to c. 468 Ma (Chew et al. 2008). U-Pb zircon dating of rare arc-related S-type muscovite granite which intrudes the Tyrone Plutonic Group will provide a minimum age for the timing of its emplacement. Ophiolite obduction may have occurred as late as c. 470 Ma coeval with the accretion of the Tyrone Volcanic Group (Chapter 5). The timing of accretion may have important implications for why the Tyrone ophiolite was obducted and not underplated to the composite Laurentian margin (see Chapter 4). Ar-Ar dating of boudinaged hornblende from the contact between the Tyrone Plutonic Group and Tyrone Central Inlier will further constrain the timing of ophiolite emplacement. Amphibolite-facies conditions within gabbros of the Tyrone Plutonic Group are in excess of 500-550 °C above closure temperature estimates for hornblende. Thus, Ar-Ar dating would record post-metamorphic cooling through this temperature. Arc-emplacement has been constrained to c. 470 Ma (Cooper et al. 2011)

Samples have been collected for U-Pb zircon and amphibole/muscovite/biotite Ar-Ar geochronology from across the Tyrone Igneous Complex. Several samples have been collected for U-Pb zircon dating. Funding allows five samples to be dated by ID-TIMS.

(i) Plagiogranite (associated with sheeted dykes) from Craigballyharky Quarry will further constrain the age of the Tyrone ophiolite
(ii) S-type muscovite granite from Tremoge Glen stitches the Tyrone ophiolite in its present structural position and will provide a minimum age for timing of its emplacement
(iii) Porphyritic andesite from Copney will date the lower Tyrone Volcanic Group (Loughmacrory Formation)
(iv) Rhyolite from Crosh will date the uppermost Tyrone Volcanic Group (Broughderg Formation)
(v) Rhyolitic tuff from Beaghbeg will date the Beaghmore Formation (=backarc of the Tyrone Volcanic Group)

Five samples have been collected for Ar-Ar geochronology:

(i) Amphibolite-facies pegmatitic gabbros which are coeval with dolerite dykes of the Tyrone ophiolite
(ii) Hornblende-bearing lava from the Tyrone arc

(iii) Boudinaged and rotated amphibole from a newly discovered obduction contact between the Tyrone ophiolite and its metamorphic basement
(iv) Late-stage, I-type and calc-alkalic biotite-bearing granite (c. 464 Ma)
(v) Post-orogenic muscovite bearing-pegmatites

Some detailed Ar-Ar geochronology has already been carried out on the Tyrone Central Inlier (see Chew et al. 2008). Minerals for Ar-Ar geochronology have been hand picked. Amphibole, biotite and muscovite mineral closure temperatures are well established in the literature and will constrain the thermal evolution of the rocks through a window of ~300 to 550˚C. Discrepancies between U-Pb zircon and Ar-Ar geochronology, due to uncertainties in the ages of Ar-Ar standards and radioactive decay rates, have recently been discussed by Kuiper et al. (2008). Corrections at 475 Ma would be within error of U-Pb zircon and Ar-Ar dates.

8.2.2 Pb isotopes

Petrochemical suites:
No Pb isotope work has been carried out over the Tyrone Igneous Complex. Samples analysed from the Tyrone Volcanic Group for whole rock geochemical analysis, Nd and Sr isotopes should be analysed for Pb isotopes. This would provide important constraints on the sources for the different petrochemical suites identified in the Tyrone Volcanic Group (e.g. IAT, Fe-Ti eMORB, OIB-like, CAB, Alk – see Chapter 4) and link them to specific source regions (e.g. DM, HIMU, etc).

Hidden basement and its implications:
Pb isotope work on the Tyrone Igneous Complex and Tyrone Central Inlier may also help to constrain the nature of the basement beneath County Tyrone. High LILE, LREE enrichement and strongly negative εNd_t values within the Tyrone Volcanic Group suggest either the Tyrone arc formed on a fragment of continental material (the model favoured herein) or was contaminated by the subduction of continental material (accepting a model of diachronous collision). Furthermore, Pb isotope work may shed further light on the nature of the basement beneath the Tyrone Central Inlier, as recent work by Flowerdew et al. (2009) has suggested there may be hidden Archean crust at depth under NW Ireland.

Link to Curraghinalt?
Mesothermal Au, shear-zone-hosted hosted Au, and stratiform Pb-Zn ± Au mineralization is widespread within the Dalradian Supergroup of Counties Tyrone and Londonderry, Northern Ireland (e.g. Curraghinalt, Scotch Town, Glenlark targets

respectively) (e.g. Lusty et al. 2009). A Pb isotope study on the individual targets, their host successions (Dalradian Supergroup), and the Tyrone Volcanic Group may help to address the source of the contained metals at mineralized showings across the Sperrin Mountains of Northern Ireland and economic deposits such as Curraghinalt. Curraghinalt, a large mesothermal Au deposit located several km NW of the Omagh Thrust, consists of at least seven primary Au bearing quartz veins ranging in width from 0.5 to 3.0m. Approximately 26 km of drilling (>250 drillholes) has defined a NI 43-101 compliant measured resource of 0.02 Mt at 21.51 g/t Au, an indicated resource of 1.1 Mt at 12.84 g/t Au, and an inferred resource of 5.45 Mt at 12.74 g/t Au (www.dalradian.com). This makes it the UK's largest Au deposit by some margin.

As the Tyrone Volcanic Group structurally underlies the Neoproterozoic host succession of Curraghinalt (Dalradian Supergroup), and the along-strike Au deposit Cavanacaw (=16,000 Oz measured, 88,000 Oz indicated, 295,800 Oz inferred: www.galantas.com), it has long been though of as the source of the contained metal (i.e. Au, Pb, Cu, etc) (e.g. Parnell et al. 2000). This is consistent with similar $\delta^{34}S_{CDT}$ values from sulphides at Cashel Rock, Curraghinalt, Cavanawaw, Charlestown and regional Au-bearing quartz veins (Parnell et al. 2000). Pb isotopes from Charlestown are similar to those from Cavanacaw suggesting an extension of the underthrust Tyrone Igneous Complex was the most likely source of Pb at Cavanacaw (Parnell et al. 2000). No Pb isotope data from Curraghinalt was presented by Parnell et al. (2000), which is characterized by more a Cu-dominated mineral assemblage.

Recent unpublished Ar-Ar dating of muscovite in wallrock clasts of quartz veins at Curraghinalt has produced high precision ages of 459-458 Ma slightly younger than peak metamorphism during the Grampian orogeny (Clive Rice personal communication 2012). Similar ages of c. 454 Ma have been produced for sericite from veinlets (with and without molybdenite) cutting Au-bearing veins. These ages are consistent with recent re-Os dating of molybdenite (c. 459 Ma) by Dave Selby which suggests an Ordovician age for Au mineralization (Rice pers comm.). One sample of sericite has produced an older age of 420 Ma, which may suggest the Ar-Ar system of this sample was reset during the Late Caledonian.

Au mineralization is widespread along either side of the Omagh Thrust both within the Tyrone Volcanic Group at Broughderg, Crosh, Tullybrick, Mulnafye, Cashel Burn and Cashel Rock (Clifford et al. 1992), and within the Dalradian Supergroup (e.g. Rylagh, Glenlark, Glenmacoffer, Scotch Town, Alwories, Golan Burn, Glenerin, Glensass, Coneyglen, Bessy Bell: e.g. Lusty et al. 2009). This is part of a wider trend of Au mineralization along the Fair Head – Clew Bay line of Ireland and its continuations: the

Highland Boundary Fault of Scotland and the Baie Verte – Brompton line of Newfoundland (e.g. van Staal 2007, Ryan & Dewey 2011). Establishing a link to the underthrust arc-related volcanics would be of considerable interest to the mining community as the majority of Au occurrences in the north of Ireland appear to be restricted to Ireland 10's of kms from the Fair Head - Clew Bay Line or deep seated crustal sutures such as the Donegal lineament further north (e.g. Parnell et al. 2000, Lusty et al. 2009).

8.2.3 'Gaps in the Grampian'

To further constrain the evolution of the Grampian orogeny there are several important studies which should be undertaken. Only when the origin and evolution of each terrane is understood can accurate models for the orogen in the British and Irish Caleonides be developed.

Ballantrae Ophiolite Complex:

The Ballantrae Ophiolite Complex of Scotland forms an integral part of the orogen and is one of the most extensively studied oceanic tracts of the British and Irish Caledonides. However, despite decades of research, the age of arc-related tuffs and within-plate lavas are still poorly constrained (Chapter 5). Old Sm-Nd ages (e.g. Sm-Nd age of 501 ± 12 Ma: Thirwall & Bluck 1984) are entrenched in the literature and are extremely unreliable. Zircon ages of tuffs from Ballantrae by Sawaki et al. (2010) are also associated with large errors (typically ± >15 Ma) and need improvement. High resolution ID-TIMS dating of tuffs, lavas and within-plate gabbro from Ballantrae should be carried as a high priority to constrain the evolution of these often understudied parts of its succession. As detailed in Chapter 5, strong temporal, geochemical and lithological similarities exist between the Ballantrae Ophiolite Complex and the Tyrone Igneous Complex; however correlation is hampered by insufficient and/or imprecise geochronology.

Highland Border Complex

The Highland Border Complex, broadly analogous to the Clew Bay Complex of Ireland (Chew et al. 2003; Tanner & Sutherland 2007; Chew et al. 2010), is intermittently exposed along the Highland Boundary Fault as a series of Lower Paleozoic deep marine sedimentary rocks with isolated occurrences of mafic and ultramafic rocks (described in Henderson & Robertson 1982; Curry et al. 1984; Bluck 2002; Tanner & Sutherland 2007; Henderson et al. 2009; Bluck 2010). Poor exposure and heavy faulting across the complex has resulted in its internal stratigraphy and place within the Grampian orogeny becoming contentious issues (e.g. Tanner & Sutherland 2007; Bluck 2010). Although recent studies have suggested the majority of the sequence is in 'stratigraphic continuity' with the Dalradian (Tanner & Sutherland 2007), evidence presented by Bluck (2010) clearly demonstrates a number of sequences young NW towards the Dalradian, not SE as proposed by Tanner and Sutherland (2007). Although it is generally accepted the revised stratigraphy of Tanner and Sutherland (2007) is largely correct and the complex comprises the autochthonous Trossachs Group of the Dalradian Supergroup overlain by an obducted ophiolite (Highland Border Ophiolite), there are clearly several areas which require further investigation (see Bluck 2010).

Charlestown Group:

As detailed in Chapter 6, geochemistry and geochronology within the Charlestown Group is limited. No detailed trace-element, REE or Nd-isotope work exists in the literature. Strong lithological, geochemical and temporal similarities exist between the Tyrone Volcanic and Charlestown groups. Furthermore, the Charlestown Cu deposit (O'Connor & Poustie (1986) bears a striking similarity to the Cashel Rock VMS target (Hollis 2012 unpublished report). Selected U-Pb zircon dating and geochemistry would provide valuable insights into the evolution of this arc succession and its role in the Irish Caledondies. Recollection and investigation of a graptolite fauna may prove useful as at Slieve Gallion (e.g. Cooper et al. 2008). The Charlestown volcanics were visited by the author, Richard Herrington and Mark Cooper during early 2012; samples have been collected for geochemical analysis and possible U-Pb geochronology for a masters project. Some fragmentary graptolites were collected for analysis at the Natural History Museum.

Appendix

List of files on attached DVD

Chapter 2:

Word files

- Laboratory procedures

Excel files

- T2-x- Precision and accurary for SPH prefixed repeats
- T2-x2- XRF precision and accuracy for international standards
- T2-x3- ICP-MS precision and accuracy for international standards

Chapter 3:

Word files

- T3.1- U-Pb zircon geochronology data
- T3.2- Geochemistry data

Chapter 4:

Word files

- T4.1- Petrochemical suites summary table from manuscript
- T4.2- U-Pb zircon geochronology data
- T4.3- Summary of all geochronology in TIC

Excel files

- T4.x- Geochemistry data

Chapter 5:

Word files

- T5.1- U-Pb zircon geochronology data

Excel files

- T5.x- Geochemistry data (whole rock and mineral chemistry)

Chapter 6:

Word files

- T6.1- Geochemistry data
- T6.2- U-Pb zircon geochronology data

Chapter 7:

*Word files – **Additional information***

- Introduction to regional semiconformable and mineralization-proximal hydrothermal alteration
- Ironstone geochemistry and associated units
- Mineral chemistry of the Tyrone Volcanic Group

- Deformation in the Tyrone Volcanic Group
- Element mobility in the lower Tyrone Volcanic Group

Excel files

- T7.x- Ironstone geochemistry data
- T7.x2- Drillcore geochemistry data
- T7.x3- Mineral chemistry data

Reference list

AFONSO, J.C. & ZLOTNIK, S. 2011. The subductability of continental lithosphere, in BROWN, D. & RYAN, P.D. (eds.). *Arc-Continent Collision.* Frontiers in Earth Sciences, 53-86.

ALLEN, R.L., WEIHED, P., BLUNDELL, D.J., CRAWFORD, T., DAVIDSON, G., GALLEY, A., GIBSON, H., HANNINGTON, M., HERRINGTON, R., HERZIG, P., LARGE, R., LENTZ, D., MASLENNIKOV, V., MCCUTCHEON, S., PETER, J. & TORNOS, F. 2002. Global comparisons of volcanic-associated massive sulphide districts, in BLUNDELL, D ET AL. (eds). *The timing and location of major ore deposits in an evolving orogen.* Geological Society of London Special Publication, **204**, 13-37.

ALSOP, G.I. & HUTTON, D.H.W. 1993. Major southeast directed Caledonian thrusting and folding in the Dalradian rocks of mid-Ulster: Implications for Caledonian tectonics and mid-crustal shear zones. *Geological Magazine*, **130**, 233-244.

ALT, J.C. & TEAGLE, D.A.H. 2000. Hydrothermal alteration and fluid fluxes in ophiolites and oceanic crust, in DILEK, Y., MOORES, E.M., ELTHON, D. & NICOLAS, A. (eds). *Ophiolites and Oceanic Crust: New insights from field studies and the Ocean Drilling Program.* Boulder, Colorado, Geological Society of America Special Paper, **349**, 273-282.

ANDERTON, R. 1982. Dalradian deposition and the late Precambrian-Cambrian history of the N Atlantic region: a review of the early evolution of the Iapetus Ocean. *Journal of the Geological Society, London*, **139**, 421431.

ANGUS, N.S. 1962. Oscellar hybrids from the Tyrone Igneous Series, Ireland. *Geological Magazine,* **99**, 9-26.

ANGUS, N.S. 1970. A Pyroxene-Hornfels from the Basic Plutonic Complex, Co. Tyrone, Ireland. *Geological Magazine*, **107**, 277-287.

ANGUS, N.S. 1977. The Craigballyharky granitic complex within the Tyrone Igneous Series. *Proceedings of the Royal Irish Academy, Section B – Biological, Geological and Chemical Science*, **77**, 181-199.

ANONYMOUS. 1972. Penrose field conference on ophiolites. *Geotimes*, **17**, 24-55.

BALL, T.K. & BLAND, D.J. 1985. The Cae Coch volcanogenic massive sulphide deposit, Trefriw, North Wales. *Journal of the Geological Society, London,* **142**, 889-898.

BARRETT, T.J. & MACLEAN, W.H. 1994. Mass changes in hydrothermal alteration zones associated with VMS deposits of the Noranda area. *Exploration and Mining Geology,* **3**, 131-160.

BARRETT, T.J., & MACLEAN, W.H. 1999. Volcanic sequences, lithogeochemistry, and hydrothermal alteration in some bimodal volcanic-associated massive sulfide systems. In BARRIE, C.T., AND HANNINGTON, D. (eds) *Volcanic-associated massive*

sulfide deposits: processes and examples in modern and ancient environments. Society of Economic Geologists, *Reviews in Economic Geology*, **8**, 101-131.

BARRETT, T.J., JARVIS, I. & JARVIS, K.E. 1990. Rare earth element geochemistry of massive sulfide-sulfates and gossans on the southern Explorer Ridge. Geology, **18**, 583-586.

BARRIE, C.T. & HANNINGTON, M.D. 1999. Introduction: Classification of VMS deposits based on host rock composition, *in* BARRIE, C.T. & HANNINGTON, M.D. (eds.). *Volcanic-Associated Massive Sulfide Deposits: Processes and Examples in Modern and Ancient Settings.* Reviews in Economic Geology, **8**, 2-10.

BARRIE, C.T., LUDDEN, J.N. & GREEN. T. 1993. Geochemistry of volcanic rocks associated with Cu-Zn and Ni-Cu deposits in the Abitibi subprovince. *Economic Geology,* **88**, 1341-1358.

BARRIE, C.T. & PATTISON, J. 1999. Fe-Ti basalts, high silica rhyolites, and the role of magmatic heat in the genesis of the Kam-Kotia volcanic-associated massive sulphide deposit, western Abitibi Subprovince, Canada. *Economic Geology monographs,* **10**, 577-592.

BAXTER, E.F., AGUE, J.J. & DEPAOLO, D.J. 2002. Prograde temperature-time evolution in the Barrovian type-locality constrained by Sm/Nd garnet ages from Glen Cova, Scotland. *Journal of the Geological Society, London*, **159**, 71-82.

BAYSWATER URANIUM. 2012. http://www.bayswateruranium.com/avoca.html

BEAMISH, D., CUSS, R.J., LAHTI, M., SCHEIB, C. & TARTARAS, E. 2007. The Tellus airborne geophysical survey of Northern Ireland: Final processing report. *British Geological Survey Internal Report,* IR/06/136, pp. 74.

BICKLE, M.J. & TEAGLE, D.A.H. 1992. Strontium alteration in the Troodos ophiolite: implications for fluid fluxes and geochemical transport in mid-ocean ridge hydrothermal systems. *Earth and Planetary Science Letters*, **113**, 219-237.

BIERLEIN, F.P., GROVES, D.I. & CAWOOD, P.W. 2009. Metallogeny of accretionary orogens – The connection between lithospheric processes and metal endowment. *Ore Geology Reviews*, **36**, 282-292.

BLUCK, B. J. 1985. The Scottish paratectonic Caledonides. *Scottish Journal of Geology*, **21**, 437-464.

BLUCK, B.J. 2002. The Midland Valley terrane, in TREWIN, N.H. (ed.). *The Geology of Scotland.* Geological Society of London, 149-166.

BLUCK, B.J. 2007. Anomalies on the Cambro-Ordovician passive margin of Scotland. *Proceedings of the Geologists' Association*, **118**, 55-62.

BLUCK, B.J. 2010. The Highland Boundary Fault and the Highland Border Complex. *Scottish Journal of Geology*, **46**, 113-124.

BLUCK, B.J., HALLIDAY, A.N., AFTALION, M. & MACINTYRE, R.M. 1980. Age and origin of the Ballantrae ophiolite and its significance to the Caledonian orogeny and Ordovician time scale. *Geology*, **8**, 492-495.

BLUCK, B. J., GIBBONS, W. & IINGHAM, J. K. 1992. Terranes. In Cope, J. C. W., Ingham, J. K and Rawson, P. F. (eds) Atlas of Palaeogeography and Lithofacies, *Geological Society of London, Memoirs*, **13**, 1-4.

BOURCIER, W.L. & BARNES, H.L. 1987. Ore solution chemistry. VII Stabilities of chloride and bisulphide complexes of zinc to 350 °C. *Economic Geology,* **82**, 1839-1863.

BOUTELIER, D. & CHEMENDA, A. 2011. Physical modeling of arc-continent collision: a review of 2D, 3D, purely mechanical and thermomechanical experimental models, in BROWN, D. & RYAN, P.D. (eds.). *Arc-Continent Collision.* Frontiers in Earth Sciences, 445-473.

BRADSHAW, G.D., ROWINS, S.M., PETER, J.M. & TAYLOR, B.E. 2008. Genesis of the Wolverine volcanic sediment-hosted massive sulfide deposit, Finlayson Lake District, Yukon, Canada: Mineralogical, mineral chemical, fluid inclusion, and sulfur isotope evidence. *Economic Geology*, **103**, 35-60.

BRITISH GEOLOGICAL SURVEY. 1986. Metamorphic Rocks – The crystalline Caledonides, in *British Regional Geology: Northern Ireland*, 5-17.

BROWN, D., RYAN, P.D., AFONSO, J.C., BOUTELIER, D., BURG, J.P., BYRNE, T., CALVERT, A., COOK, F., DEBARI, S., DEWEY, J.F., GERYA, T.V., HARRIS, R., HERRINGTON, R., KONSTANTINOVSKAYA, E., RESTON, T., AND ZAGOREVSKI, A. 2011a. Arc continent collision: the making of an orogen, in BROWN, D. & RYAN, P.D. (eds.*). Arc-Continent Collision.* Frontiers in Earth Sciences, 477-493.

BROWN, D., HERRINGTON, R. & ALVAREZ-MARRON, J. 2011b. Processes of arc-continent collision in the Uralides, in BROWN, D. & RYAN, P.D. (eds.). *Arc-Continent Collision.* Frontiers in Earth Sciences, 311-340.

BYRNE, T., CHAN, Y.-C., RAU, R.-J., LU, C.-Y, LEE, Y.-H. & WANG, Y.-J. 2011. The arc-continent collision in Taiwan, in BROWN, D. & RYAN, P.D. (eds.). *Arc-Continent Collision.* Frontiers in Earth Sciences, 213-245.

CALVERT, A.J. 2011. The seismic structure of island arc crust, in BROWN, D. & RYAN, P.D. (eds.). *Arc-Continent Collision.* Frontiers in Earth Sciences, 87-119.

CAMERON, I.B. & OLD, R.A. 1997. Geology of the country around Cookstown. 1:50 000 Geological Sheet 27 (Cookstown). Geological Survey of Northern Ireland. *Technical Report* GSNI/97/7.

CAMPBELL, I.H., COAD, P., FRANKLIN, J.M., GORTON, M.P., HART, T.R., SCOTT, S.D., SOWA, J., & THURSTON, P.C. 1981. Grant 80: Rare earth elements in felsic volcanic rocks associated with Cu-Zn massive sulphide mineralization. *Ontario Geological Survey Miscellaneous Paper* 98, 45-53.

CARVALHO, D. BARRIGA, F.J.A.S. & MUNHA, J. 1999. Bimodal-siliciclastic systems - The case of the Iberian Pyrite Belt, in BARRIE, C.T. & HANNINGTON, M.D. (eds.). *Volcanic-Associated Massive Sulfide Deposits: Processes and Examples in Modern and Ancient Settings*. Reviews in Economic Geology, **8**, 375-402.

CATHELINEAU, M. 1988. Cation site occupancy in chlorites and illites as a function of temperature. *Clay minerals*, **23**, 471-485.

CAWOOD, P.A., NEMCHIN, A.A., STRACHAN, R., PRAVE, T. & KRABBENDAM, M. 2007. Sedimentary basin and detrital zircon record along East Laurentia and Baltica during assembly and breakup of Rodinia. *Journal of the Geological Society, London*, **164**, 257-275.

CHACKSFIELD, B.C. 2010. A preliminary interpretation of Tellus airborne magnetic and electromagnetic data for Northern Ireland. *British Geological Survey Internal Report*, IR/07/041, pp.51.

CHARLESWORTH, H.A.K. 1960. The Lower Palaeozoic inlier of the Curlew Mountains anticline. *Proceedings of the Royal Irish Academy*, **61B**, 37-50.

CHEW, D.M. 2009. Grampian orogeny, in HOLLAND, C.H. & SANDERS, I.S. (eds) *The Geology of Ireland. 2nd edition*, 69-93.

CHEW, D.M., DALY, J.S., PAGE, L.M. & KENNEDY, M.J. 2003. Grampian orogenesis and the development of blueschist facies metamorphism in western Ireland. *Journal of the Geological Society, London*, **160**, 911-924.

CHEW, D.M., GRAHAM, J.R. AND WHITEHOUSE, M.J. 2007. U-Pb zircon geochronology of plagiogranites from the Lough Nafooey (= Midland Valley) arc in western Ireland: constraints on the onset of the Grampian orogeny. *Journal of the Geological Society, London,* **164**, 747-750.

CHEW, D.M., FLOWERDEW, M.J., PAGE, L.M., CROWLEY, Q.G., DALY, J.S., COOPER, M. R., & WHITEHOUSE, M.J. 2008. The tectonothermal evolution and provenance of the Tyrone Central Inlier, Ireland: Grampian imbrication of an outboard Laurentian microcontinent?. *Journal of the Geological Society, London*, **165**, 675-685.

CHEW, D.M., DALY, J.S., MAGNA, T., PAGE, L.M., KIRKLAND, C.L., WHITEHOUSE, M.J. & LAM, R. 2010. Timing of ophiolite obduction in the Grampian orogen. *Geological Society of America Bulletin*, **122**, 1787–1799.

CHRISTIE, D.M. & SINTON, J.M. 1981. Evolution of abyssal lavas along propagating segments of the Galapagos spreading centre. *Earth and Planetary Science Letters*, **56**, 321-335.

CHRISTIE, D.M. & SINTON, J.M. 1986. Major element constraints on melting, differentiation and mixing of magmas from the Galapagos 95.5°W propagating rift system. *Contributions to Mineralogy and Petrology*, **94**, 274-288.

CLIFF, R.A., YARDLEY, B.W.D., & BUSSY, F. 1996. U-Pb and Rb-Sr geochronology of magmatism and metamorphism in the Dalradian of Connemara, W. Ireland. *Journal of the Geological Society, London,* **153**, 109-120.

CLIFFORD, J.A., EARLS, G., MELDRUM, A.H. & MOORE, N. 1992. Gold in the Sperrin Mountains, Northern Ireland: an exploration case history, in BOWDEN, A.A., EARLS G., O'CONNOR, P.G. & PYNE. J.F. (eds). *The Irish Minerals Industry 1980-1990*. Irish Association for Economic Geology, Dublin, 77-87.

CLIFT, P.D., & RYAN, P.D. 1994. Geochemical evolution of an Ordovician island arc, South Mayo, Ireland. *Journal of the Geological Society, London*, **151**, 329-342.

COBBING, E.J. 1969. Schistosity and folding in a banded gabbro from Tyrone. *Bulletin of the Geological Survey of Great Britain*, **30**, 89-97.

COBBING, E.J., MANNING, P.I. & GRIFFITH, A.E. 1965. Ordovician-Dalradian unconformity in Tyrone. *Nature*, **206**, 1132-50.

COLMAN, T.B. & COOPER, D.C. 2000. Exploration for Metalliferous and Related Minerals in Britain: A guide. 2nd Edition. British Geological Survey, DTI Minerals Programme Publication, No. 1, pp.78

COLMAN-SADD S.P., STONE, P., SWINDEN, H.S. & BARNES R.P. 1992. Parallel geological development in the Dunnage Zone of Newfoundland and the Lower Palaeozoic terranes of southern Scotland: an assessment. *Transactions of the Royal Society of Edinburgh: Earth Sciences*, **83**, 571-594.

CONDON, D., SCHOENE, B., BOWRING, S., PARRISH, R., MCLEAN, N., NOBLE, S. & CROWLEY, Q. 2007. EARTHTIME; isotopic tracers and optimized solutions for high-precision U-Pb ID-TIMS geochronology. *Eos, Transactions, American Geophysical Union*, **88**, no. 52, Suppl.

COOPER, R.A. & LINDHOLM, K. 1990. A precise worldwide correlation of early Ordovician graptolite sequences. *Geological Magazine*, **127**, 497-525.

COOPER, M.R. & MITCHELL, W.I. 2004. Midland Valley Terrane, in MITCHELL, W.I. (ed)., *The Geology of Northern Ireland. Our Natural Foundation, second edition.* Geological Survey of Northern Ireland.

COOPER, M.R., CROWLEY, Q.G. & RUSHTON, A.W.A. 2008. New age constraints for the Ordovician Tyrone Volcanic Group, Northern Ireland. *Journal of the Geological Society, London*, **165**, 333-339.

COOPER, M.R., CROWLEY, Q.G., HOLLIS, S.P., NOBLE, S.R., ROBERTS, S., CHEW, D., EARLS, G., HERRINGTON, R. & MERRIMAN, R.J. 2011. Age constraints and geochemistry of the Ordovician Tyrone Igneous Complex, Northern Ireland: implications for the Grampian orogeny. *Journal of the Geological Society, London*, **168**, 837-850.

COOPER, M.R., ANDERSON, H., WALSH, J.J., VAN DAM, C.L., YOUNG, M.E., EARLS, G. & WALKER, A. 2012. Palaeogene Alpine tectonics and Icelandic plume-related magmatism and

deformation in Northern Ireland. *Journal of the Geological Society, London*, **169**, 29-36.

CORFU, F. & NOBLE, S.R. 1992. Genesis of the southern Abitibi greenstone belt, Superior Province, Canada: Evidence from zircon Hf-isotope analyses using a single filament technique. *Geochimica et Cosmochimica Acta*, **56**, 2081-2097.

CUMMINS, W.A. 1954. An Arenig volcanic series near Charlestown, Co. Mayo.. *Geological Magazine*, **91**, 102-104.

CURRY, G.B., BLUCK, B.J., BURTON, C.J., INGHAM, J.K., SIVETER, D.J. & WILLIAMS, A. 1984. Age, evolution and tectonic history of the Highland Border Complex, Scotland. *Transactions of the Royal Society of Edinburgh*: *Earth Sciences*, **75**, 113-133.

CUTTS, J.A., ZAGOREVSKI, A., MCNICOLL, V., & CARR, S.D. 2012. Tectono-stratigraphic setting of the Moreton's Harbour Group and its implications for the evolution of the Laurentian margin: Notre Dame Bay, Newfoundland. *Canadian Journal of Earth Sciences*, **49**, 111-127.

DALY, J.S. 2009. Precambrian, in HOLLAND, C.H. & SANDERS, I.S. (eds) *The Geology of Ireland. 2nd edition*, 7-42.

DEBARI, S.M. & GREENE, A.R. 2011. Vertical stratification of composition, density, and inferred magmatic processes in exposed arc crustal sections, in BROWN, D. & RYAN, P.D. (eds.). *Arc-Continent Collision.* Frontiers in Earth Sciences, 121-144.

DEER, W.A., HOWIE, R.A. & ZUSSMAN, J. 1989. *An introduction to the rock forming minerals.* New York, pp.528.

DEMPSTER, T.J. & BLUCK, B.J. 1991. The age and tectonic significance of the Bute Amphibolite, Highland Border Complex, Scotland. *Geological Magazine*, **128**, 77-80.

DEPAOLO, D.J. 1981. Trace element and isotopic effects of combined wallrock assimilation and fractional crystalization. *Earth and Planetary Science Letters*, **53**, 189-202.

DEPAOLO, D.J. 1988. *Neodynium Isotope Geology.* New York, Springer Verlag, p187.

DEPAOLO, D.J. & WASSERBURG, G.J. 1976. Nd isotopic variations and petrogenetic models. *Geophysical Research Letters*, **3**, 249-252.

DERONDE, C.E.J. 1995. Fluid chemistry and isotope characteristics of seafloor hydrothermal systems and associated VMS deposits: potential for magmatic contributions. *Mineralogical Association of Canada Short Course*, **23**, 479-510.

DEWEY, J.F. 2003. Ophiolites and lost oceans: rifts, ridges, arcs and/or scrapings. *Journal of the Geological Society of America, Special Paper*, **373**, 153-158.

DEWEY, J.F. 2005. Orogeny can be very short. *Proceedings of the National Academy of Sciences of the United States of America*, **102**, 15286-15293.

DEWEY, J.F. & CASEY, J.F. 2011. The origin of obducted large-slab ophiolite complexes, in BROWN, D. & RYAN, P.D. (eds.). *Arc-Continent Collision.* Frontiers in Earth Sciences, 431-444.

DEWEY, J.F. & MANGE, M.A. 1999. Petrography of Ordovician and Silurian sediments in the western Irish Caledonides: tracers of a short-lived Ordovician continent-arc collision orogeny and the evolution of the Laurentian Appalachian-Caledonian margin. In MacNiocaill, C. & Ryan, P.D. (eds) *Continental Tectonics*. Geological Society of London, Special Publication, **164**, 55-107.

DEWEY, J.F. & RYAN, P.D. 1990. The Ordovician evolution of the South Mayo Trough, western Ireland. *Tectonics*, **9**, 887-901.

DEWEY, J.F. & SHACKLETON, R.M. 1984. A model for the evolution of the Grampian tract in the early Caledonides and Appalachians. *Nature*, **312**, 115-121.

DEWEY, J.F., RICKARDS, R.B. & SKEVINGTON, D.G. 1970. New light on the age. Of the Dalradian deformation and metamorphism in western Ireland. *Norsk Geologisk Tidsskrift*, **50**, 19-54.

DEWOLFE, M.D., GIBSON, H.L. & PIERCEY, S.J. 2009. Petrogenesis of the 1.9 Ga mafic hanging wall sequence to the Flin Flon, Callinan, and Triple 7 massive sulphide deposits, Flin Flon, Manitoba, Canada. *Canadian Journal of Earth Sciences*, **46**, 509-527.

DILEK, Y. & FURNES, H. 2011. Ophiolite genesis and global tectonics. Geochemical and tectonic fingerprinting of ancient oceanic lithosphere. *GSA Bulletin*, **123**, 387-411.

DIVI, S.R., THORPE, R.I. & FRANKLIN, J.M. 1979. Application of discriminant analysis to evaluate compositional controls of stratiform massive sulphide deposits in Canada. Journal of the International Association for Mathematical Geology, **11**, 391-406.

DOUVILLE, E., BIENVENU, P., CHARLOU, J.L., DONVAL, J.P., FOUQUET, Y., APPRIOU, P. & GAMO, T. 1999. Yttrium and rare earth elements in fluids form various deep-sea hydrothermal systems. *Geochimica et Cosmochimica Acta*, **63**, 627-643.

DOYLE, M.G. & ALLEN, R.L. 2003. Sub sea floor replacement in volcanic-hosted massive sulfide deposits. *Ore Geology Reviews,* **23**, 183-222.

DRAUT, A.E. & CLIFT, P.D. 2001. Geochemical evolution of arc magmatism during arc-continent collision, South Mayo, Ireland. *Geology*, **29**, 543-546.

DRAUT, A.E., CLIFT, P.D., CHEW, D.M., COOPER, M.J., TAYLOR, R.N. & HANNIGAN, R.E. 2004. Laurentian crustal recycling in the Ordovician Grampian Orogeny: Nd isotopic evidence from western Ireland. *Geological Magazine*, **114**, 195-207.

DRAUT, A.E., CLIFT, P.D., AMATO, J.M., BLUSZTAJN, J. & SCHOUTEN, H. 2009. Arc-continent collision and the formation of continental crust: a new geochemical and isotopic record from the Ordovician Tyrone Igneous Complex, Ireland. *Journal of the Geological Society, London*, **166**, 485-500.

DUNNING, G.R. & KROGH, T.E. 1985. Geochronology of ophiolites in the Newfoundland Appalachians. *Canadian Journal of Earth Sciences*, **22**, 1659-1670.

DUNNING, G.R., KEAN, B.F., THURLOW, J.G. & SWINDEN, H.S. 1987. Geochronology of the Buchans, Roberts Arm, and Victoria Lake groups and Mansfield Cove Complex, Newfoundland. *Canadian Journal of Earth Sciences*, **24**, 1175-1184.

EASTOE, C.J., SOLOMON, M. & WALSHE, J.L. 1987. District-scale alteration associated with massive sufide deposits in the Mount Read volcanics, western Tasmania. *Economic Geology*, **82**, 1239-1258.

ELDERFIELD, H. & GREAVES, M.J. 1982. The rare earth elements in seawater. Nature, **296**, 214-218.

ELDRIDGE, C.S., BARTON, P.B. JR. & OHMOTO, H. 1983. Mineral textures and their bearing on the formation of Kuroko orebodies. *Economic Geology Monograph,* **5**, 241-281.

EMBLY, R.W., JONASSON, I.R., PERFIT, M.R., FRANKLIN, J.M., TIVEY, M.A., MALAHOFF, A., SMITH, M.F. & FRANCAIS, T.J.G. 1988. Submersible investigation of an extinct hydrothermal system on the Galapagos Ridge: sulphide mounds, stockwork zone, and differentiated lavas. *Canadian Mineralogist,* **26**, 517-539.

ERNST, W.G. & LIU, J. 1998. Experimental phase equilibrium study of Al- and Ti-contents of calcic amphibole in MORB - A semiquantitative thermobarometer. *American Mineralogist*, **83**, 952-969.

FLINN, D. & OGLETHORPE, R.J.D. 2005. A history of the Shetland Ophiolite Complex. *Scottish Journal of Geology*, **41**,141-148.

FLOWERDEW, M.J., DALY, J.S., & WHITEHOUSE M.J. 2005. 470 Ma granitoid magmatism associated with the Grampian Orogeny in the Slishwood Division, NW Ireland. *Journal of the Geological Society, London*, **162**, 563-575.

FLOWERDEW, M.J., CHEW, D.M., DALY, J.S. & MILLAR, I.L. 2009. Hidden Archaean and Palaeoproterozoic crust in NW Ireland? Evidence from zircon Hf isotopic data from granitoid intrusions. *Geological Magazine*, **146**, 903-916.

FORNARI, D.J., PERFIT, M.R., MALAHOFF, A. & EMBLEY, R. 1983. Geochemical studies of abyssal lavas recovered by DSRV Alvin from Eastern Galapagos Rift, Inca Transform, and Ecuador Rift, 1, Major Element Variations in Natural glasses and spacial distribution of lavas. *Journal of Geophysical Research*, **88**, 10519-10529.

FRANKLIN, J.M., LYDON, J.W. & SANGSTER, D.F. 1981. Volcanic-associated massive sulfide deposits, in SKINNER, B.J. (ed.). *Economic Geology 75th Anniversary Volume*. Society of Economic Geologists, 485-627.

FRANKLIN, J.M., HANNINGTON, M.D., JONASSON, I.R. & BARRIE, C.T. 1998. Arc-related volcanogenic massive sulphide deposits. Proceedings of Short Course on Metallogeny of Volcanic Arcs, January 24-25, Vancouver: *British Columbia Geological Survey Open-File* 1998-8, N1-N32.

FRANKLIN, J.M., GIBSON, H.L., JONASSON, I.R. & GALLEY, A.G. 2005. Volcanogenic Massive Sulfide Deposits, *in* HEDENQUIST, J.W., THOMPSON, J.F.H., GOLDFARB, R.J. AND RICHARDS, J.P. (eds.). *Economic Geology 100th Anniversary Volume.* The Economic Geology Publishing Company, 523-560.

FRIEDRICH, A.M., HODGES, K.P., BOWRING, S.A., & MARTIN, M.W. 1999a. Geochronological constraints on the magmatic, metamorphic and thermal evolution of the Connemara Caledonides, western Ireland. *Journal of the Geological Society, London*, **156**, 1217-1230.

FRIEDRICH, A.M., BOWRING, S., MARTIN, M.W. & HODGES, K.V. 1999b. Short-lived continental magmatic arc at Connemara, western Irish Caledonides: Implications for the age of the Grampian orogeny. *Geology*, **27**, 27-30.

FRYER, B.J., KERR, A., JENNER, G.A. & LONGSTAFFE, F.J. 1992. Probing the crust with plutons: regional isotopic geochemistry of granitoid intrusions across insular Newfoundland. *Current Research - Newfoundland and Labrador Department of Natural Resources*, Report 92-1, 119-140.

GALE, G.H. 2003. Vectoring volcanogenic massive sulphide deposits using rarth earth elements and other pathfinder elements at the Ruttan mine, Manitoba (NTS 63B5), in Report of Activities 2003, Manitoba Industry, Trade and Mines, Manitoba Geological Survey, 54-73.

GALE, G.H., FEDIKOW, M.A.F. & HUTCHINSON, R.W. 2002. Distinguishing barren from productive exhalative strata and vectoring toward hydrothermal vent sites using Eu [abs]. *Geological Society of America Abstracts with Programs,* **34**, 113.

GALLEY, A.G. 2003. Composite synvolcanic intrusions associated with Precambrian VMS-related hydrothermal systems. *Mineralium Deposita,* **38**, 443-473.

GALLEY, A.G., HANNINGTON, M.D. & JONASSON, I.R. 2007a. Volcanogenic massive sulphide deposits, *in* GOODFELLOW, W.D. (ed.). *Mineral Deposits of Canada: A Synthesis of Major Deposit-Types, District Metallogeny, the Evolution of Geological Provinces, and Exploration Methods: Geological Association of Canada, Mineral Deposits Division,* Special Publication, **5**, 141-161.

GALLEY, A.G., SYME, R. & BAILES, A.H. 2007b. Metallogeny of the Paleoproterozoic Flin Flon Belt, Manitoba and Saskatchewan, *in* GOODFELLOW, W.D. (ed.). *Mineral Deposits of Canada: A Synthesis of Major Deposit-Types, District Metallogeny, the Evolution of Geological Provinces, and Exploration Methods: Geological Association of Canada, Mineral Deposits Division,* Special Publication, **5**, 509-531.

GEMMELL, J.B. & FULTON, R. 2001. Geology, genesis and exploration implication of the footwall and hanging-wall alteration associated with the Hellyer volcanic associated massive sulfide deposit, Tasmania, Australia. *Economic Geology*, **96**, 1003-1035.

GSNI. 1979. Pomeroy, Northern Ireland Sheet 34, solid. *Ordnance Survey for the Geological Survey of Northern Ireland, scale 1:50,000, 1 sheet.*

GSNI. 1983. Cookstown, Northern Ireland Sheet 27, solid. *Ordnance Survey for the Geological Survey of Northern Ireland, scale 1:50,000, 1 sheet.*

GSNI. 1995. Draperstown. Northern Ireland Sheet 26, solid and Drift Geology. *British Geological Survey, scale 1:50,000, 1 sheet.*

GSNI. 2007. The Tellus project: Proceedings of the end-of-project conference, Belfast, October 2007. See
http://www.bgs.ac.uk/gsni/tellus/conference/index.html).

GERBI, C.C., JOHNSON, S.E. & ALEINIKOFF, J.N. 2006. Origin and orogenic role of the Chain Lakes massif, Maine and Quebec. *Canadian Journal of Earth Sciences*, **43**, 339-366.

GERYA, T.V. 2011. Intra-oceanic subduction zones, in BROWN, D. & RYAN, P.D. (eds.). Arc-Continent Collision. Frontiers in Earth Sciences, 23-51.

GIBSON, H.L. & WATKINSON, D.H. 1990. Volcanogenic massive sulphide deposits of the Noranda cauldron and shield volcano, Quebec, in RIVE. M (ed.). *The Northwestern Quebec Polymetallic Belt: A summary of 60 years of mining exploration.* Special Publication of the Canadian Institute of Mining, **43**, 119-132.

GIBSON, H.L. & GALLEY, A.L. 2007. Volcanogenic massive sulphide deposits of the Archean, Noranda District, Quebec, in GOODFELLOW, W.D. (ed.). *Mineral Deposits of Canada: A Synthesis of Major Deposit-Types, District Metallogeny, the Evolution of Geological Provinces, and Exploration Methods.* Geological Association of Canada, Mineral Deposits Division, Special Publication, **5**, 533-552.

GILLIS, K.M. & THOMPSON, G. 1993. Metabasalts from the Mid-Atlantic Ridge: new insights into hydrothermal systems in slow-spreading crust. *Contributions to Mineralogy and Petrology*, **113**, 502-523.

GILLIS, K.M., COOGAN, L.A. & PEDERSEN R. 2005. Strontium isotope constraints on fluid flow in the upper oceanic crust at the East Pacific Rise. *Earth and Planetary Science Letters*, **232**, 83-94.

GOODENOUGH, K.M., STYLES M.T., SCHOFIELD D., THOMAS R.J., CROWLEY Q.G., LILLY R.M., MCKERVEY, J., STEPHENSON, D. & CARNEY, J., Architecture of the Oman - UAE Ophiolite: evidence for a multi-phase magmatic history, *Arabian Journal of Geosciences*, In Press.

GOODFELLOW, W.D. 2007. Metallogeny of the Bathurst Mining Camp, Northern New Brunswick, in GOODFELLOW, W.D. (ed.). *Mineral Deposits of Canada: A Synthesis of Major Deposit-Types, District Metallogeny, the Evolution of Geological Provinces, and Exploration Methods.* Geological Association of Canada, Mineral Deposits Division, Special Publication, **5**, 449-469.

GOODFELLOW, W.D. & PETER, J.M. 1999. Reply: sulfur isotope composition of the Brunswick No. 12 massive sulphide deposit, Bathurst Mining Camp, New Brunswick: implications for ambient environment, sulphur source, and ore genesis. *Canadian Journal of Earth Sciences,* **36**, 127-134.

GOODFELLOW, W.D., MCCUTCHEON, S.R. & PETER, J.M. 2003. Massive sulfide deposits of the Bathurst Mining Camp, New Brunswick and Northern Maine: Introduction and summary of findings, in GOODFELLOW, W.D., MCCUTCHEON, S.R. & PETER, J.M. (eds.). Massive Sulfide Deposits of the Bathurst Mining Camp, New Brunswick and Northern Maine. *Economic Geology Monograph,* **11**, 1-16.

GRAHAM, C.M. 1986. The role of the Cruachan Lineament during Dalradian Evolution. *Scottish Journal of Geology,* **22**, 257-270.

GRAHAM, J.R. 2009. Ordovician of the North, in HOLLAND, C.H. & SANDERS, I.S. (eds). *The Geology of Ireland*, 2nd edition. 43-67.

GRENNE, T. & SLACK, J.F. 2003. Bedded jaspers of the Ordovician Løkken ophiolite, Norway: seafloor deposition and diagnetic maturation of hydrothermal plume-derived silica-iron gels. *Mineralium Deposita,* **38**, 625-639.

GUNN, A.G., LUSTY, P.A.J., MCDONNELL, P.M. & CHACKSFIELD, B.C. 2008. A preliminary assessment of the mineral potential of selected parts of Northern Ireland. *British Geological Survey, Economic Minerals Programme, Commissioned Report, CR/07/149, pp. 161.*

HAMILTON, P.J., O'NIONS, R.K., BRIDGWATER, D. & NUTMAN, A. 1983. Sm-Nd studies of Archaean metasediments and metavolcanics from West Greenland and their implications for the Earth's early history. *Earth and Planetary Science Letters*, **62**, 263-272.

HAMILTON, P.J., BLUCK, B.J. & HALLIDAY, A.N. 1984. Sm-Nd ages from the Ballantrae Complex, SW Scotland. *Transactions of the Royal Society of Edinburgh: Earth Sciences*, **75**, 183-187.

HAMMARSTROM, J.M. & ZEN, E-A. 1986. Aluminum in hornblende: An empirical igneous geobarometer. *American Mineralogist*, **71**, 1297-1313.

HANNINGTON, M.D., JONASSON, I.R., HERZIG, P.M. & PETERSEN, S. 1995. Physical and chemical processes of seafloor mineralization and mid-ocean ridges, in HUMPHRIS, SE., ZIERENBERG, R.A., MULLINEAUX, L.S. & THOMSON, R. (eds.). *Seafloor Hydrothermal Systems: Physical, Chemical, Biological, and Geological Interactions.* Geophysical Monograph Series, **91**, 115-157.

HANNINGTON, M.D., GALLEY, A.G., HERZIG, P.M. & PETERSEN, S. 1998. Comparison of the TAG mound and stockwork complex with Cyprus-type massive sulfide deposits. *Proceedings of the Ocean Drilling Program, Scientific Results Volume 158*, 389-415.

HANNINGTON, M.D., POULSEN, K.H., THOMPSON, J.F.H. & SILLITOE, R.H. 1999. Volcanogenic gold in the massive sulphide environment. *Reviews in Economic Geology,* **8**, 325-356.

HANNINGTON, M.D., SANTAGUIDA, F., KJARSGAARD, I.M. & CATHLES, L.M. 2003a. Regional-scale hydrothermal alteration in the Central Blake River Group, western Abitibi

subprovince, Canada: implications for VMS prospectivity. *Mineralium Deposita*, **38**, 393-422.

HANNINGTON, M.D., KJARSGAARD, I.M., GALLEY A.G. & TAYLOR, B. 2003b. Mineral-chemical studies of metamorphosed hydrothermal alteration in the Kristineberg volcanogenic massive sulfide district, Sweden. *Mineralium Deposita*, **38**, 423-442.

HANNINGTON, M.D., DE RONDE, C.E.J. & PETERSEN, S. 2005. Sea-floor tectonics and submarine hydrothermal systems *in* HEDENQUIST, J.W., THOMPSON, J.F.H., GOLDFARB, R.J. AND RICHARDS, J.P. (eds.). *Economic Geology 100th Anniversary Volume*. The Economic Geology Publishing Company, 111-141.

HARPER, G.D. 1984. The Josephine Ophiolite, northwestern California. *GSA Bulletin*, **95**, 1009-1026.

HARPER, G.D. 2003. Fe-Ti basalts and propagating-rift tectonics in the Josephine Ophiolite. *Geological Society of America Bulletin*, **115**, 771-787.

HARRIS, R. 2011. The nature of the Banda arc-continent collision in the Timor region, in BROWN, D. & RYAN, P.D. (eds.). *Arc-Continent Collision.* Frontiers in Earth Sciences, 163-211.

HARRIS, P.M., FARRAR, E., MACINTYRE, R.M., MILLER, J.A. & YORK, D. 1965. Potassium-argon age measurements on two igneous rocks from the Ordovician system of Scotland. *Nature*, **205**, 352-353.

HART, T., GIBSON, H.L. & LESHER, C.M. 2004. Trace element geochemistry and petrogenesis of felsic volcanic rocks associated with volcanogenic Cu-Zn-Pb massive sulphide deposits. *Economic Geology,* **99**, 1003-1013.

HARTLEY, J.J. 1933. The geology of north-eastern Tyrone and the adjacent portions of County Londonderry. *Proceedings of the Royal Irish Academy, Section B- Biological, Geological and Chemical Science*, **41**, 218-285.

HARTLEY, J.J. 1936. The age of the igneous series of Slieve Gallion. *Geological Magazine*, **73**, 226-8.

HASTIE, A.R., KERR, A.C., PEARCE, J.A. & MITCHELL, S.F. 2007. Classification of altered volcanic island arc rocks using immobile trace elements: development of the Th-Co discrimination diagram. *Journal of Petrology*, **48**, 2341-2357.

HENDERSON, W.G. & ROBERTSON, A.H.F. 1982. The Highland Border rocks and their relation to marginal basin development in the Scottish Caledonides. *Journal of the Geological Society, London*, **139**, 433-450.

HENDERSON, W.G., TANNER, P.G.W. & STRACHAN, R.A. 2009. The Highland Border Ophiolite of Scotland: observations from the Highland Workshop field excursion of April 2008. *Scottish Journal of Geology*, **45**, 13-18.

HERRINGTON, R.J. & BROWN, D. 2011. The generation and preservation of mineral deposits in arc-continent collision environments, in BROWN, D. & RYAN, P.D. (eds.). *Arc-Continent Collision.* Frontiers in Earth Sciences, 145-159.

HERRINGTON, R., MASLENNIKOV, V., ZAYKOV, V., SERAVKIN, I., KOSAREV, A., BUSCHMANN, B., ORGEVAL, J-J., HOLLAND, N., TESALINA, S., NIMIS, P. & ARMSTRONG, R. 2005. Classification of VMS deposits: Lessons from the South Uralides. *Ore Geology Reviews,* **27**, 203-237.

HERRINGTON, R.J., SCOTNEY, P.M., ROBERTS, S., BOYCE, A.J. & HARRISON, D. 2011. Temporal association of arc-continent collision, progressive magma contamination in arc volcanism and formation of gold-rich massive sulphide deposits on Wetar Island (Banda arc). *Gondwana Research*, **19**, 583-593.

HERRMANN, W. & HILL, A.P. 2001. The origin of chlorite-tremolite-carbonate rocks associated with the Thalanga volcanic-hosted massive sulfide deposit, North Queensland, Australia. *Economic Geology*, **96**, 1149-1173.

HERZIG, P.M. & HANNINGTON, M.D. 1995. Polymetallic massive sulfides at the modern seafloor: A review. *Ore Geology Reviews,* **10**, 95-115.

HEY, R.N., JOHNSON, G.L. & LOWRIE, A. 1977. Recent tectonic evolution of the Galapagos area and plate motions in the east Pacific. *Geological Society of America Bulletin*, **88**, 1404-1420.

HEY, R.N., DUENNEBIER, F.K. & MORGAN, W.J. 1980. Propagating rifts on mid-ocean ridges. *Journal of Geophysical Research*, **85**, 3647-3658.

HODGES, D.J. & MANOJLOVIC, P.M. 1993. Application of lithogeochemistry to exploration for deep VMS deposits in high grade metamorphic rocks, Snow Lake, Manitoba. *Journal of Geochemical Exploration,* **48**, 201-224.

HOLLIS, S.P. 2012. Licence DG2. Period – 1st January 2010 to 31st December 2011. Technical Report. Submitted to Department of Enterprise, Trade and Investment & Crown Mineral Agent.

HOLLIS, S.P., ROBERTS, S., COOPER, M.R., EARLS, G., HERRINGTON, R.J., CONDON, D.J., COOPER, M.J., ARCHIBALD, S.M. & PIERCEY, S.J. 2012. Episodic-arc ophiolite emplacement and the growth of continental margins: Late accretion in the Northern Irish sector of the Grampian-Taconic orogeny. *GSA Bulletin,* **124**, 1702-1723.

HUSELBEE, M.Y. & THOMAS, A.T. 1998. Olenellus and conodonts from the Durness Group, NW Scotland, and the correlation of the Durness succession. *Scottish Journal of Geology*, **34**, 83-88.

HUTTON, D.H.W & HOLLAND, C.H. 1992, An Arenig-Llanvirn age for the black shales of Slieve Gallion, County Tyrone. *Irish Journal of Earth Sciences*, **11**, 187-189.

HUTTON, D.H.W., AFTALION, M. & HALLIDAY, A.N. 1985. An Ordovician ophiolite in County Tyrone, Ireland. *Nature*, **315**, 210-212.

HYNES, A. 1980. Carbonatisation and mobility of Ti, Y and Zr in Ascot Formation metabasites, SE Quebec. *Contributions to Mineralogy and Petrology*, **75**, 79-87.

ISHIKAWA, Y., SAWAGUCHI, T., IWAYA, S. & HORIUCHI, M. 1976. Delineation of prospecting targets for Kuroko deposits based on modes of volcanism of underlying dacite and alteration halos. *Mining Geology*, **26**, 105-117.

JACOBSEN, S.B. & WASSERBURG, G.J. 1979. Nd and Sr isotopic study of the Bay of Islands ophiolite complex and the evolution of the source of mid-ocean ridge basalts. *Journal of Geophysical Research*, **84**, 7429-7445.

JAFFEY, A.H., FLYNN, K.F., GLENDENIN, L.E., BENTLEY, W.C. & ESSLING, A.M. 1971. Precision measurements of half-lives and specific activities of ^{235}U and ^{238}U. *Physics Press,* **C4**, 1889–1906.

JENNER, G.A. 1996. Trace element geochemistry of igneous rocks: geochemical nomenclature and analytical geochemistry, in: WYMAN, D.A. (ed) *Trace element geochemistry of volcanic rocks: applications for massive sulfide exploration.* Geological Association of Canada, Short Course Notes, 51-77.

JOHNSON, M.C. & RUTHERFORD, M.J. 1989. Experimental calibration of the aluminium-in-hornblende geobarometer with application to Long Valley caldera (California) volcanic rocks. *Geology*, **17**, 837-841.

JOWETT, E.C. 1991. Fitting iron and magnesium into the hydrothermal chlorite geothermometer. *GAC/MAC/SEG Joint Annual Meeting (Toronto, May 27-29), Program with Abstracts* **16**, A62.

KALOGERPOULOS, S.I. & SCOTT, S.D. 1983. Mineralogy and geochemistry of tuffaceous exhalites (tetsusekiei) of the Fukazawa mine, Hokuroku district, Japan. *Economic Geology Monograph*, **5**, 412-432.

KALOGERPOULOS, S.I. & SCOTT, S.D. 1989. Mineralogy and geochemistry of an Archean tuffaceous exhalite: the Main Contact Tuff, Millenbach mine area, Noranda, Quebec. *Canadian Journal of Earth Science,* **26**, 88-105.

KEAN, B.A., EVANS, D.T.W. & JENNER G.A. 1995. Geology and mineralization of the Lushs Bight Group. *Newfoundland Department of Natural Resources*, Report 95-2, pp. 204.

KERR, A. 1996. New perspectives on the stratigraphy, volcanology, and structure of island-arc volcanic rocks in the Ordovician Robert's Arm Group, Notre Dame Bay. *Current Research Report*, Report: 96-1, 283–310.

KERRICH, R. & WYMAN, D.A. 1996. The trace element systematics of igneous rocks in mineral exploration: An overview. *Geological Association of Canada Short Course Notes,* **12**, 1-50.

KERRICH, R., & WYMAN, D.A. 1997. Review of developments in trace-element fingerprinting of geodynamic settings and their implications for mineral exploration. *Australian Journal of Earth Sciences*, **44**, 465-487.

KNUCKEY, M.J., COMBA, C.D.A. & RIVERIN, G. 1982. Structure, metal zoning and alteration at the Millenbach deposit, Noranda, Quebec. *Geological Association of Canada, Special Paper,* **25**, 255-295.

KRANIDIOTIS, P. & MACLEAN, W.H. 1987. Systematics of chlorite alteration at the Phelps Dodge massive sulfide deposit, Matagami, Quebec. *Economic Geology*, **82**, 1898-1911.

KROGH, T.E. 1973. A low contamination method for the hydrothermal decomposition of zircon and extraction of U and Pb for isotopic age determinations. *Geochimica et Cosmochimica Acta*, **37**, 485-494.

KROGH, T.E. 1982. Improved accuracy of U-Pb zircon ages by the creation of more concordant systems using an air-abrasion technique. *Geochimica et Cosmochimica Acta*, **46**, 637-649.

KUIPER, K.F., DEINO, A., HILDEN, F.J., KRIJGSMAN, W., RENNE, P.R. & WIJBRANS, J.R. 2008. Synchronizing rock clocks of Earth history. Science, **320**, 500-504.

LAIRD, J. 1988. Chlorites: metamorphic petrology. *Reviews in Mineralogy and Geochemistry*, **19**, 405-453.

LARGE, R.R. 1992. Australian volcanic-hosted massive sulphide deposits: features, styles and genetic models: Economic Geology, **87**, 471-510.

LARGE, R.R., GEMMELL, J.B. & PAULICK, H. 2001. The alteration box plot: a simple approach to understanding the relationship between alteration mineralogy and lithogeochemistry associated with volcanic-hosted massive sulfide deposits. *Economic Geology*, **96**, 957-971.

LEAT, P.T., JACKSON, S.E., THORPE, R.S. & STILLMAN, C.J. 1986. Geochemistry of bimodal basalt-subalkaline/peralkaline rhyolite provinces within the Southern British Caledonides. *Journal of the Geological Society, London*, **143**, 259-273.

LEISTEL, J.M., MARCOUX, E. & DESCHAMPS, Y. 1999. Chert in the Iberian Pyrite Belt. *Mineralium Deposita,* **33**, 59-81.

LENTZ, D.R. 1998. Petrogenetic evolution of felsic volcanic sequences associated with Phanerozoic volcanic-hosted massive sulphide systems: the role of extensional geodynamics. *Ore Geology Reviews,* **12**, 289-327.

LENTZ, D.R., HALL, D.C. & HOY, L.D. 1997. Chemostratigraphic, alteration, and oxygen isotopic trends in a profile through the stratigraphic sequence hosting the Heath Steele B zone massive sulfide deposit, New Brunswick. *Canadian Mineralogist*, **35**, 841-874.

LESHER, C.M., GIBSON, H.L. & CAMPBELL, I.H. 1986. Composition-volume changes during hydrothermal alteration of andesite at Buttercup Hill, Noranda district, Quebec. *Geochimica et Cosmochimica Acta,* **50**, 2693-2705.

LEYSHON, P.R. & CAZALET, P.C.D. 1978. Base-metal exploration programme in Lower Palaeozoic volcanic rocks, Co. Tyrone, Northern Ireland. *Institution of Mining and Metallurgy*, **85**, B91-B99.

LIAGHAT, S. & MACLEAN, W.H. 1992. The key tuffite, Matagami mining district: origin of the tuff component and mass changes. *Exploration and Mining Geology,* **1**, 197-207.

LISSENBERG, C.J., BÉDARD, J.H. & VAN STAAL, C.R. 2004. The structure and geochemistry of the gabbro zone of the Annieopsquotch Ophiolite, Newfoundland: implications for lower crustal accretion at spreading ridges. *Earth and Planetary Science Letters*, **229**, 105-123.

LISSENBERG, C.J., ZAGOREVSKI, A., MCNICOLL, V.J., VAN STAAL, C.R. & WHALEN, J.B. 2005. Assembly of the Annieopsquotch Accretionary Tract, Newfoundland Appalachians: Age and Geodynamic Constraints from Syn-Kinematic Intrusions. *Journal of Geology*, **113**, 553-570.

LISSENBERG, C.J. & VAN STAAL, C.R. 2002. The relationships between the Annieopsquotch Ophiolite Belt, the Dashwoods Block and the Notre Dame Arc in southwestern Newfoundland. *Current Research, Newfoundland Department of Mines and Energy*, Report 02-1, 145-153.

LISSENBERG, C.J. & VAN STAAL, C.R. 2006. Feedback between deformation and magmatism in the Lloyds River Fault Zone, an example of episodic fault reactivation in an accretionary setting, Newfoundland Appalachians. *Tectonics*, **25**, TC4004

LONG, C.B., MCCONNELL, B.J. & PHILCOX, M.E. 2005. Geology of South Mayo: A geological description of South Mayo to accompany the bedrock geology 1:100,000 scale map series, sheet 11, South Mayo. Geological Survey of Ireland.

LUDWIG, K. R. 1991. Isoplot - a plotting and regression program for radiogenic isotope data: *USGS Open File Report*, 91-445.

LUDWIG, K.R. 1998. On the treatment of concordant uranium-lead ages. *Geochimica, Cosmochimica Acta*, **62**, 665-676.

LUDWIG, K.R. 2003. Isoplot/Ex version 2.06. A Geochronological toolkit for Microsoft Excel. *Berkeley Geochronology Center Special Publication*, *No.*4, 70p.

LUSTY, P.A.J., GUNN, A.G., MCDONNELL, P.M., CHACKSFIELD, B.C., COOPER, M.R. & EARLS, G. 2009. Gold potential of the Dalradian rocks of north-west Northern Ireland: prospectivity analysis using Tellus data. *Applied Earth Science*, **118**, 162-177.

LYDON, J.W. 1984. Some observations on the morphology and ore textures of volcanogenic sulfide deposits of Cyprus. Geological Survey of Canada, *Current Research*, Paper 84-01A, 601-610.

MACLEAN, W.H. 1990. Mass change calculations in altered rock series. *Mineralium Deposita*, **25**, 44-49.

MACLEAN, W.H. & HOY, L.D. 1991. Geochemistry of hydrothermally altered rocks at the Horne Mine, Noranda, Quebec. *Economic Geology*, **86**, 506-528.

MANGE, M.A., DEWEY, J. & WRIGHT, D.T. 2003. Heavy minerals solve structural and stratigraphic problems in Ordovician strata of the western Irish Caledonides. *Geological Magazine*, **140**, 25-30.

MANGE, M., IDLEMAN, B., YIN, Q.Z., HIDAKA, H. & DEWEY, J. 2010. Detrital heavy minerals, white mica and zircon geochronology in the Ordovician South Mayo Trough, western Ireland: signatures of the Laurentian basement and the Grampian orogeny. *Journal of the Geological Society, London*, **167**, 1147-1160.

MASLENNIKOV, V.V., AYUPOVA, N.R., HERRINGTON, R.J., DANYUSHEVSKIY, L.V. & LARGE, RR. 2012. Ferruginous and manganiferous haloes around massive sulphide deposits of the Urals. *Ore geology reviews*, **47**, 5-41.

MATTINSON, J.M. 2005. Zircon U–Pb chemical abrasion ('CA-TIMS') method: Combined annealing and multi-step partial dissolution analysis for improved precision and accuracy of zircon ages. *Chemical Geology*, **220**, 47–66.

MATTSSON, H.B. & OSKARSSON, N. 2005. Petrogenesis of alkaline basalts at the tip of a propagating rift: Evidence from the Heimaey volcanic centre, south Iceland. *Journal of Volcanology and Geothermal Research*, **147**, 245-267.

MAX, M.D. & RIDDIHOUGH, R.P. 1975. Continuation of the Highland Boundary Fault in Ireland. *Geology*, **3**, 306-210.

MAX, M.D., RYAN, C.G. & INAMDAR, D.D. 1983. A magnetic deep structural geology interpretation of Ireland. *Tectonics*, **2**, 431-451.

MCCONNELL, B.J., STILLMAN, C.J. & HERTOGEN, J. 1991. An Ordovician basalt to peralklaine rhyolite fractionation series from Avoca, Ireland. *Journal of the Geological Society, London*, **148**, 711-718.

MCCONNELL, B., RIGGS, N., & CROWLEY, Q.G. 2009. Detrital zircon provenance and Ordovician terrane amalgamation, western Ireland. *Journal of the Geological Society, London*, **166**(3), 473-484.

MCDONOUGH, W.F. & SUN. S.-S. 1995. The composition of the Earth. *Chemical Geology*, **120**, 223-254.

MCFARLANE, J.A.S., COOPER, M.R. & CHEW, D.M. 2009. New geological and geophysical insights into the Dalradian Lack Inlier, Northern Ireland: Implications for lithostratigraphy and gold mineralization. *Irish Association for Economic Geology, Annual Review*, 57-59.

MCLEOD, R.L. & STANTON, R.L. 1984. Phyllosilicates and associated minerals in some Paleozoic stratiform sulfide deposits of southeastern Australia. *Economic Geology*, **79**, 1-22.

MERCIER-LANGEVIN, P., HANNINGTON, M.D., DUBÉ, B. & BÉCU, V. 2011. The gold content of volcanogenic massive sulfide deposits. *Mineralium Deposita,* **46**, 509-539.

MERRIMAN, R.J. & HARDS, V.L. 2000. Petrographic notes on igneous and metamorphic rocks from Northern Ireland. *British Geological Survey Short Report MPSR/00/7.*

MESCHEDE, M. 1986. A method of discriminating between different types of mid-ocean ridge basalts and continental tholeiites with the Nb-Zr-Y diagram. *Chemical Geology*, **56**, 207-218.

MESSINA MINERALS, 2012. http://www.messinaminerals.com/s/Resources.asp

MICHARD, A. & ALBAREDE, F. 1986. The REE content of some hydrothermal fluids. *Chemical Geology,* **55**, 51-60.

MILLER, C., HALLEY, S., GREEN, G. & JONES, M. 2001. Discovery of the West 45 volcanic-hosted massive sulfide deposit using oxygen isotopes and REE geochemistry. *Economic Geology,* **96**, 1227-1237.

MILLS, R.A. & ELDERFIELD, H. 1995. Rare earth element geochemistry of hydrothermal deposits from the active TAG mound, 26°N Mid-Atlantic Ridge. *Geochimica Cosmochimica Acta*, **59**, 3511-3524.

MITRA, A., ELDERFIELD, H. & GREAVES, M.J. 1994. Rare earth elements in submarine hydrothermal fluids and plumes from the Mid-Atlantic Ridge. *Marine Chemistry,* **46**, 217-235.

MIYASHIRO, A. 1973. The Troodos Complex was probably formed in an island arc. *Earth and Planetary Science Letters*, **73**, 217-222.

MORTON, R.L. & FRANKLIN, J.M. 1987. Two-fold classification of Archean volcanic-associated massive sulphide deposits. *Economic Geology,* **82**, 1057-1063.

MURPHY, J.B., & HYNES, A.J. 1986. Contrasting secondary mobility of Ti, P, Zr, Nb and Y in two metabasaltic suites in the Appalachians. *Canadian Journal of Earth Sciences*, **23**, 1138-144.

NANCE, R.D., GUTIÉRREZ-ALONSO, G., KEPPIE, J.D., LINNEMANN, U., MURPHY, J.B., QUESADA, C., STRACHAN, R.A. & WOODCOCK, N.H. 2010. Evolution of the Rheic Ocean. *Gondwana Research*, **17**, 194-222.

NOBLE, S.R., TUCKER, R.D. & PHARAOH, T.C. 1993. Lower Palaeozoic and Precambrian igneous rocks from eastern England, and their bearing on late Ordovician closure of the Tornquist Sea: constraints from U-Pb and Nd isotopes. *Geological Magazine*, **130**, 835-846.

O'BRIEN, B.H. 2007. Geology of the Buchans–Robert's Arm volcanic belt, near Great Gull Lake. *Current Research – Newfoundland Geological Survey Branch*, Report 07-1, 85–102.

O'CONNOR, P.G. 1987. Volcanology, geochemistry and mineralization in the Charlestown Ordovician inlier, Co. Mayo. *Unpublished PhD thesis, National University of Ireland*

O'CONNOR, P.G. & POUSTIE, A.1986. Geological setting of, and alteration associated with, the Charlestown mineral deposit, in ANDREW, C.J., CROWE, R.W.A. FINLAY, S., PENNELL,

W.M. & PYNE, J.F. *Geology and genesis of mineral deposits in Ireland*, Irish Association for Economic Geology, 89-101.

OLIVER, G.J.H., STONE, P. & BLUCK, B.J. 2002. The Ballantrae Complex and Southern Uplands terrane, in TREWIN, N.H. (ed)., *The Geology of Scotland*, 4th edition, 167-200.

PARK, R.G., STEWART, A.D. & WRIGHT, D.T. 2002. The Hebridean terrane, in TREWIN, N.H. (ed)., *The Geology of Scotland*. 4th edition, 45-80.

PARNELL, J., EARLS, G., WILKINSON, J.J., HUTTON, D.H.W., BOYCE, A.J., FALLICK, E., ELLAM, R.M., GLEESON, S.A., MOLES, N.R., CAREY, P.F., & LEGG, I. 2000. Regional fluid flow and gold mineralization in the Dalradian of the Sperrin Mountains, Northern Ireland. *Economic Geology*, **95**, 1389-1416.

PEARCE, J.A. 1983. Role of the sub-continental lithosphere in magma genesis at active continental margins, in: HAWKESWORTH, C.J. (ed) *Continental basalts and mantle xenoliths*, 230-249

PEARCE, J.A. 1996. A user's guide to basalt discrimination diagrams. *Geological Association of Canada Short Course Notes,* **12**, 79-113.

PEARCE, J.A. & CANN, J.R. 1973. Tectonic setting of basic volcanic rocks determined using trace element analyses. *Earth and Planetary Science Letters*, **19**, 290-300.

PEARCE, J.A. & NORRY, M.J. 1979. Petrogenetic implications of Ti, Zr, Y and Nb variations in volcanic rocks. *Contributions to Mineralogy and Petrology*, **69**, 33-47.

PEARCE, J.A., HARRIS, N.B.W., & TINDLE, A.G. 1984a. Trace element discrimination diagrams for the tectonic interpretation of granitic rocks. *Journal of Petrology*, **25**, 956-983.

PEACE, J.A., LIPPARD, S.J. & ROBERTS, S. 1984b. Characteristics and tectonic significance of suprasubduction zone ophiolites, in GASS, I.G., LIPPARD., S.J. & SHELTON, A.W. (eds) *Ophiolites and Oceanic Lithosphere*. Geological Society, London, Special Publications, **16**, 77-94.

PEARCE, J.A., ERNEWEIN, M., BLOOMER, S.H., PARSON, L.M., MURTON, B.J. & JOHNSON, L.E. 1994. Geochemistry of Lau Basin volcanic rocks: Influence of ridge segmentation and arc proximity, in MELLIE, J.L. (ed.). *Volcanism associated with extension at consuming plate margins*. Geological Society of London, Special Publication, **81**, 53-75.

PEATFIELD, G.R. 2003. Updated technical review report on the Tyrone mineral exploration property, (prospecting licences UM 11/96 and UM 12/96, County Tyrone, Northern Ireland – 20 January, 2003. Published report for Tournigan Gold Corporation.

PERFIT, M.R., RIDLEY, W.I. & JONASSON, I.R. 1999. Geologic, petrologic, and geochemical relationships between magmatism and massive sulphide mineralization along the Eastern Galapagos Spreading Centre. *Reviews in Economic Geology,* **8**, 75-100.

PETER, J.M. 2003. Ancient iron-rich metalliferous sediments (iron formations): their genesis and use in the exploration for stratiform base metal sulphide deposits,

with examples from the Bathurst Mining Camp, in LENTZ, D.R. (ed.*). Geochemistry of Sediments and Sedimentary Rocks: Evolutionary Considerations to Mineral Deposit-Forming Environments, GEOtext 4*. Geological Association of Canada, 145-173.

PETER, J.M. & GOODFELLOW, W.D. 1996. Mineralogy, bulk and rare earth element geochemistry of massive sulphide-associated hydrothermal sediments of the Brunswick Horizon, Bathurst Mining Camp, New Brunswick. *Canadian Journal of Earth Sciences,* **33**, 252-283.

PETER, J.M. & GOODFELLOW, W.D. 2003. Hydrothermal sedimentary rocks of the Heath Steele belt, Bathurst Mining Camp, New Brunswick: part 3: application of mineralogy and mineral bulk compositions to massive sulphide exploration. *Economic Geology Monograph,* **11**, 417-433.

PETER, J.M., KJARSGAARD, I.M. & GOODFELLOW, W.D. 2003a. Hydrothermal sedimentary rocks of the Heath Steele Belt, Bathurst Mining Camp, New Brunswick: Part 1. Mineralogy and Mineral Chemistry. *Economic Geology Monograph,* **11**, 361-390.

PETER, J.M., GOODFELLOW, W.D. & DOHERTY, W. 2003b. Hydrothermal sedimentary rocks of the Heath Steele Belt, Bathurst Mining Camp, New Brunswick: Part 2. Bulk and rare earth element geochemistry and implications for origin. *Economic Geology Monograph*, **11**, 391-415.

PIERCEY, S.J. 2007a. Volcanogenic massive sulphide (VMS) deposits of the Newfoundland Appalachians: An overview of their setting, classification, grade-tonnage data, and unresolved questions. In PEREIRA, C.G.P. & WALSH, D.G. (eds) Current Research. Newfoundland Department of Natural Resources, Geological Survey, Report 07-01, 169-178.

PIERCEY, S.J. 2007b. An overview of the use of petrochemistry in regional exploration for volcanogenic massive sulfide (VMS) deposits. In MILKEREIT, B. (ed) Proceedings of Exploration 07: Fifth Decennial International Conference on Mineral Exploration, 223-246.

PIERCEY, S.J. 2009. Lithogeochemistry of volcanic rocks associated with volcanogenic massive sulfide (VMS) deposits and applications to exploration. In COUSENS, B.L. & PIERCEY, S.J. (eds) Subaqueous Volcanism and Mineralization. Mineral Deposits Division-Volcanology and Igneous Petrology Division, Geological Association of Canada, Short Course Notes, **19**, 15-40.

PIERCEY, S.J. & HINCHEY, J. 2012. Field Trip Guide Book – B4. Volcanogenic massive sulphide (VMS) deposits of the Central Mobile Belt, Newfoundland. GAC-MAC-AGC-AMC Joint Annual Meeting, St. John's, Canada.

PIERCEY, S.J. MURPHY, D.C. MORTENSEN, J.K. & PARADIS, S. 2001. Boninitic magmatism in a continental margin setting, Yukon-Tanana terrane, southeastern Yukon, Canada. *Geology,* **29**, 731-734.

POLLOCK, J.C., HIBBARD, J.P. & SYLVESTER, P.J. 2009. Early Ordovician rifting of Avalonia and birth of the Rheic Ocean: U–Pb detrital zircon constraints from Newfoundland. *Journal of the Geological Society, London*, **166**, 501–515.

POULSEN, H. AND HANNINGTON, M. 1995. Auriferous Volcanogenic Sulfide Deposits, *in* ECKSTRAND, O.R., SINCLAIR, W.D. AND THORPE, R.I. (eds.*). Geology of Canadian Mineral Deposit Types.* Geology of Canada, no. 8, Decade of North American Geology (DNAG): Geological Society of America, Part 1, 183-196.

PRAVE, A.R. 1999. The Neoproterozoic Dalradian Supergroup of Scotland: an alternative hypothesis. *Geological Magazine*, **136**, 609-617.

RAVEGGI, M., GILES, D., FODEN, J. & RAETZ, M. 2007. High Fe-Ti magmatism and tectonic setting of the Paleoproterozoic Broken Hill Block, NSW, Australia. *Precambrian Research*, **156**, 55-84.

Reston, T. 2009. The structure, evolution and symmetry of the magma-poor rifted margins of the North and Central Atlantic: a synthesis. *Tectonophysics*, **468**, 6-27.

RESTON, T. & MANATSCHAL, G. 2011. Rifted margins: building blocks of later collision, in BROWN, D. & RYAN, P. (eds). *Arc-continent collision.* Frontiers in Earth Sciences, 3-21.

ROBERTSON, A.H.F. & HENDERSON, W.G. 1984. Geochemical evidence for the origins of igneous and sedimentary rocks of the Highland Border, Scotland. *Transactions of the Royal Society of Edinburgh: Earth Sciences*, **75**, 135-150.

ROBINSON, P.T., MALPAS, J., DILEK, Y. & ZHOU, M-F. 2008. The significance of sheeted dyke complexes in ophiolites. *GSA Today*, **18**, 4-10.

ROGERS, N. 2004. Red Indian Line geochemical database. *Geological Survey of Canada Open File*:4605.

ROGERS, N. & VAN STAAL., C.R. 2003. Volcanology and tectonic setting of the northern Bathurst mining Camp: Part II, mafic volcanic constraints on backarc opening. *Econonic Geology Monograph,* **11**, 181-201.

ROGERS, N., VAN STAAL, C.R., ZAGOREVSKI, A., SKULSKI, T., PIERCEY, S. & MCNICOLL, V.J. 2007. Timing and tectonic setting of volcanogenic massive sulphide bearing terranes within the Central Mobile Belt of the Canadian Appalachians, in MILKEREIT, B. *Proceedings of Exploration 07: Fifth Decennial International Conference on Mineral Exploration*, 1199-1205.

ROLLINSON, H.R. 1993. *Using geochemical data: evaluation, presentation, interpretation.* Longman Group, U.K., Ltd. Harlow, U.K.

ROSS, P.-S., & BÉDARD, J.H. 2009. Magmatic affinity of modern and ancient subalkaline volcanic rocks determined from trace-element discriminant diagrams. *Canadian Journal of Earth Sciences*, **46**, 823-839.

RYAN, P.D. & DEWEY, J.F. 2004. The South Connemara Group reinterpreted: A Subduction-accretion complex in the Caledonides of Galway Bay, western Ireland. *Journal of Geodynamics*, **37**, 513-529.

RYAN, P.D. & DEWEY, J.F. 2011. Arc-continent collision in the Ordovician of western Ireland: stratigraphic, structural and metamorphic evolution, in BROWN D. & RYAN, P.D. *Arc-continent collision*, Frontiers in Earth Sciences, 373-401.

RYAN, P.D., FLOYD, P.A. & ARCHER, J.B. 1980. The stratigraphy and petrochemisty of the Lough Nafooey Group (Tremadocian), western Ireland. *Journal of the Geological Society of London*, **137**, 443-458.

RYAN, P.D., SAWAL, V.K. & ROWLANDS, A.S. 1983. Ophiolitic mélange separates ortho- and para-tectonic Caledonides in western Ireland. *Nature*, **302**, 50-52.

SADLER, P.M. COOPER, R.A., & MELCHIN, M. 2009. High-resolution, early Paleozoic (Ordovician-Silurian) time scales. *GSA Bulletin*, **121**, 887-906.

SAEKI, Y. & DATE, J. 1980. Computer application to the alteration data of the footwall dacite lava at the Ezuri Kuroko deposits, Akita prefecture. *Mining Geology*, **30**, 241-250.

SANGSTER, D.F. 1972. Precambrian volcanogenic massive sulphide deposits in Canada. A review. *Canadian Geological Survey Paper,* 72-22, pp.44.

SANGSTER, D.F. 1980. Quantitative characteristics of volcanogenic massive sulphide deposits I. Metal content and size distribution of massive sulphide deposits in volcanic centres. *CIM Bulletin*, 73, 74-81

SAWAKI, Y., SHIBUYA, T., KAWAI, T., KOMIYA, T., OMORI, S., IIZUKA, T., HIRATA, T., WINDLEY, B.F. & MARUYAMA, S. 2010. Imbricated ocean-plate stratigraphy and U-Pb zircon ages from tuff beds in cherts in the Ballantrae complex, SW Scotland. *GSA Bulletin*, **122**, 454-464.

SAWKINS, F.J. 1976. Massive sulphide deposits in relation to geotectonics. *Geological Association of Canada Special Paper,* **14**, 222-240.

SCHÄRER, U. 1984. The effect of initial ^{230}Th disequilibrium on young U-Pb ages: the Makalu case, Himalaya. *Earth and Planetary Science Letters*, **67**, 191-204.

SCHOFIELD, D.I., VAN STAAL, C.R. & WINCHESTER, J.A. 1998. Tectonic setting and regional significance of the 'Port aux Basques Gneiss', SW Newfoundland. *Journal of the Geological Society, London*, **155**, 323-334.

SCHMIDT, J.M. 1988. Mineral and whole-rock compositions of seawater-dominated hydrothermal alteration at the Arctic volcanogenic massive sulfide prospect, Alaska. *Economic Geology*, **83**, 822-842.

SCHMIDT, M.W. 1992. Amphibole composition in tonalite as a function of pressure: an experimental calibration of the Al-in-hornblende barometer. *Contributions to Mineralogy and Petrology*, **110**, 304-310.

SCHMITZ, M. D. & SCHOENE, B. 2007. Derivation of isotope ratios, errors, and error correlations for U-Pb geochronology using Pb-205-U-235-(U-233)-spiked isotope dilution thermal ionization mass spectrometric data. *Geochemistry Geophysics Geosystems*, **8**, Q08006.

SCOTNEY, P.M., ROBERTS, S., HERRINGTON, R.J., BOYCE, A.J. & BURGESS, R. 2005. The development of volcanic hosted massive sulfide and barite-gold orebodies on Wetar Island, Indonesia. *Mineralium Deposita,* **40**, 76-99.

SENGÖR, A.M.C. & NATAL'IN, B.A. 2004. Phanerozoic analogues of Archaean oceanic basement fragments – altaid ophiolites and ophirags, in KUSKY, T.M. (ed.). *Precambrian Ophiolites and Related Rocks*. Elsevier, 671-721.

SHAND, S.J. 1943. Eruptive Rocks. Their genesis, composition, classification, and their relation to ore-deposits with a chapter on meteorite. New York: John Wiley & Sons.

SHAW, H.F. & WASSERBURG, G.J. 1984. Isotopic constraints on the origin of Appalachian mafic complexes. *American Journal of Science*, **284**, 319-349.

SHERVAIS, J.W. 1982. Ti-V plots and the petrogenesis of modern ophiolitic lavas. *Earth and Planetary Science Letters*, **59**, 101-118.

SHUKUNO, H., TAMURA, Y., TANI, K., CHANG, Q., SUZUKI, T. & FISKE, R.S. 2006. Origin of silicic magmas and the compositional gap at Sumisu submarine caldera, Izu-Bonin arc, Japan. *Journal of Volcanology and Geothermal Research,* **156**, 187-216.

SINTON, J.M., WILSON, D.S., CHRISTIE, D.M., HEY, R.N. & DELANEY, J.R. 1983. Petrologic consequences of rift propagation on oceanic spreading ridges. *Earth and Planetary Science Letters*, **62**, 193-207.

SKULSKI, T., CASTONGUAY, S., MCNICOLL, V., VAN STAAL, C., KIDD, W., ROGERS, N., MORRIS, W., UGALDE, H., SLAVINSKI, H., SPICER, W., MOUSSALLAM, Y. & KERR, I. 2010. Tectonostratigraphy of the Baie Verte Oceanic Tract and its ophiolite cover sequence on the Baie Verte Peninsula. *Current Research – Newfoundland and Labrador Department of Natural Resources*, Report 10-1, 315-335.

SPRAY, J.G. & DUNNING, G.R. 1991. A U/Pb age for the Shetland Islands oceanic fragment, Scottish Caledonides - evidence from anatectic plagiogranites in layer 3 shear zones. *Geological Magazine*, **128**, 667-671.

SLACK, J.F., FOOSE, M.P., FLOHR, M.J.K., SCULLY, M. & BELKIN, H.E. 2003. Exhalative and subsea-floor replacement processes in the formation of the Bald Mountain massive sulfide deposit, Northern Maine. *Economic Geology Monograph,* **11**, 513-547.

SLACK, J.F., GRENNE, T., BEKKER, A., ROUXEL, O.J. & LINDBERG, P.A. 2007. Suboxic deep seawater in the late Paleoproterozoic: evidence from hematitic chert and iron formation related to seafloor-hydrothermal sulfide deposits, central Arizona. *Earth and Planetary Science Letters,* **255**, 243-256.

SMELLIE, J.L. & STONE, P. 2001. Geochemical characteristics and geotectonic setting of early Ordovician basalt lavas in the Ballantrae Complex ophiolite, SW Scotland. *Transactions of the Royal Society of Edinburgh: Earth Sciences*, **91**, 539-555.

SPITZ, G. & DARLING, R. 1978. Major and minor element lithogeochemical anomalies surrounding the Louvem copper deposit, Val d'Or, Quebec. *Canadian Journal of Earth Sciences*, **15**, 1161-1169.

SPRY, P.G., PETER, J.M. & SLACK, J.F. 2000. Meta-exhalites as exploration guides to ore, in SPRY, P.G., MARSHALL, B. & VOKES, F.M. (eds.). Metamorphosed and Metamorphogenic Ore Deposits. *Reviews in Economic Geology,* **11**, 163-201.

STACEY, J.S. & KRAMERS, J.D. 1975. Approximation of terrestrial lead isotope evolution by a two-stage model. *Earth and Planetary Science Letters*, **26**, 207-221.

STERN, R.J. 2004. Subduction initiation: spontaneous and induced. *Earth and Planetary Science Letters*, **226**, 275-292.

STRACHAN, R.A., SMITH, M., HARRIS, A.L. & FETTES, D.J. 2002. The Northern Highland and Grampian terranes in TREWIN, N.H. (ed)., *The Geology of Scotland*, 4th edition, 81-147.

STYLES, M, ELLISON, R. ARKLEY, S., CROWLEY, Q.G., FARRANT, A., GOODENOUGH, K.M., MCKERVEY, J, PHARAOH, T., PHILLIPS, E., SCHOFIELD, D. & THOMAS, R.J. *The geology and geophysics of the United Arab Emirates : Volume 2, Geology.*, Abu Dhabi, United Arab Emirates, United Arab Emirates, Ministry of Energy, Petroleum and Minerals, 2006, 1-351.

SUN, S.-S., & MCDONOUGH, W.F. 1989. Chemical and isotopic systematics of oceanic basalts: implications for mantle composition and processes. In Saunders, A.D., and Norry, M.J. (eds) *Magmatism in the Ocean Basins. Geological Society, London, Special Publications*, **42**, 313-345.

SVERJENSKY, D.A. 1984. Europium redox equilibria in aqueous solution. *Earth and Planetary Science Letters,* **67**, 70-78.

SWINDEN, H.S. 1996. Geochemistry of volcanic rocks in the Moreton's Harbour-Twillingate area, Notre Dame Bay. *Current Research – Newfoundland Geological Survey Branch*, Report 96-1, 207-226.

SWINDEN, H.S., JENNER, G.A. & SZYBINSKI, Z.A. 1997. Magmatic and tectonic evolution of the Cambrian-Ordovician Laurentian margin of Iapetus: geochemical and isotopic constraints from the Notre Dame Subzone, Newfoundland. *Geological Society of America Memoir*, **191**, 337-365.

TANNER, P.W.G. 2007. The role of the Highland Border ophiolite in the ~470 Ma Grampian event, Scotland. *Geological Magazine*, **144**, 597-602.

TANNER, P.W.G. & SUTHERLAND, S. 2007. Highland Border Complex in Scotland: a paradox resolved. *Journal of the Geological Society, London*, **164**, 111-116.

THIRLWALL, M.F. & BLUCK, B.J. 1984. Sr-Nd isotope and geological evidence that the Ballantrae "ophiolite", SW Scotland, is polygenetic, in GASS, I.G., LIPPARD, S.J. & SHELTON, A.W., (eds.) *Ophiolites and Oceanic Lithosphere*. Geological Society of London. Special Publications, **13**, 215-230.

TREMBLAY, A., RUFFET, G. & BÉDARD, J.H. 2011. Obduction of Tethyan-type ophiolites – A case study from the Thetford-Mines ophiolitic Complex, Quebec Appalachians, Canada. *Lithos*, **125**, 10-26.

THURLOW, J.G. 2010. Great Mining Camps of Canada 3. The history and geology of the Buchans mine, Newfoundland and Labrador. *Geoscience Canada*, **37**, 145-173.

URABE, T. & SCOTT, S.D. 1983. Geology and footwall alteration of the South Bay massive sulphide deposit, northwestern Ontario, Canada. *Canadian Journal of Earth Sciences*, **20**, 1862-1879.

VAN STAAL, C.R. 2005. The Northern Appalachians, in Selley, R.C., Robin, L., Cocks, M., and Pilmer, I.R. (eds). *Encyclopedia of Geology*. Elsevier, Oxford, v.4, p81-91.

VAN STAAL, C. R. 2007. Pre-Carboniferous tectonic evolution and metallogeny of the Canadian Appalachians. In GOODFELLOW, W.D. (ed) *Mineral Deposits of Canada: A synthesis of major deposit-types, district metallogeny, the evolution of geological provinces, and exploration methods.* Geological Association of Canada, Mineral Deposits Division, Special Publication, **5**, 793-818.

VAN STAAL, C.R., FYFFE, L.R., LANGTON, J.P. & MCCUTCHEON, S.R. 1992. The Ordovician Tetagouche Group, Bathurst camp, northern New Brunswick, Canada: History, tectonic setting, and distribution of massive-sulfide deposits. *Exploration and Mining Geology,* **1**, 93-101.

VAN STAAL, C. R., DEWEY, J. F., MAC NIOCAILL, C. & MCKERROW, W. S. 1998. The Cambrian-Silurian tectonic evolution of the northern Appalachians and British Caledonides: history of a complex, west and southwest Pacific-type segment of Iapetus. In BLUNDELL, D.J. & SCOTT, A. C. (eds) *Lyell: The Past is the Key to the Present.* Geological Society, London, Special Publications, **143**, 199-242.

VAN STAAL, C.R., WILSON, R.A., ROGERS, N., FYFFE, L.R., LANGTON, J.P., MCCUTCHEON, S.R., MCNICOLL, V. & RAVENHURST, C.E. 2003. Geology and tectonic history of the Bathurst Supergroup, Bathurst Mining Camp, and its relationships to coeval rocks in southwestern New Brunswick and adjacent Maine - a synthesis, in GOODFELLOW, W.D. MCCUTCHEON, S.R. AND PETER, J.M. (eds.). *Massive Sulfide Deposits of the Bathurst Mining Camp, New Brunswick and Northern Maine.* Economic Geology Monograph, **11**, 37-60.

VAN STAAL, C.R., WHALEN, J.B., MCNICOLL, V.J., PEHRSSON, S.J., LISSENBERG, C.J., ZAGOREVSKI, A., VAN BREEMAN, O. & JENNER, G.A. 2007. The Notre Dame arc and the Taconic Orogeny in Newfoundland, in HATCHER, J., CARLSON, M.P., MCBRIDE, J.H., AND MARTÍNEZ CATALÁN, J.R., (eds). *The 4D framework of continental crust*. Geological Society of America, Memoirs, **200**, 511-552.

VAN STAAL, C.R., WHALEN, J.B., VALVERDE-VAQUERO, P., ZAGOREVSKI, A. & ROGERS, N. 2009. Pre-Carboniferous, episodic accretion-related, orogenesis along the Laurentian margin of the northern Appalachians, in MURPHY, J.B., KEPPIE, J.D. & HYNES, A.J. (eds). *Ancient Orogens and Modern Analogues.* Geological Society London, Special Publications, 271-316.

WALDRON, J.W.F. & VAN STAAL, C.R. 2001. Taconian Orogeny and the accretion of the Dashwoods Block: a peri-Laurentian microcontinent in the Iapetus Ocean. *Geology*, **29**, 811-814.

WENDT, I. & CARL, C. 1991. The statistical distribution of the mean squared weighted deviation. *Chemical Geology: Isotope Geoscience section*, **86**, 275-285.

WHALEN, J.B., JENNER, G.A., LONGSTAFFE, F.J., GARIEPY, C. & FRYER, B.J. 1997. Implications of granitoid geochemical and isotopic (Nd, O, Pb) data from the Cambrian-Ordovician Notre Dame arc for the evolution of the Central Mobile Belt, Newfoundland Appalachians, in SINHA, A.K., WHALEN, J.B. & HOGAN, J.P. *The nature of magmatism in the Appalachian orogen*. Geological Society of America, Memoir, **191**, 367-395.

WIER, M.W. 1986. The formation of the base-metal deposits of the Tyrone Volcanic – Igneous Complex, Northern Ireland. Unpublished Master of Scienc thesis, University of Leeds, UK.

WILLIAMS, H., COLMAN-SADD, S.P., & SWINDEN, H.S. 1988. Tectonostratigraphic subdivisions of central Newfoundland. *Geological Survey of Canada, Current Research, Part B,* Paper 88-1b.

WINCHESTER, J.A., & FLOYD, P.A. 1977. Geochemical discrimination of different magma series and their differentiation products using immobile elements. *Chemical Geology*, **20**, 325-343.

WINCHESTER, J.A. & VAN STAAL, C.R. 1995. Volcanic and sedimentary terrane correlation between the Dunnage and Gander Zones of the Canadian Appalachians and the British Caledonides reviewed, in HIBBARD, J.P., VAN STAAL, C.R. & CAWOOD, P.A. (eds)., *Current perspectives in the Appalachian - Caledonian Orogen*. Geological Association of Canada, Special Paper, **41**, 95-114.

WRIGHT, C.A., BARNES, C.R. & JACOBSEN, S.B. 2002. Neodymium isotopic composition of Ordovician conodonts as a seawater proxy: Testing paleogeography. *Geochemistry, Geophysics, Geosystems*, **3**, doi: 10.1029/2001GC00195.

WOOD, D.A. 1980. The application of a Th-Hf-Ta diagram to problems of tectonomagmatic classification and to establishing the nature of crustal contamination of basaltic lavas of the British Tertiary volcanic province. *Earth and Planetary Science Letters*, **50**, 11-30.

WRAFTER, J.P. & GRAHAM, J.R. 1989. Ophiolitic detritus in the Ordovician sediments of South Mayo, Ireland. *Journal of the Geological Society of London,* **146**, 213-215.

WYMAN, D., BLEEKER, W. & KERRICH, R. 1999. A 2.7 Ga komatiite, low Ti tholeiite, arc tholeiite transition, and inferred proto-arc geodynamic setting of the Kidd Creek deposit: evidence from precise trace element data. *Economic Geology Monographs,* **10**, 525-542.

WYMAN, D.A. 2000. High-precision exploration geochemistry: applications for volcanogenic massive sulfide deposits. *Australian Journal of Earth Sciences,* **47**, 861-871.

YOUNG, S.A., SALTZMAN, M.R., FOLAND, K.A., LINDER, J.S. & KUMP, L.R. 2009. A major drop in seawater $^{87}Sr/^{86}Sr$ during the Middle Ordovician (Darriwilian): Links to volcanism and climate? *Geology*, **37**, 951-954.

ZAGOREVSKI, A. 2008. Preliminary geochemical database of the Buchans-Robert's Arm Belt, central Newfoundland. Geological Survey of Canada Open File 5986.

ZAGOREVSKI, A. & VAN STAAL., C.R. 2011. The Record of Ordovician Arc-Arc and Arc-Continent Collisions in the Canadian Appalachians During the Closure of Iapetus: in BROWN, D., AND RYAN, P.D. (eds.). *Arc-Continent Collision*, Frontiers in Earth Sciences, 341-371.

ZAGOREVSKI, A., ROGERS, N., VAN STAAL, C.R., MCNICOLL, V., LISSENBERG, C.J. & VALVERDE-VAQUERO, P. 2006. Lower to Middle Ordovician evolution of peri-Laurentian arc and backarc complexes in Iapetus: constraints from the Annieopsquotch Accretionary Tract, central Newfoundland. *GSA Bulletin*, **118**, 324-342.

ZAGOREVSKI, A., VAN STAAL, C.R., MCNICOLL, V.J., ROGERS, N. & VALVERDE-VAQUERO, P. 2008. Tectonic architecture of an arc-arc collision zone, Newfoundland Appalachians, in DRAUT, A.E., CLIFT, P.D. & SCHOLL, D.W. (eds.) *Formation and Application of the Sedimentary Record in Arc Collision Zones*. Geological Society of America, Special Paper, **436**, 309-333.

ZAGOREVSKI, A., LISSENBERG, C.J. & VAN STAAL, C.R. 2009a. Dynamics of accretion of arc and backarc crust to continental margins: Inferences from the Annieopsquotch accretionary tract, Newfoundland Appalachians. *Tectonophysics*, **479**, 150-164.

ZAGOREVSKI, A., VAN HEES, G. & ROGERS, N. 2009b. Provisional nomenclature of the volcanic rocks in the Buchans area, central Newfoundland. Geological Survey of Newfoundland and Labrador Open House, St. John's, Newfoundland.

ZAGOREVSKI, A., ROGERS, N. & HASLAM, R. 2010. Geology and significance of the Harry's River mafic volcanic rocks, Buchans area, Newfoundland. *Current Research 2010, Newfoundland and Labrador Department of Natural Resources*, 373-384.

ZAGOREVSKI, A., VAN STAAL, C.R. & ROGERS, N. 2012. Making and breaking of an arc: recurring extensional magmatism in the Annieopsquotch Accretionary Tract, Newfoundland Appalachians. GAC-MAC-AGC-AMC Joint Annual Meeting, St. Johns 2012. Abstract Volume 35, p.154.

ZALASIEWICZ, J.A., TAYLOR, L., RUSHTON, A.W.A., LOYDELL, D.K., RICKARDS, R.B. & WILLIAMS, M. 2009. Graptolites in British Stratigraphy. *Geological Magazine*, **146**, 785-850.

ZAYKOV, V.V., ZAYKOVA, E.V. & MASLENNIKOV, V.V. 2000. Volcanic complexes and ore mineralization in spreading basins of the southern Urals, in MEZHELOVSKY, N.V., MOROZOV, A.F., GUSEV, G.S. & POPOV, V.S. (eds.). Geodynamics and Metallogeny:

theory and implications for applied geology. Ministry of Natural Resources of the RF and GEOKART Ltd., Moscow, p315-337 (in Russian).

ZHANG, W. & FYFE, W. 1995. Chloritization of the hydrothermally altered bedrock at the Igarapé Bahia gold deposit, Carajás, Brazil. *Mineralium Deposita*, **30**, 30-38.